Methods in Molecular Biology 2237

Springer Protocols

Kelly C. Whittaker
Ruo-Pan Huang *Editors*

Antibody Arrays

Methods and Protocols

MOREMEDIA

Humana Press

METHODS IN MOLECULAR BIOLOGY

Series Editor
John M. Walker
School of Life and Medical Sciences
University of Hertfordshire
Hatfield, Hertfordshire, UK

For further volumes:
http://www.springer.com/series/7651

For over 35 years, biological scientists have come to rely on the research protocols and methodologies in the critically acclaimed *Methods in Molecular Biology* series. The series was the first to introduce the step-by-step protocols approach that has become the standard in all biomedical protocol publishing. Each protocol is provided in readily-reproducible step-by-step fashion, opening with an introductory overview, a list of the materials and reagents needed to complete the experiment, and followed by a detailed procedure that is supported with a helpful notes section offering tips and tricks of the trade as well as troubleshooting advice. These hallmark features were introduced by series editor Dr. John Walker and constitute the key ingredient in each and every volume of the *Methods in Molecular Biology* series. Tested and trusted, comprehensive and reliable, all protocols from the series are indexed in PubMed.

Antibody Arrays

Methods and Protocols

Edited by

Kelly C. Whittaker and Ruo-Pan Huang

RayBiotech, Peachtree Corners, GA, USA,
RayBiotech Life, Peachtree Corners, GA, USA

Humana Press

Editors
Kelly C. Whittaker
RayBiotech
Peachtree Corners, GA, USA

Ruo-Pan Huang
RayBiotech Life
Peachtree Corners, GA, USA

ISSN 1064-3745 ISSN 1940-6029 (electronic)
Methods in Molecular Biology
ISBN 978-1-0716-1063-3 ISBN 978-1-0716-1064-0 (eBook)
https://doi.org/10.1007/978-1-0716-1064-0

Preface

The completion of the Human Genome Project and implementation of genome-wide association studies have advanced our understanding of polymorphisms and mutations within disease-related genes. However, the molecular underpinnings of many diseases cannot be realized by DNA analysis alone; they require interrogation of protein activity, protein post-translational modification, or interactions of proteins with other biomolecules. Indeed, high-throughput methodologies of investigating protein function have become an essential tool to understand the molecular basis of disease and to generate meaningful data that informs treatment decisions. In particular, due to the heterogeneous nature of health and disease in human populations, high-throughput protein analysis has considerable potential to empower approaches for the implementation of precision medicine.

An example of a high-throughput protein analysis method is the antibody array. Antibody arrays can simultaneously measure the levels of tens to thousands of proteins within single biological samples. The term "antibody array" or "antibody microarray" refers to a planar solid support constructed of glass, plastic, or a flexible material such as nitrocellulose membrane, which has a grid of antibody spots on its surface. Analogous to a DNA microarray, this design allows specific analytes to be captured at fixed spot locations, where a discrete signal reporting on the abundance of the analyte is generated and computationally processed.

The detection principle of antibody arrays most commonly employs a sandwich immunoassay, but other methods may be used. When a matched antibody pair is not available, the antigen may be directly labeled (biotinylation) or alternatively, label-free methods may be used. Antibodies can be substituted with other capture agents to profile various molecular interactions. Recombinant proteins, peptides, aptamers, or even biological samples have been useful as multi-analyte probes and may be adapted to a researcher's desired application.

Antibody array platforms have been used to measure protein levels in a variety of samples, including blood, urine, cerebrospinal fluid, bone marrow extract, tears, saliva, tissue lysate, or conditioned medium. Dysregulated protein levels detected by anybody arrays have been the springboard to establishing a molecular explanation for many idiopathic conditions. For example, over the past 20 years, antibody arrays have been used extensively to elucidate the molecular basis of cancer, autoimmunity, neurodegeneration, and numerous other disease processes. Such studies have identified target proteins for therapeutic intervention and discovered biomarkers for the early diagnosis or prognosis of disease.

The complexity of the molecular landscape of disease, along with persistent efforts by the research community to improve precision medicine, has driven significant advancements in antibody array technology. Most notably, an increasing number of antibodies have been validated for array applications. A larger pool of antibodies enables ever larger array panels that permit broader screens capable of richer discoveries. Other recent achievements include antibody barcoding and "SNAP" chip technology, both of which can, to some degree, overcome limitations on antibody array panel design in order to better harness the power of the vast cache of array-validated antibodies available.

This volume aims to present the reader with a technical overview and practical methodology of a variety of antibody array formats and technologies. Antibody array types wherein the methods, advantages, and disadvantages of the technology are explained, as well as

practical applications of antibody arrays pertaining to investigations of specific research topics and biological processes and guidance on the methods of processing, analysis, and storage of array data are presented.

The techniques described here are a representative collection of tested and proven antibody array-related methodologies, each contributed by an expositor with first-hand practical experience in the application described. Our goal is to empower the reader with the required information to select the most appropriate array for their research application, with the technical knowledge to use and process the array with minimal pitfalls, and with the knowledge to perform analysis that realizes maximum benefit from the data generated.

Peachtree Corners, GA, USA *Kelly C. Whittaker*
Ruo-Pan Huang

Contents

Preface . . . . . *v*
Contributors . . . . . *ix*

1 Sandwich-Based Antibody Arrays for Protein Detection 1
Ying Qing Mao, Brianne Petritis, and Ruo-Pan Huang

2 Well-Based Antibody Arrays 11
Robert S. Matson

3 One-Step Antibody Arrays 39
Ying Qing Mao and Lin-Hai Li

4 Global Detection of Proteins by Label-Based Antibody Array 45
Zhizhou Kuang, Li-Pai Chen, Ruochun Huang, and Ruo-Pan Huang

5 Surface Plasmon Resonance Imaging-Mass Spectrometry Coupling on Antibody Array Biochip: Multiplex Monitoring of Biomolecular Interactions and On-Chip Identification of Captured Antigen 55
Anastasiia Halushkina, William Buchmann, Nathalie Jarroux, and Régis Daniel

6 Multiplexed Protein Biomarker Detection with Microfluidic Electrochemical Immunoarrays 69
Abby Jones, Patricia Czarnecki, Lasangi Dhanapala, and James F. Rusling

7 Cytometry Multiplex Bead Antibody Array 83
Benyue Zhang, Gang Xiao, Ying Qing Mao, Zhiqiang Lv, and Ruo-Pan Huang

8 Antibody Arrays: Barcode Technology 93
Liwei Yang and Jun Wang

9 Reverse Phase Protein Arrays 103
Justin B. Davis, Sydney Andes, and Virginia Espina

10 Enhanced Protein Profiling Arrays for High-Throughput Quantitative Measurement of Cytokine Expression 123
Ruochun Huang, Chun-Hui Gao, Wenjuan Wu, and Ruo-Pan Huang

11 Methods for Membranes and Other Absorbent Surfaces 129
Jarad J. Wilson, Yun Xi, Ruochun Huang, and Ruo-Pan Huang

12 Precise Chip-to-Chip Reagent Transfer for Cross-Reactivity-Free Multiplex Sandwich Immunoassays 141
François Paquet-Mercier, David Juncker, and Sébastien Bergeron

13 Antibody Printing Technologies 151
Valentin Romanov and Benjamin D. Brooks

14 Self-Assembling Peptide Hydrogels for 3D Microarrays 179
Greta Bergamaschi, Alessandro Strada, Roberto Frigerio, Marina Cretich, and Alessandro Gori

15 Surface Modification of Glass Slides with Aminosilanes for Microarray Use 191
Chris Stuart

16 Dried Blood-Based Protein Profiling Using Antibody Arrays 199
Kelly C. Whittaker, Ying Qing Mao, Siwei Zhu, Zhiqiang Lv, and Ruo-Pan Huang

17 Profiling Glycoproteins on Functionalized Reverse Phase Protein Array 207
Ying Zhang, Liyuan Zhang, Anton Iliuk, and W. Andy Tao

18 Determining Protein Phosphorylation Status Using Antibody Arrays and Phos-Tag Biotin 217
Eiji Kinoshita, Emiko Kinoshita-Kikuta, and Tohru Koike

19 Analyzing Signaling Pathways Using Antibody Arrays 225
Hao Tang, Chaohui Duan, Zhizhou Kuang, and Ruo-Pan Huang

20 Using Antibody Arrays for Biomarker Discovery 237
Shuhong Luo, Yunbiao Ling, Li-Pai Chen, and Ruo-Pan Huang

21 Immune Cell Isolation from Murine Intestine for Antibody Array Analysis 247
Joshua A. Owens and Rheinallt M. Jones

22 Database Development for Antibody Arrays 257
Zhaowei Xu, Likun Huang, and Sheng-Ce Tao

23 Data Analysis for Antibody Arrays 263
Huihua Zhang, Ying Qing Mao, Brianne Petritis, and Ruo-Pan Huang

24 Statistical Analysis Options for Antibody Array Data 277
Jingqiao Lu

Index 315

Contributors

Sydney Andes • *Center for Applied Proteomics and Molecular Medicine, George Mason University, Manassas, VA, USA*

Greta Bergamaschi • *National Research Council of Italy—Istituto di Scienze e Tecnologie Chimiche (SCITEC-CNR), Milan, Italy*

Sébastien Bergeron • *Parallex BioAssays Inc., St-Basile-le-Grand, QC, Canada*

Benjamin D. Brooks • *Biomedical Sciences, Rocky Vista University, Ivins, UT, USA*

William Buchmann • *Université Paris-Saclay, Univ Evry, CNRS, LAMBE, Evry-Courcouronnes, Paris, France; CY Cergy Paris Université, CNRS, LAMBE, Cergy, Paris, France*

Li-Pai Chen • *Department of Gynaecologic Oncology, Affiliated Cancer Hospital and Institute of Guangzhou Medical University, Guangzhou, Guangdong, China*

Marina Cretich • *National Research Council of Italy—Istituto di Scienze e Tecnologie Chimiche (SCITEC-CNR), Milan, Italy*

Patricia Czarnecki • *Department of Chemistry, University of Connecticut, Storrs, CT, USA*

Régis Daniel • *Université Paris-Saclay, Univ Evry, CNRS, LAMBE, Evry-Courcouronnes, Paris, France; CY Cergy Paris Université, CNRS, LAMBE, Cergy, Paris, France*

Justin B. Davis • *Center for Applied Proteomics and Molecular Medicine, George Mason University, Manassas, VA, USA*

Lasangi Dhanapala • *Department of Chemistry, University of Connecticut, Storrs, CT, USA*

Chaohui Duan • *Department of Clinical Laboratory, Sun Yat-sen Memorial Hospital, Sun Yat-sen University, Guangzhou, Guangdong, China*

Virginia Espina • *Center for Applied Proteomics and Molecular Medicine, George Mason University, Manassas, VA, USA*

Roberto Frigerio • *National Research Council of Italy—Istituto di Scienze e Tecnologie Chimiche (SCITEC-CNR), Milan, Italy*

Chun-Hui Gao • *Intensive Care Unit, Affiliated Cancer Hospital and Institute of Guangzhou Medical University, Guangzhou, Guangdong, China*

Alessandro Gori • *National Research Council of Italy—Istituto di Scienze e Tecnologie Chimiche (SCITEC-CNR), Milan, Italy*

Anastasiia Halushkina • *Université Paris-Saclay, Univ Evry, CNRS, LAMBE, Evry-Courcouronnes, Paris, France; CY Cergy Paris Université, CNRS, LAMBE, Cergy, Paris, France*

Likun Huang • *Key Laboratory of Systems Biology, Shanghai Center for Systems Biomedicine, Shanghai Jiao Tong University, Shanghai, China*

Ruochun Huang • *RayBiotech Life, Peachtree Corners, GA, USA*

Ruo-Pan Huang • *RayBiotech Life, Peachtree Corners, GA, USA; RayBiotech, Inc., Guangzhou, Guangdong, China; South China Biochip Research Center, Guangzhou, Guangdong, China; Affiliated Cancer Hospital and Institute of Guangzhou Medical University, Guangzhou Medical University, Guangzhou, Guangdong, China*

Anton Iliuk • *Tymora Analytical Operations, West Lafayette, IN, USA*

Nathalie Jarroux • *Université Paris-Saclay, Univ Evry, CNRS, LAMBE, Evry-Courcouronnes, Paris, France; CY Cergy Paris Université, CNRS, LAMBE, Cergy, Paris, France*

Abby Jones • *Department of Chemistry, University of Connecticut, Storrs, CT, USA*
Rheinallt M. Jones • *Division of Pediatric Gastroenterology, Hepatology, and Nutrition, Department of Pediatrics, Emory University School of Medicine, Atlanta, GA, USA*
David Juncker • *McGill University and Génome Québec Innovation Centre, Montreal, QC, Canada; Biomedical Engineering Department, McGill University, Montreal, QC, Canada*
Eiji Kinoshita • *Department of Functional Molecular Science, Institute of Biomedical and Health Sciences, Hiroshima University, Hiroshima, Japan*
Emiko Kinoshita-Kikuta • *Department of Functional Molecular Science, Institute of Biomedical and Health Sciences, Hiroshima University, Hiroshima, Japan*
Tohru Koike • *Department of Functional Molecular Science, Institute of Biomedical and Health Sciences, Hiroshima University, Hiroshima, Japan*
Zhizhou Kuang • *RayBiotech Life, Peachtree Corners, GA, USA; RayBiotech, Inc., Guangzhou, Guangdong, China*
Lin-Hai Li • *Department of Laboratory Medicine, General Hospital of Southern Theatre Command of PLA, Guangzhou, Guangdong, China*
Yunbiao Ling • *Hepatobiliary Surgery, The Third Affiliated Hospital of Sun Yat-sen University, Guangzhou, Guangdong, China*
Jingqiao Lu • *RayBiotech, Peachtree Corners, GA, USA*
Shuhong Luo • *RayBiotech, Peachtree Corners, GA, USA*
Zhiqiang Lv • *RayBiotech, Inc., Guangzhou, Guangdong, China*
Ying Qing Mao • *RayBiotech Life, Peachtree Corners, GA, USA*
Robert S. Matson • *QuantiScientifics, LLC, Orange, CA, USA*
Joshua A. Owens • *Division of Pediatric Gastroenterology, Hepatology, and Nutrition, Department of Pediatrics, Emory University School of Medicine, Atlanta, GA, USA*
François Paquet-Mercier • *Parallex BioAssays Inc., St-Basile-le-Grand, QC, Canada*
Brianne Petritis • *RayBiotech Life, Peachtree Corners, GA, USA*
Valentin Romanov • *Victor Chang Cardiac Research Institute, Darlinghurst, NSW, Australia*
James F. Rusling • *Department of Chemistry, University of Connecticut, Storrs, CT, USA; Institute of Materials Science, University of Connecticut, Storrs, CT, USA; Department of Surgery and Neag Cancer Center, University of Connecticut Health Center, Farmington, CT, USA; School of Chemistry, National University of Ireland Galway, Galway, Ireland*
Alessandro Strada • *National Research Council of Italy—Istituto di Scienze e Tecnologie Chimiche (SCITEC-CNR), Milan, Italy*
Chris Stuart • *RayBiotech Life, Peachtree Corners, GA, USA*
Hao Tang • *RayBiotech Life, Peachtree Corners, GA, USA*
Sheng-Ce Tao • *Key Laboratory of Systems Biology, Shanghai Center for Systems Biomedicine, Shanghai Jiao Tong University, Shanghai, China*
W. Andy Tao • *Tymora Analytical Operations, West Lafayette, IN, USA; Department of Biochemistry, Purdue University, West Lafayette, IN, USA; Department of Chemistry, Purdue University, West Lafayette, IN, USA; Center for Cancer Research, Purdue University, West Lafayette, IN, USA*
Jun Wang • *Multiplex Biotechnology Laboratory, Department of Biomedical Engineering, Stony Brook University, State University of New York, Stony Brook, NY, USA*
Kelly C. Whittaker • *RayBiotech, Peachtree Corners, GA, USA*
Jarad J. Wilson • *RayBiotech Life, Peachtree Corners, GA, USA*

Wenjuan Wu • *Department of Gynaecologic Oncology, Cancer Institute and Hospital, Guangzhou Medical University, Guangzhou, Guangdong, China*
Gang Xiao • *Department of Laboratory Medicine, Third Affiliated Hospital of Southern Medical University, Guangzhou, Guangdong, China*
Yun Xi • *The Third Affiliated Hospital of Sun Yat-sen University, Guangzhou, Guangdong, China*
Zhaowei Xu • *Key Laboratory of Systems Biology, Shanghai Center for Systems Biomedicine, Shanghai Jiao Tong University, Shanghai, China*
Liwei Yang • *Multiplex Biotechnology Laboratory, Department of Biomedical Engineering, Stony Brook University, State University of New York, Stony Brook, NY, USA*
Benyue Zhang • *RayBiotech Life, Peachtree Corners, GA, USA*
Huihua Zhang • *RayBiotech, Inc., Guangzhou, Guangdong, China*
Liyuan Zhang • *Key Laboratory of Proteomics, Dalian Medical University, Dalian, China*
Ying Zhang • *Institutes of Biomedical Sciences, Fudan University, Shanghai, China*
Siwei Zhu • *RayBiotech, Inc., Guangzhou, Guangdong, China*

Chapter 1

Sandwich-Based Antibody Arrays for Protein Detection

Ying Qing Mao, Brianne Petritis, and Ruo-Pan Huang

Abstract

Sandwich-based antibody arrays enable the detection of multiple proteins simultaneously, thus offering a time- and cost-effective alternative to single-plex platforms. The protein of interest is "sandwiched" between an antibody that captures it to the array and a second antibody that is used for detection. Here we describe a 1-day procedure to process samples, such as serum or cell lysates, with a quantitative sandwich-based antibody array on a glass substrate using fluorescence.

Key words Antibodies, Antibody array, Array, Fluorescence, Immunoassay, Quantitative array, Sandwich immunoassay

1 Introduction

The feasibility of immobilizing antibodies in an arrayed format to capture and analyze antigens was first demonstrated in the late 1990s [1, 2]. Since then, different formats of the antibody array have been developed [3, 4] for use in basic and clinical research to study the protein profiles of signaling pathways, diseases, and patient response to treatment [5, 6]. Their ability to measure the expression of multiple proteins at one time offers a time- and cost-effective alternative to using single-plex detection platforms like enzyme-linked immunosorbent assays (ELISA). Furthermore, antibody arrays have low sample volume requirements, which is an attracting option with limited samples (e.g., clinical samples).

Sandwich-based antibody arrays employ an antibody pair to detect each protein of interest: a "capture" antibody (CAb) immobilized on the array substrate and a "detection" antibody (DAb) that binds to a different epitope of the same protein [3]. The use of two antibodies per target results in excellent specificity. Briefly, CAbs are arrayed in an addressable format on a membrane (e.g., nitrocellulose), glass, or bead substrate. The protein (i.e., antigen), if it's expressed, is bound by its specific CAb when the sample is incubated on the array. After unbound proteins are removed with a

Kelly C. Whittaker and Ruo-Pan Huang (eds.), *Antibody Arrays: Methods and Protocols*, Methods in Molecular Biology, vol. 2237, https://doi.org/10.1007/978-1-0716-1064-0_1,

washing step, a mixture of DAbs is added (Fig. 1). The DAb will bind to its antigen if it has been captured by the CAb; thus, the protein of interest will be "sandwiched" between the antibody pair. Finally, the detection antibody enables chemiluminescence or fluorescence via its conjugated enzyme (e.g., horseradish peroxidase, biotin, or fluorophore). Because the antibodies are arrayed in an addressable format, the chemiluminescence or fluorescence signal can be assigned accurately to a specific protein. For example, each target is represented by its own spot on a membrane- or glass-based array (Fig. 2), or by a detection antibody with a unique fluorophore on a bead-based array. The signal is proportional to the amount of the protein in the sample.

Both qualitative and quantitative analyses are performed with sandwich-based arrays. Relative protein expression differences across samples are ascertained with qualitative arrays. Quantitative arrays, on the other hand, determine protein concentration (e.g., ng/mL) by extrapolating the standard curve to sample signal. The standard curve is produced by adding a known amount of purified antigen in serial dilutions.

Cross-reactivity and sample matrix effects are important issues to consider with sandwich-based antibody arrays. Antibody cross-reactivity, or non-specific binding, between detection antibodies can sometime occur, thus restricting which antibodies can be placed together on the same array [3]. Therefore, antibody cross-reactivity testing during array production is necessary. Sample matrix effects are a common cause of nonlinear dilution responses in immunoassays [3, 7]. This can occur when proteins or other components within the sample affect the immunoreactivity of the target molecule. These matrix components can also affect the ability of the antibody to recognize its target within the sample. Autoantibodies, binding proteins, hemolysis, or certain disease states (e.g., highly lipemic samples) can contribute to this phenomenon. Sample dilution and centrifugation can help minimize matrix effects, and a minimum twofold dilution should be used for all samples. The only exception to this rule is urine, which can be analyzed without dilution due to its low protein content. Notably, the optimal sample dilution for all samples must be determined empirically.

In this chapter, we describe the steps and materials needed to process samples using a quantitative sandwich-based antibody array called Quantibody®. Using a standard glass slide, 16 identical sub-arrays are printed and separated from each other with a 16-well gasket secured on top of the slide. Biotinylated DAbs on the array are detected using a streptavidin molecule conjugated to a Cy3 equivalent dye. Prior to scanning, the gasket is removed, and the fluorescent signal is analyzed using a Cy3-capable laser scanner.

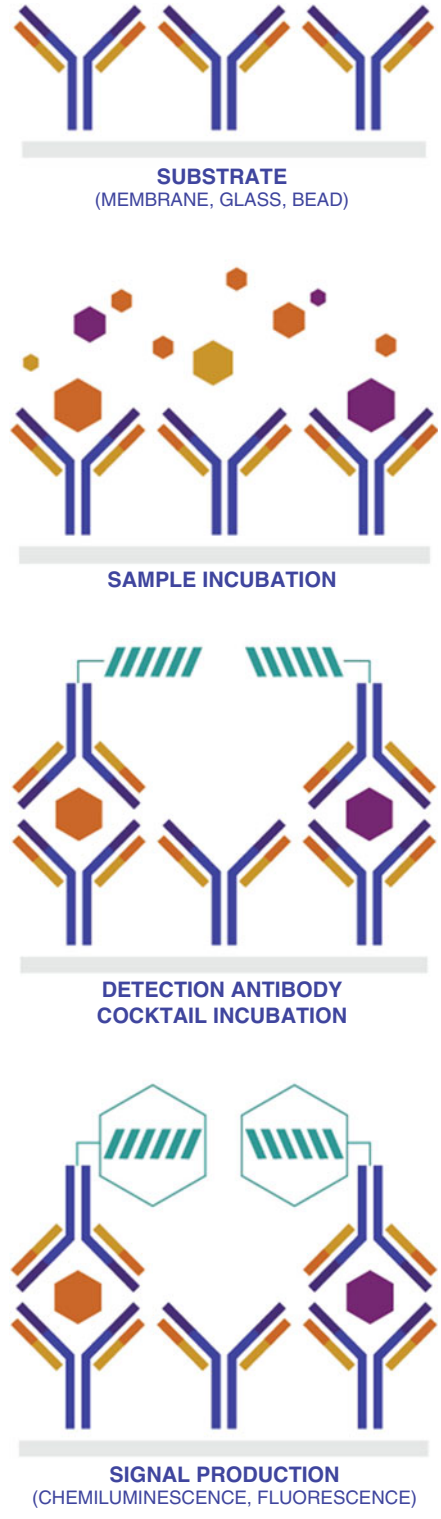

Fig. 1 General steps of a sandwich-based array

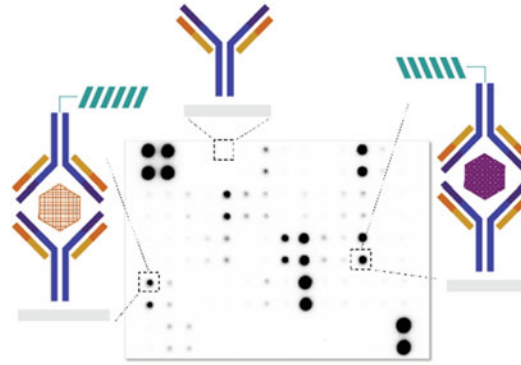

Fig. 2 Each spot on a membrane- or glass-based antibody array represents a unique target protein

2 Materials

1. InnoScan 710AL laser scanner (Innopsys) with Mapix software.
2. Scienion SX non-contact arrayer (Berlin, Germany).
3. 16-well removable gasket.
4. Inflammation Antibody Array Slide: one standard glass slide; ten inflammatory cytokines, IL-1 alpha, IL-1 beta, IL-4, IL-6, IL-8, IL-10, IL-13, MCP-1, IFN gamma, and TNF alpha; and biotin-labelled bovine IgG. Each slide is spotted with 16 wells of identical cytokine antibody arrays. Each antibody, together with the biotin-labelled bovine IgG (positive control), is arrayed in quadruplicate with the non-contact arrayer. The 16-well removable gasket is applied to the printed slide, and the slide is sealed with film (*see* **Note 1**).
5. BSA.
6. Casein.
7. Tween-20.
8. Black microcentrifuge tubes.
9. Microcentrifuge tubes.
10. 1× PBS: 137 mM NaCl, 2.7 mM KCl, 10 mM Na_2HPO_4, 1.8 mM KH_2PO_4, pH 7.4.
11. 1× Sample Diluent: 5% BSA in 1× PBS.
12. 20× Wash Buffer II: 400 mM Tris–HCl, 3 M NaCl, pH 7.5 in dH_2O.
13. 1× Wash Buffer II: 20 mM Tris–HCl, 150 mM NaCl, pH 7.5 in dH_2O.
14. 20× Wash Buffer I: 2% Tween-20 (w/v), 400 mM Tris–HCl, 3 M NaCl, pH 7.5 in dH_2O.

15. 1× Wash Buffer I: 0.1% Tween-20 (w/v), 20 mM Tris–HCl, 150 mM NaCl, pH 7.5 in dH_2O.
16. 0.1% BSA/PBS: 0.1% BSA (w/v) in 1× PBS.
17. Cy3 Equivalent Dye-Conjugated Streptavidin Working Stock: 1.4 mL of 1× Sample Diluent, 5 μL of Cy3 Equivalent Dye-Conjugated Streptavidin (100 μg/mL) in a black microcentrifuge tube.
18. Cytokine Antigen Mix: 100 ng each of IL-1 alpha, IL-1 beta, IL-4, IL-6, IL-10, IL-13, MCP-1, and TNF alpha, 500 ng of IFN gamma, and 20 ng of IL-8 in 1 mL of 0.1% BSA/PBS. Aliquot 10 μL to each tube and freeze dry (*see* **Note 2**).
19. Detection Biotin-Conjugated Anti-Cytokine Antibody Mix: mix proper amount of biotin-conjugated antibodies to IL-1 alpha, IL-1 beta, IL-4, IL-6, IL-8, IL-10, IL-13, MCP-1, IFN gamma, and TNF alpha (ranging from 1 to 250 ng/mL) in 1.4 mL of 1× Sample Diluent.
20. 4-Slide Washer/Dryer.
21. Thermo Orbital Shaker.
22. Human serum sample.

3 Methods

3.1 Slide, Sample, and Standard Preparation

1. Completely air dry the Inflammation Antibody Array Slide by peeling off the cover film and letting it air dry at room temperature for 1–2 h (*see* **Note 3**).
2. Label the Cytokine Antigen Mix Working Stock as Std1.
3. Label 6 clean microcentrifuge tubes as Std2 to Std7. Add 200 μL of 1× Sample Diluent to each of the tubes.
4. Pipette 100 μL of Std1 into the tube labeled Std2 and mix gently. Perform five more serial dilutions by adding 100 μL of Std2 to the tube labeled Std3 and so on (Fig. 3).
5. Add 100 μL of 1× Sample Diluent to another tube labeled as CNTRL. Do not add the cytokine antigens or samples to the CNTRL tube, which will be used as negative control. For best results, include a set of standards on each slide (*see* **Note 4**).
6. Thaw the human serum samples on ice, and pipette 50 μL of human serum into a clean 1.5 mL tube. Add 50 μL 1× Sample Diluent to make a 2× diluted serum sample.

3.2 Blocking and Incubation

1. Add 100 μL of 1× Sample Diluent into each well, and incubate at room temperature for 30 min to block slides (*see* **Note 5**).
2. Decant the 1× Sample Diluent from each well. Add 100 μL of the standards (Std1–Std7 and CNTRL) and 2× diluted serum

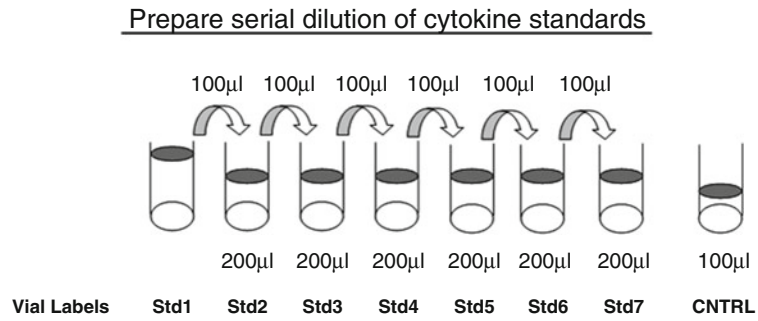

Fig. 3 Prepare serial dilution of cytokine standards

samples to corresponding wells. Incubate at room temperature for 1–2 h (*see* **Note 6**).

3. Decant the liquid from each well (*see* **Note 7**), and wash five times (5 min each) with 150 µL of 1× Wash Buffer I at room temperature with gentle shaking. Completely remove the wash buffer in each wash step (*see* **Note 8**).
4. Decant the 1× Wash Buffer I from each well, and wash two times (5 min each) with 150 µL of 1× Wash Buffer II at room temperature with gentle shaking. Completely remove the wash buffer in each wash step.
5. Add 80 µL of the Detection Biotin-Conjugated Anti-Cytokine Antibody Mix to each well. Incubate at room temperature for 1–2 h (*see* **Note 9**).
6. Decant the Detection Biotin-Conjugated Anti-Cytokine Antibody Mix from each well.
7. Wash five times (5 min each) with 150 µL of 1× Wash Buffer I at room temperature with gentle shaking. Completely remove the wash buffer in each wash step.
8. Wash two times (5 min each) with 150 µL of 1× Wash Buffer II at room temperature with gentle shaking. Completely remove the wash buffer in each wash step.
9. Add 80 µL of Cy3 Equivalent Dye-Conjugated Streptavidin Working Stock to each well. Incubate at room temperature for 1 h (*see* **Notes 10** and **11**).
10. Decant the Cy3 Equivalent Dye-Conjugated Streptavidin Working Stock from each well, and wash five times (5 min each) with 150 µL of 1× Wash Buffer I at room temperature with gentle shaking. Completely remove the wash buffer in each wash step (*see* **Note 12**).

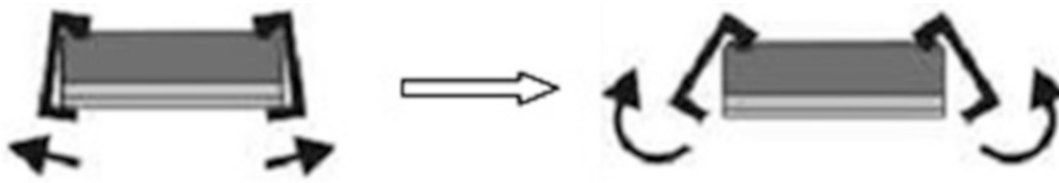

Fig. 4 The gentle release of the glass slide from the chip

3.3 Fluorescence Detection and Image Analysis

1. Carefully remove the slide from the 16-well removable gasket (Fig. 4).
2. Place the slide in the 4-Slide Washer/Dryer, and add 30 mL of 1× Wash Buffer I. Gently shake at room temperature for 15 min.
3. Decant Wash Buffer I. Add 30 mL of 1× Wash Buffer II, and gently shake at room temperature for 5 min (*see* **Note 13**).
4. Decant Wash Buffer II. Remove 1× Wash Buffer II completely by a compressed N2 stream. Or gently apply suction with a pipette to remove water droplets. Do not touch the array, only the sides.
5. The signals can be visualized through use of a laser scanner equipped with a Cy3 wavelength such as Axon GenePix and Innopsys InnoScan (excitation, 555 nm; emission, 565 nm; resolution, 10 μm). A Dynamic Range Extension (XDR) mode scan is recommended for Innopsys scanners (*see* **Note 14**).
6. Data extraction can be done with most microarray analysis software. A linear curve is recommended for low abundant proteins, while a log-log curve is recommended for median to high abundant proteins.

4 Notes

1. If the slide will not be used immediately after printing, package with a moisture absorbing pad, and store in −20 °C until use.
2. Complete reconstitution of the lyophilized standard is critical for accurate protein concentration quantification. It is critical to ensure that the lyophilized standard powder is in the bottom of the tube for reconstitution. A quick spin of the Cytokine Antigen Mix can ensure this. After adding 500 μL of Sample Diluent to the tube, reconstitute it at room temperature for 15–30 min with gentle agitation. Avoid vigorous vortexing to prevent protein denaturation. Reconstitute the Cytokine Antigen Mix within 1 h of usage. If you must use the standard for two different days, store at −80 °C.

3. If the slide was stored prior to use, let it equilibrate to room temperature inside the sealed plastic bag for 20–30 min prior to opening and continuing with **step 1** of Subheading 3.1. Room temperature equilibration is important to prevent moisture condensation upon the slide surface, as the antibody printed on the glass slide may become loosely bound after thawing. If the slide is not completely dry, adding Sample Diluent to the array may cause the translocation of the unbound antibodies to adjacent locations, which causes the formation of "comet tails." Drying the slide for 1–2 h at room temperature or in a vented hood can almost completely prevent this phenomenon.
4. A full set of standards is needed for a single slide experiment. However, if multiple slides of the same array are run simultaneously, not all the slides need a full set of standards. When running multiple slides, a full set of standards should be included on every four slides. For the other slides, a negative control and one standard (e.g., Std3) should be included for inter-slide normalization purposes.
5. Blocking can lower the background and may give a more consistent result. However, it is not needed for most sample types (culture media, serum, gingival crevicular fluid, and other body fluids). A blocking step is recommended for lysate samples which tend to have higher background.
6. To minimize matrix effects, we recommend that all the samples are diluted at least twofold with 1× Sample Diluent. Cover the slide with adhesive film during incubations if less than 70 μL of sample or reagent is used. Longer incubation times are preferable for higher signals. If many slides are run simultaneously, this step can be done overnight at 4 °C with gentle shaking. The next morning, however, the slides need to be re-equilibrated to room temperature for 1 h before continuing to the next step. Signals will be lower if you directly process slides incubated at 4 °C overnight.
7. Pipette suction with vacuum pump is recommended for liquid removal. In order to prevent cross-well contamination, wash the pipette tip between the removal from each well, and avoid buffer overflow of the initial wash with 1× Wash Buffer I.
8. Thorough washing after sample incubation is critical for the success of the experiment. 1× Wash Buffer I contains 0.1% Tween-20 and is the key wash buffer to remove non-specific signals. A longer incubation with Wash Buffer I will produce a cleaner background but may also lower the signal. For cell and tissue lysates, an extra wash with 1× Wash Buffer I at room temperature with gentle shaking for 20 min is recommended.

9. Longer incubation times with the detection antibody will result in higher signals; however, the background noise will also increase. One-and-a-half-hour incubation with the detection antibody is sufficient for optimal detection.
10. Photobleaching-resistant Cy3 equivalent dye is our first choice for green laser detection. For systems with higher background in the green laser (such as nitrocellulose-coated slides), a Cy5 equivalent dye can also be used for red laser detection in this step. Based upon our experience, the Cy3 equivalent dyes are generally more resistant to photobleaching and yield a higher signal intensity.
11. The streptavidin-biotin complex is the strongest known non-covalent interaction ($K_d = 10^{-15}$ M) between a protein and ligand. The bond formation between biotin and streptavidin is very rapid and efficient. A longer incubation of dye-conjugated streptavidin in the reaction can only marginally increase the detection signal.
12. Since the Cy3 equivalent dye-conjugated streptavidin reaction system has very high fluorescence, trace of it can cause very high background. It is crucial to use a pipette to completely remove the buffer residue around the well corners in each wash.
13. This step is necessary to remove any possible remaining dye in the well corner of the frame. It can also lower the non-specific signals of the sample, especially cell or tissue lysates. A longer incubation of Wash Buffer I will lower the background. However, we do not recommend Wash Buffer I incubation of more than 2 h since the real signal may also be removed.
14. The signal intensity for different cytokines can differ greatly in the same array; in such cases, multiple scans are recommended, with a higher PMT for low signal cytokines and a low PMT for high signal cytokines. If the scanner is equipped with XDR functionality, an XDR mode scan is recommended. Using the XDR mode, the signal detection dynamic range can be extended up to two extra logs.

References

1. Rowe CA, Scruggs SB, Feldstein MJ, Golden JP, Ligler FS (1999) An array immunosensor for simultaneous detection of clinical analytes. Anal Chem 71(2):433–439. https://doi.org/10.1021/ac980798t
2. Guschin D, Yershov G, Zaslavsky A, Gemmell A, Shick V, Proudnikov D, Arenkov P, Mirzabekov A (1997) Manual manufacturing of oligonucleotide, DNA, and protein microchips. Anal Biochem 250(2):203–211. https://doi.org/10.1006/abio.1997.2209
3. Ruo-Pan H, Brett B, Valerie Sloane J, Wei-Dong J, Ying-Qing M, Qiao-Lin C, Zhi S (2012) Cytokine antibody arrays in biomarker discovery and validation. Curr Proteomics 9(1):55–70. https://doi.org/10.2174/157016412799746209
4. Sauer U (2017) Analytical protein microarrays: advancements towards clinical applications. Sensors (Basel) 17(2):256. https://doi.org/10.3390/s17020256

5. Chen Z, Dodig-Crnković T, Schwenk JM, Tao S-C (2018) Current applications of antibody microarrays. Clin Proteomics 15:7–7. https://doi.org/10.1186/s12014-018-9184-2
6. Huang Y, Zhu H (2017) Protein array-based approaches for biomarker discovery in cancer. Genomics Proteomics Bioinformatics 15(2): 73–81. https://doi.org/10.1016/j.gpb.2017.03.001
7. Tu J, Bennett P (2017) Parallelism experiments to evaluate matrix effects, selectivity and sensitivity in ligand-binding assay method development: pros and cons. Bioanalysis 9(14): 1107–1122. https://doi.org/10.4155/bio-2017-0084

Chapter 2

Well-Based Antibody Arrays

Robert S. Matson

Abstract

Multiplex immunoassays are important tools in basic research and diagnostics. The ability to accurately quantify the presence of several antigens within an individual sample all at once has been useful in developing a proteomics view of biology. This in turn has enabled the development of disease-associated immunodiagnostic panels for better prognosis and well-being. Moreover, it is well understood that such multiplexing approaches lend themselves to automation, thereby reducing labor while providing the ability to dramatically conserve both reagent and sample all of which will reduce the cost per test. Here we describe various methods to create and use multiplex immunoassays in the wells of microtiter plates or similar formats.

Key words Antibody, Sourcing, Multiplex, ELISA, Immunoassay, Antibody array, Microwell, Microplate, Microarray, Self-assembly, Tethered, Immobilization, Molecular bridging, Oligonucleotide, Conjugate, Cross-reactivity, Image analysis, Quantitation

1 Introduction

In this chapter we describe steps in preparing a quantitative multiplex immunoassay in a microplate format based upon various means to tether antibodies and other proteins onto different solid-phase supports. The chapter is divided into three main antibody solid-phase immobilization strategies: physical adsorption, covalent coupling, and molecular bridging. In addition, related methods for protein microarraying and assay development are provided.

1.1 The Elephant in the Room-Antibody Sourcing

It cannot be overstated that the most critical factor in the successful development of any immunoassay, whether a conventional singleplex assay or an array-based multiplex ELISA, is antibody performance. Simply put, you need to use well-characterized antibodies and understand their limitations in terms of sensitivity, specificity, and stability. A word of caution, there has been considerable concerns over the quality of commercial antibodies raised by the research community [1–4] prompting the formation of an international working group to address such problems [5]. However,

Kelly C. Whittaker and Ruo-Pan Huang (eds.), *Antibody Arrays: Methods and Protocols*, Methods in Molecular Biology, vol. 2237, https://doi.org/10.1007/978-1-0716-1064-0_2,

Table 1
Antibody sourcing

	Vendor A			Vendor B		
Analyte	**Capture Ab**	**2° Ab**	**Antigen**	**Capture Ab**	**2° Ab**	**Antigen**
Hu IL-6	500 µg $449	50 µg $405	5 µg $359	50 µg $70	50 µg $85	4 x 5 ng $80
ELISA	matched pair	biotin	full length active	matched pair	biotin	partial seq E.coli
Host	mouse mAb	rabbit pAb	recombinant	rat IgG1 MQ2-13A5	rat IgG2a MQ2-39C3	recombinant
Conditions	4.0-8.0 µg/mL	0.5-1.0 µg/mL	7.8-500 pg/mL	0.5-2.0 µg/mL	0.5-2.0 µg/mL	8-1000 pg/mL

Comparison of vendor immunoassay component products (e.g., human IL-6) in terms of quantity, pricing, matched antibody pairs, secondary antibody label, antigen source, host, clones and ELISA conditions for capture antibody, secondary (2° Ab) and the assay sensitivity range for antigen detection

unless you have the capability to produce your own supply of antibodies, it will be necessary to rely on commercial sources either to prepare custom antibodies for you or furnish catalog materials. It is therefore prudent to source antibodies from at least 2–3 suppliers and perhaps more if you require matched pairs for a sandwich format. Most vendors maintain an extensive library of unconjugated antibodies to choose from for use as a capture antibody. Not all vendors provide a complementary secondary (reporter) antibody or matched pairs; and fewer will be able to supply the native antigen to use as a standard or control (Table 1).

As shown in Table 1, it is important to map out the availability and alternative product offering that could be potentially used in preparing the antibody array. These will help frame the assay design, including cost considerations. In this example, the biotin-labeled secondary antibodies permit the user to evaluate the suitability of a variety of labels based upon streptavidin-dye or streptavidin-enzyme conjugate (e.g., streptavidin-Cy5/streptavidin-Cy3, Alexa dyes, streptavidin-alkaline phosphatase, streptavidin-HRP, etc.). However, use of directly labeled antibody conjugates may be advantageous in terms of cost and performance, especially in view of the newly recognized problem with exogenous biotin interference with tests due to the use of megadose supplements [6, 7]. Once the signaling agent(s) for the assay are narrowed down, a directly labeled antibody conjugate (e.g., HRP-antibody) could be evaluated and those issues resolved.

In designing a multiplex sandwich immunoassay, pay careful attention to the specificity of the primary (capture) antibody and secondary (reporter) antibody pairs. Monoclonal antibodies bind to well-defined epitopes, so using the same clone for the pair will not work. Referring to Table 1, in the case of Vendor B, rat monoclonal MQ2-13A5 is used for the capture while an antibody

from MQ2-39C3 is used as the reporter. Likewise, Vendor A provides a monoclonal capture antibody and a polyclonal reporter antibody. In this instance, specificity is assured by the monoclonal capture, while the antibody population within the polyclonal pool undoubtedly favors a different epitope binding site. This is not always true, often requiring screening of various polyclonal antibodies for optimal binding. Once the matched pairs have been selected, it is advisable to perform the immunoassay directly on the solid-phase that is intended to be used for assay development. That is because the antibody performance may vary depending upon the nature of the solid-phase [8]. If the assay does not work well, try flipping the primary and secondary antibodies, using the secondary for capture and the primary as the reporter.

It is advisable to obtain the specification reports and/or certificates of analysis (CoA) if available from the vendor. These will provide useful information on the antibody isotype, host, clonality, cross-reactivity, purity, stability, handling conditions, and utility or intended use. Some antibodies are recommended for Western blots and others for immunoprecipitation, cellular staining (immunohistochemistry), flow cytometry, etc. but not so much for ELISA. If at all possible, choose antibodies that have been developed for immunoassays! Many vendors will provide the recommended concentrations or dilution ranges for the antibodies to be used in the immunoassay. Also, recombinant antigens are now widely used to prepare antibodies. As a result, recombinant antigens are often available as standards for the immunoassay. However, these surrogates may not be fully representative of the antibody's binding capacity for native antigen. It is recommended to compare the recombinant standard against an endogenous positive control during the validation of a diagnostic immunoassay. In selecting antibodies, the buyer needs to be aware of any access restrictions to the purchase. Many vendors offer their products for research only (RUO). If the intended use is for in vitro diagnostics (IVD) purposes, a license from the vendor may be required.

For the multiplex immunoassay, the assay development process should include a determination of the optimal surface loading capacity (i.e., the antibody surface density) for each capture antibody. Antibodies may vary in their antigen binding efficiency on a particular surface. Overloading can result in steric hindrance, thereby reducing the effective binding capacity, while too low an antibody density may lead to saturation and early plateauing in the standard curve [9]. Likewise, adjustment to the secondary antibody concentration may be necessary to further improve sensitivity.

1.2 Cross-Reactivity

Particularly with multiplex immunoassays, cross-talk (cross-reactivity), especially with secondary (2° Ab) antibodies, is a major concern and should be dealt with early on. The likelihood of cross-reactivity increases with the size of the multiplex [10]. There are

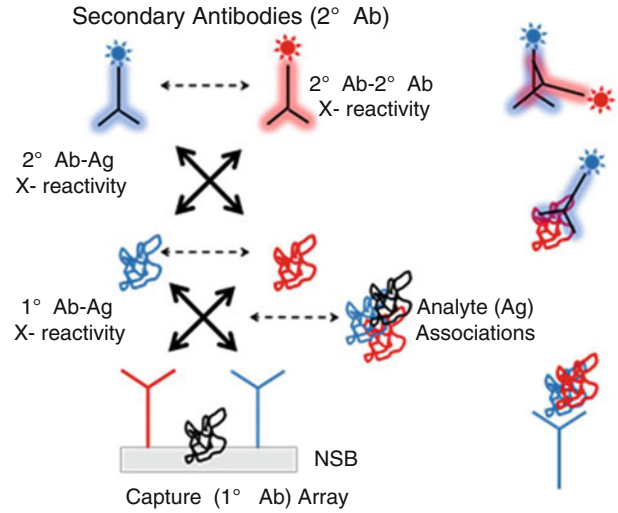

Fig. 1 Cross-reactivity in multiplex immunoassay. Examination of various levels of cross-reactivity in a multiplex sandwich ELISA. At the primary (1° Ab) level: non-specific binding (NSB) on the solid-phase; antibody-antigen cross-reactivity; antigen-antigen complex formation (association). At the secondary (2° Ab) level: antibody-antibody complex formation; antibody-antigen cross-reactivity

various conditions that may lead to a perceived cross-reactivity (Fig. 1). The simplest and most common issue is with non-specific binding (NSB) of the antigen and/or secondary antibody to the surface. The surface adsorption of proteins is dependent upon a number of factors including the protein's secondary structure, stability under different pH and ionic conditions, temperature, hydrophobicity, as well as the physical-chemical properties of the solid-phase and the buffer. Thus, different proteins are likely not to bind to the surface to the same extent. The remedy is to find a surface blocking agent that is suitable for the assay. Test for the NSB of the antigen, secondary antibodies, and signaling reagents.

The other issues of secondary antibody cross-reactivity for antigens, antibody-antibody interaction, and antigen-antigen aggregation are more difficult to sort out. One approach is to examine the individual assay components. For example, one may prepare a series of antibody array plates with variation in capture antibody (C), target antigen standard (T), and secondary (detection) antibodies (D) to determine the extent of cross-talk in the assay. For example, consider a 9-plex sandwich immunoassay:

Condition #1: (C, T, D) = (+9, +9, +9)—*for a 9-plex antibody array assay with all components.*

Condition #2: (+9, +1, +9) = **target cross-reactivity**—*determine each individual antigen target (standard) response for the 9-plex array with all detection antibodies present.*

Condition #3: (+9, +9, +1) = **detection cross-reactivity**—*determine each individual detection antibody response for the array with all antigens present.*

Condition #4: (+1, +9, +1) = **capture cross-reactivity**—*determine that a single capture antibody and detection antibody show target specificity with all antigens present.*

A modified "checkerboard" approach for performing these tests is described in Fig. 2. In this particular example, we find that the matched pair of capture antibody and detection antibody for target 1 are specific with no observed cross-reactivity. However, under condition #3, the detection antibody for target 2 also picks

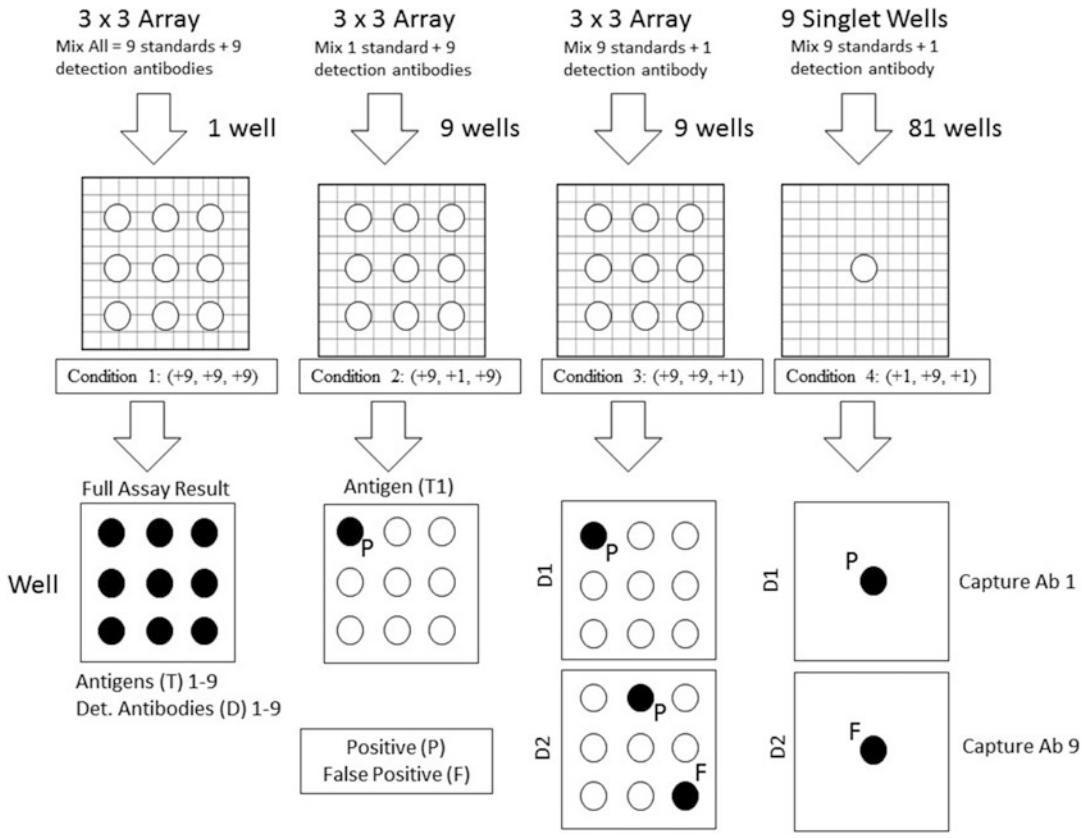

Fig. 2 "Checkerboard" determination of cross-reactivity. Utilizing well-based antibody arrays to systematically determine the extent of cross-reactivity for antibodies and antigens. **Condition 1:** *Determine the level of sensitivity for each analyte.* Using all components perform the full multiplex assay. **Condition 2:** *Determine whether or not the antigen cross-reacts with other capture antibodies.* Apply a single antigen standard to the array well, and then add all detection antibodies. Do this for all antigens. **Condition 3:** *Determine whether or not the detection antibody cross-reacts with other antigens.* Apply a pool of all antigens to the array well, and then add a single detection antibody. Do this for all detection antibodies. **Condition 4:** *Confirm whether or not there is cross-reactivity of antigen with different capture antibodies.* Print a single capture antibody (or array) in a single well, and then apply all of the antigen standards to each well. Add a single detection antibody to each well. Do this for all wells

up signal for target 9 suggesting the possibility that detection antibody 2 recognizes epitopes associated with target 9 as well. Using wells with separate capture antibody, signal from the addition of detection antibody 2 is picked up on the well containing only capture antibody 9, thus confirming the cross-reactivity.

1.3 Printing Aspects

The specific details surrounding antibody printing using various dispensing technologies are largely outside the scope of this chapter. Essentially, most arraying devices consist of a high-precision *xyz* platform to which various fluid dispensing tools are attached to deliver quantitative volumes of reagent (ink) in a confined space such as a slide or microplate well [11]. The dispensing occurs either by non-contact, with the substrate by jetting of droplets to the surface, or by contact printing, which transfers fluid directly to the surface. There are various non-contact dispensing units available based upon either piezo or solenoid valve action to eject droplets from a nozzle. Contact printing is largely accomplished using quills comprising notched stainless steel rod in the form of a split pin. Solid pins are also used. Non-contact printing requires aspiration of the sample into the nozzle (aspiration-dispense mode), while split or solid pins are dipped into the sample and the tip is stamped into or at a distance very close to the surface such that fluid is efficiently transferred. Arraying into plates requires additional time when compared to printing onto a slide. For optimal spotting the nozzle (or pin tip) needs to be within 1–2 mm from the surface (Fig. 3). This is to allow precise delivery of the droplet without a skew in the trajectory such that the spot is centered true. Plastic plates can also build up static electricity which can deflect the droplet resulting in the spot being off-center if the dispense height is not optimal. Static charge buildup can be minimized by wiping the plate surfaces with alcohol, the use of static discharge devices, and most effectively

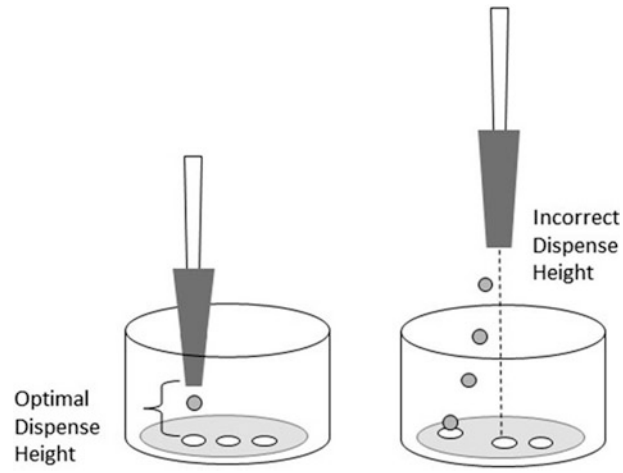

Fig. 3 Dispense height. Illustration of the proper dispenser tip height relative to substrate for optimal printing conditions

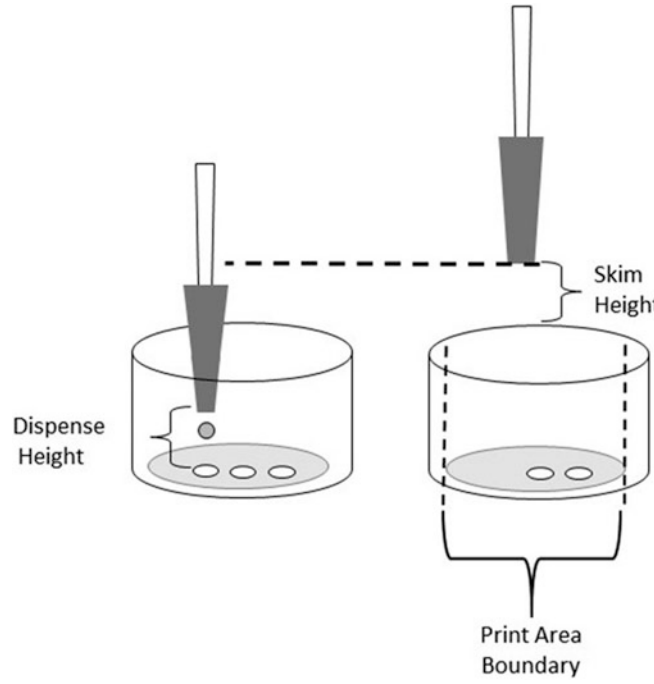

Fig. 4 Skim height. Illustration of setting a dispenser skim height necessary to provide clearance moving in and out of adjacent wells during printing, as well as avoiding collision at the walls by setting a print area boundary

pre-equilibrating the plate in the microarray dispenser with humidity set at RH >50%.

Because the superstructure of the plate (Fig. 4) presents an obstacle to the dispenser, the *z*-axis must be adjusted (programmed) such that the tip safely enters and exits each well at a collision-free height above the plate (skim height). This up-and-down translation adds significant time to the print cycle when compared to a slide which can be printed "on-the-fly" at a fixed skim height across the slide.

Spot size is controlled by a number of parameters, starting with droplet formation, where backing fluid compression, sample viscosity, nozzle coatings, and dispenser design interplay, to droplet acceleration, temperature, relative humidity, substrate properties, and surface wetting [12].

As shown in Table 2, the type of dispenser used tends to determine the spot size range, which in turn limits the spotting density (spots/cm^2) achievable within a plate well. Moreover, the plate well sidewalls prevent the disperser tip's breadth of reach within the well. For that reason, some vendors offer square-well plates with increased area to accommodate higher density arrays. Obviously, one can calculate the upper limit on spot density for a given plate and dispenser given the spot diameter and spot center-

Table 2
Arraying devices, dispense volumes, substrates

Dispenser Characteristics				Plate Substrate Material			
Printing Mechanism	Dispenser Type	Dispensed Drop Volume	Spot Diameter on surface	Glass	Plastic	NC	Comments
Non-Contact	Piezo dispense capillary (PDC)	50-800 pL	80-250 µm	☑	☑	☑	control spotting to various surfaces by PCD type, orifice, piezo tuning & number of droplets
Non-Contact	Piezo	100 pL-10 nL	90-500 µm	☑	☑	☑	
Non-Contact	Solenoid valve	20 nL 2.6 nL to 2 µL 1.3 nL to 1 µL	300-600 µm	☑ ☑ ☑	☑ ☑ ☑	☒ ☒ ☑	Very large spots Spot diffusion Use 1-3 nL dispense to NC
Contact	Split Pin Solid Pin	0.5-1.2 nL 0.7- 1.8 nL	62.5-125 µm 100-160 µm	☑ ☑	☑ ☑	☒ ☑	Pin fouling on NC (nitrocellulose membrane or coating)

A list of different printing mechanisms used to dispense antibodies onto surfaces. Contact or non-contact dispensing is reviewed in terms of the dispensed volume and spot diameter ranges expected using different dispensers. The suitability of various dispensers for spotting onto glass, plastic, and nitrocellulose (NC) substrates
☑ compatible, ☒ not recommended

to-center spacing. A general "rule of thumb" would be to set a minimum spot spacing at about three times the spot radius (Fig. 5). There are a variety of dispenser technologies available (Table 2). For creation of higher density antibody arrays in plate wells, smaller spots are required. Piezo dispensers delivering pico-liter size droplets can produce 100s of spots/well with spot diameters of approximately 100 µm. Split pin printing covers similar spot densities depending upon the pin tip selected. However, while non-contact dispensers are suitable for most substrates, the use of split pins with nitrocellulose substrates is not recommended due to fouling or clogging of the slot, as well as the potential for damage to the substrate surface. Solenoid valve-driven dispensers will produce droplets in the nanoliter range, leading to larger diameter spots, thus reducing the spot density per well. For a standard well area, expect to achieve between 25 and 50 spots/well.

1.4 Preparation of Antibodies for Printing

For the development of multiplex immunoassays, the most important consideration is preservation of the antibody binding capacity. Many vendors provide their antibodies in a stabilization buffer. Usually, PBS buffer, pH 7.4 but also Borate buffer, pH 8.2 along with such additives as BSA, trehalose, glycerol, gelatin, and sodium azide are common. If azide or other preservatives are not added, then the preparations are sterile filtered. Some vendors do offer carrier-free preparations (lacking BSA or sodium azide) but at a higher cost.

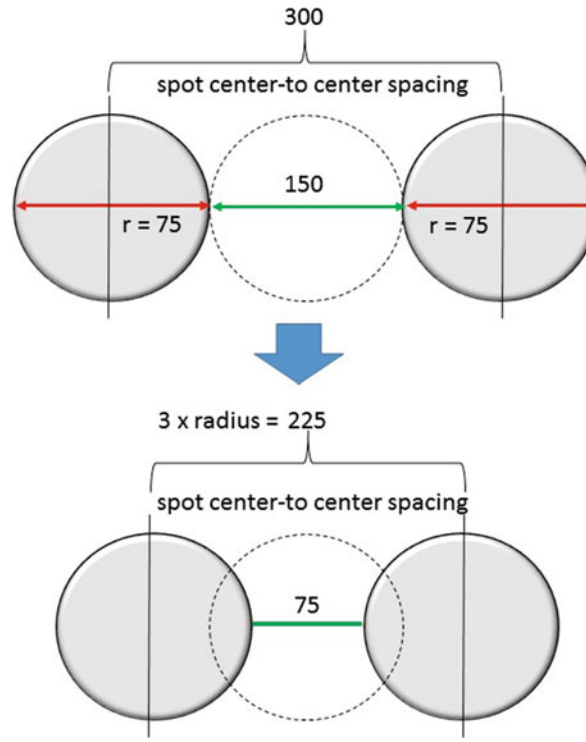

Fig. 5 Spot spacing. Setting the minimum spot center-to-center spacing to achieve maximum spot density in the array

It is important to know the buffer composition of the antibody product whether provided in liquid form or lyophilized. In the case of the solid form, carefully follow the vendor's directions for reconstitution, and avoid substituting buffers until the stability of the antibody has been determined. There may be incompatibilities leading to such conditions as salting out (precipitation) of the antibody, aggregation, or denaturation due to a pH shift. Be patient; lyophilized powders require time to rehydrate. Avoid vortexing or excessive, forceful agitation leading to foaming, which is an indicator of potential denaturation. Instead, allow the solution to stand for 30 min, and then gently swirl to completely dissolve the contents. The addition of BSA is especially problematic for printing because it may compete with the antibody for binding to the surface. Thus, the BSA needs to be removed from the antibody. An antibody cleanup kit is recommended. Once the antibody is free of BSA, it is a good idea to exchange the antibody into the desired print buffer. This can be accomplished by gel filtration or dialysis. These steps will also remove other additives such as trehalose or glycerol. If needed, the antibody can be "gently" concentrated using a molecular weight cutoff (MWCO) spin filter.

2 Materials

2.1 Immobilization by Physical Adsorption

1. Solid phase: polystyrene-based, flat bottom microtiter plates, high binding for proteins.
2. Capture antibodies: purified, carrier-free (no BSA), concentration ~1 mg/mL.
3. Antibody cleanup kit (*see* **Note 1**).
4. Print buffer: 0.01 M phosphate-buffered saline (PBS), pH 7.4.
5. Filtration device: 0.2 μm sterile filtration of buffers.
6. Dialyzer: buffer exchange of antibody solutions, Sigma-Aldrich PURD35010 (*see* **Note 2**).
7. Magnetic stirrer.
8. Graduated cylinder, beakers.
9. Micro BCA Protein Assay Kit.
10. Protein concentrator: 10 K MWCO spin filter.
11. Source plate: non-binding, 384-well (*see* **Note 3**).
12. Microarray dispenser: capable of droplet dispense from ~1 to 10 nL (*see* **Note 4**).
13. Microcentrifuge: 0–2000 rpm.
14. Pipettor: single-channel; multi-channel.
15. Pipet tips: 1–10 μL; 100–1000 μL capacity.
16. Plate reader or spectrophotometer (*see* **Note 5**).

2.2 Colorimetric Immunoassay Development

1. Blocking buffer: 1% BSA in PBS, pH 7.4.
2. Wash buffer: 0.05 M Tris-buffered saline, 0.05% Tween-20, pH 8.0, at 25 °C.
3. Antibody-HRP conjugate: labeled secondary (reporter) antibody paired with each capture antibody to be used in the multiplex sandwich ELISA.
4. TMB, insoluble formulation: ready-to-use precipitating enzyme (HRP) substrate (*see* **Note 6**).

2.3 Immobilization by Covalent Attachment

2.3.1 Activated Polypropylene Plate

1. CDT-activated polypropylene plate (QuantiScientifics).
2. Capture antibodies: purified, carrier-free (no BSA), concentration ~1 mg/mL.
3. Print buffer: 50 mM sodium borate, pH 9.3.
4. *N*-Lauroylsarcosine, sodium salt (NLS): anionic surfactant.
5. Distilled deionized (DDI) water: 18 MΩ or equivalent.
6. 50 mM sodium bicarbonate, 150 mM NaCl, pH 9.0 (Solution A): dissolve 4.2 g $NaHCO_3$ and 8.77 g NaCl into a final volume of 1 L with DDI water. The resulting solution is pH

~ 8. Adjust to pH 9.2 ± 0.2 with NaOH (1 M) and HCl (6 N). Sterile filter. Label and then store at 2–8 °C.

7. Blocker Casein (Solution B): 1% Hammersten Casein in 25 mM Tris-HCl, 150 mM NaCl, pH 7.4 with Kathon. Label and store at 2–8 °C.
8. Casein Quench Buffer: 0.1% casein in bicarbonate buffer; mix 90 parts Solution A with 90 parts Solution B, then sterile filter, label, and store at 2–8 °C.
9. PBST: 20× PBS with 0.05% (v/v) Tween® 20, pH 7.4.

2.3.2 Epoxy-Activated Glass Surface

1. Solid phase: epoxy-activated glass slide or plate.
2. Capture antibodies: purified, carrier-free (no BSA), concentration ~1 mg/mL.
3. Print buffer: phosphate-buffered saline (PBS), pH 7.4.
4. Casein Quench Buffer: **item 6** of Subheading 2.3.1.
5. PBST: **item 7** of Subheading 2.3.1.

2.4 Immobilization by Molecular Bridging

1. Polystyrene plate: flat bottom, high-binding, 96-well.
2. 50 mM MES buffer, pH 6—2-(*N*-Morpholino) ethanesulfonic acid hydrate: dissolve 1 g MES hydrate into 75 mL DDI water ~ pH 4.5, adjust pH to 6.0 with 2 N NaOH, final volume to 100 mL with DDI water, and sterile filter.
3. NHS: *N*-hydroxysuccinimide.
4. EDAC: 1-ethyl-3-(3-dimethylaminopropyl)carbodiimide hydrochloride.
5. BSA: bovine albumin, Fraction V.
6. 1 M sodium phosphate dibasic, pH 7.5.
7. PBS.
8. Amino-oligonucleotides: 5′ or 3′ amino-oligonucleotide (*see* **Note 23**).
9. Micro BCA Protein Assay Kit.
10. Pipettor: single- or multi-channel.
11. Pipet tips: 20–200 µL capacity.
12. Plate reader.
13. Platform shaker (gyratory).
14. Magnetic stirrer.
15. Centrifuge.
16. Protein concentrator: Pierce 88513, 10 K MWCO spin filter.
17. BSA coupling solution: weigh out 15.4 mg BSA (V), and dissolve in ~1.5 mL MES buffer, pH 6 to achieve ~10 mg/mL.

18. EDAC stock solution: weigh out ~1–2 mg EDAC, dissolve in MES buffer, pH 6, and determine volume to achieve 0.4 mg per 10 mg BSA (2 mM).
19. NHS stock solution: weigh out ~2–4 mg NHS, dissolve in MES buffer, pH 6, and determine volume to achieve, 0.6 mg per 10 mg BSA (5 mM).

2.5 Fluorescent Multiplex ELISA/ Fluorescent Immunoassay (FIA)

1. Oligo-BSA Antibody Array Plate.
2. Wash buffer: TBST (1×).
3. PBS-BSA buffer: 1% BSA in PBS, pH 7.4.
4. Streptavidin-alkaline phosphatase: ~3 mg/mL in 10 mM Tris-HCl, 0.15 M NaCl, 0.1 mM $ZnCl_2$, 0.1 mM $MgCl_2$, pH 8.0, 50% glycerol; 1:10,000 (v/v) yields ~0.3 μg/mL working stock.
5. Enzyme substrate: ELF97 precipitating substrate; Lumi-Phos WB or Lumi-Phos 530.
6. Biotinylated antibody: antigen-specific, matched to capture antibody.
7. Streptavidin-dye: SureLight 488.

3 Methods

3.1 Physical Adsorption

This protocol is for the preparation of antibody arrays by direct adsorption within the wells of polystyrene plates. Plate manufacturers modify the polystyrene surface features in order to promote efficient binding of antibodies. Generally, a high-binding plate is used for immunoassays. Here, the capture antibody is prepared in a print buffer and dispensed to the surface (well bottom) using a microarray dispenser. After drying of the protein droplets, a blocking agent is added to the wells to reduce non-specific binding during assay development.

3.1.1 Printing of the Capture Antibody Array Plate

It is highly recommended that the user wear gloves during these procedures to avoid contamination issues and accumulation of debris on surfaces.

1. Prepare the antibodies for printing at 0.2–1 mg/mL in PBS, pH 7 (*see* **Note 7**).
2. Place 70 μL of each antibody solution in an assigned well of a 384-well source plate.
3. Put a lid on the plate.
4. Spin the plate at 2000 rpm (400 × *g*) for 5 min to remove air.
5. Set up the microarray dispenser for printing. Critical conditions are relative humidity (RH), temperature, and dispenser cleaning. Set RH ~ 60% and Temp ~ 25 °C (*see* **Note 8**).

6. Place the source plate on the deck of the microarray dispenser.
7. Carefully position a clean, flat bottom, polystyrene high-binding plate to be used for creation of the well arrays on the deck.
8. Conduct the print run cycles.
9. Keep the printed plate on the print deck under humidity for 1 h or transfer to a humidity chamber for the incubation period. Be careful not to jar the plate during transfer.
10. Allow the printed droplets on the plate to completely dry down in a clean environment.
11. Block the plate wells in 1% BSA-PBS, pH 7.4 or other suitable blocking agent (*see* **Note 9**). Carefully dispense 100 µL of the blocking agent into wells. Do not touch the bottom surface in order to prevent damage to the array.
12. Allow the plate to stand at room temperature for 1 h. Next, remove the liquid by rapid inversion over a sink to expel. Carefully rinse the wells with 100 µL DDI water. Repeat using the inversion method.
13. Air-dry the plate, and then store in a moisture barrier bag with desiccant under refrigeration.

3.1.2 Colorimetric Immunoassay Development

1. Allow the plate to reach room temperature. Rehydrate the wells of the plate to be used in the assay with 100 µL TBST wash buffer, 5 min. Remove solution by rapid inversion prior to use.
2. Prepare samples: dilute plasma 1:100 (v/v) in blocking buffer and gently mix. Avoid foaming (*see* **Note 10**).
3. Deliver 100 µL to each well and set aside. Incubate for 1 h at ambient temperature (22–25 °C) without mixing or shaking (*see* **Note 11**).
4. Remove liquid by rapid inversion of the strip over a sink or waste container.
5. Deliver 100 µL wash buffer (1×) to each well. Remove solution. Repeat rinse two times, and then let it soak for 5 min. Following the soak, rinse additionally for three times. Do not allow the wells to dry out. After the final rinse, blot the strip using lint-free towels.
6. Prepare fresh enzyme conjugate: dilute stock 1:1000 (v/v) in blocking buffer (*see* **Note 12**).
7. Deliver 100 µL to each well and set aside. Incubate for 30 min. No mixing or shaking.
8. Remove liquid and rinse as previously described.
9. Prepare substrate: bring TMB solution to room temperature prior to use. Deliver 100 µL to each well and set aside. Incubate for 15 min. No mixing or shaking. Do not discard solution.

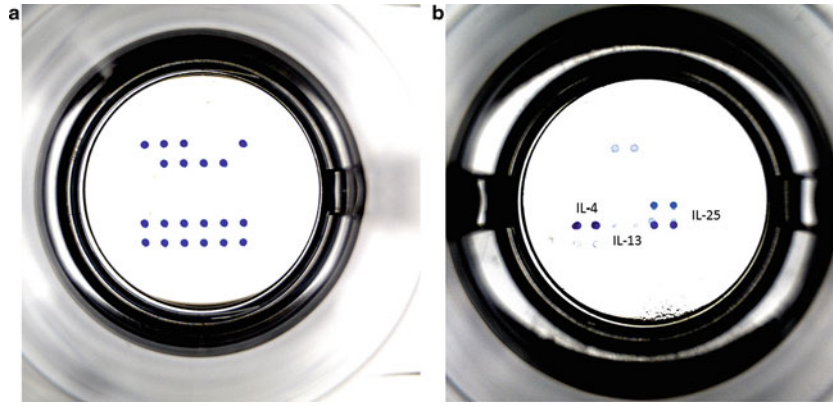

Fig. 6 Developed multiplex antibody array well. (**a**) Antibody array printed with capture antibodies (0.5 mg/mL PBS, pH 7.4) at 900 pL per spot (~45 ng) into a high-binding polystyrene plate (sciFLEXPLATE, Type 2) using an S3 sciFLEXARRAYER. Signal was developed using biotinylated anti-goat IgG (1 μg/mL) and streptavidin-HRP/TMB according to Subheading 3.1.2. (**b**) An array well with three cytokines doped into diluted plasma as the sample. The assay was performed by multiplex sandwich ELISA for IL-4, IL-13, and IL-25 based upon a biotinylated anti-cytokine secondary antibody pool. Signal developed as in (**a**) using a sciREADER CL2. Relative signal strength IL-4 > IL-25 ≫ IL-13. Possible cross-reactivity with other proteins detected

10. Read the strips using a colorimetric imaging reader (Fig. 6; *see* **Note 13**).

3.1.3 Imaging and Data Analysis

For the analysis of plate-based antibody array immunoassays, a plate well imaging system is required with at least the ability to obtain raw pixel intensity values for the region of interest (ROI). For example, the ROI could be a collection of spots (array format) within a single well such that individual well images are processed separately and then stitched together to obtain all the data from the 96 wells of the plate; conversely, a single image of the developed plate could be captured and the individual wells treated as sub-arrays for the purpose of analysis. Both approaches are valid. The imaging device could be a digital microscope, phone camera, or a commercial imaging reader. Image files (.tif/.tiff; jpeg; bmp) can be exported to stand-alone image analysis programs such as ImageJ (*see* **Note 14**).

3.1.4 ImageJ Analysis of Well-Based Antibody Arrays

1. Capture an image of the desired ROI using an imaging system (*see* **Note 15**).
2. Convert the image to .jpeg or other supported file type.
3. Import into ImageJ.
4. Locate the image under the **File tab**.
5. Move over to the **Image tab**; convert to desired **Type**, e.g., 8-bit (grayscale).
6. Under the **Edit tab**, select **Invert** *depending upon if analyzing colorimetric or fluorescent signal* (*see* **Note 16**).

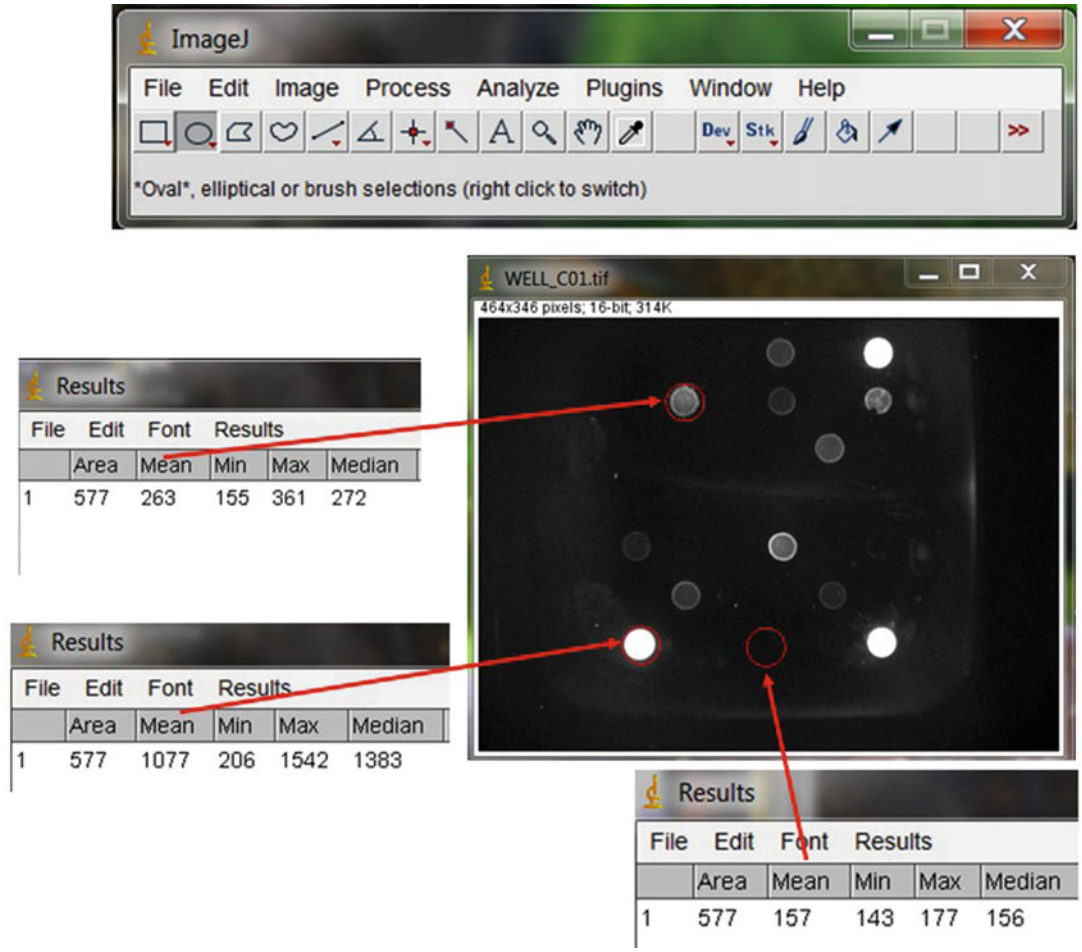

Fig. 7 ImageJ analysis of array in well. Image of an array within a single well being analyzed. Measurement results are shown for different spots

7. Save the new file, as, e.g., 8-bit invert .jpeg or other descriptor of choice (Fig. 7).
8. Under the **Analyze tab**, first select **Clear Results** and then **Set Measurements** (select parameters).
9. Highlight the "oval" icon to measure spots with the parameters selected above
10. Drag oval over desired spot to measure.
11. Select under the Analyze tab **Measure** (*see* **Note 17**).
12. The **Results** box will appear on the screen. This can be saved as an Excel worksheet (*see* Fig. 8).
13. Once the pixel intensity data has been placed into an Excel worksheet, then statistical analysis, curve fitting of standards, and estimation of sample from the extrapolation can be achieved. For multiplex immunoassay quantification, macros can be run in Excel such as AssayFit (IVDtools, Inc.) (*see* Fig. 9).

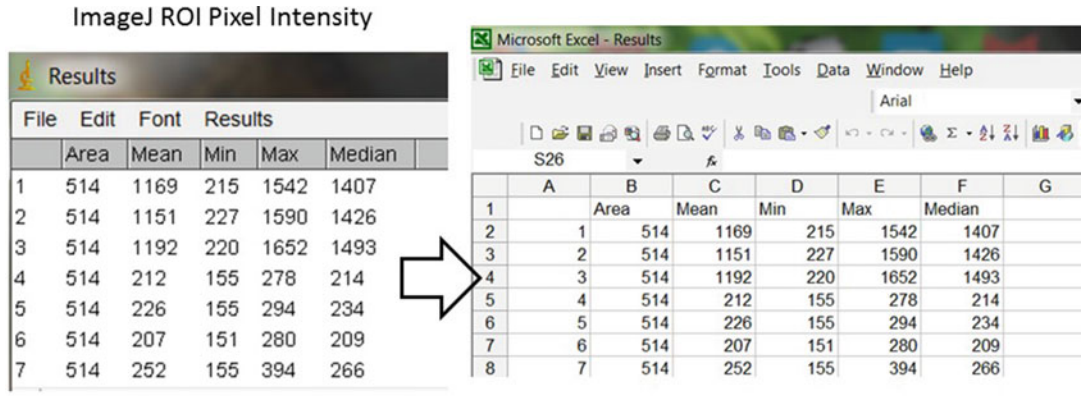

Fig. 8 Export of ImageJ results into Excel

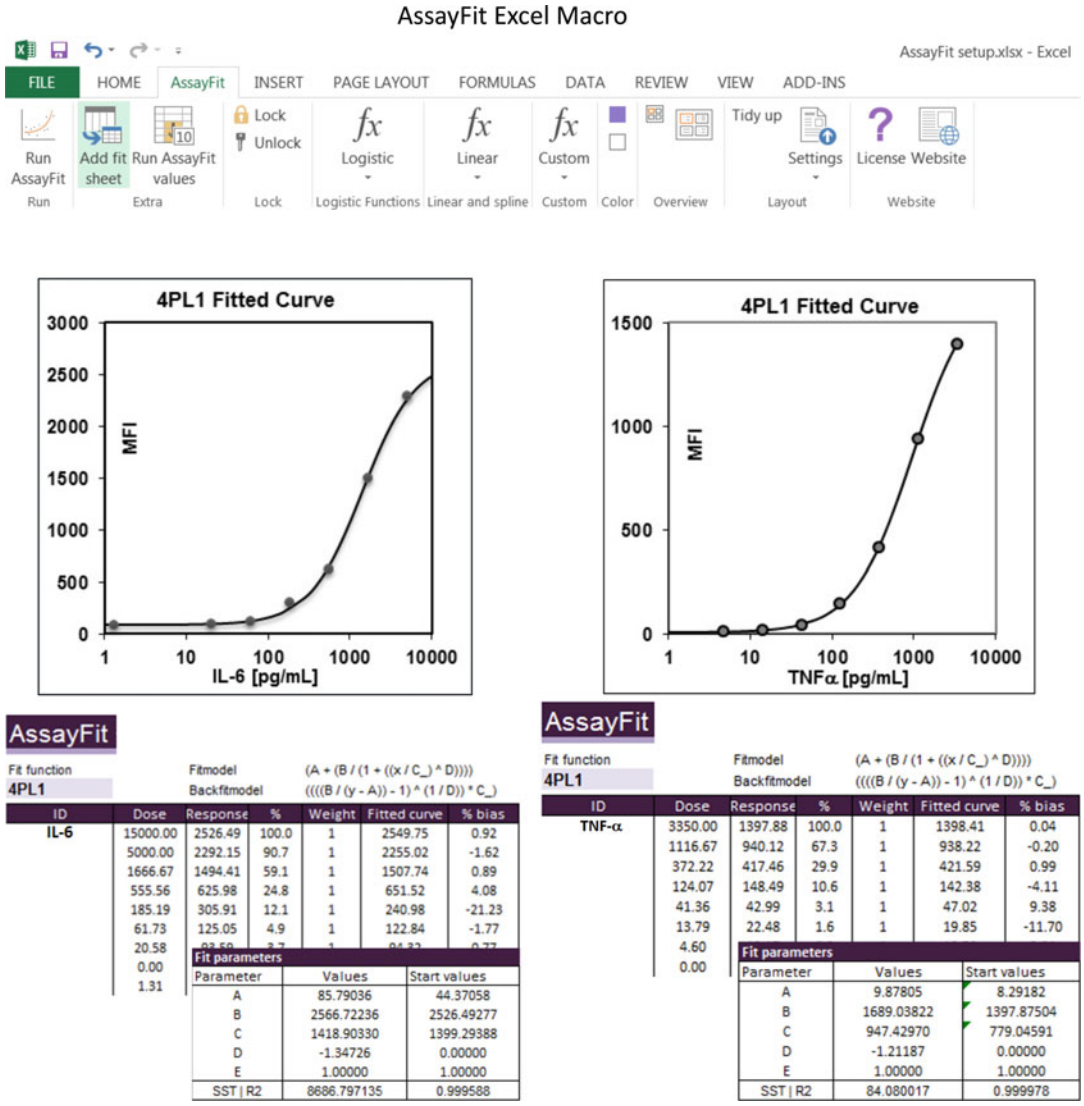

Fig. 9 Analysis of ImageJ Excel data using AssayFit. The pixel intensity results imported from ImageJ are pasted into the AssayFit worksheet macro and the standard curve fit (4PL) created for analytes IL-6 and TNF-α

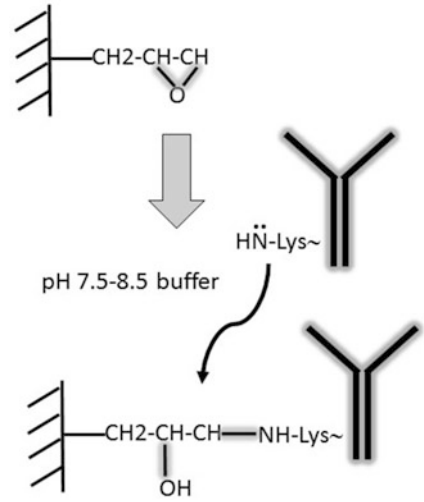

Fig. 10 Epoxide reaction. Covalent coupling of an antibody to a solid support by opening of the surface epoxide ring via lysine amino acid residues of the antibody

3.2 Covalent Coupling

The covalent immobilization of antibodies to activated surfaces may be required for higher sensitivity immunoassays (Fig. 10). In this protocol, surfaces that have been modified with amine reactive groups are employed to tether antibodies to that surface. For example, epoxy-activated glass (2D surface) and glass with an epoxy hydrogel layer (3D surface) are popular slide formats. These can be subsequently converted for well-based immunoassays using a well overlay superstructure.

Plastic plates have also been surface modified for covalent attachment of proteins either by a chemical means or the addition of a reactive coating such as a hydrogel. A very stable surface chemistry is provided by the conversion of amine-modified plastics with 1,1′-carbonyl-di-(1,2,4-triazole). The resulting triazolide is highly reactive with the lysine side groups of antibodies [13] (Fig. 11).

3.2.1 Covalent Cross-Linking of Antibodies to Activated Polypropylene

1. Purified antibodies are prepared in 50 mM sodium borate, pH 9.3 containing NLS surfactant (0.00002%) at 0.25–1 mg/mL protein (*see* **Note 18**).
2. Place 70 μL of each antibody solution in a non-binding 384-well source plate for printing.
3. Antibodies are arrayed in the bottom of the CDT-activated polypropylene plate essentially as described in **steps 3–10** of Subheading 3.1.1.
4. Following air-drying, inactivate any residual CDT by adding 200 μL of Casein Quench Buffer (CQB) to each well. The CQB must be at room temperature prior to dispensing (*see* **Note 19**).

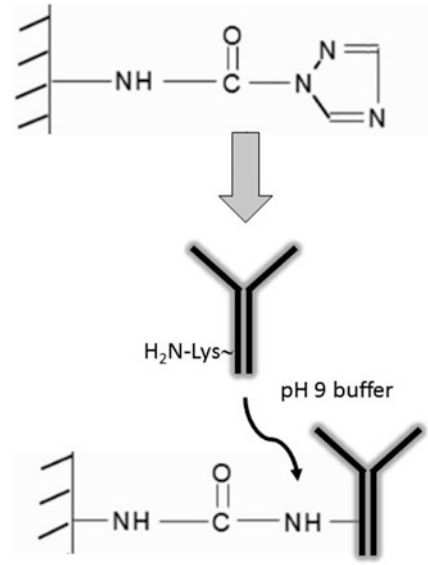

Fig. 11 CDT reaction. Displacement of the triazole leaving group by the antibody's lysine residue resulting in covalent coupling of the antibody to the solid support

5. Allow the plate to stand for 1 h with CQB.
6. Remove the CQB by forcibly inverting the plate over a sink.
7. Tap the plate on an absorbent wipe.
8. Fill wells with DDI water and soak for 5 min.
9. Remove water and rinse the wells two more times with DDI water without a soak.
10. After the completion of the water rinse, remove any residual water from the plates by forcibly tapping both sides of each plate onto an absorbent wipe.
11. Allow the plate to air-dry.
12. Package and seal in a moisture barrier bag with desiccant.

3.2.2 Covalent Attachment of Antibodies onto Epoxy Glass Surfaces

1. Purified antibodies are prepared in PBS, pH 7.5–8.5 at 0.05–0.2 mg/mL protein (*see* **Note 20**).
2. Place 70 μL each antibody solution in a non-binding 384-well source plate for printing.
3. Antibodies are arrayed in the bottom of the epoxy-activated glass plate (**steps 3–10** in Subheading 3.1.1).
4. Following air-drying, inactivate residual epoxy groups in CQB as previously described in **steps 4–10** of Subheading 3.2.1 (*see* **Note 21**).
5. Remove the casein solution, and rinse the wells with 100 μL PBST.

6. Discard the PBST rinse buffer, and repeat **step 5**, twice more.
7. Rinse the plate in DDI water.
8. Allow to air-dry, and then package in a moisture barrier pouch with desiccant. Store under refrigeration at 2–8 °C.

3.3 Molecular Bridging

The immobilization of antibodies to planar surfaces via intermediary scaffolding was first explored in the 1990s. Cantor's group at Boston University described oligonucleotide-directed self-assembly of proteins [14]. First, biotinylated oligo was attached to the wells of a polystyrene plate coated with streptavidin. Antibodies attached to complementary oligos were applied under hybridization conditions to achieve an antibody array. Meyer et al. [15] described the main advantages of the DNA-directed immobilization (DDI) approach, that being a "chemically mild and highly efficient method for generating (micro) structured patterns of proteins on surfaces."

A similar approach to antibody immobilization via oligonucleotide tethering is offered by QuantiScientifics (Orange, CA) under the $A^{2®}$ trademark. The A^2 technology developed at Beckman Coulter Inc. [16, 17] utilizes capture oligonucleotides covalently linked to the wells of a 96-well polypropylene plate. A detailed description along with protocols for use has been described in an earlier volume of Springer Protocols [18]. While polypropylene offers a chemically resilient platform, the attachment of short oligonucleotides to the more commonly used polystyrene plate is problematic, requiring photo cross-linking or the preparation of reactive polymer coatings. Alternatively, the use of bridging molecules that bind strongly to polystyrene might provide a convenient scaffold for presentation of capture oligonucleotides. For instance, milk proteins such as casein as well as serum albumin can be effectively used as blocking agents to counter non-specific binding of macromolecules on a variety of surfaces including plastic and glass. Elaine Tronic in her dissertation work [19] determined that bovine serum albumin (BSA) could be adsorbed on polystyrene to a level fourfold higher than to that of glass substrate, at about 400 ng/cm^2. Moreover, the adsorbed layer appeared to be very stable. The following protocols exploit these findings to migrate the A^2 format over to other substrates for use in multiplex immunoassays [20]. First, carboxyl groups on BSA are converted to an activated ester form using 1-ethyl-3-(3-dimethylaminopropyl) carbodiimide with *N*-hydroxysuccinimide (EDAC + NHS) chemistry. An amino-modified oligonucleotide is added to the esterified BSA and subsequently covalently coupled by displacement of the ester (Fig. 12). The resulting Oligo-BSA conjugates are immobilized (via dispensing) to the polystyrene surface of the plate as arrays in the bottom of the wells. Subsequently, the antibody array is formed by self-assembly of the complementary oligo-antibody conjugates during hybridization (Fig. 13).

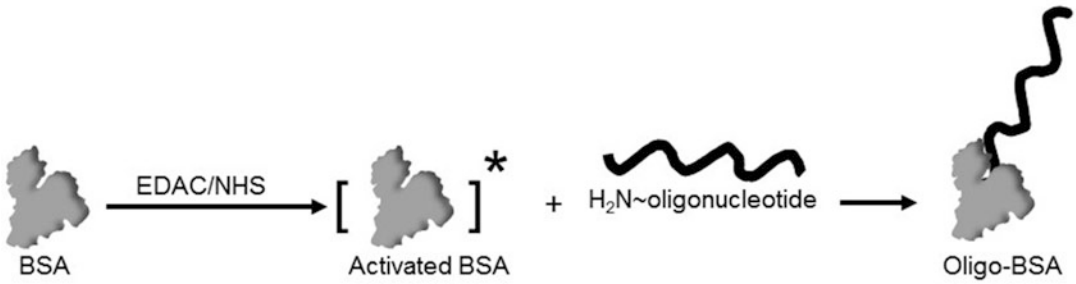

Fig. 12 Coupling of capture oligonucleotide to BSA. Bovine serum albumin carboxyl groups are converted to NHS esters to form activated BSA. The BSA-NHS ester reacts with amine-terminated oligonucleotides, resulting in the formation of oligo-modified BSA

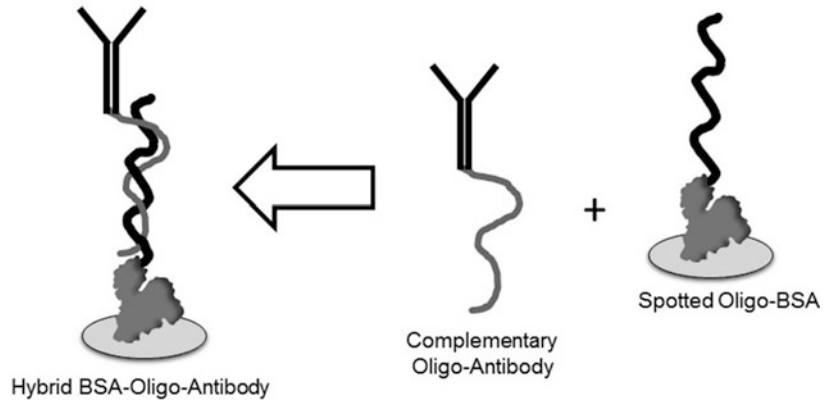

Fig. 13 Assembly of the BSA-oligo-antibody array. Capture oligos linked to BSA are printed in an array format in the wells of polystyrene microplates. Complementary oligos with capture antibodies are pooled and applied to the array under hybridization conditions to form the antibody array

3.3.1 Preparation of Oligonucleotide-BSA Conjugates

1. Prepare BSA coupling solution at ~10 mg/mL in MES buffer: determine the protein concentration of the BSA in MES buffer using a micro-BCA method, and then dilute to desired concentration in MES buffer (*see* **Note 22**).
2. Prepare EDAC stock solution, 2 mM in MES buffer.
3. Prepare NHS stock solution, 5 mM in MES buffer.
4. Add the EDAC and NHS stock solutions to the BSA solution immediately! Incubate with shaking for 15 min.
5. Prepare the Amino-Oligo at 100 OD_{260}/mL DDI water. 5 OD = 50 μL (*see* **Note 23**).
6. Add 50 μL of the Amino-Oligo to the BSA solution reaction (*see* **step 5**).
7. Add 100 μL 1.0 M sodium phosphate buffer, pH 7.5 to shift the pH 6 → pH 7 (*see* **Note 24**).

8. Incubate with shaking or tumbling for 2 h at room temperature.
9. Dialyze using MWCO filters (3.5 K) against 3 L of PBS buffer, pH 7.4 overnight (15–20 h) with at least 1 buffer change of 1 L PBS buffer prior to recovery.
10. Determine the protein concentration of dialysate using the micro-BCA method.
11. Adjust the concentration of the conjugate as needed.
12. Store under refrigeration at 2–8 °C.

3.3.2 Immobilization of the Oligo-BSA-Antibody onto Polystyrene Plates

1. The Oligo-BSA conjugate concentration is adjusted to ~1 mg/mL protein with a PBS buffer.
2. Conjugates are placed in a non-binding 384-well source plate for printing.
3. Follow **steps 3–10** in Subheading 3.1.1.
4. Block in 1% BSA-PBS, 100 μL per well (*see* **Note 25**).
5. Rinse two times with 200 μL TBST per well.
6. Air-dry at least 4 h to overnight at room temperature.
7. Prepare the hybridization cocktail comprising of the complementary oligo-antibody in hybridization buffer (*see* **Note 26**).
8. Apply 50 μL per well.
9. Incubate for 1 h with shaking.
10. Rinse each well with 200 μL hybridization buffer, followed by two rinses using TBST.
11. Allow to air-dry, then seal in a pouch with desiccant, and store under refrigeration.

3.4 Multiplex Immunoassays

This protocol is for the performance of an immunoassay using the Oligo-BSA Antibody Array Plate. The previously prepared oligo-antibody conjugates are pooled and applied to the arrayed Oligo-BSA capture probes under hybridization conditions, resulting in the self-assembly of a capture antibody array in each well of the 96-well plate [18, 20].

3.4.1 Oligo-BSA Antibody Array Fluorescent Multiplex ELISA

1. Bring the Oligo-BSA Antibody Array plate to room temperature prior to removing from its pouch.
2. Rehydrate wells in 100 μL of wash buffer (1×). Allow to stand for 5–10 min.
3. Remove the wash buffer, but do not allow the plate to dry out.
4. Tap the plate upside down onto several layers of clean towels to remove residual buffer.

5. Prepare samples or antigen standards in PBS-BSA buffer, and deliver 100 µL to each well.
6. Incubate for 1 h at room temperature with shaking.
7. Remove solution and rinse with wash buffer.
8. Deliver 100 µL of streptavidin-AP prepared in PBS-BSA to each well (*see* **Note 27**).
9. Incubate for 30 min at room temperature with shaking.
10. Remove solution and rinse in wash buffer.
11. Bring the enzyme substrate to room temperature, and then deliver 100 µL per well.
12. Cover the plate with foil, or place in the dark.
13. Incubate for 30 min at room temperature **without** shaking (*see* **Note 28**).
14. Carefully remove most of the solution from wells, but do not rinse.
15. Wipe off the bottom of the plate with ethanol using a scratch-free and lint-free cloth.
16. Read the semi-wet plate on a fluorescent imaging system (Fig. 14) (*see* **Note 29**).

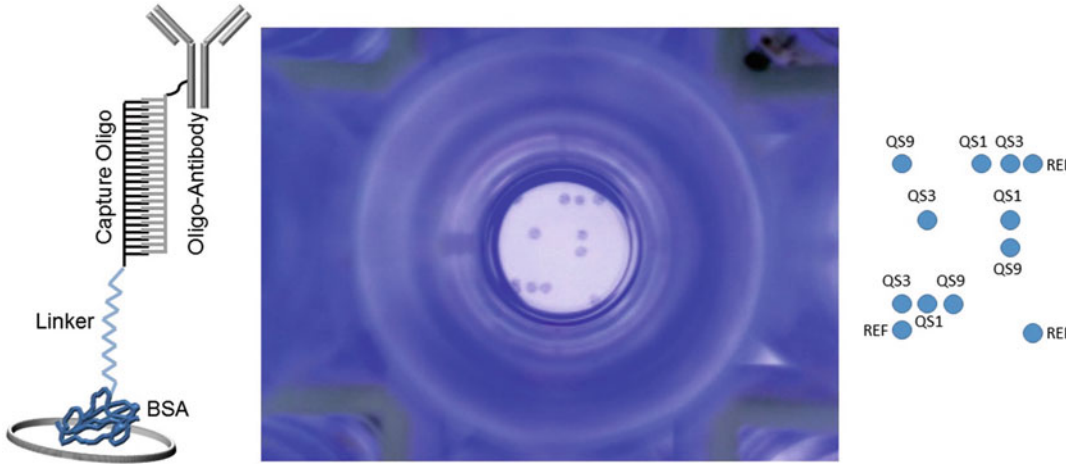

Fig. 14 Digital microscope fluorescent imaging of the oligo-BSA antibody array. An array of capture oligo-BSA (QS1, QS3, QS9 from QuantiScientifics) and a biotinylated reference oligo (REF) are printed. QS complementary oligo-antibodies are pooled and hybridized in the well to form the antibody array. In this case, a rabbit antibody was attached to all of the complementary oligos. A biotinylated anti-rabbit antibody was applied and signal developed with streptavidin-alkaline phosphatase using a Lumi-Phos fluorescent precipitating substrate. Images of the well were captured under blue LED light using a digital microscope (Dino-Lite Edge Digital Microscope, AM4115T-GFBW)

3.4.2 Oligo-BSA Antibody Array FIA

1. Follow **steps 1–7** of Subheading 3.4.1.
2. Prepare a pool of biotinylated secondary antibodies, and apply 100 μL to each well.
3. Incubate for 30 min with shaking.
4. Remove solution and rinse in wash buffer.
5. Prepare streptavidin-488 at 1:1000 (v/v), and apply 100 μL to each well.
6. Incubate for 30 min with shaking.
7. Remove solution, and rinse in wash buffer.
8. Wipe off the bottom of the plate with ethanol using a scratch-free and lint-free cloth.
9. Read the semi-wet plate on a fluorescent imaging system (*see* **Note 29**).

4 Notes

1. Stabilization of antibodies is required to preserve binding activity. BSA is often added in excess. The problem arises during antibody immobilization or conjugation steps. When BSA is present in significant molar excess to that of antibody, it effectively outcompetes or diminishes the antibody reaction (e.g., for adsorption or covalent linking to a surface). Antibody spin column-based cleanup kits are available from several vendors: Pierce 44600-Melon IgG Purification Support; Abcam-ab102778; and Expedeon-AbPure Kit.
2. Commercial antibodies are supplied in a number of different buffers with stabilizing agents and other additives. As a consequence, there may be differences in spot morphologies, solid-phase coupling efficiency, and antibody-antigen binding activity among several capture antibodies used in the multiplex. It is recommended that the antibodies be prepared in the same print buffer composition. This can be accomplished by dialysis of the antibody solution against the print buffer resulting in a buffer exchange after removal of any BSA. If the antibodies are supplied in lyophilized form, add the PBS directly to the vial, and allow to hydrate at least 30 min at room temperature or overnight with refrigeration.
3. Proteins (also nucleic acids) will bind to most microtiter plates, especially polystyrene plates that are commonly used in immunoassays. These should not be used as source plates for printing antibodies. Instead, use plates that are certified as non-binding surfaces (NBS) such as available from Greiner Bio-One 781901 or the Corning NBS plate. These are surface-treated

polystyrene flat bottom plates. Polypropylene plates are also available and generally considered non-binding. The 384-well plate is preferred since there is less tendency for surface evaporation, and it uses much less volume than a 96-well plate while providing fourfold greater capacity for storage of samples and probes. If the source plate has been previously sealed and stored under refrigeration, it is advisable first to allow the plate to reach room temperature. Carefully remove the seal and replace with a clean lid. Centrifugation of a sealed, refrigerated plate may cause a vacuum to develop in the wells. This can lead to suction of the well contents out of the plate as the seal is removed leading to potential cross contamination.

4. The choice of available microarrayers or automated low volume dispensers is limited. As discussed in Subheading 1.3 (*see* Table 2), dispenser selection is linked to the desired array density, which, in turn, is largely predicated by the dispensed volume (spot diameter) and spot center-to-center spacing precision that can be achieved. The following are commercial manufacturers of low volume dispensing equipment that offer high-precision dispensing: Scienion AG, Berlin, Germany (www.scienion.com); BioDot, Irvine, CA (www.biodot.com); ArrayJet, United Kingdom (www.arrayjet.co.uk); GeSiM mbH, Germany (www.gesim.de); and M2-Automation, Berlin, Germany (www.m2-automation.com).
5. There is often confusion over the need for a plate reader. If one is performing a protein determination assay with a colorimetric endpoint, then a conventional microplate reader or spectrophotometer can be used. However, for quantifying well-based microarrays, an imaging plate reader is required that is capable of focusing on the well bottom (to view the microarray) either from the top or the bottom of the well. Similarly, for a fluorescent assay, a fluorescent signal imaging reader is needed (*see* **Notes 13** and **15**).
6. For the development of the HRP signal, a TMB substrate is widely used with immunoassays. TMB comes in either soluble or insoluble forms. For microarrays, the insoluble TMB is used for development since it forms a stable, highly colored precipitant on spots: Thermo Scientific, 1-Step Ultra TMB-Blotting Solution #37574, Moss, Inc. (Pasadena, MD: www.MossBio.com), offers TMBX formulated for microarrays and immunoblotting.
7. Since different antibodies may adsorb differently leading to variation in spot morphologies and antigen binding reactivity on a particular surface, the antibody print concentration may need to be adjusted for optimal performance.

8. The relative humidity (RH) needs to be set in the range of about 50–70% at 25 °C ± 3 °C to avoid evaporation of the print buffer from the dispenser and leaving buffer residue and adsorbed proteins. If not checked, there is a risk in clogging of the tip which results in no spots printed or, if partially obstructed, a divergence of the droplet trajectory and/or dispensed volume. This leads to erratic performance such as spot alignment, morphology issues, and satellites. RH also reduces the buildup of static electricity within the system. Avoid higher RH which can lead to bulk wetting out of the printed surfaces, thereby coalescing and/or enlarging the print droplets.
9. While BSA is widely used as a blocking agent to reduce non-specific binding (NSB), there are other suitable blocking agents available. These include both protein and non-protein (polymer) blockers. However, certain blocking reagents were designed to be used for membranes (Western blots) or coated nitrocellulose slides and may not be applicable for use with plastic microplates. Other blockers, albeit, identified as stabilizing agents are used to stabilize antibodies on coated microplates or preserve enzymatic activity. These may be suitable as NSB blockers: G-Biosciences (www.gbiosciences.com) and Surmodics (www.surmodics.com).
10. Plasma is used here as an example of a complex sample matrix. The extent of dilution depends upon the assay sensitivity range and analyte levels that may be present in the sample. Due to the viscosity of plasma, dilution is recommended to at least ½ (v/v) in a suitable diluent with buffering capacity that maintains solubility and reduces NSB. Avoid excessive mixing action that causes foaming to prevent protein denaturation.
11. The no shake protocol is used to prevent sluffing or dissolution of the developed TMB precipitant from the spot. This can occur when excessive amounts of enzyme conjugate are applied or too high a loading of the capture antibody has been spotted.
12. The dilution of the enzyme conjugate (HRP-antibody) used for detection is dependent upon the enzyme's specific activity. This information is usually available from the vendor who may recommend an appropriate range of dilutions for ELISA. In this case, 1/1000 dilution was based upon achieving an enzyme concentration of about 1 μg/mL which was found to be sufficient for signal development. It is advisable to prepare fresh working solutions and discard them after use.
13. There is a limited selection of colorimetric imaging readers. The images shown in Fig. 6 were captured using the sciREADER CL2 (www.scienion.com). Other colorimetric readers designed for imaging microplates include SensoSpot Colorimetry (www.sensovation.com) and Array Reader C-Series (www.biovendor-instruments.com).

14. ImageJ is a public domain image software program that can be downloaded for free and run on most computer platforms. It supports the following file types: .tiff, .gif, .jpeg, .bmp, as well as others. https://imagej.nih.gov/ij/download.html.
15. Other imaging readers with exportable ImageJ supported image files including digital microscopes, camera phones, as well as fluorescent and chemiluminescent scanners may be used.
16. ImageJ allows various transformations such as image signal inversion and conversion to RGB and grayscale. In doing so, it is advisable to set the intensity scale such that the background is minimal and signal is a positive value. For example, 8-bit grayscale for intensity measurement is set to background min = 0 and signal max = 254.
17. Under the **Analyze** pull down tab, first select **Set Measurements** (contains the measurement parameters), then select **Clear Results** (removes previous data), and finally select **Measure** which will record the new data set in **Results**.
18. Coupling antibodies to CDT-activated surfaces is accelerated under basic pH conditions. Depending upon the wetting properties of the plastic surface, the addition of a surfactant such as NLS may be necessary to achieve the desired spot diameter and morphology. In using surfactants remember to use concentrations below their critical micelle concentration (CMC).
19. CQB efficiently neutralizes the reactive surface with the added benefit of blocking.
20. Epoxide coupling reaction conditions for immobilization of proteins are generally conducted under slightly basic conditions where they are more stable.
21. Capping of epoxides can be accomplished using 0.1 M ethanolamine, pH 9. A blocking step would be required prior to performing the immunoassay.
22. Further optimization of the Oligo/BSA molar ratio to achieve a desired hybridization efficiency may be required. This can be accomplished by varying the concentration of the BSA.
23. The OD260 input can be varied as well, to scale the reaction or alter the molar ratio.
24. It is recommended to determine pH shift conditions in advance.
25. Following the dispensing of the Oligo-BSA conjugates, it is important to fully dry the arrayed wells prior to performing the blocking step.

26. The hybridization buffer needs to be chemically compatible with the polystyrene surface while providing stability for the oligo-antibody conjugate. SSC (saline-sodium citrate buffer) or SSPE (saline-sodium phosphate, EDTA buffer) work well.
27. Depending upon enzyme specificity, the streptavidin-alkaline phosphate concentration needs to be titrated in advance to determine optimal signal response.
28. Signal begins to develop within a few minutes of reagent addition. Incubation time for signal can be adjusted to achieve the desired level.
29. Various fluorescent imaging systems are available, but the instrumentation model selection will be dependent upon the choice of the fluorescent signaling reporter excitation/emission wavelengths:
    (a) ELF97—Ex 345/Em 530.
    (b) Lumi-Phos WB—Ex 480/Em 535.
    (c) SureLight 488—Em 496/Ex 517.

References

1. Soper CB (2005) Editorial—An open letter to our readers on the use of antibodies. J Comp Neurol 493:477–478
2. Couchman JR (2009) Commercial antibodies: the good, bad, and really ugly. J Histochem Cytochem 57(1):7–8
3. Ascoli CA, Birabaharan J (2015) The antibody dilemma: shortcuts taken by antibody manufacturers and end-users have led to a reproducibility crisis. Genet Eng Biotechnol 35(14):8–9
4. Weller MG (2016) Quality issues of research antibodies. Anal Chem Insights 11:21–27. https://doi.org/10.4137/ACI.S31614
5. Uhlen M, Bandrowski A, Carr S et al (2016) A proposal for validation of antibodies. Nat Methods 13:823–827
6. Chun KY (2017) Biotin interference in diagnostic tests. Clin Chem 63(2):619–620
7. Colon PJ, Greene DN (2018) Biotin interference in clinical immunoassays. J Appl Lab Med 2(6):941–951
8. Gerdtsson AS, Dexlin-Mellby L, Delfani P et al (2016) Evaluation of solid supports for slide- and well-based recombinant antibody microarray. Microarrays 5(16):1–17. https://doi.org/10.3390/microarrays5020016
9. Matson RS, Little MC (1988) Strategy for the immobilization of monoclonal antibodies on solid-phase supports. J Chromatogr 458:67–77
10. Juncker D, Bergeron S, Laforte V, Li H (2014) Cross-reactivity in antibody microarrays and multiplexed sandwich assays: shedding light on the dark side of multiplexing. Curr Opin Chem Biol 18:29–37
11. Martinsky T (2009) Chapter 10: Printing methods. In: Matson RS (ed) Microarray methods & protocols. CRC Press, Boca Raton, FL, pp 157–186
12. Matson RS (2013) Chapter 4: Arraying processes. In: Matson RS (ed) Applying genomic and proteomic microarray technology in drug discover, 2nd edn. CRC Press, Baco Raton, FL, pp 103–132
13. Matson RS (2014) Oligonucleotide tethering of proteins for multiplex assay migration to mobile applications. In: AACC emerging diagnostics conference, San Jose, CA
14. Niemeyer CM, Sano T, Smith CL, Cantor CR (1994) Oligonucleotide-directed self-assembly of proteins: semisynthetic DNA-streptavidin hybrid molecules as connectors for the generation of macroscopic arrays and the construction of supramolecular bioconjugates. Nucleic Acids Res 22:5530–5539
15. Meyer R, Giselbrecht S, Rapp BE, Hirtz M, Niemeyer CM (2014) Advances in DNA-directed immobilization. Curr Opin Chem Biol 18:8–15

16. Lu N, Boyer D, Moheb S et al (2005) Multiplex measurement of human cytokine levels in serum samples using the A2™ multiplex system. In: Presented at the 96th annual meeting of the American Association for Cancer Research, 17 Apr 2005, Anaheim, CA
17. Robbins MA, Li M, Leung I, Li H et al (2006) Stable expression of shRNAs in human CD34+ progenitor cells can avoid induction of interferon responses to siRNAs in vitro. Nat Biotechnol 24:566–571
18. Matson RS (2015) Chapter 18: Multiplex ELISA using oligonucleotide tethered antibodies. In: Hnasko R (ed) ELISA methods and protocols, Springer protocols. Humana Press, New York
19. Tronic E (2012) Surface analysis of adsorbed proteins: a multi-technique approach to characterize surface structure. PhD dissertation, University of Washington, Pub. No. 3552866. http://search.proquest.com/docview/1313207756
20. Matson RS (2017) Design and use of multiplex immunoassays based on oligonucleotide tethering. Am Lab 49(3):8–11

Chapter 3

One-Step Antibody Arrays

Ying Qing Mao and Lin-Hai Li

Abstract

The sandwich-based immunoassay is renowned for its specificity and sensitivity for protein detection, where the antigen is "sandwiched" by a pair of antigen epitope-specific antibodies. The capture antibody-antigen-detection antibody complex will be formed if all the components are present in a proper reaction system. A one-step rapid sandwich-based antibody array can be developed through fixing the capture antibody on a glass slide with a fluorescence-labelled detection antibody. In this chapter, we describe the process of a one-step mouse immunoglobulin isotyping array for use in hybridoma culture supernatants.

Key words Antibody array, Sandwich assay, Fluorescence detection, One-step

1 Introduction

The traditional sandwich-based assay contains multiple steps including blocking, sample incubation, the addition of the detection antibody, and signal generation through fluorescence or chemiluminescence detection methods [1, 2]. While this method works well for most immunoassay development, it is time-consuming and may not be the best choice for time-sensitive assays. Minimal processing steps can not only save time but also lower the system CV. Since a longer incubation time is not necessary for the detection of abundant proteins, a one-step rapid assay can be developed in an array format and completed within 1–2 h. In this chapter we will present a one-step assay development for mouse immunoglobulin isotyping.

Immunoglobulins are key elements of the immune response in vertebrates against parasitic invasion. While different vertebrates produce different types of immunoglobulins, their serological concentrations are usually very abundant, ranging from microgram to milligram per milliliter. In addition, the growth and widespread use of mouse monoclonal antibody technology has created a need for a fast, accurate, and simple means of determining immunoglobulin class and subclass.

Kelly C. Whittaker and Ruo-Pan Huang (eds.), *Antibody Arrays: Methods and Protocols*, Methods in Molecular Biology, vol. 2237, https://doi.org/10.1007/978-1-0716-1064-0_3,

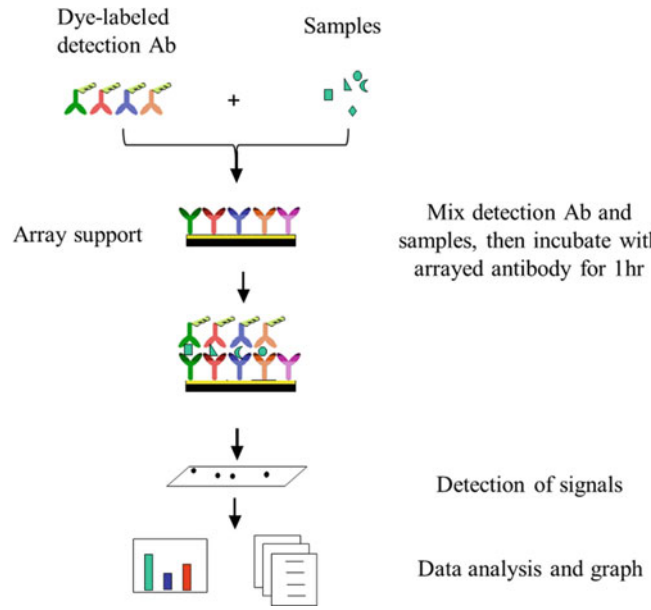

Fig. 1 Process outline of a one-step sandwich-based antibody array

Based upon the variation of the constant region of the heavy chain, eight immunoglobulin heavy chain isotypes are found in mice, IgA, IgD, IgE, IgM, IgG1, IgG2a, IgG2b, and IgG3, with two types of light chains: lambda and kappa. Taking advantage of array technology and the availability of isotype-specific monoclonal antibodies, a mouse immunoglobulin isotype array can be quickly developed using the sandwich-based technology for the determination of the eight mouse immunoglobulin subclasses (IgG1, IgG2a, IgG2b, IgG3, IgA, IgD, IgE, and IgM) and the two light chain types [3].

In this system, samples and Cy3 equivalent dye-labelled detection antibody are added together to the array. After washing away the non-bound proteins, the arrays can be visualized with a laser scanner (Fig. 1). This assay provides a highly sensitive approach (within the nanogram range) to simultaneously detect eight immunoglobulin subclasses and the two light chain types in culture supernatants and purified mouse monoclonal antibodies. The experimental procedure is simple and can be performed in any laboratory.

2 Materials

1. Non-contact arrayer.
2. Microarray scanner.
3. 16-well gasket (Grace Bio).

4. Aminosilane-coated glass slides.
5. Antibodies: anti-mouse isotype-specific antibodies (IgA, IgD, IgE, IgM, IgG1, IgG2a, IgG2b, and IgG3, lambda, and kappa).
6. Cy3-labelled bovine IgG.
7. Alexa 555-labelled goat anti-mouse Ig. This antibody can react with all murine immunoglobulin isotypes.
8. 1× PBS: 137 mM NaCl, 2.7 mM KCl, 10 mM Na_2HPO_4, 1.8 mM KH_2PO_4, pH 7.4.
9. Sample diluent: 5% BSA in 1× PBS.
10. Wash buffer: 0.1% Tween-20 (w/v), 20 mM Tris–HCl, 150 mM NaCl, pH 7.5.
11. Eppendorf tubes.
12. Microcentrifuge.
13. Hybridoma culture supernatant samples.

3 Methods

3.1 Preparation of the Antibody Array Glass Chip

1. Dilute the eight murine isotype-specific and the two light chain-specific capture antibodies to 200 μg/mL with 1× PBS.
2. Add 1 μL of Cy3-labelled bovine IgG (1 mg/mL) to 499 μL of 1× PBS to prepare a 500× diluted solution of the positive control (POS1).
3. Dilute 10 μL of POS1 in 90 μL of 1× PBS to prepare another 5000× diluted positive control (POS2) (*see* **Note 1**).
4. Array the murine isotype-specific antibodies, together with two positive controls in quadruplicate with 16 identical sub-arrays on 1 standard glass slide with the non-contact arrayer. The spot-to-spot distance should be 600 nm (*see* **Note 2**).
5. After printing, dry the slides overnight at 4 °C.
6. Vacuum dry the slides for 2 h, and then assemble with the 16-well gasket. The slide chip is now ready for sample testing (*see* **Note 3**).

3.2 Sample Processing

1. Add 1.6 mL of sample diluent into a clean Eppendorf tube and add 1 μL of Alexa 555-labelled goat anti-mouse Ig (1 mg/mL). Spin briefly (*see* **Note 4**).
2. Based upon the sample numbers, pipette 90 μL of the diluted Alexa 555-labelled goat anti-mouse Ig to the corresponding number of wells on the glass chip.
3. Dilute the hybridoma culture supernatant samples 90× using sample diluent.

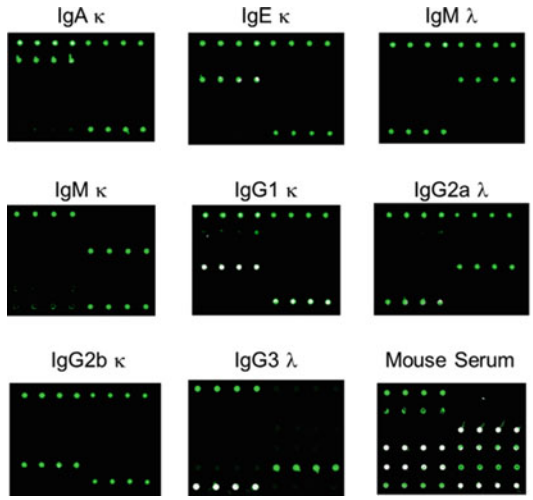

POS1	POS2
IgA	IgD
IgE	IgM
IgG1	IgG2a
IgG2b	IgG3
Lambda	Kappa

Fig. 2 Typical examples of sample results

4. In each well, add 1 μL of each 90× diluted hybridoma culture supernatant sample, and mix well through pipetting. Incubate at room temperature for 0.5–1 h (*see* **Note 5**).
5. Decant the samples from each well, and wash five times with wash buffer at room temperature. Rinse briefly, and then completely remove the wash buffer in each wash step (*see* **Note 6**).
6. Disassemble the 16-well gasket from the slide by pushing the clips outward from the slide side. Carefully remove the slide from the gasket (*see* **Note 7**).
7. Remove any wash buffer droplets completely by gently applying suction with a pipette. Do not touch the array, only the sides.

3.3 Imaging and Data Analysis

1. Scan the slide with the laser microarray scanner with the following settings: wavelength 532 nm, PMT 600, power 100%, and resolution 10 μm (*see* **Note 8**).
2. Data analysis: Results can be evaluated qualitatively by visual inspection or semi-quantitatively through data extraction with GenePix software. In a typical set of results for hybridoma supernatants or purified monoclonal antibodies, except for the positive controls, only one of the eight heavy chains and one of the light chains will show positive signals in each array (*see* **Note 9**) (Fig. 2).

4 Notes

1. The concentration of these capture antibodies may vary from 0.1 to 1 mg/mL, with the higher protein concentration, the higher detection signal, and the higher background. The two different positive controls will be used for array visualization and inter-well signal normalization.
2. For data accuracy, we use quadruplicate spots for the same target. Each spot has 333 pL of antibody with a spot size of 130 μm in diameter. To avoid spot overlapping, the spot-to-spot distance is recommended to be over 450 μm.
3. Overnight 4 °C incubation and vacuum drying are necessary for the absorption of the capture antibody to the glass surface. The finished slides can be stored at 4 °C for a few months prior to testing. For long-term storage, it is recommended that the slides are sealed with desiccant and stored at −20 °C.
4. The final working solution of this detection antibody can be 0.1–1 μg/mL. In our system, the detection antibody concentration is optimized to be around 0.6 μg/mL.
5. This dilution is optimized for a hybridoma supernatant. For purified mouse monoclonal antibodies, dilute with sample diluent to 100 μg/mL prior to adding on the array. For serum/plasma/ascites, add 1 μL of sample to 99 μL of sample diluent to make a 100× sample dilution first, and then use 1 μL for sample testing.
6. Pipette suction with a vacuum pump is recommended for sample and wash buffer removal. In order to prevent cross-well sample contamination, wash the pipette tip between each sample removal. Thorough washing after sample incubation is critical for a clean background. The wash buffer contains 0.1% Tween-20 to remove non-specific signals. Longer incubations with the wash buffer will have cleaner background but may also lower the signal. In order to prevent cross-well contamination, avoid buffer overflow of the initial several washings of wash buffer.
7. Since the reaction system has very high fluorescence, traces of it can cause very high background. It is crucial to use a pipette to completely remove the buffer residue around the corner in the last wash before disassembly.
8. Any Cy3 compatible laser scanner will work for imaging. We recommend a minimum 10 μL resolution for data to be extracted for quantitative analysis.
9. For mouse serum, plasma, or ascitic fluids, since it contains all eight isotypes, the most abundant isotypes (IgG1, IgG2a, IgG2b, IgG3, and IgM) will generally have much stronger

signals than the lower abundant groups (IgA, IgD, and IgE). In general, the light chain kappa is more dominant than the lambda chain. While this protocol is for qualitative determination of isotyping, nonetheless, the mouse immunoglobulin concentrations can be determined if a set of mouse immunoglobulin standards were run in parallel in **step 4** of Subheading 3.2.

References

1. Engvall E (1972) Enzyme-linked immunosorbent assay, Elisa. J Immunol 109(1):129–135. ISSN: 0022-1767
2. Zhou Q, Mao YQ, Jiang WD, Chen YR, Huang RY, Zhou XB, Wang YF, Shi Z, Wang ZS, Huang RP (2012) Development of IGF signaling antibody arrays for the identification of hepatocellular carcinoma biomarkers. PLoS One 7(10):e46851. https://doi.org/10.1371/journal.pone.0046851. Epub 2012 Oct 11
3. Shao W, Zhang C, Liu E, Zhang L, Ma J, Zhu Z, Gong X, Qin Z, Qiu X (2016) Identification of liver epithelial cell-derived Ig expression in μ chain-deficient mice. Sci Rep 6:23669. https://doi.org/10.1038/srep23669

Chapter 4

Global Detection of Proteins by Label-Based Antibody Array

Zhizhou Kuang, Li-Pai Chen, Ruochun Huang, and Ruo-Pan Huang

Abstract

Because of narrow availability of antibody pairs and potential cross-reactivity between antibodies, the development of sandwich-based antibody arrays which need a pair of antibodies for each target has been restricted to higher density resulting in limited proteomic breadth of detection. Label-based array is one way to overcome this obstacle by directly labeling all targets in samples with fluorescent dyes such as Cy3 and Cy5. The labeled samples are then applied on the antibody array chip composed of capture antibodies. In this chapter, we will introduce this technology including array production and sample detection assay.

Key words Antibody array, Biotin labeling

1 Introduction

Antibody arrays have been successfully used in recent years as a powerful platform for global protein expression profiling, functional determination, and biomarker screening using various sample types, including serum [1], plasma [2], cell-cultured media [3, 4], cell/tissue lysates [5, 6], body fluids such as cerebrospinal fluid [7], urine [8], abscess fluid [9], bronchoalveolar lavage [10], sputum [11], breath condensates [12], saliva [4], tears [13], prostatic fluid [14], and milk and colostrum [15]. The methodology behind most antibody arrays is sandwich-based, much like that of a standard ELISA, which endows the arrays with high detection sensitivity, specificity, reproducibility, and high-throughput measurement capabilities. However, the requirement of a pair of antibodies for each target restricts the development of higher density antibody arrays resulting in limited proteomic breadth of detection, because of narrow availability of antibody pairs and potential cross-reactivity between antibodies. The higher the number of antibody pairs required in the array, the harder it is to eliminate false signals between targets.

One way to overcome this obstacle is to directly label all targets in samples with fluorescent dyes such as Cy3 and Cy5. The labeled

Kelly C. Whittaker and Ruo-Pan Huang (eds.), *Antibody Arrays: Methods and Protocols*, Methods in Molecular Biology, vol. 2237, https://doi.org/10.1007/978-1-0716-1064-0_4,

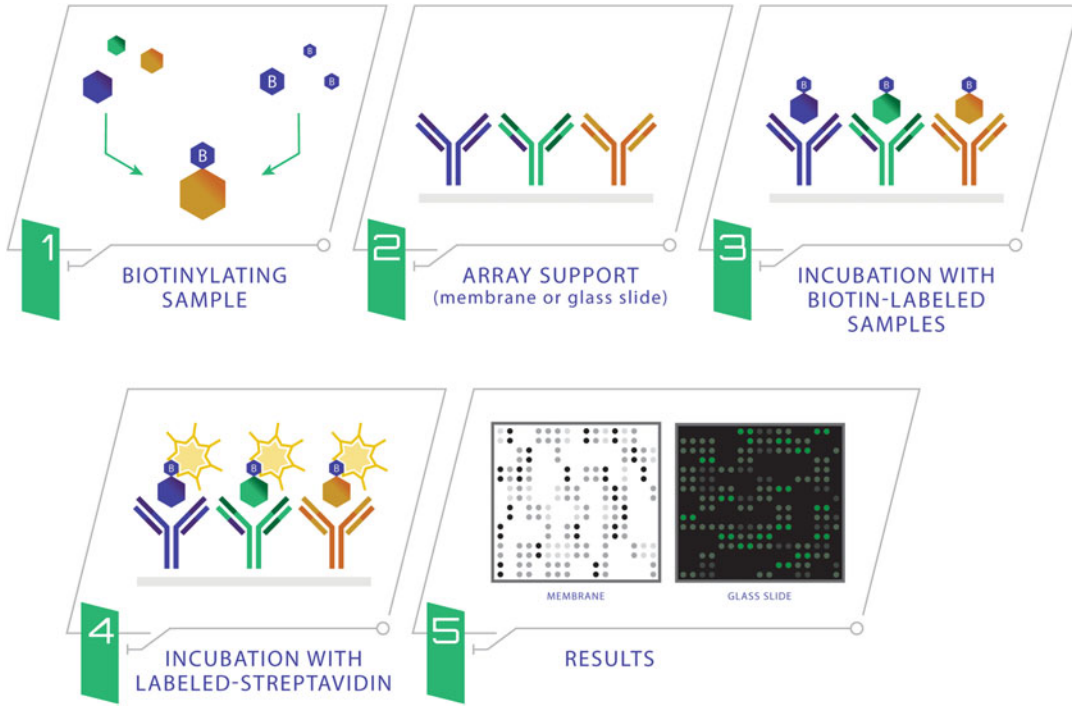

Fig. 1 Diagram of a label-based antibody array

samples are then applied on the antibody array chip composed of capture antibodies. The chips are washed extensively, and bound proteins are then visualized by laser scanner (Fig. 1). Since only capture antibodies are required, this approach offers the possibility to develop antibody arrays with much higher density, capable of detecting thousands of target proteins simultaneously [16]. Recently, we have successfully built up a label-based antibody array with 2000 targets, which is the largest commercially available antibody array to date. With this array, a broad, panoramic view of protein expression, including cytokines, chemokines, adipokines, growth factors, angiogenic factors, proteases, soluble receptors, soluble adhesion molecules, and other proteins, is obtained. In this chapter, we will introduce this technology including array production using a glass platform and sample detection assay.

2 Materials

Prepare all solutions using ultrapure water (prepared by purifying deionized water, to attain a sensitivity of 18 MΩ cm at 25 °C) and analytical grade reagents. Prepare and store all reagents at room temperature (unless indicated otherwise). Centrifuge at 2–8 °C with fixed angel rotors and swing rotors. Different sizes of pipetman from 0.1 to 1000 μL.

2.1 Array Printing

1. 25 mm × 75 mm aminopropyl silane-coated glass slides
2. Antibodies against 500 different targets.
3. Biotin-labeled IgG with three different concentrations used as positive control.
4. Glass slide array printer.
5. 384-well plate
6. Incubation chamber and snap-on side that matches printed glass slide array.
7. Plastic slide incubation chambers.

2.2 Sample Preparation and Storage

1. Cell lysis buffer: 20 mM Tris–HCl, pH 7.5, 150 mM NaCl, 1 mM Na_2EDTA, 1 mM EGTA, 1% NP-40, 1% sodium deoxycholate, 2.5 mM sodium pyrophosphate, 1 mM b-glycerophosphate, 1 mM Na_3VO_4, 1 μg/mL leupeptin.
2. 1× PBS: 0.137 M NaCl, 0.0027 M KCl, 0.01 M Na_2HPO_4, and 0.0018 M KH_2PO_4.
3. Labeling reagent: 10 mg/mL biotin in 1× PBS.
4. Labeling buffer: 1× PBS.
5. Biotin labeling stop reagent: 0.5 M Tris–HCl, pH 8.0.
6. Dialysis tubes (sample volume determined size).
7. Floating dialysis rack.
8. Clean microfuge tube and bench centrifuge.

2.3 Sample Detection

1. Printed L-Series Human Antibody Array AAH-BLG-3 (glass slide array).
2. Blocking buffer: 3% BSA in 1× PBS.
3. 20× wash buffer: 20× PBS with 1% Tween-20.
4. Cy3-conjugated streptavidin.
5. 30 mL centrifuge tube
6. Microarray scanner.

3 Methods

3.1 Array Printing

1. According to the instruction of array printer, load the glass slides on the deck of printer (*see* **Notes 1** and **2**).
2. Design the array map with all positive control, negative control, and antibody spots for 500 targets with duplicates for each (Fig. 2).
3. Transfer 50 μL of each antibody at the working concentration and the biotin-labeled IgG concentrations to a 384-well plate (*see* **Note 3**).

	1	2	3	4	5	6	7	8	9	10	11	12	13	14	15	16	17	18	19	20	21	22	23	24	25	26	27	28	29	30
1	P1a	P1a	P2a	P2a	P3a	P3a	neg	neg	5	5	6	6	7	7	8	8	9	9	10	10	11	11	12	12	13	13	14	14	15	15
2	16	16	17	17	18	18	19	19	20	20	21	21	22	22	23	23	24	24	25	25	26	26	27	27	28	28	29	29	30	30
3	31	31	32	32	33	33	34	34	35	35	36	36	37	37	38	38	39	39	40	40	41	41	42	42	43	43	44	44	45	45
4	46	46	47	47	48	48	49	49	50	50	51	51	52	52	53	53	54	54	55	55	56	56	57	57	58	58	59	59	60	60
5	61	61	62	62	63	63	64	64	65	65	66	66	67	67	68	68	69	69	70	70	71	71	72	72	73	73	74	74	75	75
6	76	76	77	77	78	78	79	79	80	80	81	81	82	82	83	83	84	84	85	85	86	86	87	87	88	88	89	89	90	90
7	91	91	92	92	93	93	94	94	95	95	96	96	97	97	98	98	99	99	100	100	101	101	102	102	103	103	104	104	105	105
8	106	106	107	107	108	108	109	109	110	110	111	111	112	112	113	113	114	114	115	115	116	116	117	117	118	118	119	119	120	120
9	121	121	122	122	123	123	124	124	125	125	126	126	127	127	128	128	129	129	130	130	131	131	132	132	133	133	134	134	135	135
10	136	136	137	137	138	138	139	139	140	140	141	141	142	142	143	143	144	144	145	145	146	146	147	147	148	148	149	149	150	150
11	151	151	152	152	153	153	154	154	155	155	156	156	157	157	158	158	159	159	160	160	161	161	162	162	163	163	164	164	165	165
12	166	166	167	167	168	168	169	169	170	170	171	171	172	172	173	173	174	174	175	175	176	176	177	177	178	178	179	179	180	180
13	181	181	182	182	183	183	184	184	185	185	186	186	187	187	188	188	189	189	190	190	191	191	192	192	193	193	194	194	195	195
14	196	196	197	197	198	198	199	199	200	200	201	201	202	202	203	203	204	204	205	205	206	206	207	207	208	208	209	209	210	210
15	211	211	212	212	213	213	214	214	215	215	216	216	217	217	218	218	219	219	220	220	221	221	222	222	223	223	224	224	225	225
16	226	226	227	227	228	228	229	229	230	230	231	231	232	232	233	233	234	234	235	235	236	236	237	237	238	238	239	239	240	240
17	241	241	242	242	243	243	244	244	245	245	246	246	247	247	248	248	249	249	250	250	251	251	252	252	253	253	254	254	255	255
18	256	256	257	257	258	258	259	259	260	260	261	261	262	262	263	263	264	264	265	265	266	266	267	267	268	268	269	269	270	270
19	271	271	272	272	273	273	274	274	275	275	276	276	277	277	278	278	279	279	280	280	281	281	282	282	283	283	284	284	285	285
20	P1b	P1b	P2b	P2b	P3b	P3b	neg	neg	290	290	291	291	292	292	293	293	294	294	295	295	296	296	297	297	298	298	299	299	300	300
21	301	301	302	302	303	303	304	304	305	305	306	306	307	307	308	308	309	309	310	310	311	311	312	312	313	313	314	314	315	315
22	316	316	317	317	318	318	319	319	320	320	321	321	322	322	323	323	324	324	325	325	326	326	327	327	328	328	329	329	330	330
23	331	331	332	332	333	333	334	334	335	335	336	336	337	337	338	338	339	339	340	340	341	341	342	342	343	343	344	344	345	345
24	346	346	347	347	348	348	349	349	350	350	351	351	352	352	353	353	354	354	355	355	356	356	357	357	358	358	359	359	360	360
25	361	361	362	362	363	363	364	364	365	365	366	366	367	367	368	368	369	369	370	370	371	371	372	372	373	373	374	374	375	375
26	376	376	377	377	378	378	379	379	380	380	381	381	382	382	383	383	384	384	385	385	386	386	387	387	388	388	389	389	390	390
27	391	391	392	392	393	393	394	394	395	395	396	396	397	397	398	398	399	399	400	400	401	401	402	402	403	403	404	404	405	405
28	406	406	407	407	408	408	409	409	410	410	411	411	412	412	413	413	414	414	415	415	416	416	417	417	418	418	419	419	420	420
29	421	421	422	422	423	423	424	424	425	425	426	426	427	427	428	428	429	429	430	430	431	431	432	432	433	433	434	434	435	435
30	436	436	437	437	438	438	439	439	440	440	441	441	442	442	443	443	444	444	445	445	446	446	447	447	448	448	449	449	450	450
31	451	451	452	452	453	453	454	454	455	455	456	456	457	457	458	458	459	459	460	460	461	461	462	462	463	463	464	464	465	465
32	466	466	467	467	468	468	469	469	470	470	471	471	472	472	473	473	474	474	475	475	476	476	477	477	478	478	479	479	480	480
33	481	481	482	482	483	483	484	484	485	485	486	486	487	487	488	488	489	489	490	490	491	491	492	492	493	493	494	494	495	495
34	496	496	497	497	498	498	499	499	500	500	501	501	502	502	503	503	504	504	505	505	506	506	507	507	508	508	neg	neg	neg	neg
35	neg	neg	neg	neg	neg	neg	neg	neg	neg	neg	neg	neg	neg	neg	neg	neg	neg	neg	neg	neg	neg	neg	neg	neg	positiv	positiv	positiv	positiv	positiv	positiv

Fig. 2 Production map of array with 500 detection targets. P1a-P3a, P1b-P3b, and P1c-P3c: three different concentration of positive control. Neg: negative control

4. Print the corresponding reagents on the slides using the printer control software.
5. Assemble the printed glass slide into the incubation chamber by applying the slide to the incubation chamber with the barcode facing upward (Fig. 3a). Then, gently snap one edge of a snap-on side (Fig. 3b), press against a lab bench, and push the slide in the lengthwise direction (Fig. 3c). Repeat with the other side (Fig. 3d) (*see* **Notes 4** and **5**). If not running the assay immediately, seal the assembled slide with adhesive film, and place in a plastic bag filled with desiccant and store at −20 °C.

3.2 Sample Preparation

1. Dilute 20 μL serum or plasma with 80 μL 1× PBS (fivefold dilution).
2. Add sample into a dialysis tube, and carefully place dialysis tubes into floating dialysis rack (*see* **Note 6**).
3. Place the floating dialysis rack into ≥500 mL 1× PBS in a large beaker, and place the beaker on a stir plate and dialyze for at least 3 h at 4 °C, stirring the buffer gently (*see* **Note 7**).
4. Exchange the dialysis buffer, and repeat **step 3**.

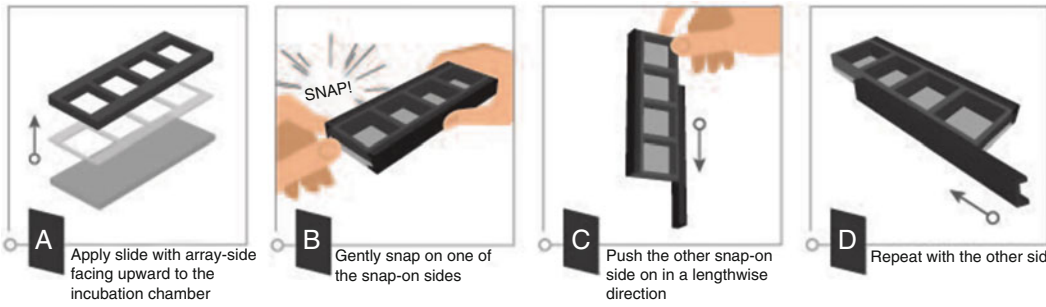

Fig. 3 Glass slide assembly instructions

5. Transfer the dialyzed sample to a clean microfuge tube (*see* **Note 8**).
6. Spin the dialyzed samples for 5 min at 10,000 × *g* to remove any particulates or precipitates, and then transfer the supernatants to a clean microfuge tube.
7. Prepare 1× biotin labeling reagent immediately prior to use. Briefly spin down the labeling reagent tube. Add 100 µL 1× PBS into the tube, and then pipette up and down or vortex slightly to dissolve the lyophilized reagent (*see* **Note 9**).
8. Add 22 µL of 1× labeling reagent solution into a new tube containing 35 µL dialyzed serum or plasma sample and 155 µL labeling buffer (*see* **Note 10**).
9. Incubate at room temperature (RT) with gentle rocking or shaking for 30 min. Mix the reaction solution by gently tapping the tube every 5 min.
10. Add 3 µL biotin labeling stop reagent into each reaction tube. Collect each sample, and immediately dialyze according to **steps 3–5** (*see* **Note 11**).

3.3 Sample Detection

1. Place the assembled glass slide in clean environment for 15 min at RT.
2. Add 400 µL of blocking buffer into each well of the assembled glass slide, and incubate at RT for 30 min. Ensure that there are no bubbles on the array surface (*see* **Note 12**).
3. Immediately prior to sample incubation, spin down biotin-labeled samples for 5 min at 10,000 × *g* to remove any particulates or precipitates. 20-fold dilute samples with blocking buffer (*see* **Note 13**).
4. Completely remove blocking buffer from each well (*see* **Note 14**). Add 400 µL of diluted samples into appropriate wells (*see* **Note 15**). Remove any bubbles on the array surface. Incubate with gentle rocking or shaking for 2 h at RT.

5. Separately dilute the required amounts of 20× Wash Buffer I and 20× Wash Buffer II concentrate with ddH_2O.
6. Decant the samples from each well, and wash three times with 800 μL of 1× Wash Buffer I at RT with gentle rocking or shaking for 5 min per wash.
7. Place the assembled glass slide into "a container" with 200 mL of 1× Wash Buffer I to completely cover the entire assembly, and remove any bubbles in the wells. Wash two times at RT with gentle rocking or shaking for 10 min per wash.
8. Decant the Wash Buffer I from each well, place the assembled glass slide into a container with 200 mL of 1× Wash Buffer II to completely cover the entire assembly, and remove any bubbles in wells. Wash two times at RT with gentle rocking or shaking for 5 min per wash.
9. Briefly spin down the tube containing the Cy3-conjugated streptavidin immediately before use.
10. Add 1000 μL of blocking buffer to the Cy3-conjugated streptavidin to prepare a concentrated Cy3-conjugated streptavidin stock solution. Pipette up and down to mix gently (do not store the stock solution for later use).
11. Add 200 μL of the concentrated Cy3-conjugated streptavidin stock solution to a tube with 800 μL of blocking buffer to prepare a 1× Cy3-conjugated streptavidin. Mix gently.
12. Carefully remove the assembled glass slide from the container, and remove all of Wash Buffer II from the wells. Add 400 μL of 1× Cy3-conjugated streptavidin to each well. Cover the incubation chamber, and incubate at RT for 2 h with gentle rocking or shaking (*see* **Note 16**).
13. Decant the solution, and disassemble the glass slide from the incubation frame and chamber. Disassemble the device by pushing clips outward from the side, as shown in Fig. 4. Carefully remove the glass slide from the gasket.
14. Gently place the glass slide into a 30 mL centrifuge tube, and add 30 mL of 1× Wash Buffer I. Wash with gentle rocking or shaking for 10 min. Remove the wash buffer. Repeat two times for a total of three washes.

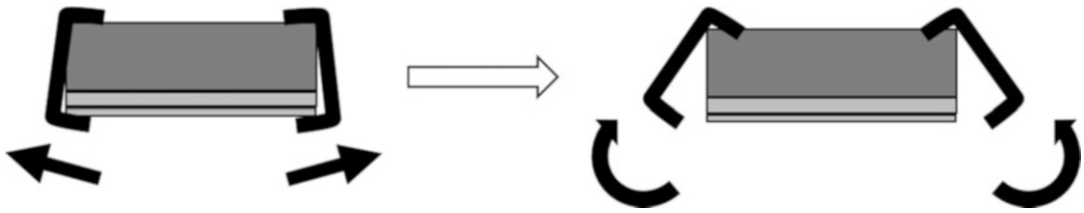

Fig. 4 Disassemble the glass slide from the incubation frame and chamber

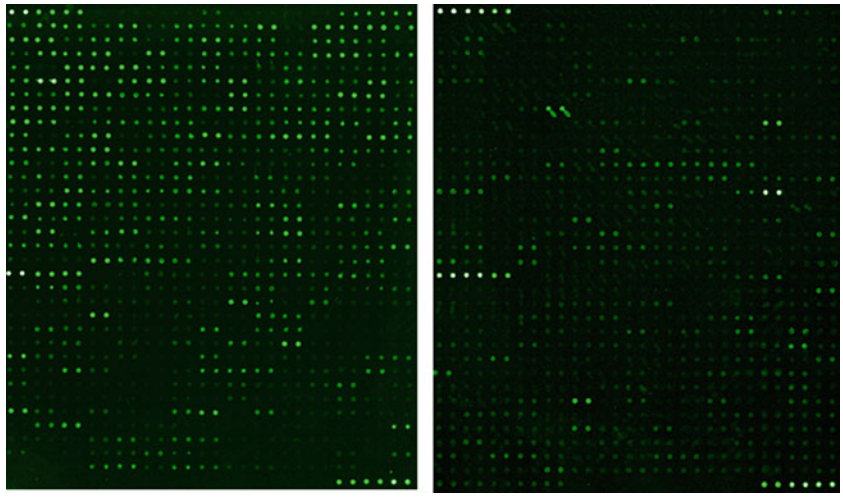

Fig. 5 Sample detection results

15. Add 30 mL of 1× Wash Buffer II. Wash with gentle rocking or shaking for 5 min. Remove the wash buffer. Repeat one more time for a total of two washes.
16. Add 30 mL of ddH_2O, and incubate for 5 min. Remove the glass slide, and decant the water from the centrifuge tube. Remove any excess water droplets from the slide completely by gently applying suction with a pipette to remove buffer droplets (*see* **Note 17**).

3.4 Fluorescence Detection (Fig. 5)

1. Proceed immediately to scanning the slide using microarray scanner (*see* **Note 18**).

4 Notes

1. The microarray slides are delicate. Please do not touch the array surface with pipette tips, forceps, or your fingers. Hold the slides by the edges only.
2. Handle the slides with powder-free gloves and in a clean environment.
3. Dilute the antibodies to proper concentrations following the vendor's instruction.
4. Do not remove the glass slide from the chamber assembly until **step 13** of Subheading 3.3, and take great care not to break the glass slide when doing so.
5. Permanent marker ink can significantly interfere with fluorescent signal detection. Never mark anywhere on the front (arrayed) side of the slide. It's best to avoid using marker completely; however, if you need to number the slide, please

add a small mark only on the back of the slide along the top or bottom edge using a green or blue ultra-fine point Sharpie® brand marker, only after the slide is completely dry.

6. If the samples appear to be cloudy, transfer the samples to a clean tube, and centrifuge them at 16,000 × *g* for 20 min at 2–8 °C before dialysis. If the samples are still not clear, store them at −20 °C for 20 min. Remove them from the freezer, and immediately centrifuge them at 16,000 × *g* for 20 min at 2–8 °C.
7. The dialysis procedure may proceed overnight.
8. The sample volume may change during dialysis.
9. Amines (e.g., Tris, glycine) and azides quench the biotinylation reaction. Avoid contaminating samples with these chemicals prior to biotinylation.
10. To normalize serum concentrations during biotinylation, measure sample volume before and after dialysis. Then adjust the volumes of dialyzed serum/plasma and labeling buffer to compensate. For example, if the sample volume doubles after dialysis, then use twice as much serum/plasma in the labeling reaction (70 μL) and reduce the labeling buffer to 120 μL.
11. Biotinylated samples can be stored at −20 or −80 °C until you are ready to proceed with the assay.
12. The glass slide should be completely dry before adding blocking buffer to wells.
13. The optimal sample dilution factor will depend on the abundance of target proteins. If the background or antigen-specific antibody signals are too strong, the sample can be diluted further in subsequent experiments. If the signal is too weak, more concentrated samples can be used.
14. Remove reagents/sample by gently applying suction with a pipette to the corners of each well. Do not touch the printed area of the array, only the sides. Protect the slide from dust or other contaminants.
15. Avoid the flow of sample into neighboring wells.
16. Avoid exposure to light after adding Cy3-conjugated streptavidin by covering the assembled glass slide with aluminum foil or incubate in a dark room.
17. Protect the glass slides from temperatures above RT, and store them in the dark. Do not expose glass slide to strong light, such as sunlight or a UV lamp.
18. Make sure the finished glass slide is completely dry before scanning or storing.

References

1. Hashimoto I, Wada J, Hida A, Baba M, Miyatake N, Eguchi J, Shikata K, Makino H (2006) Elevated serum monocyte chemoattractant protein-4 and chronic inflammation in overweight subjects. Obesity (Silver Spring) 14(5):799–811
2. Ray S, Britschgi M, Herbert C, Takeda-Uchimura Y, Boxer A, Blennow K, Friedman LF, Galasko DR, Jutel M, Karydas A, Kaye JA, Leszek J, Miller BL, Minthon L, Quinn JF, Rabinovici GD, Robinson WH, Sabbagh MN, So YT, Sparks DL, Tabaton M, Tinklenberg J, Yesavage JA, Tibshirani R, Wyss-Coray T (2007) Classification and prediction of clinical Alzheimer's diagnosis based on plasma signaling proteins. Nat Med 13(11):1359–1362
3. Turtinen LW, Prall DN, Bremer LA, Nauss RE, Hartsel SC (2004) Antibody array-generated profiles of cytokine release from THP-1 leukemic monocytes exposed to different amphotericin B formulations. Antimicrob Agents Chemother 48(2):396–403
4. De CF, Dassencourt L, Anract P (2004) The inflammatory side of human chondrocytes unveiled by antibody microarrays. Biochem Biophys Res Commun 323(3):960–969
5. Haddad G, Belosevic M (2009) Transferrin-derived synthetic peptide induces highly conserved pro-inflammatory responses of macrophages. Mol Immunol 46(4):576–586
6. Argas DL, Nascimbene C, Krishnan C, Zimmerman AW, Pardo CA (2005) Neuroglial activation and neuroinflammation in the brain of patients with autism. Ann Neurol 57(1): 67–81
7. Liu BC, Zhang L, Lv LL, Wang YL, Liu DG, Zhang XL (2006) Application of antibody array technology in the analysis of urinary cytokine profiles in patients with chronic kidney disease. Am J Nephrol 26(5):483–490
8. Fu SY, Su GW, McKinley SH, Yen MT (2007) Cytokine expression in pediatric subperiosteal orbital abscesses. Can J Ophthalmol 42(6): 865–869
9. Coppinger JA, O'Connor R, Wynne K, Flanagan M, Sullivan M, Maguire PB, Fitzgerald DJ, Cagney G (2007) Moderation of the platelet releasate response by aspirin. Blood 109(11):4786–4792
10. Simcock DE, Kanabar V, Clarke GW, O'Connor BJ, Lee TH, Hirst SJ (2007) Proangiogenic activity in bronchoalveolar lavage fluid from patients with asthma. Am J Respir Crit Care Med 176(2):146–153
11. Kim HB, Kim CK, Iijima K, Kobayashi T, Kita H (2009) Protein microarray analysis in patients with asthma: elevation of the chemokine PARC/CCL18 in sputum. Chest 135(2): 295–302
12. Matsunaga K, Yanagisawa S, Ichikawa T, Ueshima K, Akamatsu K, Hirano T, Nakanishi M, Yamagata T, Minakata Y, Ichinose M (2006) Airway cytokine expression measured by means of protein array in exhaled breath condensate: correlation with physiologic properties in asthmatic patients. J Allergy Clin Immunol 118(1):84–90
13. Sack RA, Conradi L, Krumholz D, Beaton A, Sathe S, Morris C (2005) Membrane array characterization of 80 chemokines, cytokines, and growth factors in open- and closed-eye tears: angiogenin and other defense system constituents. Invest Ophthalmol Vis Sci 46(4):1228–1238
14. Kverka M, Burianova J, Lodinova-Zadnikova R, Kocourkova I, Cinova J, Tuckova L, Tlaskalova-Hogenova H (2007) Cytokine profiling in human colostrum and milk by protein array. Clin Chem 53(5):955–962
15. Fujita K, Ewing CM, Sokoll LJ, Elliott DJ, Cunningham M, De Marzo AM, Isaacs WB, Pavlovich CP (2008) Cytokine profiling of prostatic fluid from cancerous prostate glands identifies cytokines associated with extent of tumor and inflammation. Prostate 68(8): 872–882
16. Lin Y, Huang R, Chen LP, Lisoukov H, Lu ZH, Li S, Wang CC, Huang RP (2003) Profiling of cytokine expression by biotin label-based protein arrays. Proteomics 3(9): 1750–1757

Chapter 5

Surface Plasmon Resonance Imaging-Mass Spectrometry Coupling on Antibody Array Biochip: Multiplex Monitoring of Biomolecular Interactions and On-Chip Identification of Captured Antigen

Anastasiia Halushkina, William Buchmann, Nathalie Jarroux, and Régis Daniel

Abstract

The coupling of surface plasmon resonance imaging (SPRi) with mass spectrometry (MS) offers a very promising multidimensional analysis. This system takes advantage of the two well-established techniques: SPR, which allows for the analysis of biomolecular interactions through the determination of kinetic and thermodynamic constants, and MS, which can characterize biological structures from mass measurements and fragmentation experiments. Here, a protocol for the coupling of SPRi with matrix-assisted laser desorption/ionization mass spectrometry (MALDI-MS) is described using a biochip grafted by antibodies in an array format. Interaction between β-lactoglobulin antibodies and the protein antigen is detected and analyzed by SPRi. Then, the arrayed biochip which fitted a commercially MALDI target was inserted in a MALDI source, and mass spectra were recorded directly from the biochip surface from each antibody spot, showing protein ions attributed to the corresponding specific protein antigens.

Key words Biomolecular interactions, Surface plasmon resonance, Mass spectrometry, Matrix-assisted laser desorption/ionization, Poly(ethylene glycol), β-Lactoglobulin, Antibodies

1 Introduction

Biomolecular interactions are at the core of numerous biological processes, and several techniques are available to determine either their thermodynamic features or their structural determinants. The hyphenation of thermodynamic and structural methods raises much interest as it allows a multidimensional and comprehensive characterization of bio-interactions. The coupling of surface plasmon resonance (SPR) with mass spectrometry (MS) from a unique surface common to both techniques, so-called SPR-MS coupling, meets this objective of full characterization as SPR provides kinetic and thermodynamic data by real-time monitoring of

Kelly C. Whittaker and Ruo-Pan Huang (eds.), *Antibody Arrays: Methods and Protocols*, Methods in Molecular Biology, vol. 2237, https://doi.org/10.1007/978-1-0716-1064-0_5,

bio-interactions [1–6] and MS allows the structural identification of the specifically captured ligands on the SPR sensor surface [7–9]. The SPR monitoring of bio-interactions requires the immobilization of one partner of interaction (i.e., receptor) on a biosensor surface or in a channel, whereas potential binding partners (ligands) are flowed over the immobilized receptors. Because SPR does not provide any structural data about the captured ligands due to the principle of SPR detection based on optical measurement, the coupling with MS provides a real added value in this respect [10].

Initial SPR-MS developments were based on the use of a sensor chip with a limited number of flow cells, requiring elution steps for the recovery of the captured biomolecules and their subsequent MS analysis [11–16]. Alternatively, a SPR-MS coupling based on a sensor chip in a microarray format has been developed in the past decade, allowing multiplexed and high-throughput SPR-MS analyses involving SPR imaging (SPRi) and matrix-assisted laser desorption/ionization (MALDI)-MS on the same sensor surface [17–22]. This chapter will describe a step-by-step procedure to implement this recently developed SPRi-MALDI-MS method, including (1) the SPRi biochip preparation, (2) the SPRi experiment allowing the determination of interaction and the ligand capture, and (3) the direct on-chip MALDI-MS detection of specifically retained ligands (Fig. 1). More precisely, the procedure will be applied to the analysis of antibody-antigen interactions as an example. We will detail in a first step the functionalization of the chip gold surface by a self-assembled monolayer (SAM) of short poly(ethylene glycol) (PEG) chains, a key step in order to reduce the nonspecific binding, especially when analyzing bio-interactions in complex mixtures such as in biological fluids. The PEG chains are terminated by a *N*-hydroxysuccinimide (NHS) group as an active end for antibody grafting. Then, we will describe the SPRi detection and recording of the complex formation between β-lactoglobulin and its corresponding antibody immobilized on the sensor surface over a range of concentrations (1–100 μg/mL ~ 54.5 nM–5.45 μM) (Fig. 2a). Last, we will describe the MALDI-MS detection and identification of the specifically retained antigen on the receptor spots directly from the biochip surface. Femtomolar amounts of captured β-lactoglobulin, as determined by SPR, were sufficient for the on-chip direct MS detection and to obtain good quality mass spectra. The mass spectra exhibited protein ions corresponding to the specific antigen, without any trace of nonspecific ligand (Fig. 2b). The biochip surface free from receptors was also devoid of nonspecifically bound proteins (Fig. 2c), indicating that the functionalization of the sensor surface by short PEG chains greatly minimizes the unspecific binding.

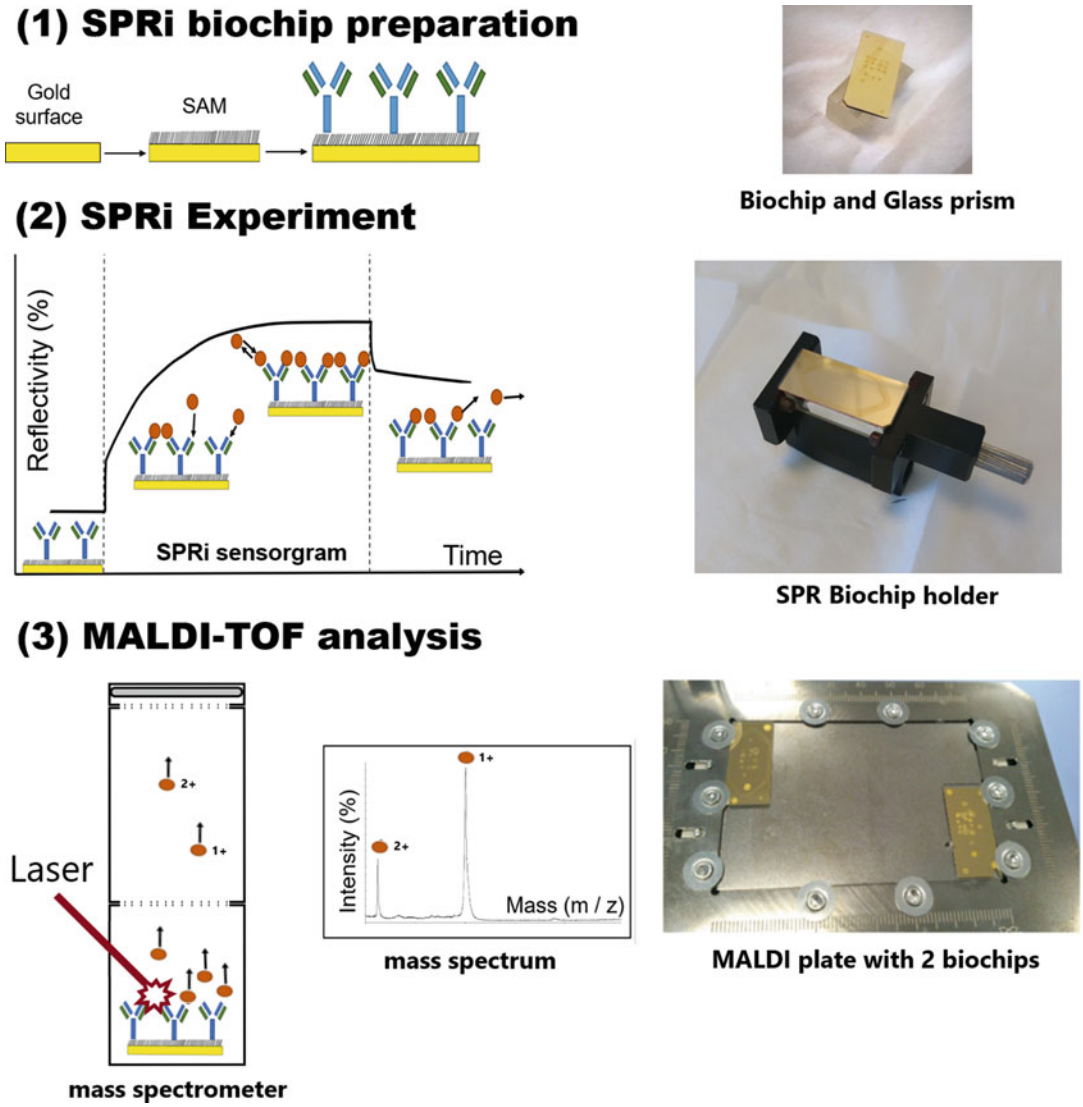

Fig. 1 Main steps of the SPRi-MALDI-MS experiment: (1) SPRi biochip preparation, (2) SPRi experiment allowing the determination of interaction and ligand capture, and (3) direct on-chip MALDI-MS detection of specifically retained ligands

2 Materials

2.1 Chemical Reagents

1. *O*-(2-Carboxyethyl)-*O′*-(mercaptoethyl)-heptaethylene glycol (PEG) aliquoted to 3.5 µL (~4 mg) and stored at −20 °C.
2. 4-Pyrrolidinopyridine.
3. *N*-Hydroxysuccinimide (NHS).
4. *N*,*N′*-Dicyclohexylcarbodiimide (DCC).

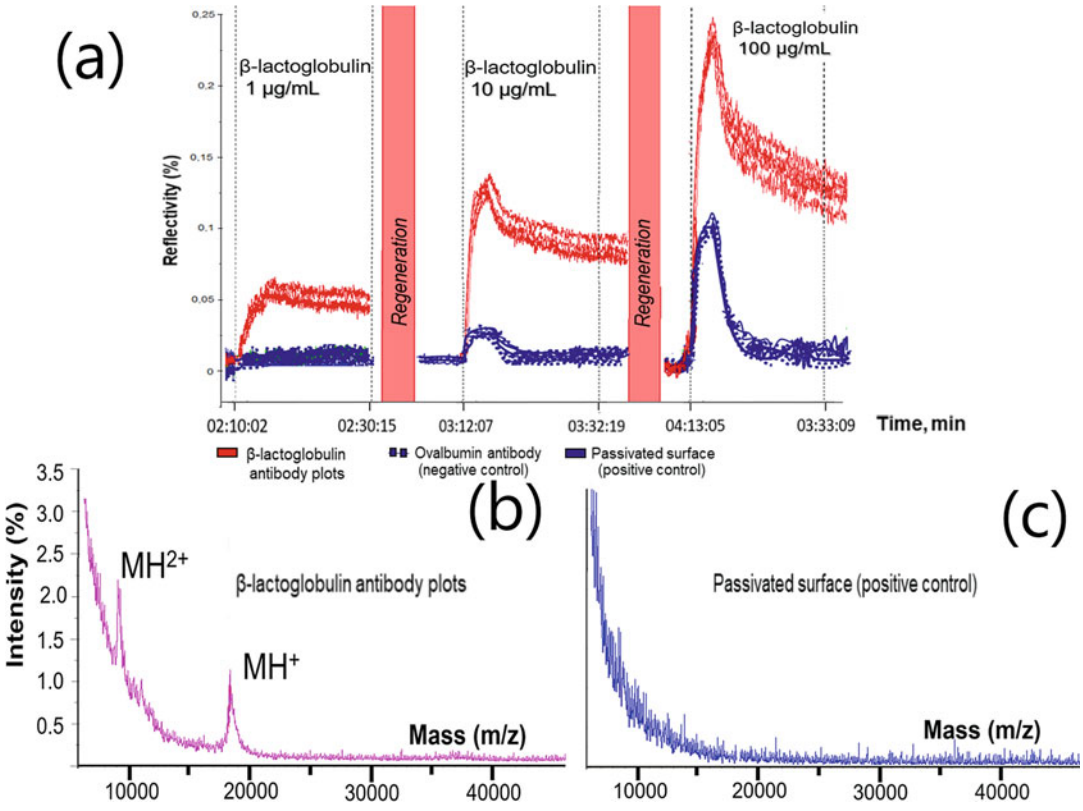

Fig. 2 (**a**) SPRi sensorgrams obtained after injections of β-lactoglobulin at different concentrations (1, 10, and 100 µg/mL) in 10 mM ammonium acetate buffer pH 7.5, (**b**) MALDI-TOF mass spectrum obtained after the SPRi experiment directly from an anti-β-lactoglobulin antibody plot of biochip surface, (**c**) MALDI-TOF mass spectrum obtained after the SPRi experiment directly from a passivated area of the biochip surface

5. 2-(4-Hydroxyphenylazo)-benzoic acid (HABA, MALDI matrix).
6. Trifluoroacetic acid (TFA).
7. High index liquid "Serie B" for connection between glass prism and SPRi-Slides (HORIBA Scientific, France).
8. 55% (v/v) Glycerol prepared by dilution in deionized water from 100% glycerol.

2.2 Proteins (Receptors and Ligands)

Protein solutions can be prepared and stored up to 1 week, at 4 °C (unless indicated otherwise).

1. β-Lactoglobulin from bovine milk.
2. Polyclonal antibody against β-lactoglobulin.
3. Monoclonal antibody against ovalbumin.

2.3 Solvents, Buffer, and Solutions for SPRi Experiment

All aqueous solutions should be prepared using ultrapure water and analytical grade reagents.

1. Ultrapure water, 18.2 MΩ cm.
2. Ethanol absolute.
3. Dimethyl sulfoxide (DMSO).
4. Current buffer for SPRi: 10 mM ammonium acetate, pH 7.5. Add about 500 mL water to a 1 L graduated cylinder or a glass beaker, and transfer 1.33 mL of 7.5 M ammonium acetate stock solution to the cylinder as well. Add water to a volume of 900 mL. Mix and adjust pH with ammonium hydroxide. Make up to 1 L with water. Store at 4 °C.
5. Passivation solution: 1 mM L-lysine. Add about 40 mL of current buffer to a 50 mL plastic flacon. Weigh 0.00731 g L-lysine, and transfer to the flacon. Dissolve the powder, and add current buffer to a final volume of 50 mL. Leave one aliquot at 4 °C for current use, and store the remaining aliquots at −20 °C.
6. Regeneration solution: 0.1 M glycine-HCl, pH 2.0. Add about 35 mL water to a 50 mL graduated cylinder or a glass beaker. Weigh 0.37535 g glycine, and transfer to the cylinder. Add water to a volume of 40 mL. Mix and adjust pH with HCl (*see* **Note 1**). Add water to a final volume of 50 mL with water. Store at 4 °C.

2.4 Equipment

1. UV-ozonolyzer.
2. Laboratory rocker.
3. Light table.
4. Petri dish.
5. Polystyrene box.
6. Box filled with ice.
7. Empty squeeze bottle.
8. 50 mm diameter glass beakers.
9. Plastic flacons 50 mL.
10. Aluminum foil.
11. Parafilm.
12. Lens wipes (no-dust optic wipes).
13. Plastic tweezers.

2.5 Instrument

2.5.1 SPR

1. SPR imaging (SPRi) experiments should be performed using an SPRi-Plex imager (HORIBA Scientific, France) equipped with 660 nm light-emitting diode (LED) and charge-coupled device (CCD) camera or imager with similar specifications. Data acquisition and instrument control should be performed via SPRi-View P4.1.0, and quantitative analysis of the experimental data should be done with the software SPRi-Analysis 1.2.1 or equivalent.
2. SPRi glass prism.
3. Gold-covered glass slides: thickness × length × width = 0.5 mm × 28 mm × 12 mm, chromium bonding layer 1–2 nm, gold layer 50 nm, roughness: maxi 7 Å (*see* **Note 2**).

2.5.2 MALDI-TOF Mass Spectrometry

1. MALDI-TOF experiments should be performed using an Autoflex Speed MALDI-TOF/TOF MS instrument or equivalent. This instrument is equipped with a SmartBeam II™ laser (modified Nd:YAG laser) pulsed with 1 kHz frequency. Mass spectra acquisition and instrument control should be performed via FlexControl 3.4. Mass spectra should be processed using FlexAnalysis software (version 3.3.80.0) or equivalent.
2. TLC adapter MALDI target plate (i.e., target plate for MALDI imaging with fixations).
3. Customized transparent plastic film, used as a mask figuring the array pattern to guide the manual spot deposition (*see* **Note 3**).
4. Matrix solution: 0.05 M 2-(4-Hydroxyphenylazo)-benzoic acid (HABA) in acetonitrile/water 50%/50% (v/v), 0.2% trifluoroacetic acid (TFA). Weigh 12.1 mg of HABA in a plastic vial. Add 1 mL of acetonitrile/water 50/50% (v/v), 0.2% TFA. Dissolve matrix and mix solution thoroughly to ensure that matrix solution is homogeneous.

3 Methods

Preparation steps described in Subheadings 3.1–3.3 are for the preparation of two biochips (*see* **Note 4**).

3.1 Gold Surface Cleaning

Prior to use, the gold surface of the glass slides is systematically cleaned by ozonolysis. Glass slide handling should be performed exclusively with plastic tweezers.

1. Rinse the gold-covered glass slides with copious amounts of acetone, and dry with airflow using an empty squeeze bottle nozzle (*see* **Note 5**).

2. Rinse glass slides with copious amounts of ethanol absolute, and dry again as in **step 1**.
3. Drop glass slides off (gold side up) in the UV-ozonolyzer for 30 min.

3.2 PEG Self-Assembled Monolayer

1. Dissolve aliquot (3.5 µL ~ 4 mg) of PEG in 3.48 mL of ethanol absolute to obtain a 2.5 mM PEG solution, and mix it thoroughly. Transfer solution into a 50 mL beaker. Tightly cover the beaker with parafilm and aluminum foil (*see* **Note 6**).
2. Immerse the UV-ozonolysis cleaned biochips (gold side up) one by one in the PEG solution. Take care not to overlay them.
3. Cover the beaker with several layers of parafilm and aluminum foil. Put the covered beaker inside a polystyrene box, and close the lid.
4. Place the polystyrene box on the laboratory rocker, and rock at 50 rpm for 6 h.
5. Stop the rocker, and take out the beaker with the biochips. Take the biochips out one by one, rinse them with ethanol absolute, and immerse them into another beaker filled with ethanol absolute.
6. Repeat **step 3**, and leave the box on the laboratory rocker and rock at 50 rpm for 5 min.
7. Stop the rocker, and take out the beaker with the biochips. Take the biochips out, and rinse them again with ethanol absolute. Handling the biochips one by one, place them (gold side up) on a paper towel, and dry them using airflow from an empty squeeze bottle.
8. Transfer biochips to a Petri dish and close the lid. Cover the Petri dish with aluminum foil.

3.3 PEG Activation

1. Mix 727 µL of 715 mM DCC in DMSO with 727 µL of 660 mM NHS in DMSO and 727 µL of 660 mM 4-pyrrolidinopyridine in DMSO (or dissolve 55.2 mg of NHS, 106 mg of DCC, and 7 mg of 4-pyrrolidinopyridine in 2.17 mL of DMSO; *see* **Note 7**) in a beaker.
2. Take the biochips out of the Petri dish, and immerse them one by one in the activation solution mixture prepared in **step 1**.
3. Cover the beaker with several layers of aluminum foil. Put the covered beaker inside the polystyrene box, and close the lid.
4. Place the polystyrene box on the laboratory rocker, and rock at 50 rpm for 16 h.
5. Stop the rocker, and take out the beaker with the biochips. Take biochips out, rinse them with DMSO, and immerse them into another beaker filled with DMSO.

6. Repeat **step 3**, and leave on the laboratory rocker rocking at 50 rpm for 5 min.
7. Stop the rocker, and take out the beaker with the biochips. Take the biochips out, rinse them with water, and immerse them into another beaker filled with water.
8. Repeat **step 3**, and leave on the laboratory rocker rocking at 50 rpm for 5 min.
9. Stop the rocker, and take out the beaker with the biochips. Take the biochips out one by one, and rinse them with water again.
10. Place the biochips (gold side up) on a paper towel, and dry them using airflow from an empty squeeze bottle.
11. Transfer the biochips into separate empty, labelled flacons. Tightly close the lids, and wrap the flacons with aluminum foil. Store at 4 °C (*see* **Note 8**).

3.4 Antibody Grafting

1. Take the flacon with the biochip from the fridge, and leave it for 1 h at room temperature before immobilization of antibodies. Do not remove the aluminum foil before using the biochip.
2. Prepare 6 μM antibody solution containing 5% glycerol: To each 5 μL aliquot of 1 mg/mL (~6.67 μM) solution of each antibody, add 0.5 μL of 55% glycerol. Mix thoroughly and keep on ice during the spotting of the antibodies. Afterward, store at 4 °C and mix thoroughly prior to next usage.
3. Indicate the positions to be arrayed on the transparent plastic film. Then place this plastic film on the light table. Place the biochip over the transparent plastic film in order to see where to spot.
4. Spot manually 0.2 μL droplets of anti-β-lactoglobulin and control anti-ovalbumin antibody solutions (prepared in **step 2**) onto the surface of the biochip in an array format according to the spot locations indicated on the transparent plastic film placed on the light table.
5. Put the biochip inside the Petri dish with a piece of wet paper towel inside (to ensure humidity), close the lid, and wrap it tightly with parafilm and cover with aluminum foil.
6. Leave the biochips for immobilization at 4 °C for 16 h before the SPRi experiment. If time-saving is a priority, immobilization time can be reduced (*see* **Note 9**).

3.5 Biochip - SPRi Prism Assembly

1. Clean the SPRi glass prism by spraying it with ethanol absolute and wiping with lens wipes. Thoroughly dry the prism, and insert it in the prism holder of the SPRi device.

2. Depose 1 μL (or less, *see* **Note 10**) of the refractive index matching oil on the surface of the prism, and gently slide the biochip over the prism. Ensure no air bubbles remain between the glass slide and the prism (*see* **Note 11**).

3.6 Passivation of the Biochip Surface

The free reactive NHS groups remaining after antibody grafting are passivated by reaction with L-lysine.

1. Insert the prism holder containing the prism and mounted biochip inside the SPRi device, and fix it.
2. Inject 150 μL of 1 mM L-lysine in current buffer followed by injection of 150 μL of the regeneration solution (*see* **Note 12** *for injection details*). Repeat this injection sequence three times.

3.7 SPRi Experiment

1. Prepare a 100 μg/mL stock solution of β-lactoglobulin (~5.45 μM): weigh 0.2 mg of β-lactoglobulin in a plastic vial (i.e., 2 mL plastic tube), and add 2 mL of SPRi current buffer. Mix well to dissolve the powder completely. Store at 4 °C up to 1 week and mix thoroughly prior to next use.
2. Dilute the 5.45 μM β-lactoglobulin stock solution in the SPRi current buffer to obtain the tenfold analyte dilution series 545 and 54.5 nM β-lactoglobulin (*see* **Note 13**). Store at 4 °C up to 1 week, and mix thoroughly prior to next use.
3. Define the spots as regions of interest (ROIs) in the SPRi analysis software. Set the flow rate to obtain a laminar flow in the flow cell (50 μL/min when using the SPRi-Plex device (*see* **Note 14** *for experimental setup details*). Wait for the SPRi baseline stabilization.
4. Inject 150 μL of 54.5 pM (1 μg/mL) β-lactoglobulin solution, and monitor the receptor-ligand interactions (*see* **Note 12** *for the injection details*).
5. At the end of the dissociation phase, inject 150 μL of the regeneration solution.
6. Repeat **steps 4** and **5** for successive increasing concentrations of β-lactoglobulin (*see* **Note 15**).
7. For the biochip dedicated to further MALDI analysis, the last injection of β-lactoglobulin should not be followed by the regeneration step in order to keep the captured ligand on the biochip.
8. Stop the SPRi experiment, and remove the prism holder from the SPRi. Gently remove the biochip from the prism, and dry it thoroughly with airflow (*see* **Note 16**).
9. Clean the SPRi prism by spraying it with ethanol absolute and wiping with lens wipes. Thoroughly dry the prism, and store it.

3.8 MALDI-TOF MS Experiment

1. Depose 0.11 μL of the MALDI matrix solution on each receptor spot as well as on several receptor-free locations serving as controls immediately after the biochip drying (*see* **Note 17**). The spot positions are identified after the SPRi experiment by using the transparent plastic film (figuring spot location) placed over a light table.
2. Allow the matrix to crystalize (dry) completely. Put the biochip in a labelled flacon, tightly close it, and store it at 4 °C until MALDI-TOF MS experiment (*see* **Note 18**).
3. Insert the biochip into the MALDI target plate, and introduce it into the mass spectrometer source.
4. Record mass spectra using the following set of parameters: linear mode, positive ion mode, extraction delay, 450 ns; ion source 1 (IS1) voltage, 19.5 kV; ion source 2 (IS2) voltage, 17.65 kV; lens voltage, 6.5 kV. Mass range: 5000–100,000 Da. The laser intensity should be set to just above the desorption/ionization threshold. Laser shots should be accumulated over each spot to obtain a better signal-to-noise ratio (*see* **Note 19**).
5. Eject the MALDI plate (target), and recover the biochip. Put the biochip in a labelled flacon, and store it for possible further analysis at room temperature in the absence of light.

4 Notes

1. Concentrated HCl (12 M) can be used at first to narrow the gap from the starting pH to the desired pH. From then on, it would be better to use less concentrated HCl (e.g., 6 and 1 M) to avoid a sudden drop in pH beyond the target pH value.
2. At first glance, it is difficult to identify the gold side. We recommend using glass slides with a mark, for instance, a bevelled corner in order to facilitate orientation and routine manipulations.
3. A light table and a customized plastic film with marked spot localizations are required for manual spotting and matrix deposition. Alternatively, a commercial spotter can be used; in this case, refer to the settings of the manufacturer. Keep the spot deposition scheme, indicating the position of immobilized molecules—it will be required for the definition of SPRi spots and matrix deposition as well.
4. Given the duration of the activation procedure (~20 h), it is convenient to functionalize two biochips at the same time. For that purpose, all materials (including the beaker size) were adapted for preparation of two biochips. Materials, such as beaker size and chemicals, should be readjusted for different numbers of biochips.

5. Ensure that you are handling the biochips with the gold side up all the time and that the gold-covered surface does not come into contact with any objects (wipes, beaker walls, etc.) in order to avoid any contamination or damage. Take care not to damage or scratch the gold coverage during manipulations, especially with the tweezers.
6. Parafilm is used to prevent evaporation, while aluminum foil (and, eventually, the polystyrene box) ensures protection against any photochemical reaction of the thiol function of PEG.
7. We find it most convenient to prepare separate stock solutions by accurate weighing of dry DCC, NHS, and 4-pyrrolidinopyridine in distinct plastic vials (i.e., 2 mL plastic tubes). Right before the activation step, dry products should be dissolved in the proper amount of DMSO directly in the vial. We advise to use a vortex and/or ultrasound bath (short pulses) to ensure that reagents are completely dissolved. Alternatively, DCC, NHS, and 4-pyrrolidinopyridine solutions might be prepared a few hours in advance and stored in separate tightly covered glass beakers at room temperature (25 °C) in the absence of light.
8. Activated SPRi biochips can be stored up to 1 month at 4 °C, protected from humidity and in the absence of light.
9. 2 hours is the minimum required time. If time-saving is not a priority, immobilization time can be extended for better results.
10. The volume of the refractive index matching oil required for the efficient adhesion of the biochip to the prism depends strongly on the viscosity of the oil and the surface to be covered, so it should be adapted for each particular case. The volume should be sufficient to completely fill the space without air bubbles between the prism and the biochip, but not in excess to avoid oil bleed at the prism sides.
11. We suggest deposing the oil in a line shape, rather than droplet, and start sliding the biochip over the surface. We have found that relatively viscous oil deposition near the short side of the prism and slow sliding along the surface result in optimal coverage without air bubbles.
12. Each injection consists of two phases of distinct lengths: an association phase (~5 min at a 50 µL/min flow rate) and a dissociation phase (~15–30 min at a 50 µL/min flow rate), successively. The length of each phase depends on the SPRi system design and receptor-ligand couple used; thus, it should be adapted for each particular case.

13. For protein serial dilution, we recommend the use of plastic tubes with volumes slightly superior to the syringe volume used for protein loading into the flow cell. For example, the use of 2 mL plastic tubes combined with 1 mL syringe will allow the highest recovery of the solution from the bottom of the vial.
14. We are using an SPRi system with a hexagonal-shaped flow cell. It was maintained at 25 °C, and the flow rate was fixed at 50 μL/min across all experiments. The flow rate should be adapted depending on the SPR system used: it should be neither fast, nor mass transport limited, to permit efficient monitoring of molecular interactions.
15. We have found that additional injection of current buffer prior to the next analyte injection maintains the cleanliness of the loop and ensures that the obtained SPRi response is produced by the analyte interactions with the immobilized receptors only.
16. At this stage, it is possible to include a direct on-chip trypsin digestion step in order to ascertain the identification of the affinity-captured antigen protein. It is performed by directly dropping the trypsin protease on each spot of the biochip followed by MALDI-TOF MS identification of the resulting peptides according to [18, 21].
17. Control MALDI matrix spots should be located both inside and outside the SPRi flow cell area in order to control the efficiency of the surface chemistry passivation.
18. We strongly recommend performing MS analysis immediately after matrix deposition and drying. Nevertheless, storage at 4 °C in the dark for up to 1 week is also acceptable. Beyond this period, the efficiency (sensitivity) of MS analysis is seriously decreased, likely due to protein degradation.
19. We suggest accumulating hundreds of shots per spot to obtain a clear mass spectrum.

Acknowledgments

Authors are indebted to Dr. D. Lebeau for access to the MALDI-TOF/TOF MS instrument (Den-Service d'Etude du Comportement des Radionucléides, CEA, Paris-Saclay University, France); A. H. acknowledges fellowships from Université d'Evry—Paris Saclay and Région Ile-de France (Dim Analytics).

References

1. Karlsson R, Michaelsson A, Mattsson L (1991) Kinetic analysis of monoclonal antibody-antigen interactions with a new biosensor based analytical system. J Immunol Methods 145(229–240):229–240
2. Homola J (2003) Present and future of surface plasmon resonance biosensors. Anal Bioanal Chem 377(3):528–539
3. Wassaf D et al (2006) High-throughput affinity ranking of antibodies using surface plasmon resonance microarrays. Anal Biochem 351(2): 241–253
4. Homola J (2008) Surface plasmon resonance sensors for detection of chemical and biological species. Chem Rev 108(2):462–493
5. Nogues C, Leh H, Langendorf CG, Law RHP, Buckle AM, Buckle M (2010) Characterisation of peptide microarrays for studying antibody-antigen binding using surface plasmon resonance imagery. PLoS One 5(8):1–7
6. Nogues C, Leh H, Lautru J, Delelis O, Buckle M (2012) Efficient antifouling surface for quantitative surface plasmon resonance based biosensor analysis. PLoS One 7(9):e44287
7. Nedelkov D, Nelson RW (2001) Analysis of native proteins from biological fluids by biomolecular interaction analysis mass spectrometry (BIA/MS): exploring the limit of detection, identification of non-specific binding and detection of multi-protein complexes. Biosens Bioelectron 16(9–12):1071–1078
8. Gilligan JJ, Schuck P, Yergey AL (2002) Mass spectrometry after capture and small-volume elution of analyte from a surface plasmon resonance biosensor. Anal Chem 74(9): 2041–2047
9. Boireau W, Rouleau A, Lucchi G, Ducoroy P (2009) Revisited BIA-MS combination: entire 'on-a-chip' processing leading to the proteins identification at low femtomole to sub-femtomole levels. Biosens Bioelectron 24(5):1121–1127
10. Xue J, Bai Y, Liu H (2019) Hybrid methods of surface plasmon resonance coupled to mass spectrometry for biomolecular interaction analysis. Anal Bioanal Chem 411(17): 3721–3729
11. Krone JR, Nelson RW, Dogruel D, Williams P, Granzow R (1997) BIA/MS: interfacing biomolecular interaction analysis with mass spectrometry. Anal Biochem 244(1):124–132
12. Jansson Ö, Larsericsdotter H, Zhukov A, Areskoug D, Oscarsson S, Buijs J (2006) Optimizing the surface plasmon resonance/mass spectrometry interface for functional proteomics applications: how to avoid and utilize nonspecific adsorption. Proteomics 6:2355–2364
13. Bouffartigues E, Leh H, Anger-Leroy M, Rimsky S, Buckle M (2007) Rapid coupling of Surface Plasmon Resonance (SPR and SPRi) and ProteinChip™ based mass spectrometry for the identification of proteins in nucleoprotein interactions. Nucleic Acids Res 35(6):e39
14. Stigter ECA, de Jong GJ, van Bennekom WP (2009) Development of an on-line SPR-digestion-nanoLC-MS/MS system for the quantification and identification of interferon-γ in plasma. Biosensor Bioelectron 24(7): 2184–2190
15. Zhang Y et al (2015) Interface for online coupling of surface plasmon resonance to direct analysis in real time mass spectrometry. Anal Chem 87(13):6505–6509
16. Joshi S, Zuilhof H, van Beek TA, Nielen MWF (2017) Biochip spray: simplified coupling of surface plasmon resonance biosensing and mass spectrometry. Anal Chem 89(3): 1427–1432
17. Nedelkov D (2007) Development of surface plasmon resonance mass spectrometry array platform. Anal Chem 79(15):5987–5990
18. Bellon S et al (2009) Hyphenation of surface plasmon resonance imaging to matrix-assisted laser desorption ionization mass spectrometry by on-chip mass spectrometry and tandem mass spectrometry analysis. Anal Chem 81(18):7695–7702
19. Remy-Martin F et al (2012) Automated cancer marker characterization in human plasma using SUrface PLASMON Resonance in Array combined with Mass Spectrometry (SUPRA-MS). Procedia Chem 6:11–19
20. Stigter ECA, de Jong GJ, van Bennekom WP (2013) Coupling surface-plasmon resonance and mass spectrometry to quantify and to identify ligands. TrAC—Trends Anal Chem 45:107–120
21. Musso J et al (2015) Biomarkers probed in saliva by surface plasmon resonance imaging coupled to matrix-assisted laser desorption/ionization mass spectrometry in array format. Anal Bioanal Chem 407(5):1285–1294
22. Przybylski C et al (2020) Surface plasmon resonance imaging coupled to on-chip mass spectrometry: a new tool to probe protein-GAG interactions. Anal Bioanal Chem 412:507–519

Chapter 6

Multiplexed Protein Biomarker Detection with Microfluidic Electrochemical Immunoarrays

Abby Jones, Patricia Czarnecki, Lasangi Dhanapala, and James F. Rusling

Abstract

Electrochemistry is a multidisciplinary field encompassing the study of analytes in solution for detection and quantification. For the medical field, this brings opportunities to the clinical practice of disease detection through measurements of disease biomarkers. Specifically, panels of biomarkers offer an important future option that can enable physicians' access to blood, saliva, or urine bioassays for screening diseases, as well as monitoring the progression and response to therapy. Here, we describe the simultaneous detection of eight protein cancer biomarkers in a 30-min assay by a microfluidic electrochemical immunoarray.

Key words Layer-by-layer, Amperometry, ELISA, Protein detection, Biomarkers, Immunoarray, Microfluidics

1 Introduction

Conventional means of measuring proteins include enzyme-linked immunosorbent assays (ELISA) [1], electrophoretic immunoassays [2], mass spectrometry-based proteomics [3], and radioimmunoassays [4]. Modern commercial approaches have typical limits of detection (LOD) around 1–20 pg/mL for proteins and include Meso Scale Discovery®Electrochemiluminescence (MSD-ECL) [5] and Luminex [6] fluorescent bead systems for proteins that cost $150–200k. Quansys Q-Plex™ multiplexed ELISA [7] is lower cost, but not automated. Simoa HD-1 [8] single protein counting (Quanterix) detects proteins with excellent LODs of 4–70 fg/mL, but hardware currently costs $180 K [9]. Thus, existing techniques are expensive, require fully trained technicians due to complexity, often use large sample volumes, and are time consuming with sometimes insufficient sensitivity. Over the past 20 years, research has shown that measurements of panels of biomarkers offer reliable diagnostics with early detection capabilities, improved therapy

Kelly C. Whittaker and Ruo-Pan Huang (eds.), *Antibody Arrays: Methods and Protocols*, Methods in Molecular Biology, vol. 2237, https://doi.org/10.1007/978-1-0716-1064-0_6,

outcomes, and decreased mortality [10, 11]. Electrochemistry is well suited for the detection of protein panels as it offers advantages of scalability, low cost, facile sensor preparation, and high sensitivity and specificity with the ability to reach ultra-low detection limits [12, 13].

By utilizing layer-by-layer multilayer films fashioned by electrostatic binding, densely decorated nanoparticle-coated electrodes can be fabricated. Their conductive surfaces, at a specified voltage, enable fast electron transfer to and from the redox enzymes, offering a sensitive, versatile biosensor platform [14]. Here, we describe the experimental details of a simple, easily, and cheaply fabricated microfluidic electrochemical immunoarray for the rapid measurement of eight protein biomarkers in serum. The system features a syringe pump, 4-port switching valve, manual injector, and dual channel microfluidic device. The device is fabricated with two flat poly(methylmethacrylate) (PMMA) plates and channels molded using polydimethylsiloxane (PDMS) [15]. Upon optimizing the conditions of the assay, four biomarkers were detected simultaneously proceeded by another four biomarkers with a total system assay time of 30 min and detection limits below 1 fg/mL.

2 Materials

Prepare all solutions using ultrapure water (water purified with a Hydro Nanopure system or equivalent). Prepare and store all reagents at room temperature, unless indicated otherwise. Follow all waste disposal regulations when disposing of waste materials.

2.1 Preparation of Immunoassays

1. Petri dishes.
2. 5¾″ Pasteur pipettes.
3. Phosphate-buffered saline (PBS) buffer: 0.12 M sodium chloride, 2.7 mM potassium chloride, 0.0059 M sodium phosphate dibasic, 0.0039 M sodium phosphate monobasic, pH 7.4 ± 0.1. Weigh out and add 24.82 g sodium chloride, 0.7240 g potassium chloride, 3.015 g sodium phosphate dibasic, and 1.987 g sodium phosphate monobasic directly to a 3.6 L glass bottle. Add 3.0 L of water to the bottle, mix and adjust pH with sodium hydroxide (*see* **Note 1**). Make up to 3.6 L with water. Filter solution using 0.22 μm PES Bottle Top filter.
4. PBS buffer Tween-20 (PBS-T20): 0.12 M sodium chloride, 2.7 mM potassium chloride, 0.0059 M sodium phosphate dibasic, 0.0039 M sodium phosphate monobasic, and 0.05% Tween-20, pH 7.4 ± 0.1. Weigh out and add 24.82 g sodium chloride, 0.7240 g potassium chloride, 3.015 g sodium phosphate dibasic, and 1.987 g sodium phosphate monobasic directly to a 3.6 L glass bottle. Add 3.0 L of water to the bottle,

mix and adjust pH with sodium hydroxide (*see* **Note 1**). Make up to 3.6 L with water. Filter solution using 0.22 μm PES Bottle Top filter. Add 1.8 mL of Tween-20 to the filtered solution and mix.

5. 2% Bovine serum albumin (BSA): Weigh out 0.2 g of BSA and add to a conical vial. Add 10 mL water to the BSA and secure on a shake plate until completely in solution. Store at 4 °C.
6. 0.01% BSA: Add 50 μL of 2% BSA to 4.95 mL of water in a conical vial. Store at 4 °C.
7. Poly(diallyldimethylammonium chloride) PDDA: 2 mg/mL PDDA, 0.5 M sodium chloride. Weigh out 0.0585 g sodium chloride, add 1.8 mL of water and mix. Add 200 μL PDDA, mix and store at 4 °C.
8. Glutathione gold nanoparticles (GSH-AuNPs): 5 nm GSH-AuNPs in 20 mM HEPES buffer [16].
9. 1-(3-(Dimethylamino)propyl)-3-ethylcarbodiimide hydrochloride (EDC): 400 mM EDC in water. Weigh out 0.0383 g of EDC (*see* **Note 2**).
10. *N*-hydroxysulfosuccinimide (Sulfo-NHS): 100 mM Sulfo-NHS in water. Weigh out 0.0109 g of Sulfo-NHS (*see* **Note 2**).
11. 8 Electrode carbon screen-printed electrode arrays (700 μm thick) (Kanichi Research Services Ltd.).
12. Hydroquinone (HQ, ≥99%): 1 mM HQ. Weigh out 0.011 g HQ, dissolve in 1 mL of nitrogen gas purged PBS buffer, add to 100 mL of nitrogen gas purged PBS buffer.
13. Hydrogen peroxide (H_2O_2, 30%): 0.1 mM H_2O_2 in water. Add 10 μL H_2O_2 to 990 μL of water, vortex and store at 4 °C.
14. Streptavidin poly-HRP: 2 μg/mL streptavidin poly-HRP in 0.01% BSA. Add 4 μL of streptavidin poly-HRP to 996 μL of 0.01% BSA, vortex and store at 4 °C.
15. Sterile filtered bovine calf serum.
16. Kim wipes.
17. Parafilm.
18. 0.6 and 1.5 microcentrifuge tubes.
19. 150 mL glass jar.
20. Aluminum foil.

2.2 Microfluidic System (Fig. 1)

1. PEEK Tubing: 1/16″ OD × 0.010″ ID.
2. PEEK Tubing: 1/16″ OD × 0.005″ ID.
3. Low pressure 4-port switching valves, bulkhead version.
4. VacuTight Ferrule Tefzel™.
5. RheFlex® Fittings, PEEK 1/16″.

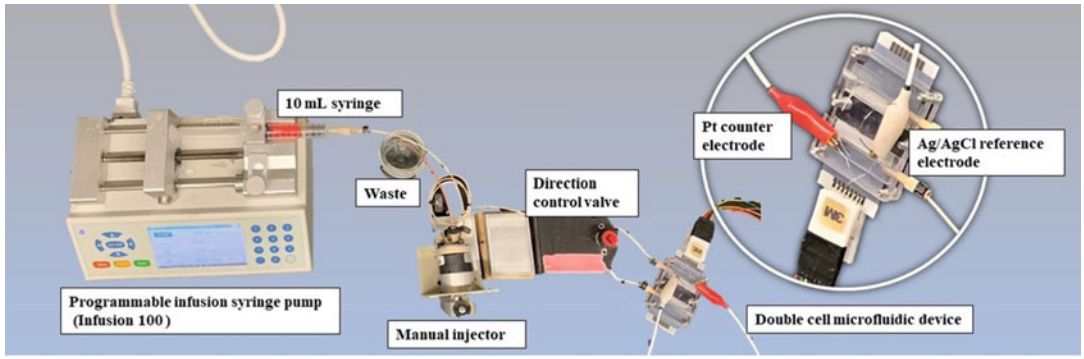

Fig. 1 Microfluidic system showing attachment of all individual pieces

6. Analytical PEEK valve with sensing switch (9725i).
7. Harvard Apparatus Pump 33.
8. 10 mL syringes.
9. 1 mL syringes.
10. 3M IC Test clip 16 Pin.
11. Alligator clips.
12. Breadboard jumper wires.
13. Electrical tape.

2.3 Antigens and Conjugates

1. Purified monoclonal antibody, polyclonal antibody, and recombinant protein.

2.4 Detection Chamber

1. Sylgard 184 Silicone Elastomer Kit: 10 parts base to 1 part curing agent. Use this kit to form the polydimethylsiloxane (PDMS) channels for the detection chambers.
2. Poly(methyl methacrylate) (PMMA) machine shop cut and adapted for a conjunction of two cells housing two reference and counter electrode setups, in addition to, two inlets and two outlets (Fig. 2).

3 Methods

Carry out procedures at room temperature unless specified otherwise.

3.1 Preparation of Modified Arrays

1. Prepare humidity chambers: Fold a Kim wipe into 1/4th its original size, place into a petri dish, and dampen the Kim wipe with water (*see* **Note 3**).
2. Prepare arrays for modification: Wash with high purity water and dry completely under nitrogen. Cut the arrays by removing the outer edge of the sheet for each individual array (*see* **Note 4**). Place the cut arrays into individual humidity chambers.

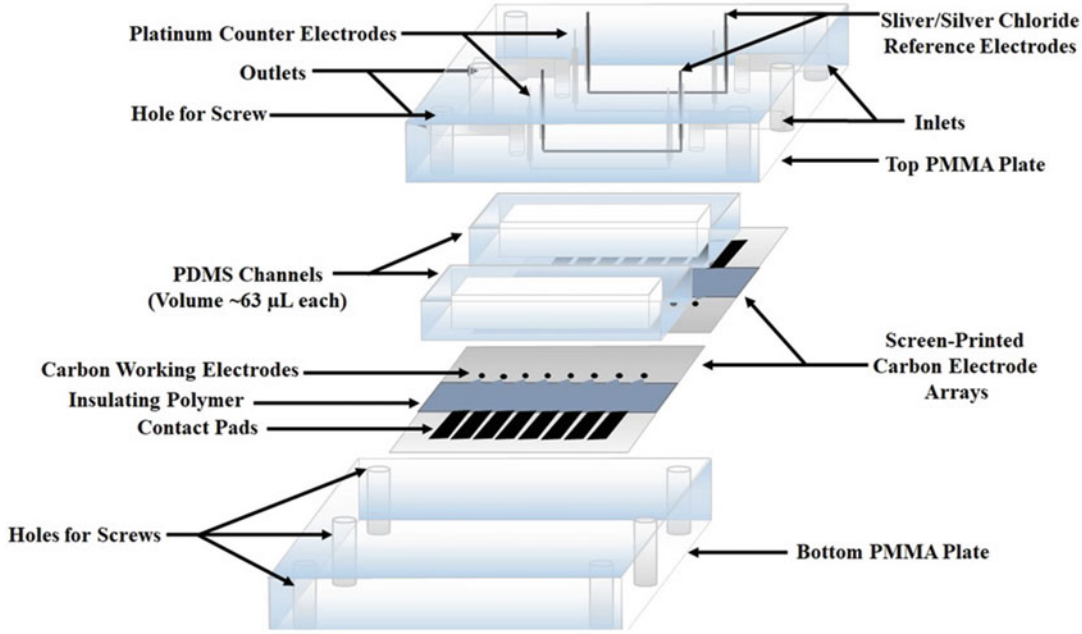

Fig. 2 Components of the microfluidic device made of micro-machined PMMA, PDMS microfluidic channel, and screen-printed carbon 8-electrode arrays

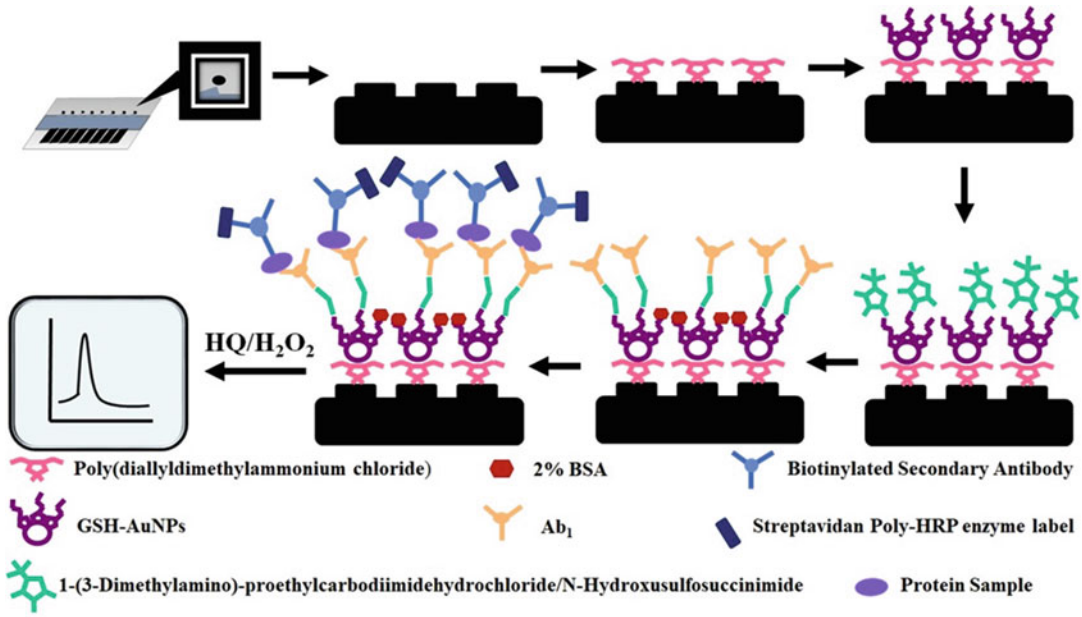

Fig. 3 Strategy for electrochemical detection by amperometric immunosensors

3. Spot approximately 1.5 µL of 2 mg/mL PDDA onto each individual electrode (*see* **Note 5**) (Fig. 3).
4. Incubate all arrays for 20 min in their humidity chambers.

5. Wash arrays twice using a Pasteur pipette with high purity water (*see* **Note 6**).
6. Dry each array under nitrogen (*see* **Note 7**).
7. Spot approximately 1.5 μL of GSH-AuNPs onto each individual electrode.
8. Incubate all arrays for 20 min in their humidity chambers.
9. During the GSH-AuNPs incubation, weigh out EDC and Sulfo-NHS in individual microcentrifuge tubes (*see* **Note 2**).
10. Repeat the washing and drying procedure (**steps 5** and **6**).
11. Add 500 μL of water to EDC and mix with a vortex.
12. Transfer the EDC solution to the Sulfo-NHS microcentrifuge tube and mix with a vortex.
13. Spot approximately 1.5 μL of the EDC/Sulfo-NHS mixture onto each individual electrode.
14. Incubate all arrays for 10 min in their humidity chambers.
15. Repeat washing and drying procedures (**steps 5** and **6**).
16. Spot approximately 1.5 μL of primary antibody (Ab_1) to each electrode. Two electrodes are designated for each antibody (Ab): Ab1—electrodes 1 and 2, Ab2—electrodes 3 and 4, Ab3—electrodes 5 and 6, Ab4—electrodes 7 and 8.
17. Store all modified arrays at 4 °C to incubate overnight (18–24 h).
18. Prepare 0.01% and 2% BSA and store at 4 °C (*see* **Note 8**).

3.2 Multiplexed Detection

1. Measure 100 mL of PBS buffer, using a graduated cylinder, and pour into a 150 mL glass jar, cover with Parafilm, and surround the jar with aluminum foil (*see* **Note 9**). Purge under nitrogen in a Styrofoam container of ice.
2. Block arrays that have been incubated overnight at 4 °C by washing the arrays twice using a Pasteur pipette with PBS-T20 (follow the technique described in **Note 6**). Using a Kim wipe, remove excess buffer around the electrodes (*see* **Note 10**) and add approximately 50 μL of 2% BSA to the electrodes using a Pasteur pipette.
3. Incubate the arrays, in their humidity chambers, at 4 °C for 1 h.
4. Prepare 0.1 mM H_2O_2.
5. Prepare 2 μg/mL streptavidin poly-HRP.
6. Prepare the secondary antibody mixture for Chamber 1: Allow antibodies to thaw at room temperature. Add the optimized concentrations of each secondary antibody to a 1.5 mL microcentrifuge tube and bring to volume with 0.01% BSA. Vortex for 25 s and store at 4 °C.
7. Repeat **step 6** for biomarkers in Chamber 2.

8. Prepare 5 times diluted bovine calf serum: Add 4 mL of PBS buffer to a 10 mL glass vial followed by the addition of 1 mL bovine calf serum. Vortex for 25 s and store at 4 °C.
9. Prepare the antigen mixture from known concentrations of clinical interest for Chamber 1. First allow the antigens to thaw at room temperature. Add the volume of each corresponding antigen to the 0.6 mL microcentrifuge tube and bring to a final volume of 500 μL with 5× bovine calf serum. Vortex for 25 s and store at 4 °C.
10. Prepare a serial dilution of the antigen mixture below that of the concentrations of interest in 0.6 mL microcentrifuge tubes. Store all dilutions at 4 °C.
11. Repeat **steps 9** and **10** for biomarkers used in Chamber 2.
12. Prepare 1 mM Hydroquinone: To a 1.5 mL microcentrifuge tube weigh out 0.011 g of hydroquinone. To the hydroquinone add 1 mL of PBS buffer that has been purging under nitrogen for at least 30 min. Vortex the hydroquinone for 1 min or until all the hydroquinone has gone into solution. Add the dissolved hydroquinone solution back into the purging PBS solution and continue to purge under nitrogen (*see* **Note 11**).
13. Once the 1 h timer has gone off for the blocked arrays, rinse the blocked arrays twice with PBS-T20 using a Pasteur pipette (follow the technique described in **Note 6**). Dry excess solution around the electrodes using a Kim wipe (*see* **Note 10**). Add approximately 50 μL of PBS-T20 to each dried array, ensuring all electrodes have solution covering them. Store the arrays inside their humidity chambers at 4 °C until use.
14. Place the first two arrays in the cell and attach to the system:
    (a) Place the two PDMS microfluidic channels on the top PMMA plate such that the counter and reference electrodes and the cell inlet and outlet ports are centered inside the channel (*see* **Note 12**).
    (b) Place the two arrays on the bottom PMMA plate so that the electrodes face towards each other on opposite sides. Next set the top PMMA plate on top of the arrays with the electrodes centered in between the counter and reference electrodes (*see* **Notes 13** and **14**).
    (c) Carefully tighten the screws such that the system components are held in place (*see* **Note 15**).
    (d) Attach the assembled microfluidic cell to the system with VacuTight™ Ferrels and RheFlex® Fittings.
15. Fill the double cell detection chambers housing the modified arrays with PBS-T20 pumping at a rate of 100 μL/min. Check for any air bubbles that may have entered the system and remove (*see* **Notes 16** and **17**).

16. Remove the Ab_2 corresponding to Chamber 1, control (5× bovine calf serum) and streptavidin poly-HRP from 4 °C and vortex each for approximately 10 s.
17. To a 0.6 mL microcentrifuge tube, add 50 μL of Ab_2, 50 μL of the control and 50 μL of streptavidin poly-HRP (*see* **Notes 18** and **19**). Vortex for 10 s.
18. Repeat **steps 16** and **17** for Ab_2, control and poly-HRP corresponding to Chamber 2.
19. Start flow of PBS-T20 to Chamber 1 and load the mixture prepared in **step 17** (*see* **Notes 20** and **21**).
20. Inject Chamber 1 solution at a flow rate of 100 μL/min for 1 min (*see* **Note 22**).
21. Start a timer for a 10-min incubation (*see* **Note 23**).
22. Return the Analytical PEEK valve to the load position and wash the loop three times with PBS-T20.
23. After 4 min change the position of the switching valve to Chamber 2, load the mixture prepared in **step 18**, and inject at a flow rate of 100 μL/min for 1 min.
24. Incubate for 20 min (*see* **Notes 24**–**26**).
25. Repeat **step 22**.
26. After a 10-min incubation, place a Kim wipe back into the Chamber 1 outlet and wash Chamber 1 with PBS-T20 for 2 min at a flow rate of 100 μL/min (*see* **Note 27**).
27. Prepare the H_2O_2/HQ mixture: To a 10 mL glass vial, add 10 mL of 1 mM HQ (prepared in **item 12** of Subheading 2.1) and 10 μL 0.1 mM H_2O_2. Vortex and store on ice.
28. Change the syringe from PBS-T20 to purged HQ and wash Chamber 1 for 2 min at 100 μL/min or until any air bubbles have appeared (*see* **Note 28**).
29. Continue the flow of purged HQ to Chamber 1 and attach the 3M clip that leads to Chamber 1s' array, counter, and reference electrodes (*see* **Notes 29**–**31**).
30. For the first array only, run a cyclic voltammetry (CV) test to determine that the HQ has reached the electrodes properly and characteristic peaks are observed (Fig. 4).
31. Play the CHI and allow the current to baseline (this will take approximately 50 s).
32. Stop the CHI followed by restarting it and allow the current to continue for 30–40 s before injecting the H_2O_2/HQ mixture and obtain an amperometric curve (total detection time will be approximately 400 s).
33. Save the amperometric curve of Chamber 1's control (Fig. 5) (*see* **Note 32**).

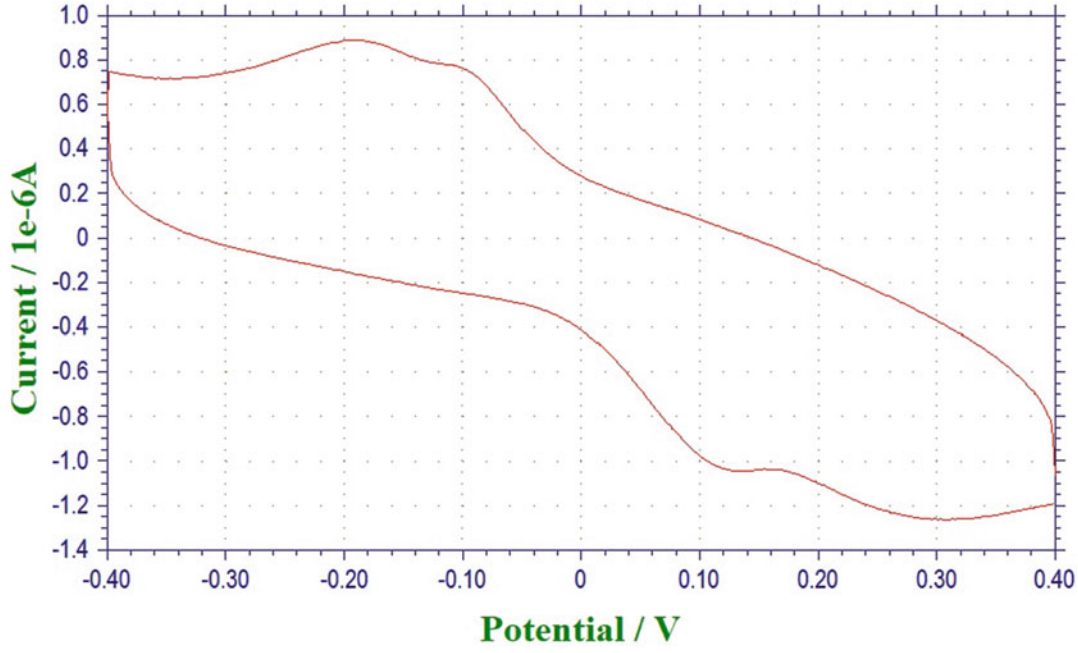

Fig. 4 Representative CV of HQ once it has reached the immune-decorated electrode

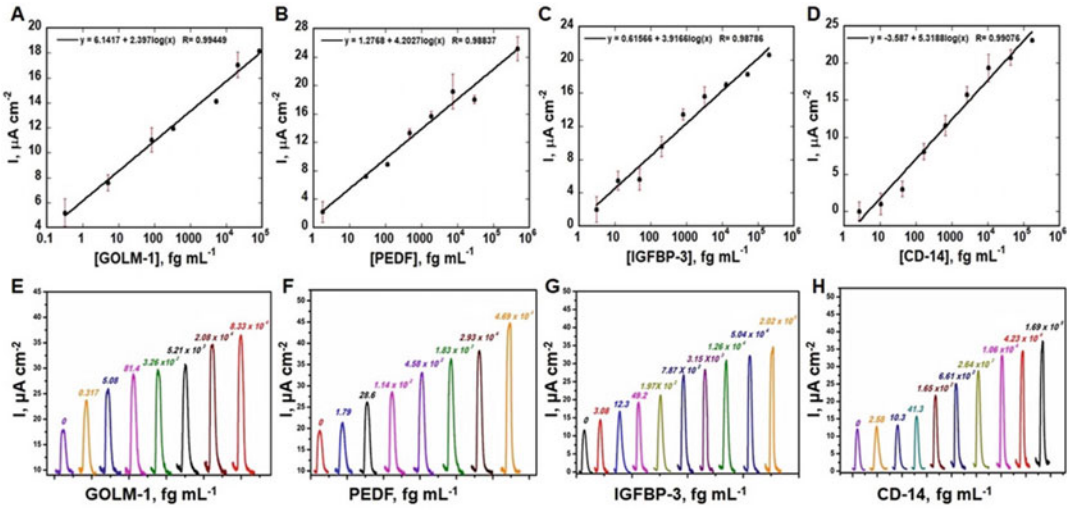

Fig. 5 Amperometric responses for Chamber 1 mixtures at −0.2 V vs Ag/AgCl developed by injecting 1 mM hydroquinone and 0.1 mM H_2O_2 after capturing analyte protein-Ab_2-poly-HRP bioconjugates on the electrodes in the microfluidic device, for (**a**) GOLM-1, (**b**) PEDF, (**c**) IGFBP-3, and (**d**) CD-14, $n = 2$. Immunoarray calibration plots of standards in diluted serum for (**e**) GOLM-1, (**f**) PEDF, (**g**) IGFBP-3, and (**h**) CD-14

34. Change the solution back to PBS-T20 and wash Chamber 1 at a flow rate of 1500 μL/min for 20 s.
35. Stop the PBS-T20 flow, return the flow rate to 100 mL/min, and switch the valve to Chamber 2.
36. Once the 20-min incubation (**step 24**) is complete for Chamber 2, repeat **steps 25–33** (*see* **Note 33**).
37. Remove the cell and wash with PBS-T20 followed by water, dry completely under nitrogen (*see* **Note 34**).
38. Wash the analytical PEEK valve 5 times with water followed by PBS-T20.
39. Wash the system with 5 mL of PBS-T20 at a flow rate of 1500 μL/min. Washing includes both Chamber 1 and 2 in the load position of the analytical PEEK valve.
40. Repeat procedure for remaining samples (*see* **Note 35**).

4 Notes

1. Remember to always calibrate the pH meter before use.
2. EDC and Sulfo-NHS can be weighed out at any step in the preparation of modified arrays (Subheading 3.1) into individual tubes, but water should not be added until immediately before use due to instability of this solution.
3. When preparing the humidity chambers, do not add too much water to the Kim wipe/paper towel, only enough to dampen. Adding too much water increases the risk of accidentally sloshing material off that has been spotted on the array.
4. Kanichi arrays come in a sheet of four. When cutting individual arrays, remove the outer gray edge only as removal of extra will result in gaps in the channel when sealing the device. This causes an incomplete seal, and solution will leak out. Also, make sure to be conscious of the placement of fingers when cutting and to touch only the edges of the arrays, never touch the electrodes directly.
5. Make sure when pipetting solution onto the individual electrodes that the solutions stay is separated and do not run into each other. If you are having difficulty with the material, rewash and dry the array and start over.
6. When washing the arrays after incubation steps, remember to never wash the electrodes directly. Wash above the electrode and allow the water or PBS-T20 to flow down over the electrodes.
7. Drying the electrodes under nitrogen requires a very soft flow. Blow on your wrist like you're trying to cool down hot food.

What your breath feels like on your wrist is what the nitrogen flow should feel like also. Use this flow as a guide for drying your arrays.

8. BSA solutions can be made a day before use as BSA takes time to go into solution and the day of running assays gets busy.
9. Purging the PBS buffer is the absolute first thing to do when preparing for detection. This is to ensure the buffer has purged as much as possible before use, as the HQ is unstable in the presence of oxygen.
10. When wiping the arrays, make sure to not wipe the electrodes. Create a rectangle around the electrodes by removing excess solution with a Kim Wipe. This will concentrate the 2% BSA, for blocking, and the PBS-T20, for storage, over the electrodes.
11. Hydroquinone is toxic, a health hazard, hazardous to the aquatic environment and corrosive to metals. Ensure all required PPE is worn when weighing out and using this chemical. Ensure complete mixture into solution before addition to the purged PBS buffer. Make sure to put used HQ into a secondary hazardous waste container at the end of the run, do not reuse for the next arrays. Once all experiments are completed, place all HQ into a primary hazardous waste container that has been properly labeled and stored.
12. Press the PDMS slabs gently into the PMMA cell, so they will not move while arranging arrays.
13. Do not wipe the electrodes on the PDMS, this has the potential to alter your fabricated layers and result in questionable results.
14. If multiplexing, it is especially important to ensure you place the array into the cell the same way every time (e.g., place the array into the device so the electrodes are read $1 \rightarrow 8$ every time). This will reduce cross reactivity and minimize your standard deviation.
15. Now that the arrays are properly placed in their respective channels, it is time to secure the top and bottom PMMA plates. It is important to not overtighten the chambers as this can result in the internal counter and reference electrodes touching. It is also important that the chambers are not too loose as this will result in leaks. One of the best ways to get a complete seal is to take a narrow micro spatula, hold it at the end with your thumb and pointer fingers and twist the first screw until it just starts to bring the PMMA plates together. Then go diagonally across the cell and do the same with that screw. Continue until all screws have been loosely tightened. Return to the first screw and tighten just as before until the screw will not move. Repeat tightening procedure with the remaining screws.

16. Pump settings are critical when running these experiments. Ensure all settings are correct before use, make sure you understand how the pump works whether you are using a manual or automated pump. Specific settings to check before starting are syringe diameter, flow rate, and whether the pump is pumping forward or in reverse.
17. When running solution through the chambers, make sure you place a Kim Wipe in the outlet to avoid flooding of the cell.
18. When preparing the injection solution, there is a specific order to add the materials to the microcentrifuge tube for a simultaneous injection: first Ab_2, second Sample (standard/patient), and third Poly-HRP.
19. Make more of the injection solution than will fill the loop (e.g., 100 μL loop, make 120–150 μL mixture). This will minimize the potential for an air bubble to be introduced into the system.
20. There are a number of different syringes in use for the addition of various solutions needed. Organize all syringes to reduce cross contamination. Color coding them with different colored tape is one of the easiest ways or to organize them.
21. Remove all bubbles from the injection solution before injecting it into the loop. If all the bubbles are not removed, this can introduce air bubbles to the cell and diminish binding to the electrodes.
22. When injecting the detection solution, make sure it is completed in one fluid motion and not "choppy," this will introduce unwanted air bubbles. "Choppy" injections feel like driving over a rumble strip and usually occur when your injector valve needs to be greased.
23. During the 10- and 20-min incubation periods, remove the Kim Wipe from the outlets to avoid wicking away of any of the sandwich assay materials.
24. Timing, if using a manual pump, is critical because you need to be conscious that your incubation and washing steps are made for the same time, every time. It is easy to set a timer, walk away, and go do something else while waiting for the timer to go off, but this also increases your chances of missing the timer going off and allowing extra incubation or washing time that other arrays will not get. This will cause fluctuations in your detection resulting in inconsistent current measurements and increased standard deviation.
25. Timing between injections should be made long enough, so the transition from detection in Chamber 1 to washing in Chamber 2 is seamless. Detection usually takes around 5 min, but there is always a chance something could go wrong and take longer so leave enough time for the unexpected.

26. Make sure to pay attention to the direction of your switching valve as you need to change the direction of it during each injection, washing, and detection steps. Also, remember to change direction during incubation times, so there is no flow to either chamber.
27. Forgetting to place the Kim Wipe back in the outlet will result in overflow/back flow and hinder the signal.
28. When attaching the HQ syringe, air is usually introduced to the system and proceeds to introduce bubbles to the chamber, so always check the chamber for bubbles before attaching the leads and detecting, as the bubbles will muddle the signal.
29. Attachment of 3M clip: Do not forget that the pin side which has jumper wires attached needs to be clipped to the array. Otherwise there will be no current flow, and no signal will appear.
30. Attachment and detachment of leads: Attach the reference lead first followed by the counter lead. Detach the counter lead first and then the reference lead. This is because the counter electrode is platinum and very fragile. By attaching it last and detaching it first, we have seen it reduces the chance of breakage and extends the wires use.
31. Never get the jumper wires wet! They will stop working, and you will need to replace all of them.
32. We aimed to detect signals of clinical interest by establishing calibration curves of protein standards in five times diluted calf serum in PBS buffer. Calf serum is an acknowledged surrogate for human serum as they have similar total protein concentration (4.0–9.0%), as reported by the manufacturer (Sigma-Aldrich). Calibrations for protein biomarkers in Chamber 1 are shown in Fig. 5, generating dynamic ranges spanning over three orders of magnitude from low fg/mL to ng/mL. Detection limits for Chamber 1 ranged from 0.317 to 3.08 fg/mL with sensitivities ranging from 2.36 to 5.32 μA/cm^2/[log C]Please check if the unit "μA/cm^2/[log C]" is presented correctly.
33. Detection limits for Chamber 2 ranged from 0.270 to 2.72 fg/mL with sensitivities ranging from 3.69 to 6.10 μA/cm^2/[log C].
34. Do not place the top PMMA plate wire side down as this can break the wires.
35. Once all the assays have been run, clean the entire system fully with PBS-T20 and water. Cleaning will be a 10 mL wash at 1500 μL/min of PBS-T20 to Chamber 1 in the load position followed in the inject position of the analytical PEEK valve. Repeat PBS-T20 wash to Chamber 2. Then repeat the entire washing procedure with water. Ensure water is the final wash as leaving PBS-T20 in the system can result in the growth of bacteria.

References

1. Santo S, Murakami A, Kuwajima A, Takehara K, Mimori T, Kawakami A, Mishima M, Suda T, Seishima M, Fujimoto M (2016) Clinical utility of an enzyme-linked immunosorbent assay for detecting anti-malanoma differentiation-associated gene 5 autoantibodies. PLoS One 11:e0154285
2. Moser AC, Hage DS (2008) Capillary electrophoresis-based immunoassays: principles and quantitative applications. Electrophoresis 16:3270–3295
3. Angel TE, Aryal UK, Hengel SM, Baker ES, Kelly RT, Robinson EW, Smith RD (2012) Mass spectrometry-based proteomics; existing capabilities and future directions. Chem Soc Rev 10:3912–1928
4. Smith JA (2006) Solution radioimmunoassay of proteins and peptides. Curr Protoc Mol Biol Chapter 10:Unit 10.24
5. BioAgilytix (2019) Meso Scale Discovery®Electrochemiluminescence (MSD-ECL). http://www.bioagilytix.com/landing-pages/meso-scale-discovery-electrochemiluminescence/. Accessed 11 Jul 2019
6. ThermoFisher Scientific (2019) Luminex Technology Multiplex Assays. https://www.thermofisher.com/us/en/home/life-science/protein-biology/protein-assays-analysis/luminex-assays.html. Accessed 11 Jul 2019
7. Quansys Biosciences (2019) Multiplex Assays http://quansysbio.com/multiplex/multiplex-assays/. Accessed 11 Jul 2019
8. Rissin DM, Kan CW, Campbell TG, Howes SC, Fournier DR, Song L, Piech T, Patel PP, Chang L, Rivnak AJ, Ferrell EP, Randall JD, Provuncher GK, Walt DR, Duffy DC (2010) Single-molecule enzyme-linked immunosorbent assay detects serum proteins at subfemtomolar concentrations. Nat Biotechnol 28:595–600
9. Rissin DM, Kan CW, Song L, Rivnak AJ, Fishburn MW, Shao Q, Piech T, Ferrell EP, Meyer RE, Campbell TG, Fournier DR, Duffy DC (2013) Multiplexed single molecule immunoassays. Lab Chip 13:2902–2911
10. Weinstein B, Joe AK (2006) Mechanisms of disease: oncogene addiction—a rationale for molecular targeting in cancer therapy. Nat Clin Pract Oncol 3:448–547
11. Cohen FD, Li L, Wang Y, Thoburn C, Afsari B, Danilova L, Douville C, Javed AA, Wong F, Mattox A, Hruban RH, Wolfgang CL, Goggines MG, Molin MD, Wang T, Roden R, Klein AP, Ptak J, Dobbyn L, Schaefer J, Stillman N, Popoli M, Vogelstein JT, Browne JD, Schoen RE, Brand RE, Tie J, Biggs P, Wong H, Mansfield AS, Jen J, Hanash SM, Falconi M, Allen PJ, Zhou S, Bettegowda C, Diaz L, Tomasetti C, Kinzier KW, Vogelstein B, Lennon AM, Papadopoulos N (2018) Detection and localization of surgically resectable cancers with a multi-analyte blood test. Science 359:926–930
12. Rusling JF, Bishop GW, Doan N, Papadimitrakopoulos F (2014) Nanomaterials and biomaterials in electrochemical arrays for protein detection. J Mater Chem B 2:12–30
13. Dixit CK, Kadimisetty K, Otieno B, Tang C, Malla S, Krause CE, Rusling JF (2016) Electrochemistry-based approaches to low cost, high sensitivity, automated, multiplexed protein immunoassays for cancer diagnostics. Analyst 141:536–547
14. Mani V, Kadimisetty K, Malla S, Joshi AA, Rusling JF (2013) Paper-based electrochemiluminescent screening for genotoxic chemicals in the environment. Environ Sci Technol 47:1937–1944
15. Otieno BA, Krause CE, Jones AL, Kremer RB, Rusling JF (2016) Cancer diagnostics via ultrasensitive multiplexed detection of parathyroid hormone-related peptides (PTHrP) with a microfluidic immunoarray. Anal Chem 88:9269–9275
16. Zheng M, Huang X (2004) Nanoparticles comprising a mixed monolayer for specific bindings with biomolecules. J Am Chem Soc 126:12047–12054

Chapter 7

Cytometry Multiplex Bead Antibody Array

Benyue Zhang, Gang Xiao, Ying Qing Mao, Zhiqiang Lv, and Ruo-Pan Huang

Abstract

The flow cytometry-based multiplex bead array is an advanced technology using antibody-conjugated multiplex beads to detect soluble targets in a liquid phase. This technology has been widely used for detection of soluble analytes like cytokines, chemokines, allergens, viral antigens, and cancer markers. RayPlex® Multiplex Beads Antibody Array series are developed by RayBiotech Life, Inc. to quantitatively detect a wide range of analytes with high sensitivity to meet increasing need of research and diagnosis.

Key words RayPlex® Multiplex Beads, Antibody array, Cytokines, Chemokines, Biomarkers

1 Introduction

The bead-based array has been widely used for high-throughput detection of soluble analytes. The flow cytometry-based multiplex bead array is an advanced technology using antibody-conjugated multiplex beads to detect soluble targets in a liquid phase. Several manufacturers have developed kits for the detection of soluble analytes like cytokines, chemokines, allergens, viral antigens, and cancer markers [1–10]. For example, RayPlex® Multiplex Beads have 3, 5, or 8 μm size beads where each is integrated with fluorescent dyes with different intensities, allowing researchers to separate them as different populations in a standard flow cytometer. Unlike traditional ELISA where antibodies are immobilized on a planar surface by adsorption, a bead-based assay has antibodies covalently conjugated to the beads' surface chemically, with a much larger reaction area. In this assay, a sandwich-based reaction similar to ELISA (Fig. 1) is utilized, and the signal is read by a flow cytometer, which can detect each single bead on the PE channel, the brightest fluorescence known to date. Because of the significantly increased reaction area and the very small volume of beads, this assay can be performed with far less sample volume while at the same time

Kelly C. Whittaker and Ruo-Pan Huang (eds.), *Antibody Arrays: Methods and Protocols*, Methods in Molecular Biology, vol. 2237, https://doi.org/10.1007/978-1-0716-1064-0_7,

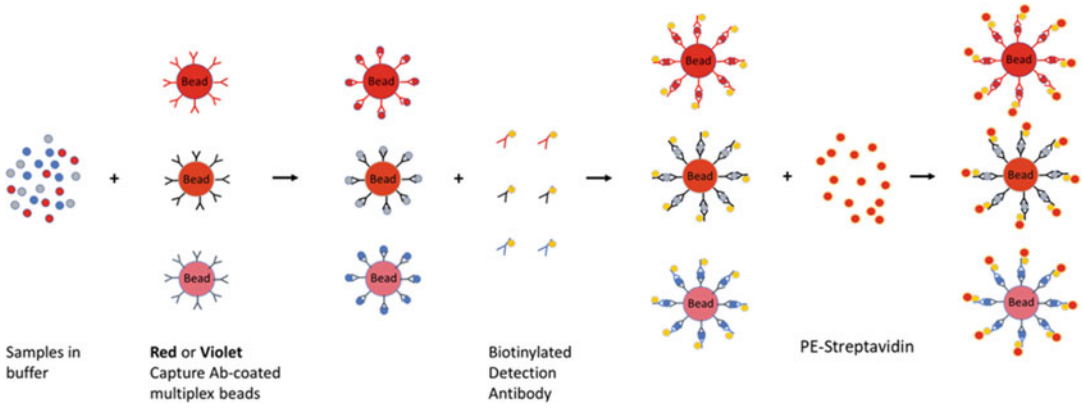

Fig. 1 Cytometry Multiplex Bead Antibody Array Diagram

reducing nonspecific binding and providing multiplexed analysis of several analytes with high sensitivity [11].

There are several benefits to using a liquid phase-based assay, including (1) the ability to simultaneously detect multiple (up to 50) targets per test; (2) significantly less sample volume required compared to traditional assays; (3) high sensitivity and reproducibility; (4) a broad linear reading range; (5) ease of use, with a readily available equipment, a simple procedure, and minimal data processing; (6) high-throughput capabilities; and (7) low cost. In this chapter, we describe a cytometry Multiplex Bead Antibody Array that utilizes this technology for the detection of 15 human cancer biomarkers, but it can easily be scaled to quantitate up to 50 targets simultaneously across numerous species and molecule classes (i.e., immune-modulatory cytokines, inflammation cytokines, viral antigens, cancer biomarkers, etc.) to meet the need for both research and clinical diagnosis.

2 Materials

All materials should be stored at 4 °C. The lyophilized protein standard mix should be stored at −80 °C. All materials can be kept for up to 6 months.

1. RayBio® Multiplex Antibody Array Bead Cocktail: comprises 2 bead sizes and 15 antibodies: AFP, CA125, CA19-9, CA72-4, CEA, NSE, pepsinogen I (PG I), pepsinogen II (PG II), SCAA1, PSA-free, PSA-total, thyroglobulin (Tg), CA153, HCG-β, and HE4. Nine antibodies are on 5 μm red beads, and six antibodies are on 8 μm red beads.
2. 10× Assay diluent: 10% BSA in 10× PBS, 0.5% Tween-20.
3. 20× Wash buffer: 20× PBS, 1% Tween-20.
4. Human serum matrix (*see* **Note 1**).

5. V-shaped 96-well microplate.
6. Lyophilized protein standard mix: contains a mixture of antigens corresponding to the antibodies contained in the Multiplex Antibody Array Bead Cocktail (*see* **Note 2**).
7. Detection antibody cocktail: contains a mixture of corresponding biotinylated antibodies to those contained in the Multiplex Antibody Array Bead Cocktail.
8. PE-conjugated streptavidin.
9. RayBright® Universal Compensation Beads coupled with antibody conjugated with PE and APC.
10. Orbital shaker (with ability to reach 1000 rpm).
11. P20, P200, and P1000 pipette.
12. Multichannel (12 channels) pipette 5–50 and 30–300 μL.
13. Vortex mixer.
14. Eppendorf microcentrifuge model 5424R or an equivalent centrifuge.
15. Eppendorf centrifuge model 5810R or an equivalent centrifuge with plate holder.
16. Flow cytometer with violet, blue, and red lasers.
17. High Throughput Sampler (for 96-well plate).
18. Aluminum foil.
19. Distilled water.
20. 1.5 mL polypropylene microcentrifuge tubes
21. Human serum sample.

3 Methods

3.1 Preparation of Sample and Reagents

1. Keep all reagents on ice.
2. Add 5 mL of the 10× assay diluent to 45 mL distilled water to make 1× assay diluent.
3. Add 2.5 mL of the 20× wash buffer to 47.5 mL distilled water to make 1× wash buffer.
4. Vortex the Multiplex Antibody Array Bead Cocktail for 30 s. Protect fluorescent multiplex beads from frequent exposure to light using aluminum foil.
5. Dilute the human serum sample twofold in 1× assay diluent to minimize matrix effects (*see* **Note 3**).
6. Dilute the detection antibody cocktail 1:100 in 1× assay diluent to make the detection antibody cocktail working stock.
7. Dilute PE-conjugated streptavidin 1:100 in 1× assay diluent to make the PE-conjugated streptavidin working stock.

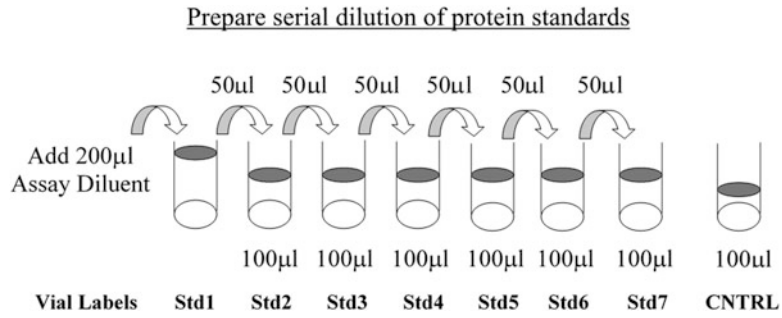

Fig. 2 Preparation of serial dilutions of protein standards

3.2 Preparation of Protein Standard Dilutions

1. Quick-spin the lyophilized protein standard mix in a mini centrifuge, and then reconstitute by adding 200 µL of 1× assay diluent. Dissolve the powder thoroughly by gentle mixing, and label this tube as Std1 (*see* **Note 4**).
2. Label six clean microcentrifuge tubes as Std2 to Std7. Add 100 µL 1× assay diluent to each of the tubes.
3. Pipette 50 µL of Std1 (*see* **step 1** of Subheading 3.3) into the tube labeled Std2, and mix gently. Perform five more serial dilutions by adding 50 µL of Std2 to the tube labeled Std3; mix and so on (Fig. 2).
4. Add 100 µL of 1× assay diluent to another tube labeled as CNTRL. Do not add standard or samples to the CNTRL tube. This tube will be used as the negative control.

3.3 Array Procedure

1. Prepare a V-shaped 96-well microplate, and mark positions for standard and samples. Duplicate tests are recommended for all standard and samples.
2. Add 25 µL of the Multiplex Antibody Array Bead Cocktail to each well, and then add 200 µL of 1× assay diluent to each well.
3. Spin down the beads at 1000 × *g* for 5 min, and remove the supernatant with a multichannel pipette without touching the beads.
4. Add 25 µL of human serum matrix to each standard well and 25 µL of 1× assay diluent to each sample well.
5. Add 25 µL of the standard dilutions and prepared serum sample to the corresponding wells. Mix and incubate at room temperature (RT) for 2 h (*see* **Note 5**).
6. Wash the beads by adding 200 µL of 1× wash buffer, spinning down at 1000 × *g* for 5 min at RT, and removing the supernatant. Repeat one more time.

Table 1
Troubleshooting options

Problem	Cause	Recommendation
Weak signal	Inadequate detection	Increase sample and beads incubation time
	Detection antibody over diluted	Increase detection antibody concentration
	Too low protein concentration in sample	Don't over dilute samples
	Too low protein concentration in sample	Don't make too low dilution or concentrate sample
	Improper storage of kit	Store kit as suggested temperature
	Reagent evaporation	Cover the incubation plate with adhesive film during incubation
Poor standard curve	Cross-contamination from neighboring wells	Avoid overflowing wash buffer
	Too much detection antibody	Optimize the detection antibody
	Standard protein degraded or not property diluted	Reconstitute the lyophilized standard well at on ice before making serial dilutions
High background	Improper flow cytometer setup and optimization	Run QC-beads before assay. Make sure high end signal not out of linear range
	Insufficient wash	Increase wash time and use more wash buffer
	Too much detection antibody	Optimize the detection antibody

7. Add 25 μL of detection antibody cocktail working stock to each well to resuspend the beads, and incubate on an orbital shaker at 500 rpm, RT for 1 h.
8. Wash once according to **step 6**, then add 50 μL of PE-conjugated streptavidin working stock to each well, and incubate on an orbital shaker at 500 rpm, RT for 30 min.
9. Wash twice according to **step 6**, and then resuspend in 300 μL of 1× wash buffer. The procedures can be optimized according to Table 1.

3.4 Flow Cytometer Setup and Data Acquisition

1. Depending on the brand of the flow cytometer, start the acquisition software, and run QC beads according to the manufacturers' protocol.
2. Adjust the voltage for FSC (forward scatter, linear mode) and SSC (side scatter, linear mode) so that major bead populations (based on sizes) are shown at prominent area.
3. Create an FSC-H/FSC-A daughter population for single bead selection to remove/limit doublets and higher.
4. Create an SSC-A/APC (use log mode for APC). Add 25 μL of Multiplex Antibody Array Bead Cocktail (unused beads cocktail) to 400 μL of 1× assay diluent, run on the flow cytometer, and adjust the SSC and APC so that all populations are well separated (*see* **Note 6**) (Figs. 3 and 4).

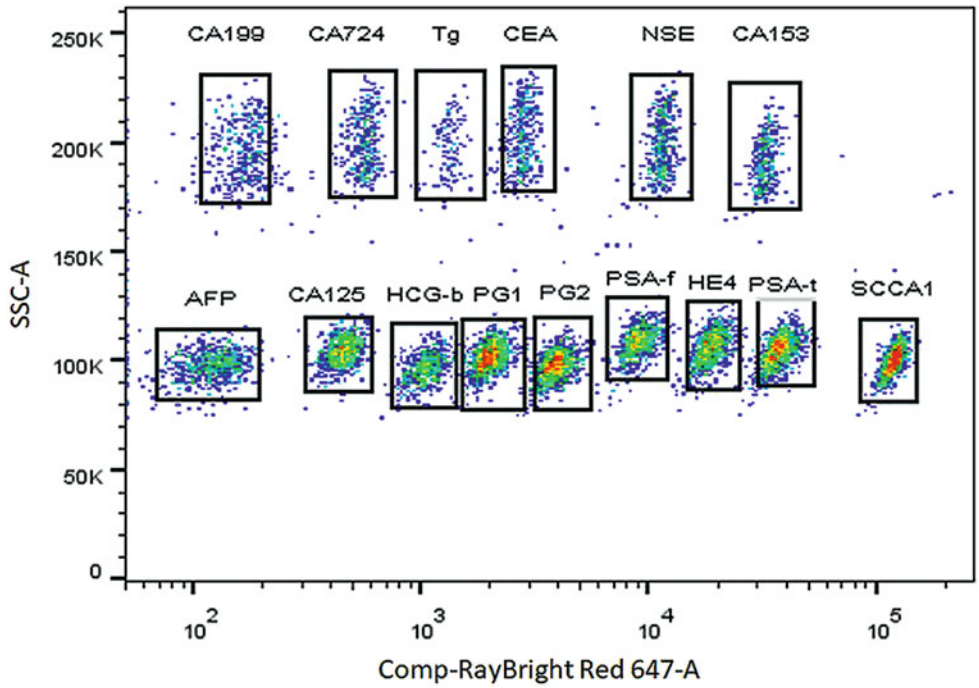

Fig. 3 RayPlex® Multiplex Beads in 5 and 8 μm sizes used in RayBio® Multiplex Antibody Array

5. Using the same Multiplex Antibody Array Bead Cocktail as in **step 4**, adjust the PE voltage so that for each population the PE MFI should be around 10–10^2 depending on the cytometer setup.
6. After PMT setup, perform compensation with RayBright® Universal Compensation Beads coupled with antibody conjugated with PE and APC (*see* **Note 7**).
7. A High Throughput Sampler (HTS) is preferred as the 96-well microplate can be used directly. If HTS is not available, transfer sample to FACS tubes for acquisition. Set the number of bead events to be acquired to at least 300 per analyte.
8. After acquisition, create and export PE geometric-mean (Geo Mean) or Median for all populations of all standards and samples to Excel, or export the whole data as FCS file for further analysis on FlowJo.

3.5 Data Analysis (Fig. 5)

1. Export the Excel file for Geo Mean (or Median) of the MFI data of PE histogram subset for each population using Table Editor of FlowJo software.
2. In Excel, create a standard curve based on cancer biomarker antigen concentrations (shown in Table 2). Calculate concentrations of all analytes of each sample based on the MFI

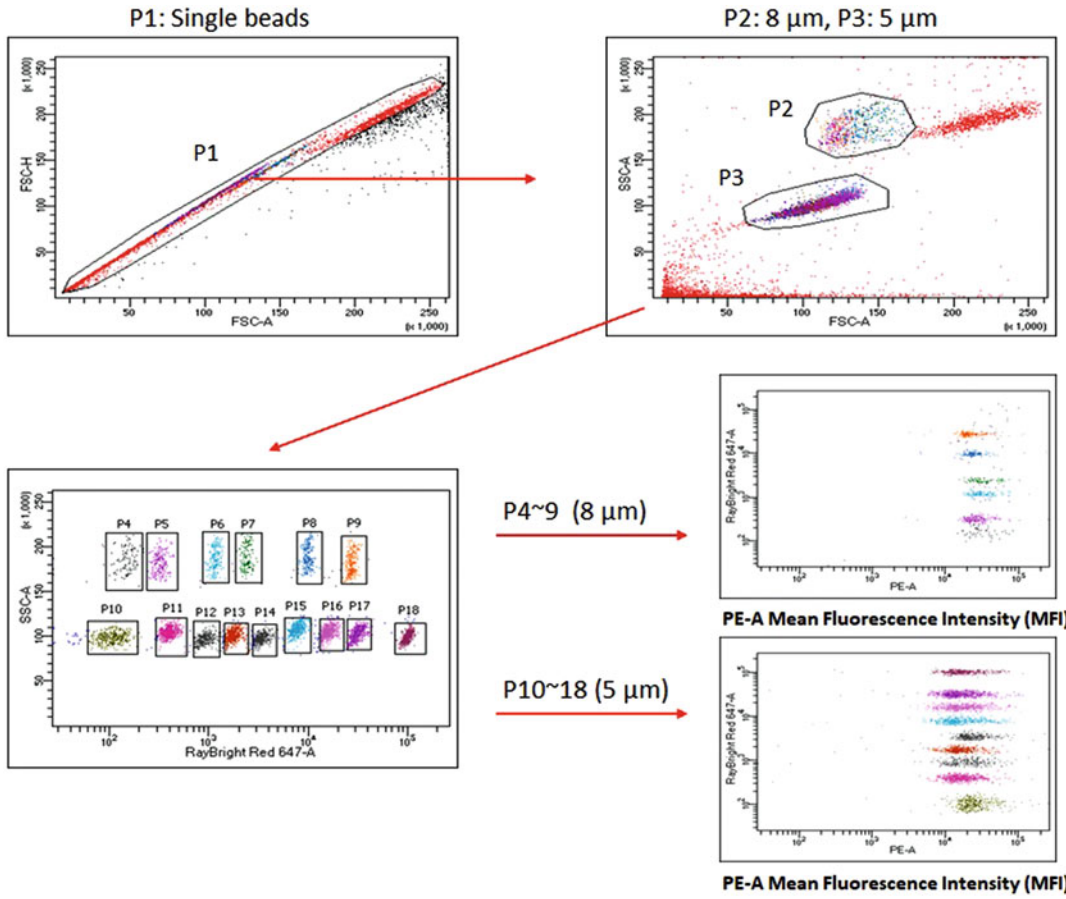

Fig. 4 Cytometry Multiplex Bead Antibody Array Flow Cytometer Gating Strategy

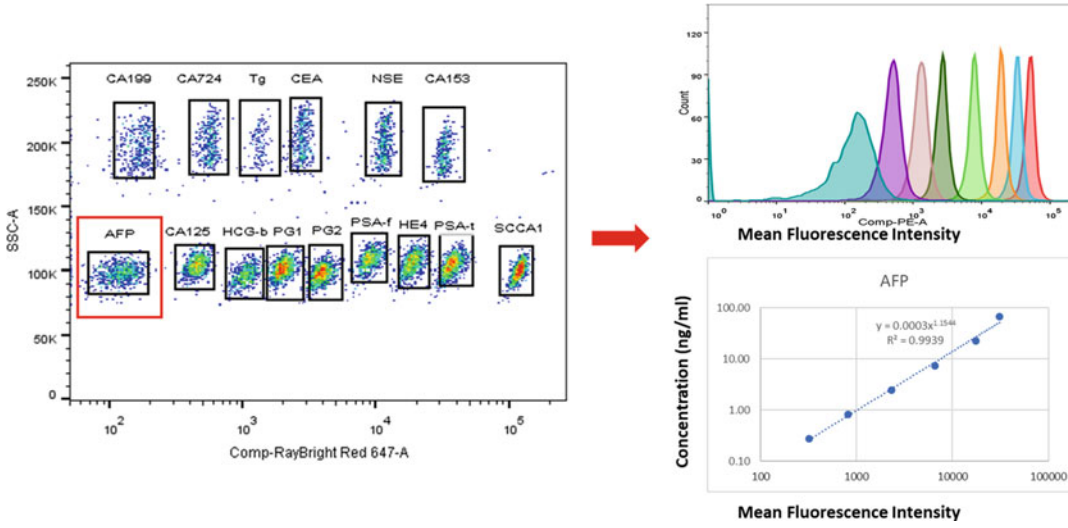

Fig. 5 Statistical analysis of Cytometry Multiplex Bead Array Data. AFP standards MFI were exported to an Excel format and analyzed with a log-log regression curve

Table 2
Standard concentration of antigens

Target antigen	Std1	Std2	Std3	Std4	Std5	Std6	Std7	Negative Ctl	Unit
AFP	200.00	66.67	22.22	7.41	2.47	0.82	0.27	0	ng/mL
CA125	2000.00	666.67	222.22	74.07	24.69	8.23	2.74	0	U/mL
CA199	2000.00	666.67	222.22	74.07	24.69	8.23	2.74	0	U/mL
CA724	200.00	66.67	22.22	7.41	2.47	0.82	0.27	0	U/mL
CEA	200.00	66.67	22.22	7.41	2.47	0.82	0.27	0	ng/mL
NSE	200.00	66.67	22.22	7.41	2.47	0.82	0.27	0	ng/mL
Pepsinogen 1	1000.00	333.33	111.11	37.04	12.35	4.12	1.37	0	ng/mL
Pepsinogen 2	200.00	66.67	22.22	7.41	2.47	0.82	0.27	0	ng/mL
SCCA1	100.00	33.33	11.11	3.70	1.23	0.41	0.14	0	ng/mL
CA153	400.00	133.33	44.44	14.81	4.94	1.65	0.55	0	U/mL
HCG-β	400.00	133.33	44.44	14.81	4.94	1.65	0.55	0	U/L
HE4	1000.00	333.33	111.11	37.04	12.35	4.12	1.37	0	pM
PSA-total	100.00	33.33	11.11	3.70	1.23	0.41	0.14	0	ng/mL
PSA-free	100.00	33.33	11.11	3.70	1.23	0.41	0.14	0	ng/mL
Tg	1000.00	333.33	111.11	37.04	12.35	4.12	1.37	0	ng/mL

Table 3
MFI data exported from FlowJo

	AFP	CA125	CA199	CA724	CEA	NSE	PG1	PG2	SCAA1	PSA-f	PSA-t	Tg	CA153	HCG-β	HE4
Std1	40843	7657	26 874	1797	16705	16266	11115	13169	9922	4850	6544	15069	13446	5737	10406
Std2	39536	4208	25 783	1372	4835	8908	7221	5684	3572	1947	2911	5175	9127	2128	3236
Std3	30969	3073	16 811	1629	1545	6190	5892	2762	1095	1051	1266	1512	7616	1283	833
Std4	17598	2345	9246	1418	784	5325	4729	1824	449	899	694	667	5510	745	325
Std5	6536	1373	4134	1375	562	3422	2976	1022	285	709	368	445	3830	403	218
Std6	2301	698	1723	1246	466	2131	1598	549	234	461	261	372	2698	203	185
Std7	810	321	742	884	375	1597	764	292	210	246	206	320	1552	132	171
Neg	83	86	217	390	295	762	212	118	192	119	152	236	586	71	142

readings. A representative MFI reading exported from FlowJo is shown in Table 3.

3. If possible, create a module in Excel, so that it can be used for the same assay in the future.

4 Notes

1. Human serum matrix contains pooled normal human serum depleted of endogenous assay targets. This is used for dilution of standards to minimize matrix effects on assay results.
2. The lyophilized protein standard should be stored at −80 °C to prevent protein breakdown.
3. Nearly any liquid sample type can be used with this assay. Optimal sample dilutions should be empirically determined for your particular sample type. Serum samples can be diluted

with 1× assay diluent. Culture supernatant or cell lysates can be tested directly without further dilution. If serum-containing conditioned media is used, it is highly recommended that a complete medium be used as a control since many types of sera contain assay targets or cross-reactive proteins.

4. Since the starting concentration of each protein standard is different, the serial concentrations from Std1 to Std7 for each protein are varied.
5. This step may be done overnight at 4 °C for best results. Longer incubation time is preferable for higher signal.
6. In the current procedure, only 5 and 8 μm red beads are used. However, additional bead colors and sizes can be used, for example, red beads (emit at APC channel) and violet beads (emit at Violet 450 nm channel). If only using red beads, a flow cytometer with blue and red lasers is required. If using both violet and red beads, a flow cytometer equipped with three lasers (violet, blue, and red) is required. Perform standard QC and optimization for the cytometer, and set up as you would for use. Run compensation for Violet 450, PE, and APC channels. (For the same setting, compensation can be reused.)
7. If both violet and red beads are used, compensation beads with antibody conjugated with Violet 450, PE, and APC will be required.

References

1. Rodrigues V, Baudier JB, Chantal I (2017) Development of a bead-based multiplexed assay for simultaneous quantification of five bovine cytokines by flow cytometry. Cytometry A 91(9):901–907. https://doi.org/10.1002/cyto.a.23170. Epub 2017 Jul 12
2. Wang Y, Yu J, Ren Y, Liu L, Li H, Guo A, Shi C, Fang F, Juehne T, Yao J, Yang E, Zhou X, Kang X (2013) Improvement for identification of heterophile antibody interference and AFP hook effect in immunoassays with multiplex suspension bead array system. Clin Chim Acta 426:68–74. https://doi.org/10.1016/j.cca.2013.09.005. Epub 2013 Sep 13
3. Moncunill G, Aponte JJ, Nhabomba AJ, Dobaño C (2013) Performance of multiplex commercial kits to quantify cytokine and chemokine responses in culture supernatants from Plasmodium falciparum stimulations. PLoS One 8(1):e52587. https://doi.org/10.1371/journal.pone.0052587. Epub 2013 Jan 2
4. Wyns H, Croubels S, Demeyere K, Watteyn A, De Backer P, Meyer E (2013) Development of a cytometric bead array screening tool for the simultaneous detection of pro-inflammatory cytokines in porcine plasma. Vet Immunol Immunopathol 151(1–2):28–36. https://doi.org/10.1016/j.vetimm.2012.09.041. Epub 2012 Oct 24
5. van der Wal FJ, Achterberg RP, de Boer SM, Boshra H, Brun A, Maassen CB, Kortekaas J (2012) Bead-based suspension array for simultaneous detection of antibodies against the Rift Valley fever virus nucleocapsid and Gn glycoprotein. J Virol Methods 183(2):99–105. https://doi.org/10.1016/j.jviromet.2012.03.008. Epub 2012 Mar 16
6. Villar-Vázquez R, Padilla G, Fernández-Aceñero MJ, Suárez A, Fuente E, Pastor C, Calero M, Barderas R, Casal JI (2016) Development of a novel multiplex beads-based assay for autoantibody detection for colorectal cancer diagnosis. Proteomics 16(8):1280–1290. https://doi.org/10.1002/pmic.201500413
7. Kranz LM, Gärtner B, Michel A, Pawlita M, Waterboer T, Brenner N (2019) Development and validation of HIV-1 multiplex serology.

J Immunol Methods 466:47–51. https://doi.org/10.1016/j.jim.2019.01.007. Epub 2019 Jan 18

8. Pomponi D, Bernardi ML, Liso M, Palazzo P, Tuppo L, Rafaiani C, Santoro M, Labrada A, Ciardiello MA, Mari A, Scala E (2012) Allergen micro-bead array for IgE detection: a feasibility study using allergenic molecules tested on a flexible multiplex flow cytometric immunoassay. PLoS One 7(4):e35697. https://doi.org/10.1371/journal.pone.0035697. Epub 2012 Apr 17
9. Christopher-Hennings J, Araujo KP, Souza CJ, Fang Y, Lawson S, Nelson EA, Clement T, Dunn M, Lunney JK (2013) Opportunities for bead-based multiplex assays in veterinary diagnostic laboratories. J Vet Diagn Investig 25(6):671–691. https://doi.org/10.1177/1040638713507256. Epub 2013 Oct 23. Review
10. Khan SS, Smith MS, Reda D, Suffredini AF, McCoy JP Jr (2004) Multiplex bead array assays for detection of soluble cytokines: comparisons of sensitivity and quantitative values among kits from multiple manufacturers. Cytometry B Clin Cytom 61(1):35–39. Erratum in: Cytometry B Clin Cytom 2005;64(1):53
11. Ooi KG, Galatowicz G, Towler HM, Lightman SL, Calder VL (2006) Multiplex cytokine detection versus ELISA for aqueous humor: IL-5, IL-10, and IFNgamma profiles in uveitis. Invest Ophthalmol Vis Sci 47(1):272–277

Chapter 8

Antibody Arrays: Barcode Technology

Liwei Yang and Jun Wang

Abstract

Antibody microarray is a fundamental, high-content technology for analyzing biomarkers with a multiplexity even at the proteomic level. Recent advancement in this field has driven the antibody array into a new territory related with single-cell analysis. Here we describe a flow pattern-based method for producing a high-density barcode antibody microarray for the detection of proteins in fluidic samples and in single cells. The antibody microarray is fabricated by a perpendicularly oriented flow patterning of single-stranded barcode DNAs, which are then converted into DNA-antibody conjugates. Compared to conventional microarrays, this barcode antibody microarray features a simple and high-throughput assay while achieving both high sensitivity and specificity. This barcode technology provides new clues for developing next-generation antibody microarrays and can be widely used in protein biomarker discovery, cell signaling network analysis, and disease diagnosis and prognosis.

Key words Proteomics, DNA barcoding, Antibody-DNA conjugation, Microarray, Antibody array, Multiplex, Protein detection, Single-cell analysis

1 Introduction

Functional proteomics, the large-scale analysis of functional proteins, is widely accepted as a powerful means for deep understanding of healthy functions and disease pathogenesis [1–3]. Advanced proteomic technologies capable of acquiring protein expression profiles in a rapid and multiplexed manner while retaining high sensitivity and specificity are highly desirable [4, 5]. In this regard, an antibody-based microarray has emerged as a prominent technology for functional proteomics studies, which enables parallel detection of multiple proteins with extremely low sample volume [6]. This type of assay embraces both high reproducibility and quantitative accuracy over large concentration ranges [7]. Furthermore, the microarray can be easily integrated with a microchip device for detecting secreted proteins and intracellular proteins at the single-cell level. For instance, we have equipped a barcode microarray with a single-cell microchip to quantify the functions of cell-cell interactions and analyze proteins from different types of

Kelly C. Whittaker and Ruo-Pan Huang (eds.), *Antibody Arrays: Methods and Protocols*, Methods in Molecular Biology, vol. 2237, https://doi.org/10.1007/978-1-0716-1064-0_8,

cells [8–10]. This technology features array elements at 10–100 μm, much smaller than the typical 150 μm size used in conventional microarray elements, thus producing high-density antibodies in an ordered pattern. The construction of these smaller array elements is achieved using a systematic flow patterning approach, which does not require the assistance of an array printer and can be performed in most research laboratories.

This protocol describes both the fabrication of the barcode antibody microarray and its potential application in the detection of proteins in fluidic samples and in single cells. The technology is based on an addressable, one-dimensional single-stranded DNA (ssDNA) microarray, which is spatially constructed on a glass slide using orthogonal oligonucleotides through flow patterning [11]. By strategically selecting the sequences of ssDNA utilized in flow patterning, each element in a given array is assigned a specific address [12]. Subsequently, the ssDNA microarray is converted into an antibody microarray through the incorporation of a cocktail of antibodies labeled with complementary ssDNA oligonucleotides, thus forming a two-dimensional antibody microarray. Proteins from fluidic samples or individual cells are captured by the antibody microarray and then quantified by using a sandwich-type immunoassay. The generated fluorescence signals are compared with a calibration curve, which is built for each protein by using protein standards, to determine the abundance of the proteins.

2 Materials

Prepare all solutions using an ultrapure water with a resistivity of 18.2 MΩ cm and analytical grade reagents. Prepare and store all reagents at room temperature (unless indicated otherwise). Perform the barcode slide fabrication and flow patterning procedures in a clean room to minimize contamination from particulate matter.

2.1 Preparation of Polydimethylsiloxane (PDMS) Chip for Barcode Flow Patterns

1. Silicon wafer with a diameter of 100 mm.
2. Piranha solution: H_2SO_4 (98%):H_2O_2 (30%) = 3:1 (v/v).
3. SU-8 2025 photoresist and developer solution (MicroChem).
4. Chrome photomask with features of flow patterns.
5. Sylgard 184 Silicone Elastomer Kit: elastomer base and curing agent.
6. Spin coater (Laurell Technologies).

2.2 Construction and Validation of One/Two-Dimensional DNA Barcode Array

1. Phosphate-buffered saline (PBS) buffer: 137 mM NaCl, 10 mM Na_2HPO_4, and 2 mM KH_2PO_4, pH 7.4.
2. Poly-L-lysine (PLL) adhesive stock solution (1% PLL in PBS buffer).

3. Bis(sulfosuccinimidyl)suberate (BS3).
4. Single-stranded DNA (ssDNA, 5′-amine modified; IDT).
5. Cyanine 3 (Cy3)-conjugated complementary DNA (Cy3-cDNA; IDT).
6. Bovine serum albumin (BSA).

2.3 Conversion of Two-Dimensional DNA Barcode Array into an Antibody Array

1. Succinimidyl 4-formylbenzoate (S-4FB).
2. Succinimidyl 6-hydrazinonicotinamide (S-HyNic).
3. Anhydrous *N*,*N*-dimethylformamide (DMF).
4. Capture and detection antibodies.
5. 7 kDa Zeba desalting columns.
6. Fast protein liquid chromatography (FPLC) system.
7. 10 kDa Amicon ultra filter.
8. Streptavidin-Alexa Fluor™ 555 conjugate.

3 Methods

3.1 Preparation of PDMS Chip for Barcode Flow Patterns

1. Immerse a silicon wafer into a piranha solution for 20–30 min (*see* **Note 1**). Wash the wafer with ultrapure water and isopropyl alcohol. Dry the wafer with a nitrogen blow gun.
2. Pour 4 mL of SU-8 2025 photoresist onto the center of the wafer, and remove any bubbles using a pipette. Use a programmable spin coater to uniformly spread the photoresist on the wafer for 10 s at 500 rpm and then 30 s at 225 × *g* (*see* **Note 2**).
3. Bake the photoresist-coated wafer at 70 °C for 3 min and then for 9 min at 105 °C. This step allows the coating to solidify.
4. Carefully position the chrome mask (Fig. 1a) on the photoresist-coated wafer (*see* **Note 3**). Expose the mask features to near-UV light with an intensity of 50 W for 90 s.
5. Bake the wafer at 70 °C for 2 min and then at 95 °C for 7 min.
6. Put the wafer into SU-8 developer with agitation for approximately 5–10 min. Wash the wafer with a small portion of fresh SU-8 developer, and then rinse with isopropyl alcohol (*see* **Note 4**). Dry the wafer using a nitrogen blow gun. Bake the wafer at 200 °C for 2 h.
7. Silanize the patterned wafer (Fig. 1b) by exposing the wafer to trimethylchlorosilane vapor in a closed petri dish for 10 min (*see* **Note 5**).
8. Combine Sylgard 184 Silicone Elastomer Base with curing agent (base:curing agent = 10:1, wt/wt). Stir the prepolymer mixture vigorously and degas under vacuum.

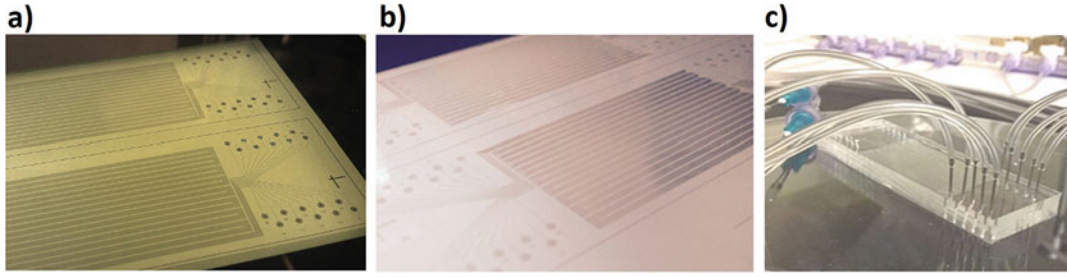

Fig. 1 Design and fabrication of PDMS chip for flow-based DNA patterning. (**a**) Chrome mask for fabricating the SU-8 master. (**b**) A silicon wafer with the flow patterns. (**c**) Setup for flow patterning. For details on the design of the chip, please *see* [11]

9. Pour the prepolymer onto the wafer with the barcode pattern. Degas the mixture to remove any remaining bubbles, and then bake the mixture at 70 °C for 1 h (*see* **Note 6**).
10. Peel off the PDMS chip from the wafer, and cut around the area of the chip that contains the barcode features. Punch 20 holes (1.0-mm diameter) through the chip using a punch (Fig. 1c). Ensure that the holes are aligned with the circular features of the barcode pattern. These holes will serve as the inlets and outlets.

3.2 Construction and Validation of One-Dimensional DNA Barcode Array

1. Perform procedure (**step 1** in Subheading 3.1) on a clean glass slide. Immerse the slide into 1% PLL solution for 2 h. Wash the slide with ultrapure water. Dry the wafer with a nitrogen blow gun.
2. Attach the PDMS chip to the slide. Ensure that the edges of the chip and the slide are aligned.
3. Bake the slide at 70 °C for 2 h to strengthen the bond between the PLL-coated slide and the PDMS chip.
4. Prepare 20 pieces of flexible polyethylene tubing (*see* **Note 7**). To one end of each piece of tubing, attach a stainless steel hollow pin. Fasten the pins to the inlets of the PDMS chip.
5. Attach the other end of the tubes to a pressure-regulated nitrogen tank setup. Allow the solution to flow through the chip using a pressure range of 0.5–1 psi.
6. Prepare 2 mM BS3 solution in PBS. Prepare 300 μM three types of ssDNA solutions (denoted as A, B, C) in PBS (*see* **Note 8**). Equivalently combine the three types of ssDNA with BS3 in PBS for each channel. A, B, and C ssDNA are designated to channels 1, 2, and 3, respectively.
7. Aspirate the BS3/DNA solutions through stainless steel pins and into the polyethylene tubing. Allow the BS3/DNA solution to flow through the chip until all channels are filled, and then stop the flow.

8. Incubate the BS3/DNA solution in the chip for 2 h. Remove the PDMS from the chip. Wash the chip with PBS, and then rinse with ultrapure water.
9. Prepare 3% BSA in PBS. Incubate the ssDNA barcode chip with 3% BSA solution for 1 h, and then wash with PBS.
10. Prepare a 200 nM cocktail of A′, B′, and C′ Cy3-conjugated oligonucleotides in 3% BSA. The sequences of A′, B′, and C′ are complementary to those of A, B, and C, respectively. Apply the Cy3-cDNA cocktail solution onto the surface of the barcode chip, and incubate for 1 h (*see* **Note 9**).
11. Pipette out the Cy3-cDNA cocktail solution and wash the chip with PBS. Observe the fluorescence under a fluorescence microscope, and then quantify the fluorescence signal.

3.3 Construction and Validation of Two-Dimensional DNA Barcode Array

1. Use a chrome mask with a flow pattern perpendicular to that of the first design, and then perform procedure (Subheading 3.1) to construct a new PDMS chip with the perpendicular pattern.
2. Perform procedure (**steps 1–8** in Subheading 3.2) to prepare a one-dimensional patterning of A, B, and C ssDNA barcode array.
3. For a two-dimensional (3 × 3) DNA barcode array (Fig. 2), prepare 300 μM stock solutions of A′-1, B′-2, C′-3, A′-4, B′-5, C′-6, A′-7, B′-8, and C′-9 DNA in 3% BSA/PBS, respectively (*see* **Note 10**). Use the guide in Fig. 2 for DNA flow patterning, and combine the DNA cocktail solutions (Solutions 1–3).
4. Flow 3% BSA/PBS solution into all channels for 1 h.

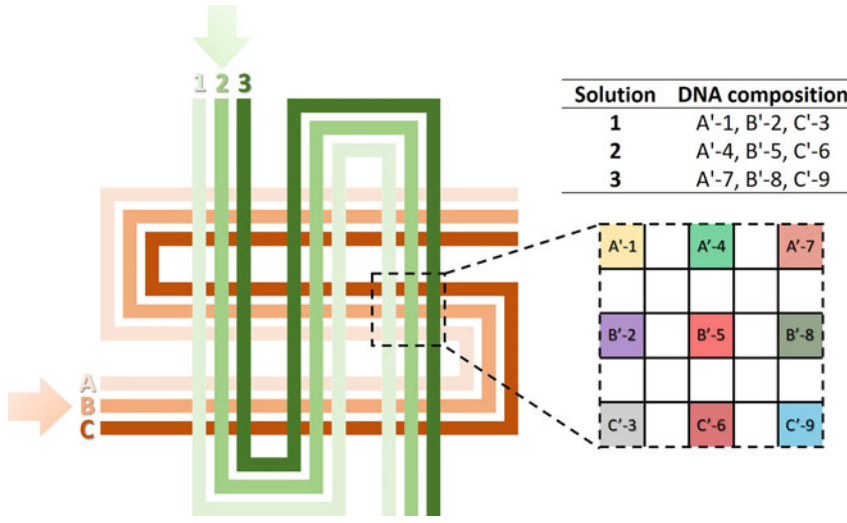

Fig. 2 Fabrication of a two-dimensional (3 × 3) DNA barcode array by flow patterning methods

5. Flow Solutions 1, 2, and 3 into channels 1, 2, and 3, respectively. After all the channels are filled, stop the flow. Incubate the DNA solutions with the PDMS chip for 2 h to allow the DNA to hybridize.
6. Flow 3% BSA/PBS solution into all channels for 1 h to remove unhybridized DNA. Carefully remove the PDMS from the barcode chip. Wash the chip with PBS, and then rinse with ultrapure water.
7. Perform procedure (**steps 9–11** in Subheading 3.2) to validate the two-dimensional DNA barcode array. Use complementary oligonucleotides 1′–9′ that are Cy3-conjugated.
8. Store the DNA barcode array in a desiccator for subsequent use (*see* **Note 11**).

3.4 Conversion of Two-Dimensional DNA Barcode Array into an Antibody Array

1. Prepare 200 mM S-4FB and 40 mM S-HyNic solutions in anhydrous DMF.
2. Prepare up to nine separate solutions of capture antibodies (1 mg/mL) in PBS (*see* **Note 12**).
3. Prepare separate 400 μM solutions of 1′–9′ DNA in PBS. Assign each capture antibody to one oligonucleotide sequence.
4. For every 100 μg of capture antibody in 1 mg/mL, add 2.2 μL of 40 mM SANH in DMF. Pipette up and down to mix the solution. Incubate the antibody/S-HyNic mixture at room temperature for 4 h.
5. Combine 40 μL of 400 μM DNA with 10 μL DMF in microcentrifuge tubes. Spin down. For each 50 μL of DNA/DMF solution, add 2.2 μL of 200 mM SFB in DMF (*see* **Note 13**). Incubate the DNA/DMF/SFB mixture at room temperature for 4 h.
6. In preparation for the antibody-DNA coupling reaction, prepare new spin columns in advance (one for each DNA solution and one for each antibody) by washing them with citrate buffer (pH 6).
7. After 4 h of incubation, put the DNA or antibody solutions into the respective Zeba desalting columns with labeled collection tubes. Spin for 2 min at 1500 × *g*. Combine the desalted DNA with the corresponding desalted antibody (Fig. 3a). Pipette up and down to mix thoroughly. Incubate for 5–6 h at room temperature. Then transfer to 4° and incubate overnight.
8. Purify the antibody-oligonucleotide conjugates at a FPLC workstation (*see* **Note 14**). After FPLC, pool the fractions containing the conjugate, and then use a 10K filter to concentrate the desired product, and store the conjugates in a 4° fridge.

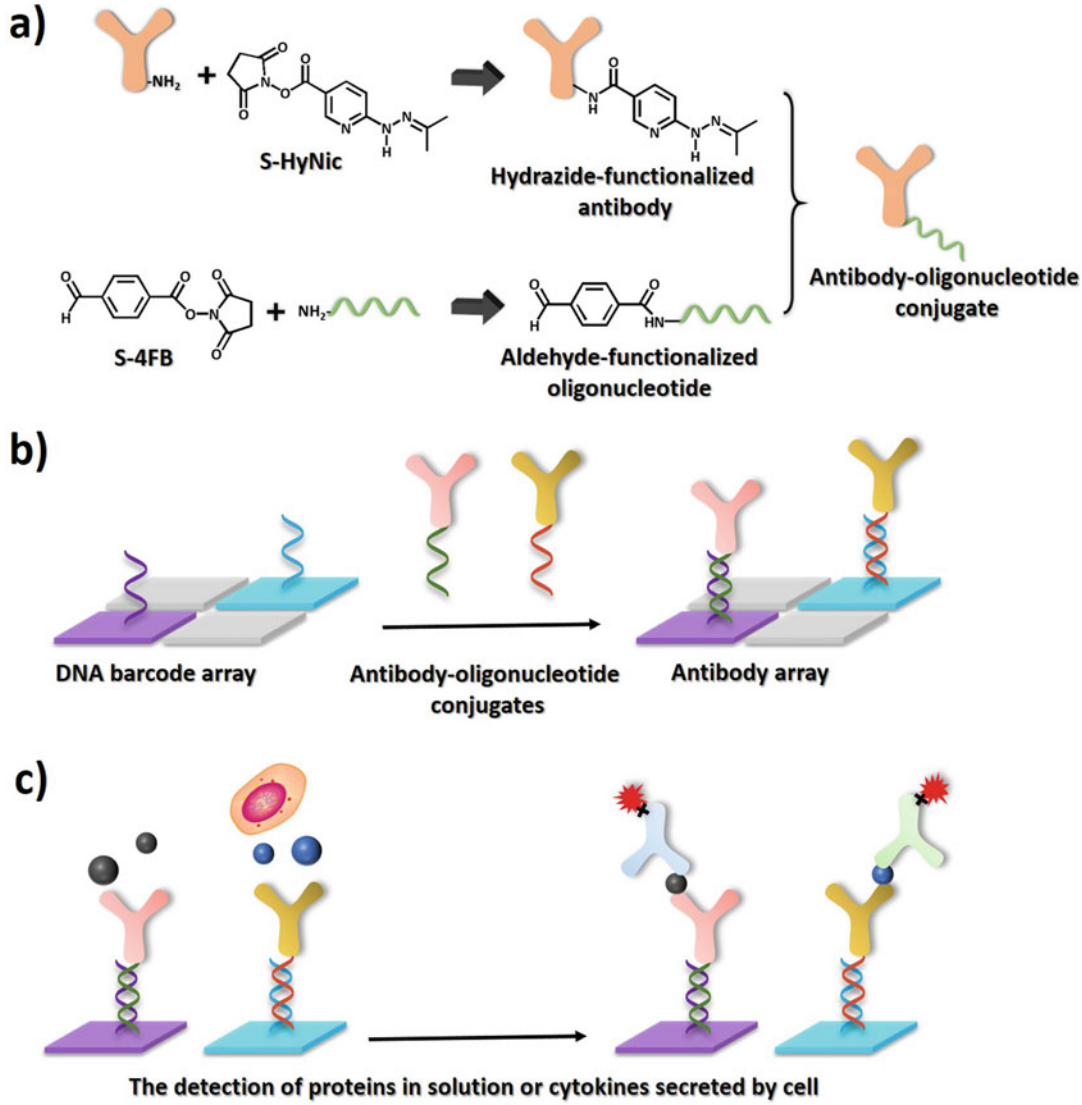

Fig. 3 Construction of an antibody array and its application on the detection of proteins. (**a**) Synthesis of antibody-oligonucleotide conjugates. (**b**) Conversion of the DNA barcode array into an antibody array through hybridization with antibody-oligonucleotide conjugates. (**c**) Protein detection based on the antibody array

9. Block the two-dimensional DNA barcode array with 3% BSA/PBS for 1 h, and then wash with PBS.
10. Prepare a cocktail of antibody-oligonucleotide conjugates at 5 μg/mL in 3% BSA/PBS. Add the cocktail solution to the DNA barcode array, and incubate for 1 h, thereby converting the DNA array to an antibody array (*see* **Note 15**, Fig. 3b).
11. Perform procedure (Subheading 3.1) to construct a new PDMS chip with microchambers or microwells, which are used for immunoassays and single-cell isolation (*see* **Note 16**).

12. Reconstitute recombinant proteins, or prepare cell samples with desired concentrations. Add the proteins or cell samples on the PDMS surface which contains features for microchannels and microchambers. Mate the antibody array with the PDMS chip using a clamp (*see* **Note 17**), and incubate for 2 h.
13. Carefully separate the PDMS part from the antibody array slide, and wash the array slide with 3% BSA/PBS. Add biotinylated detection antibodies at a concentration provided by the product datasheet. Incubate for 2 h.
14. Wash the array slide with 3% BSA/PBS, and then add Streptavidin-Alexa 555 (1 μg/mL in PBS) to complete sandwich ELISA steps (Fig. 3c). Incubate for 30 min.
15. Observe the fluorescence on the array slide under a fluorescence microscope, and quantify the fluorescence signal.

4 Notes

1. The piranha solution reacts violently with most organic materials and must be handled with extreme care in a fume hood. This solution should be prepared by adding the peroxide slowly to the acid with agitation.
2. Gradually allow spinning to slow down before stopping, which will maintain an even coating on the wafer's surface.
3. The design on the chrome mask contains 20 channels, each of which is 20 μm wide with 50 μm pitch. Each channel is flanked by two circular features which correspond to an inlet and an outlet.
4. Development with SU-8 developer solution may be carried out for a longer time if a white film is observed after washing in this step.
5. Trimethylchlorosilane is both a corrosive and an irritant chemical, which is hazardous in case of skin contact. Handle this chemical in a fume hood.
6. The height of the PDMS mixture should be about 7.5 mm or above, which will avoid adding too much tension to the PDMS-glass bond upon insertion of pins/tubing through holes.
7. The number of pieces of tubing corresponds to the number of inlets in the PDMS chip.
8. Use the BS3 solution within about 30 min after preparation because the *N*-hydroxysuccinimide ester easily undergoes hydrolysis.

9. Perform this incubation step in the dark to protect the Cy3 moiety from photobleaching.
10. These oligonucleotides serve as "bridging sequences," which connect the anchored DNA on glass slides and complementary DNA in conjugates.
11. The DNA barcode array can be stored at room temperature in a desiccator for 2–3 months.
12. If the antibody stock solutions contain sodium azide, perform buffer exchange with PBS using spin desalting columns with a 7 kDa molecular weight cutoff (MWCO).
13. DMF should be added first before adding SFB in this step; otherwise white precipitation will form.
14. Perform FPLC using a Superdex 200 gel filtration column at 0.45 mL/min isocratic flow of PBS.
15. The highest sensitivity of the antibody array can be achieved if the array is used immediately. Prolonged storage may result in loss of sensitivity.
16. The features of the PDMS chip depend on the system being studied. For instance, the detection of proteins from single-cell experiments can be performed with a PDMS chip containing microchambers with 0.15 nL volumes.
17. The clamp permits adjustment of mechanical pressure onto the microchip to seal the microchambers containing protein or single-cell samples.

Acknowledgments

The authors would like to acknowledge the start-up fund from Stony Brook University, State University of New York.

References

1. Blackstock WP, Weir MP (1999) Proteomics: quantitative and physical mapping of cellular proteins. Trends Biotechnol 17(3):121–127. https://doi.org/10.1016/s0167-7799(98)01245-1
2. Hanash S (2003) Disease proteomics. Nature 422(6928):226–232. https://doi.org/10.1038/nature01514
3. Patterson SD, Aebersold RH (2003) Proteomics: the first decade and beyond. Nat Genet 33:311–323. https://doi.org/10.1038/ng1106
4. MacBeath G (2002) Protein microarrays and proteomics. Nat Genet 32:526–532. https://doi.org/10.1038/ng1037
5. Aebersold R, Mann M (2003) Mass spectrometry-based proteomics. Nature 422(6928):198–207. https://doi.org/10.1038/nature01511
6. Wingren C, Borrebaeck CA (2008) Antibody microarray analysis of directly labelled complex proteomes. Curr Opin Biotechnol 19(1):55–61. https://doi.org/10.1016/j.copbio.2007.11.010
7. Haab BB (2005) Antibody arrays in cancer research. Mol Cell Proteomics 4(4):377–383. https://doi.org/10.1074/mcp.M500010-MCP200
8. Ma C, Fan R, Ahmad H, Shi QH, Comin-Anduix B, Chodon T, Koya RC, Liu CC,

Kwong GA, Radu CG, Ribas A, Heath JR (2011) A clinical microchip for evaluation of single immune cells reveals high functional heterogeneity in phenotypically similar T cells. Nat Med 17(6):738–U133. https://doi.org/10.1038/nm.2375

9. Wang J, Tham D, Wei W, Shin YS, Ma C, Ahmad H, Shi QH, Yu JK, Levine RD, Heath JR (2012) Quantitating cell-cell interaction functions with applications to glioblastoma multiforme cancer cells. Nano Lett 12 (12):6101–6106. https://doi.org/10.1021/nl302748q
10. Kravchenko-Balasha N, Wang J, Remacle F, Levine RD, Heath JR (2014) Glioblastoma cellular architectures are predicted through the characterization of two-cell interactions. Proc Natl Acad Sci USA 111(17):6521–6526. https://doi.org/10.1073/pnas.1404462111
11. Ramirez LS, Wang J (2016) Flow-pattern guided fabrication of high-density barcode antibody microarray. J Vis Exp 107:53644. https://doi.org/10.3791/53644
12. Bailey RC, Kwong GA, Radu CG, Witte ON, Heath JR (2007) DNA-encoded antibody libraries: a unified platform for multiplexed cell sorting and detection of genes and proteins. J Am Chem Soc 129(7):1959–1967. https://doi.org/10.1021/ja065930i

Chapter 9

Reverse Phase Protein Arrays

Justin B. Davis, Sydney Andes, and Virginia Espina

Abstract

Reverse phase protein arrays (RPPA) are used to quantify proteins and protein posttranslational modifications in cellular lysates and body fluids. RPPA technology is suitable for biomarker discovery, protein pathway profiling, functional phenotype analysis, and drug discovery mechanism of action. The principles of RPPA technology are (a) immobilizing protein-containing specimens on a coated slide in discrete spots, (b) antibody recognition of proteins, (c) amplification chemistries to detect the protein-antibody complex, and (d) quantifying spot intensity. Construction of a RPPA begins with the robotic liquid transfer of protein-containing specimens from microtiter plates onto nitrocellulose-coated slides. The robotic arrayer deposits each sample as discrete spots in an array format. Specimens, controls, and calibrators are printed on each array, thus providing a complete calibrated assay on a single slide. Each RPPA slide is subsequently probed with catalyzed signal amplification chemistries and a single primary antibody, a secondary antibody, and either fluorescent or colorimetric dyes. The focus of this chapter is to describe RPPA detection and imaging using a colorimetric (diaminobenzidine (DAB)) detection strategy.

Key words Antibody, Drug discovery, Functional phenotype, Nitrocellulose, Posttranslational modifications, Protein, Reverse phase protein array, Solid pin

1 Introduction

Signal transduction may be described as a cascade of sequential protein activation/deactivation events, initiated by an input signal. Protein posttranslational modifications, such as phosphorylation, acetylation, methylation, sumoylation, and cleavage, reflect the activity state of cellular signaling networks. Patterns of phosphorylation, for example, indicate docking events and infer protein-protein interactions. Measuring these fluctuating protein signaling events in lysed cells reflects the state of activity of ongoing signal pathway and cellular networks. This signal pathway activity ultimately depicts the functional phenotype of the cells/tissue. Measuring the functional phenotype signifies levels of the actual drug targets (proteins) in a patient's specimen and reveals a drug's on and off target effects.

Kelly C. Whittaker and Ruo-Pan Huang (eds.), *Antibody Arrays: Methods and Protocols*, Methods in Molecular Biology, vol. 2237, https://doi.org/10.1007/978-1-0716-1064-0_9,

Reverse phase protein array technology can quantify proteins in these signaling cascades. Reverse phase protein arrays (RPPA) are used to quantify proteins and posttranslational modifications across a large dynamic range, from limited specimen volumes that span low to high concentration ranges [1–4]. Protein array technology has progressed from a novel technique [5], through a research tool [1], to a laboratory developed assay for use in clinical trials [3, 6]. RPPA accommodates many specimen types, including cultured cells [7], human and animal tissues [8–10], exosomes [11], and body fluids [12]. The widespread adoption of reverse phase protein arrays stems from their ability to solve the challenges of measuring a wide diversity of low-abundance proteins and their posttranslational modifications from limited samples.

A reverse phase array differs from an antibody array because in the reverse phase format, the protein lysate specimen is deposited on a substratum and the probe molecule is a single, primary antibody [1, 2, 7, 13]. In contrast, antibody arrays consist of a multitude of antibodies deposited on a substratum, and the specimen is used as the probe. The reverse phase format allows many specimens to be quantified in a single array (slide), and multiple RPPA slides allow many proteins to be measured, with each array serving as a complete assay.

Proteins are immobilized on a nitrocellulose-coated glass slide by a robotic printing device (arrayer) [14, 15]. Array printing can be accomplished via contact deposition with solid pins or quill pins [16, 17] or noncontact piezo or inkjet printing [18]. Protein binding to the nitrocellulose occurs via multiple, poorly understood interactions consisting of van der Waals, electrostatic, and hydrophobic interactions [19]. The selection of cell lysis conditions, arrayer and pin types, and printing buffers can be optimized based on sample type, array coating, and printing conditions [14].

RPPA are an antibody-based analytical platform. Well-characterized, validated primary antibodies, directed toward a single antigen, are used to bind to a specific protein or posttranslationally modified protein within each spot. The antibody specificity must be documented by Western blotting with a complex protein lysate, such as a cell line or tissue lysate. A biotinylated secondary antibody binds to the primary antibody and is used as a base molecule for signal amplification strategies based on biotinyl tyramide/streptavidin-biotin binding. Protein signal amplification techniques based on catalyzed signal amplification using biotinyl tyramide [20–22] have been developed for chromogenic detection [1] and fluorescent detection of proteins [23]. Either chromogenic or fluorescent detection methods are compatible with RPPA [16]. The limit of detection for each protein endpoint can be determined by probing a set of RPPA slides with various concentrations of primary antibody and a constant secondary antibody concentration to determine the signal/noise ratio for each antibody dilution [2, 7].

High-quality image acquisition and spot analysis software are used to discriminate protein specimen spots from the background to precisely quantify proteins [16]. Spot analysis can be performed with any software that can adequately discriminate spots and measure the pixel intensity of each spot and the surrounding background [24].

In this chapter, we describe RPPA construction, Sypro Ruby Blot Stain for quantifying total protein in an array, RPPA immunostaining with colorimetric detection, and image acquisition.

2 Materials

2.1 Specimen Preparation

1. Protein-containing specimen: human or animal cells from laser capture microdissection, tissue (formalin or ethanol fixed or frozen), extracellular vesicles, peripheral blood mononuclear cells, vitreous fluid, etc. (*see* **Note 1**).
2. Protein printing buffer: 100 μL Bond-Breaker TCEP (tris (2-carboxyethyl)phosphine) Solution (*see* **Note 2**), neutral pH, 450 μL Tissue Protein Extraction Reagent (T-PER), and 450 μL Novex Tris-glycine SDS Sample Buffer (2×) (*see* **Note 3**).
3. Phosphate-buffered saline (PBS) without calcium or phosphate.
4. Low protein-binding microcentrifuge tubes.
5. Heat block or water bath, 85–100 °C.

2.2 Cell Culture

1. Adherent or suspension cell culture.
2. PBS, prewarmed to 37 °C.
3. Centrifuge with a swinging bucket rotor.
4. Low protein-binding microcentrifuge tubes.
5. Cell scraper for adherent cell culture.
6. 15 mL conical tubes for suspension cell culture.
7. Protein printing buffer: Use 500 μL buffer/T75 cm^2 flask for adherent cells or 100 μL lysis buffer/1 × 10^6 suspension cells.

2.3 RPPA Construction

2.3.1 RPPA Printing

1. Protein lysate in protein printing buffer.
2. Control lysates/peptide: Commercial cell lysates and/or recombinant peptides containing the protein analytes of interest.
3. Bovine serum albumin (BSA) standard, 2.0 mg/mL.
4. Robotic arrayer: Quanterix 2470 arrayer.

5. Nitrocellulose-coated glass slides (ONCYTE® nitrocellulose film slides, Grace Bio-Labs or FAST™ slides, KeraFAST) (*see* **Note 4**).
6. Protein printing buffer: 100 μL Bond-Breaker TCEP (tris (2-carboxyethyl)phosphine) Solution, neutral pH (final concentration 10%), 450 μL Tissue Protein Extraction Reagent (T-PER), and 450 μL Novex Tris-glycine SDS Sample Buffer (2×).
7. Polypropylene or polystyrene 384 well conical bottom microtiter plate with lids (Molecular Devices). The Aushon 2470 arrayer is equipped with suction cups to remove the lid from the microtiter plates. A lid *must* be placed on every microtiter plate that is loaded in the arrayer. The lid should be clean and dry, free of dust, adhesive, and liquid.
8. 70% ethanol, 5 mL.
9. Type 1 reagent grade water (deionized water).
10. Dessicant with indicator, mesh size 4 (Drierite, anhydrous calcium sulfate).
11. Ziploc style plastic storage bags.

2.3.2 RPPA Total Protein Test Print

1. RPPA slides printed with specimens, BSA, and controls.
2. Sypro Ruby Protein Blot Stain (Invitrogen).
3. Fixative solution: 7% v/v acetic acid (final concentration) and 10% v/v methanol (final concentration) added to dH_2O. Mix well. Store in a glass bottle with a screw cap lid. Stable for 2 months at room temperature.
4. Type 1 reagent grade water.
5. Orbital shaker (50 rpm) or rocker.
6. Aluminum foil.
7. Fluorescent scanner such as a UV transilluminator or laser scanner with 300 nm excitation and 618 nm emission wavelengths (*see* **Note 5**).
8. Spot analysis software: ImageQuant.

2.4 RPPA Immunostaining

1. Reverse phase protein microarrays printed with cell lysates, exosomes, vitreous, peripheral blood mononuclear cells, or other protein-containing body fluids.
2. Reblot™ Mild Antigen Stripping Solution 10× (Chemicon/Millipore): Prepare 1× solution in deionized water. Add 5 mL Reblot Mild to a screw-capped conical tube to 45 mL deionized water. Mix well.
3. PBS without calcium or magnesium.

4. I-Block™ Protein Blocking Solution (Applied Biosystems/Invitrogen): Dissolve 1 g of I-Block Protein Blocking powder in 500 mL of PBS w/o calcium or magnesium. Heat on a hot plate with constant stirring (*see* **Note 6**). Cool the solution to room temperature, and add 500 μL of Tween 20. Store I-Block solution at 4 °C for a maximum of 2 weeks.
5. Primary antibodies, unconjugated (*see* **Note 7**).
6. Biotinylated, species-specific, secondary antibodies.
7. Dako Autostainer or Autostainer Plus (Agilent/Dako).
8. Tyramide Signal Amplification System for biotinylated probes (Agilent/Dako GenPoint kit).
9. Biotin blocking system (Agilent/Dako).
10. Antibody diluent with background-reducing components (Agilent/Dako).
11. Tris-buffered saline with Tween (TBST): 0.05 mol/L Tris/HCl, 0.30 mol/L NaCl, 0.1% Tween 20, pH 7.6 (Agilent/Dako S3306).
12. Diaminobenzidine: DAB+, Liquid Substrate Chromogen System (Carcinogenic, contact hazard, wear gloves while handling) (Agilent/Dako).

2.5 RPPA Colorimetric Image Acquisition

1. UMAX Powerlook 2100XL flatbed scanner (UMAX).
2. Adobe® Photoshop Software.
3. RPPA stained with diaminobenzidine (DAB).
4. Spot analysis software (ImageQuant® GE Healthcare or similar).

3 Methods

3.1 Specimen Preparation

A Laemmli-based buffer (Novex® Tris-Glycine SDS Sample Buffer 2× plus a reducing agent and detergent) is used to create the protein lysates. The SDS and glycerol in the buffer aid in protein binding to the nitrocellulose and optimal sample diffusion within the porous nitrocellulose of the RPPA. Cell culture samples should be rinsed quickly in PBS to remove contaminating immunoglobulins or serum present in the medium, prior to cell lysis (*see* **Note 8**). The total protein concentration of each sample must be measured and adjusted to the same value, within the range of 0.25–0.5 μg/μL for RPPA printing (*see* **Note 9**):

1. Frozen cells or frozen tissue sections: add protein printing buffer to the frozen cells/tissue in a low protein-binding tube (100 μL lysis buffer/1 × 10^6 cells or 15 μL for each tissue section).

2. Vortex vigorously for 30 s.
3. Heat the sample tube in a dry heat block at 85–100 °C for 5–8 min.
4. Vortex vigorously for 30 s.
5. Spin the tube for 15 s at high speed in a microcentrifuge.
6. Allow the specimen to reach room temperature and proceed with RPPA printing.

3.2 Cell Culture

3.2.1 Adherent Cell Lines

1. Remove the culture medium.
2. Rinse adherent cells 2× in 37 °C PBS without calcium or magnesium.
3. Add protein printing buffer (500 μL/T75 cm^2 flask). Rotate the flask to ensure that the buffer covers the entire cell culture surface (bottom of the flask).
4. Use a cell scraper to dislodge the cells. Aspirate the cell lysate into a labeled 1.5 mL low protein-binding microcentrifuge tube.
5. Vortex vigorously for 30 s.
6. Heat the lysate in a dry heat block at 85–100 °C for 5–8 min.
7. Vortex vigorously for 30 s.
8. Spin the tube in briefly in a microcentrifuge.
9. Allow the specimen to reach room temperature and proceed with RPPA printing.

3.2.2 Suspension Cell Lines

1. Transfer cells and medium to a 15 mL conical tube. Spin the tube in a swinging bucket centrifuge at room temperature for 5 min at 900 × *g*.
2. Remove and discard the medium. Resuspend the cell pellet in 10 mL 37 °C PBS.
3. Spin the tube at room temperature for 5 min at 900 × *g*. Remove and discard the PBS.
4. Resuspend the cell pellet in 10 mL 37 °C PBS. Spin the tube at room temperature for 5 min at 900 × *g*. Remove and discard the PBS.
5. Add protein printing buffer to the washed cell pellet (100 μL lysis buffer/1 × 10^6 cells).
6. Vortex vigorously for 30 s.
7. Heat the lysate in a dry heat block at 85–100 °C for 5–8 min.
8. Vortex vigorously for 30 s.
9. Spin the tube in briefly in a microcentrifuge.
10. Allow the specimen to reach room temperature and proceed with RPPA printing.

3.3 RPPA Construction

The arrayer described in this protocol is the Quanterix 2470 arrayer (formerly the Aushon 2470 arrayer), equipped with 350 μm diameter solid pins. The general principles of array printing are applicable to a variety of robotic arrayers. The number of slides required for printing and immunostaining directly depends on the number of endpoints (proteins) of interest and the number of negative controls. One endpoint or control is one RPPA slide. The total number of arrays to print is determined by the sum of the endpoints, the number of arrays to be used for normalization, the number of staining batches planned, and the number of different antibody species in each run. For example, if 100 protein endpoints are to be measured, using 4 total protein stained arrays for normalization, with 4 staining batches, and the primary antibodies will include rabbit and mouse species, then a minimum of 108 arrays should be printed.

Control specimens are printed on each RPPA. Controls may include commercial cell lysates, recombinant peptides, or peptide mixtures that are known to contain the proteins of interest. Samples and controls are often printed in a dilution series to be able to create a linear dynamic range of the protein concentration for each protein of interest, thus allowing the protein's concentration to be matched to the antibody affinity. This dilution series provides a signal/noise ratio within the linear dynamic range of the RPPA for each protein-antibody pair.

3.3.1 RPPA Printing

1. Fill water wash container with type 1 reagent grade water. Empty the waste container. Fill the humidifier with type 1 reagent grade water.
2. Turn the power switch on and open the Quanterix 2470 arrayer software.
3. Click on the 384 well microtiter plate on the Library Screen to move a plate into the software library. Add as many plates as needed.
4. Click on the first microtiter plate in the library. Use the well plate grid to select the wells containing samples. The grids represent the 4 × 5 pin format (20 pins). Click on the second microtiter plate in the library, and select the wells containing the samples to be printed on the array. Repeat this process for all the microtiter plates.
5. Click "continue."
6. On the array layout screen, define the printing parameters. Top offset, 4.5 mm (*see* **Note 10**); Left offset, 5.0 mm; Feature-to-feature spacing, 1125 μM in the *x*-axis and *y*-axis; Depositions per feature, 3; Replicates, 1 (prints specimens in duplicate); and Position, linear vertical (Fig. 2) (*see* **Note 11**).

7. Select two "super arrays" if samples are loaded into rows I–P in the microtiter plate or if replicate super arrays are to be printed. Click "continue."
8. On the wash screen, choose 4 s for pin washing, with three fast immersions and one slow immersion. Click "continue."
9. On the platen load screen, select the number of slides to be loaded on each platen. Ten slides can be loaded per platen, with a total of ten platens in the arrayer.
10. Set the humidity to 50% to prevent sample evaporation and to aid in spot drying between depositions.
11. Use an adjustable pipette to load the specimens, controls, and BSA standard into 384 well conical bottom microplates, creating a 4 point, twofold dilution curve for each specimen and control. Create an 8 point, twofold dilution curve for each standard. Use protein printing buffer (900 µL T-PER, 900 µL Novex® Tris-Glycine SDS Sample Buffer 2×, and 200 µL TCEP) to make the dilutions. Figure 1 shows a specimen loading map for the microtiter plate. Well A1 will be printed in the upper left corner of the array slide, if the array is positioned horizontally with the label to the right. An example RPPA stained array is shown in Fig. 2.

Sample 1				Sample 2				Sample 3				Sample 4				Sample 5			
Neat	1:2	1:4	1:8	Neat	1:2	1:4	1:8	Neat	1:2	1:4	1:8	Neat	1:2	1:4	1:8	Neat	1:2	1:4	1:8
A1	A6	A11	A16	A2	A7	A12	A17	A3	A8	A13	A18	A4	A9	A14	A19	A5	A10	A15	A20
A1	A6	A11	A16	A2	A7	A12	A17	A3	A8	A13	A18	A4	A9	A14	A19	A5	A10	A15	A20
Sample 6				Sample 7				Sample 8				Sample 9				Sample 10			
E1	E6	E11	E16	E2	E7	E12	E17	E3	E8	E13	E18	E4	E9	E14	E19	E5	E10	E15	E20
E1	E6	E11	E16	E2	E7	E12	E17	E3	E8	E13	E18	E4	E9	E14	E19	E5	E10	E15	E20
Sample 11				Sample 12				Sample 13				Sample 14				Sample 15			
B1	B6	B11	B16	B2	B7	B12	B17	B3	B8	B13	B18	B4	B9	B14	B19	B5	B10	B15	B20
B1	B6	B11	B16	B2	B7	B12	B17	B3	B8	B13	B18	B4	B9	B14	B19	B5	B10	B15	B20
Sample 16				Sample 17				Sample 18				Sample 19				Sample 20			
F1	F6	F11	F16	F2	F7	F12	F17	F3	F8	F13	F18	F4	F9	F14	F19	F5	F10	F15	F20
F1	F6	F11	F16	F2	F7	F12	F17	F3	F8	F13	F18	F4	F9	F14	F19	F5	F10	F15	F20
Sample 21				Sample 22				Sample 23				Sample 24				Sample 25			
C1	C6	C11	C16	C2	C7	C12	C17	C3	C8	C13	C18	C4	C9	C14	C19	C5	C10	C15	C20
C1	C6	C11	C16	C2	C7	C12	C17	C3	C8	C13	C18	C4	C9	C14	C19	C5	C10	C15	C20
Sample 26				Sample 27				Sample 28				Sample 29				Sample 30			
G1	G6	G11	G16	G2	G7	G12	G17	G3	G8	G13	G18	G4	G9	G14	G19	G5	G10	G15	G20
G1	G6	G11	G16	G2	G7	G12	G17	G3	G8	G13	G18	G4	G9	G14	G19	G5	G10	G15	G20
Sample 31				Sample 32				Sample 33				Sample 34				Sample 35			
D1	D6	D11	D16	D2	D7	D12	D17	D3	D8	D13	D18	D4	D9	D14	D19	D5	D10	D15	D20
D1	D6	D11	D16	D2	D7	D12	D17	D3	D8	D13	D18	D4	D9	D14	D19	D5	D10	D15	D20
Sample 36				Sample 37				Sample 38				Sample 39				Sample 40			
H1	H6	H11	H16	H2	H7	H12	H17	H3	H8	H13	H18	H4	H9	H14	H19	H5	H10	H15	H20
H1	H6	H11	H16	H2	H7	H12	H17	H3	H8	H13	H18	H4	H9	H14	H19	H5	H10	H15	H20

Fig. 1 Reverse phase protein array print map for a Quanterix 2470 arrayer. The print head is equipped with 20, 350 µm pins in a 4 × 5 pin format. Sample 1 will be printed on the array in the upper left corner if you are looking at the array horizontally with the label on the right. The 4 × 5 print head will dip simultaneously into wells 1, 2, 3, 4, and 5 and rows A, B, C, and D. Dilutions for each sample are not placed in consecutive wells in the microtiter plate because the print head spacing allows additional spots to be printed between each pin. Dilutions are placed in every fifth well (1, 6, 11, and 16 for sample 1) but will be printed directly next to each other on the array. Any dilution scheme can be used, for example, only a 2 point dilution, a 3 point dilution, etc. A 4 point dilution generally allows signal detection across the linear range of each protein. The 384 well microtiter plate map denotes the well position and dilution for the first 40 specimens. An additional 40 specimens can be printed as a second super array from microtiter plate rows I–P

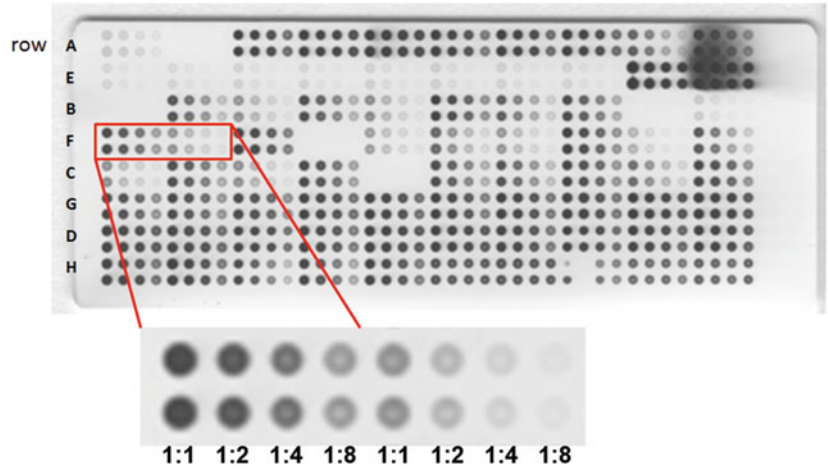

Fig. 2 DAB-stained reverse phase protein array. The row labels represent the microtiter plate row from the print map. Each sample is printed in twofold dilution series. The image in the foreground depicts two, 4 point dilution curves. The label has been cropped from the right side of the array. The dark, blooming spots in the upper right corner of the image depict saturated spots. Saturated spots can be due to a high total protein concentration and/or a primary antibody dilution that is too concentrated. To resolve blooming spot artifacts, either dilute the specimen to a lower total protein concentration or use a more dilute antibody solution

12. Place the lid on the 384 well microtiter plates (*see* **Note 12**).
13. Open the two metal clips on the plate holder. Slide the 384 well plate to the back of the holder with position A1 in the lower left corner. Close the metal clips.
14. Place the plate holder in the Quanterix 2470 arrayer specimen elevator. Ensure that the plate holder label "this end out" is visible.
15. Place the nitrocellulose-coated slides onto the slide platens with the nitrocellulose pad facing up and the label edge to the right. Ensure the slides are securely held by the three slide pins. Load each slide platen into the Quanterix 2470 arrayer.
16. Use the Quanterix 2470 arrayer software checklist to insure that the instrument/slides are ready to be printed, and click start.
17. When printing is complete, the software will prompt the user to either continue or quit. If additional slides are not being printed, select quit, save the run file, and close the software (*see* **Note 13**). Remove the microtiter plates and slides from the arrayer.
18. Place the printed microarray slides in a slide box. Store the slide box in a plastic storage bag with desiccant at −20 °C (*see* **Note 14**).
19. Turn the power off for the Quanterix 2470 arrayer.

3.3.2 RPPA Total Protein Test Print

Total protein concentration per spot is commonly used to normalize the RPPA data between specimens and spots. Variability is reduced across arrays when the total protein concentration is consistent between specimens. To measure the total protein concentration of each specimen on the array, a RPPA is constructed with the undiluted specimens only, a BSA standard dilution curve (1000, 500, 250, 125, 62.5, 31.25, 15.6, 7.8 μg/mL BSA), and a commercially available cell line control as a staining process control. This array is referred to as "total protein test print," and it is stained with Sypro Ruby Protein Blot Stain. The total protein concentration of each sample is extrapolated based on the BSA standard signal intensities. Each sample is diluted to the same concentration and then printed in a twofold dilution series on a set of arrays for subsequent immunostaining with antibodies to the proteins of interest.

Sypro Ruby Protein Blot Stain provides a fluorescent readout to quantify the total protein concentration in each spot and extrapolate the protein concentration based on a BSA standard curve. Sensitivity of Sypro Ruby Protein Blot Stain is 0.25–1 ng protein/mm^2.

1. Print protein samples on RPPA slides (two slides). Allow the sides to air dry.
2. Wash slides in type 1 reagent grade water twice for 5 min each with continuous agitation or rocking. Discard the water after each wash.
3. Place the slides in a plastic dish with a lid. Immerse the array slides in the fixative solution. Cover the dish and place on orbital shaker or rocker for 15 min.
4. Discard the fixative in a chemical waste container. Wash the array slides in type 1 reagent grade water four times for 5 min each, with continuous agitation or rocking. Discard the water after each wash.
5. Pour Sypro Ruby Protein Blot Stain onto the array slides. Incubate in the dark, protected from light, for 30 min at room temperature, on an orbital shaker or rocker. Cover the container with aluminum foil to prevent light from photobleaching the stain.
6. Discard the Sypro Ruby Protein Blot Stain in a chemical waste container. Wash the array slides in type 1 reagent grade water four times, for 1 min each, protected from light, with continuous agitation or rocking.
7. Air dry the slides at room temperature in the dark, protected from light.
8. Scan the stained slides using a fluorescent scanner with a Cy3 laser and emission filter of 618 nm. Save the images in .tiff format.

9. Quantify the pixel intensity in each spot with spot analysis software (ImageQuant or similar software).
10. Use the spot intensity values and the concentration of the BSA dilutions (1000, 500, 250, 125, 62.5, 31.25, 15.6, 7.8 μg/mL) to plot a standard curve (scatter plot in Excel). Add a linear trend line, *R*2 value, and line equation ($y = mx + b$) to the scatter plot. Using the line equation, calculate the concentration of each specimen on the array. "*y*" is the intensity value from the RPPA, "*x*" is the unknown concentration of the specimen.
11. Determine the volume of lysate needed to print the entire array set for each specimen. Adjust the total protein concentration of the lysates to 250–500 μg/mL. Dilute the specimen, if necessary with protein printing buffer. 40 μL of lysate is adequate for printing 100+ microarrays using a series of four spots, in a twofold dilution curve, in duplicate, on a Quanterix 2470 solid pin arrayer equipped with 185 or 350 μm pins.

    Example calculation to determine the volume of lysate needed to print RPPA:

    $C_1V_1 = C_2V_2$ (*to convert from μg/mL to μg/μL, divide μg/mL by 1000*)

    C_1 = Measured protein concentration on the test print array = 1.5 μg/μL

    V_1 = Volume of lysate to make the dilution (unknown)

    C_2 = Desired protein concentration = 0.5 μg/μL

    V_2 = Desired lysate volume = 40 μL

    Calculation: 1.5 μg/μL × V_1 = 0.5 μg/μL × 40 μL

    V_1 = (0.5 μg/μL × 40 μL)/1.5 μg/μL

    V_1 = 20 μg/1.5 μg/uL

    V_1 = 13.3 μL of lysate needed to make the dilution

    40 − 13.3 μL = 26.7 μL of protein printing buffer needed for the dilution

3.4 RPPA Immunostaining

Each RPPA slide is probed with a single primary antibody directed toward the antigen (protein) of interest. Multiplex analysis is achieved by staining each array with a specific antibody and then comparing specimens both within an array and between arrays. More than 100 proteins may be analyzed by printing 100+ arrays and staining each array with a different antibody.

The number of slides required for immunostaining directly depends on the number of endpoints (proteins) of interest and the number of negative control slides. A negative control slide must be included in each staining run to account for any nonspecific background staining produced by the interaction of each

sample with only the biotinylated secondary antibody. If the set of selected primary antibodies belong to different species (i.e., mouse and rabbit), it is necessary to stain a negative control array for each species of primary antibody (i.e., one anti-mouse negative control array and one anti-rabbit negative control array). We recommend staining array slides in batches so that all the primary antibodies are of the same species. This method reduces the number of negative control slides required in each staining batch. During data analysis, values for the negative control arrays are subtracted from each endpoint to eliminate any nonspecific signal generated by the secondary antibody [16]. The following RPPA staining method describes a colorimetric method using diaminobenzidine (DAB) (Fig. 2) (*see* **Note 15**).

1. Determine the number of slides to be stained, including negative controls. One array slide/protein endpoint is needed, plus one slide for each species of secondary antibody in the staining run.
2. Remove the slides from the freezer. Keep the slides dessicated (in the slide box, inside a plastic bag containing Drierite). Allow the slides to acclimate to room temperature for 10–15 min.
3. Fill the Autostainer carboys with deionized water and TBST (1×) for washes (*see* **Note 16**). Ensure that the waste carboys are empty.
4. Prepare 1× ReBlot Mild Solution.
5. Place the slides faceup in a clean, plastic dish. Do not touch the nitrocellulose surface.
6. Quickly pour 1× ReBlot Mild Solution onto the slides. Ensure that all the slides are completely wetted with Reblot.
7. Incubate the arrays in Reblot for 15 min with constant, low-speed rocking. (*see* **Note 17**).
8. Discard ReBlot solution, and wash slides with PBS without calcium or magnesium twice for 5 min each with constant, low-speed rocking.
9. Incubate slides in I-Block solution for at least 30 min at room temperature with constant, low-speed rocking. This step reduces nonspecific antibody binding. Slides can also be left in I-Block solution over night at 4 °C if needed.
10. Select the primary and biotinylated secondary antibodies. The primary and secondary antibodies must be species matched, i.e., a primary antibody raised in a rabbit requires a biotinylated anti-rabbit secondary antibody (IgG H+L).
11. Program the Dako Autostainer as described in Table 1 (*see* **Note 18**).
12. The Autostainer program automatically calculates the exact amount of each solution needed for the staining run, based

Table 1
RPPA colorimetric detection program with a Dako Autostainer

Step	Category	Dako Autostainer	Reagent name	Incubation (min)	Special instructions
1	Rinse	Agilent S3306	TBST buffer		
2	Endogenous enzyme block	Sigma 323381	Peroxide block 2	5	3% (wt%) hydrogen peroxide from any vendor
3	Rinse		TBST buffer		
5	Protein block	Agilent X0590	Avidin block	10	
6	Rinse		TBST buffer		
8	Protein block	Agilent X0590	Biotin block	10	
10	Rinse		TBST buffer		
11	Protein block	Agilent X0909	Protein block 2	5	
12	Rinse		Blow air		
13	Primary antibody		Primary antibody	30	Unconjugated
14	Rinse		TBST buffer		
17	Auxiliary		TBST wash	3	
18	Rinse		TBST buffer		
20	Secondary reagent	Vector BA-1000	Anti-rabbit IgG H+L (Biotinylated)[a]	15	Or Anti-mouse IgG
21	Rinse		TBST buffer		
24	Auxiliary		TBST wash	3	
25	Rinse		TBST buffer		
27	Auxiliary	Agilent GenPoint K062011	Primary streptavidin-HRP	15	Dilute 1:800
28	Rinse		TBST buffer		
30	Auxiliary		TBST wash	3	
31	Rinse		TBST buffer		
33	Amplification reagent	GenPoint	Biotinyl tyramide	15	Ready to use
34	Rinse		TBST buffer		
36	Auxiliary		TBST wash	3	
37	Rinse		Buffer		
39	Labeled polymer	GenPoint	Secondary streptavidin-HRP	15	Ready to use

(continued)

Table 1
(continued)

Step	Category	Dako Autostainer	Reagent name	Incubation (min)	Special instructions
40	Rinse		TBST buffer		
41	Auxiliary		TBST wash	3	
42	Rinse		TBST buffer		
43	Switch		Switch to toxic waste		
44	Chromogen	GenPoint	DAB	5	Dilute GenPoint DAB 1:100
45	Rinse		Deionized water rinse		
46	Rinse		Deionized water	3[b]	

[a]The primary and secondary antibody species must match
[b]840 minutes for an overnight staining run

on the volume of fluid deposited in each drop zone of the slide. 450 μL of reagent is required to adequately soak a 20 × 51 mm nitrocellulose pad.

13. Prepare solutions in the GenPoint kit: Dilute the *primary* streptavidin-HRP Concentrate with the streptavidin-HRP diluent at 1:800. Dilute the DAB 1:100 with DAB buffer. Load all the staining reagents into labeled Autostainer vials.
14. Dilute the primary and secondary antibodies in antibody diluent (Dako) to minimize background signal.
15. Place the reagent rack into the Autostainer.
16. Load the RPPA slides that have been blocked in I-Block solution on the Autostainer. Do not allow slides to dry during loading; 1× TBST can be used to keep the arrays wet.
17. Prime the water first, followed by TBST buffer. Start the staining run.
18. After the staining run is complete, remove the slide rack from the Autostainer. Leave the slides in the rack, and rinse the entire rack and the front and back of the slides with deionized water. The nitrocellulose pad should be completely wet with deionized water.
19. Allow the slides to air dry, protected from direct sunlight (*see* **Note 19**).

3.5 RPPA Colorimetric Image Acquisition

Image acquisition is a critical step of RPPA analysis. Arrays stained with DAB can be acquired with any high-resolution (14 bit) scanner equipped with a grayscale option. The following method

describes image acquisition with a UMAX, Powerlook 2100XL scanner [16] (*see* **Note 20**).

1. Place RPPA slides facedown (nitrocellulose against the glass) on the scanner (*see* **Note 21**).
2. Open Adobe Photoshop, and import the image from the scanner using the file menu: File/Import/MagicScan.
3. Select the "Preview" button under the scanner window. Two boxes will appear: the red box provides an outline of the "preview" area; the dotted blue box defines the "scan" area. Adjust these two boxes based on the desired scanning area.
4. Under the "Settings" window, select a 14-bit image.
5. Under the "Window" menu, choose select "Scanner Control." Enter the following scanning parameters:
   (a) Ensure "Manual Control" is checked.
   (b) Reflective.
   (c) Gray 256 scales.
   (d) Resolution 600 dpi.
   (e) No descreen.
   (f) No filter.
   (g) Image settings (eyedropper icons): 255 (white), 0 (black), 1.0 (gamma).
6. Before starting the image acquisition, adjust the dotted blue scan area box to encompass the entire slide, including the label. All scanned images will be sent to Adobe Photoshop from which they can be adjusted or saved.
7. After image acquisition is completed close the MagicScan program. The images will be open in Photoshop. Save both the original image and the color inverted image as a tiff file. Invert the color of each image to white spots on a black background: In Photoshop, after each original image is saved, use CTRL+I to invert the image, and save the inverted image with the suffix "inv" at the end of the file name (*see* **Note 22**).

4 Notes

1. If animal cell proteins will be quantified by RPPA, ensure that primary antibodies to the animal species are available and validated. Not all primary antibodies will cross-react with every species. Also ensure that the biotinylated secondary antibody will not cross-react to a high degree with the animal species.

2. TCEP is an odorless reducing agent that does not readily oxidize or react with other functional groups found in proteins. The volume of protein printing buffer required can be calculated by multiplying the number of specimens on the array by the number of dilutions and by the volume of specimen in each well of the microtiter plate. For example, 55 specimens to be printed in a fourfold dilution series, with 15 μL of specimen in each well, would require 3.3 mL of Laemmli buffer ($55 \times 4 \times 15 = 3300$ μL).
3. Novex Tris-glycine SDS Sample Buffer (2×) (Thermo Fisher catalog LC2676) may be substituted for the Laemmli buffer [25]. The Laemmli buffer recipe for cell lysis is 100 mM Tris–HCl, pH 6.8, 200 mM dithiothreitol, 4% SDS, 0.2% bromophenol blue, and 20% glycerol. Dithiothreitol should be added, just before use. Laemmli buffer without dithiothreitol can be stored at room temperature.
4. An alternative to nitrocellulose-coated slides are NEXTERION® 3-D Hydrogel-coated slides (Schott Nexterion https://www.us.schott.com/nexterion/english/products/functional-coatings/3d-hydrogel-coating.html).
5. Sypro Ruby Red stain is a permanent protein stain, detected by fluorescence with an excitation wavelength of 300 or 480 nm and an emission wavelength of 618 nm. The stain is composed of a heavy metal ruthenium complex. The stain is photostable, allowing long emission lifetime and the ability to measure fluorescence over a longer time frame, minimizing background fluorescence. A UV transilluminator, a blue-light transilluminator, or a laser scanner with excitation at 250–300 nm and emission at 618 nm can be used to detect a Sypro Ruby stained array. Example scanners are ArrayCam (Grace Bio-Labs); Tecan Power scanner; or Molecular Devices GenePix 4000B. An alternative total protein stain is the infrared dye Fast Green [26, 27].
6. Heat the I-Block solution on a hot plate at a low to medium temperature for 10–15 min. Do not allow the solution to boil. I-Block is a casein-based protein solution, and boiling will alter blocking efficiency by causing protein degradation of the casein. Mix well after adding the Tween20, but do not heat the I-Block + Tween solution.
7. Primary antibodies to be used on a RPPA must be validated by Western blotting. Samples similar to those on the array must be used to verify specificity of the antibody. A single band on a Western blot, at the specified molecular weight, provides documentation of antibody specificity. If the protein has known subunits, such as dimers or cleavage products, additional bands

at the corresponding molecular weights may also be seen on a Western blot.

8. Immunoglobulins in cell culture medium, from fetal bovine serum, can cause high nonspecific signal in the negative control array slides. Removing the cell culture medium and rinsing the cells quickly in PBS can reduce the immunoglobulin contamination, thus improving the signal/noise ratio.
9. The protein buffer determines whether or not the total protein concentration can be measured spectrophotometrically. Bromophenol blue and SDS are incompatible with the Bradford Coomassie spectrophotometric method or a NanoDrop microvolume instrument. To circumvent these problems, we print all the specimens on a RPPA with a bovine serum albumin standard. We stain the RPPA with Sypro Ruby Protein Blot Stain, and then adjust the total protein concentration of each sample to the same value, within the range of 0.25–0.5 μg/μL.
10. The top offset and left offset may vary with the nitrocellulose slide vendor due to the placement of the nitrocellulose pad and the format of the pad (single pad, four pads, eight pads, etc). Aqueous food dyes, used for baking or egg coloring, can be diluted in PBS or water to substitute as specimens for evaluating spot placement during printing. Clean the arrayer pins thoroughly following printing with food dyes. 70% ethanol in water can be used to clean the pins. To clean the pins, dispense 20 μL of 70% ethanol into wells 1–20 in rows A, B, C, and D of a 384 well microtiter plate. Load one nitrocellulose-coated slide into the arrayer. Program and execute a print run for one slide, from one microtiter plate with four unique extractions, at three depositions/feature in duplicate.
11. Approximately 30 nL of lysate will be deposited on the nitrocellulose per spot with three depositions/feature. Protein-binding capacity of nitrocellulose film slides is based on porosity and thickness of the nitrocellulose coating [19, 28]. In our experience, saturation of the nitrocellulose is reached at five depositions/spot. Very dilute specimens, with protein concentrations less than 0.125 μg/μL, can be concentrated by printing more than three depositions/feature (spot). However, spot quality may become more diffuse or inconsistent at higher depositions/feature. Printing test arrays with three, four, and five depositions/feature are helpful for assessing the trade-offs between protein concentration and spot quality.
12. A lid must be placed on every microtiter plate that is loaded in the arrayer. The lid should be clean and dry, free of dust, adhesive, and liquid. The Quanterix 2470 arrayer is equipped with two suction cups to remove the lid from the microtiter plate during sample deposition (printing). The lid is placed

back onto the microtiter plate after sample deposition is complete for that particular microtiter plate.

13. A .gal file is generated with each print run and is saved in C:\Documents and Settings\user\My Documents\user\Array Data Files. The .gal file contains the array printing layout. The .gal file can be uploaded into software analysis packages to facilitate specimen layout mapping.
14. Proteins immobilized on nitrocellulose slides are stable at −20 °C for more than 15 years if stored with desiccant.
15. RPPA slides may be stained manually or on a programmable, automated slide stainer compatible with open-source reagents. The automated slide stainer should allow various fluid volumes to be dispensed, include wash steps, and be able to completely saturate a 20 × 51 mm area of the slide. A colorimetric or fluorescent detection system can be used in conjunction with the catalyzed signal amplification method which utilizes a horseradish peroxidase-mediated deposition of biotinyl tyramide at the site of the primary/secondary antibody. The decision to use fluorescent or colorimetric detection methods depends on (a) the estimated analyte concentration, (b) type of microarray imaging system, and (c) type of sample. Fluorescent detection methods are compatible with a variety of fluorophores, such as Cy3, Cy5, Fast Green, and infrared dyes. Fluorescent detection is well suited to specimens with high total protein content and/or with high analyte concentrations, such as in cell lines where the amount of input material (cells) can be adjusted. Colorimetric detection methods are commonly used with RPPA constructed from small amounts of cells, such as laser capture microdissected specimens. Diaminobenzidine (DAB)-stained RPPA can be scanned on any high-resolution flatbed scanner. In addition, DAB-stained RPPA provide an immediate visual image of the relative abundance of each specimen, as well as any potential staining artifacts that may impact analysis.
16. Use deionized water to prepare all the solutions including TBST buffer. Clean the water and buffer containers periodically with 70% ethanol to avoid mold/bacterial growth.
17. Reblot treatment of the arrays is required for full denaturation of immobilized proteins and facilitates antibody binding. Do not exceed the ReBlot incubation time of 15 min. ReBlot is an alkaline solution that can potentially cause the nitrocellulose to detach from the glass slide. Do not use ReBlot when serum samples are printed on the arrays. The solution will cause diffusion of the serum sample on the nitrocellulose.
18. The Autostainer is designed to periodically add TBST to the slides at the end of the staining run if the operator does not

terminate the run. The TBST will cause salt crystals to form on the nitrocellulose. The salt crystals interfere with spot detection/analysis. The Autostainer can be programmed to run overnight by including an additional water rinse, for 14 h (840 min), after the slides are rinsed with water following the DAB reagent. This optional water rinse prevents the Autostainer from adding TBST to the slides until after the 840 min have elapsed and the final water rinse has been completed. Note that the operator must terminate the run after the 840 min water rinse step to prevent TBST from being added to the slides after the final water rinse.

19. DAB-stained arrays should be rinsed in running deionized water to remove TBST and DAB residue from the slide. The DAB residue can cause increased background in the scanned image. Rinse the entire Autostainer rack with the slides in running deionized water. Rinsing the Autostainer rack also helps reduce potential contamination with staining reagents between runs.
20. Each scanner should be calibrated for optimal image acquisition. The gamma setting can be adjusted using the calibrated grayscale strip provided with the scanner.
21. Cover slides with a few pieces of white copy paper to avoid light artifacts during image acquisition.
22. Images need to be inverted (white spots on a black background) in Photoshop for compatibility with ImageQuant spot analysis software.

References

1. Paweletz CP, Charboneau L, Bichsel VE et al (2001) Reverse phase protein microarrays which capture disease progression show activation of pro-survival pathways at the cancer invasion front. Oncogene 20:1981–1989
2. Liotta LA, Espina V, Mehta AI et al (2003) Protein microarrays: meeting analytical challenges for clinical applications. Cancer Cell 3:317–325
3. Mueller C, Liotta LA, Espina V (2010) Reverse phase protein microarrays advance to use in clinical trials. Mol Oncol 4:461–481
4. Mueller C, deCarvalho AC, Mikkelsen T et al (2014) Glioblastoma cell enrichment is critical for analysis of phosphorylated drug targets and proteomic–genomic correlations. Cancer Res 74:818–828
5. MacBeath G, Schreiber SL (2000) Printing proteins as microarrays for high-throughput function determination. Science 289:1760–1763
6. Espina V, Mariani BD, Gallagher RI et al (2010) Malignant precursor cells pre-exist in human breast DCIS and require autophagy for survival. PLoS One 5:e10240
7. VanMeter AJ, Rodriguez AS, Bowman ED et al (2008) Laser capture microdissection and protein microarray analysis of human non-small cell lung cancer: differential epidermal growth factor receptor (EGPR) phosphorylation events associated with mutated EGFR compared with wild type. Mol Cell Proteomics 7:1902–1924
8. Wulfkuhle JD, Berg D, Wolff C et al (2012) Molecular analysis of HER2 signaling in human breast cancer by functional protein pathway activation mapping. Clin Cancer Res 18:6426–6435
9. Bader S, Zajac M, Friess T et al (2015) Evaluation of protein profiles from treated xenograft tumor models identifies an antibody panel for formalin-fixed and paraffin-embedded (FFPE)

tissue analysis by reverse phase protein arrays (RPPA). Mol Cell Proteomics 14:2775–2785

10. van Dijk AD, Hu CW, de Bont ESJM et al (2018) Histone modification patterns using RPPA-based profiling predict outcome in acute myeloid leukemia patients. Proteomics 18:e1700379
11. Biasutto L, Chiechi A, Couch R et al (2013) Retinal pigment epithelium (RPE) exosomes contain signaling phosphoproteins affected by oxidative stress. Exp Cell Res 319:2113–2123
12. Davuluri G, Espina V, Petricoin EF et al (2009) Activated VEGF receptor shed into the vitreous in eyes with wet AMD: a new class of biomarkers in the vitreous with potential for predicting the treatment timing and monitoring response. Arch Ophthalmol 127:613–621
13. Petricoin EF, Espina V, Araujo RP et al (2007) Phosphoprotein pathway mapping: Akt/mammalian target of rapamycin activation is negatively associated with childhood rhabdomyosarcoma survival. Cancer Res 67:3431–3440
14. Austin J, Holway AH (2011) Contact printing of protein microarrays. Methods Mol Biol 785:379–394
15. Romanov V, Davidoff SN, Miles AR et al (2014) A critical comparison of protein microarray fabrication technologies. Analyst 139:1303–1326
16. Gallagher RI, Silvestri A, Petricoin EF et al (2011) Reverse phase protein microarrays: fluorometric and colorimetric detection. Methods Mol Biol 723:275–301
17. Baldelli E, Calvert V, Hodge A et al (2017) Reverse phase protein microarrays. Methods Mol Biol 1606:149–169
18. McWilliam I, Chong Kwan M, Hall D (2011) Inkjet printing for the production of protein microarrays. Methods Mol Biol 785:345–361
19. Tonkinson JL, Stillman BA (2002) Nitrocellulose: a tried and true polymer finds utility as a post-genomic substrate. Front Biosci 7:c1–c12
20. Bobrow MN, Shaughnessy KJ, Litt GJ (1991) Catalyzed reporter deposition, a novel method of signal amplification. II. Application to membrane immunoassays. J Immunol Methods 137:103–112
21. Hunyady B, Krempels K, Harta G et al (1996) Immunohistochemical signal amplification by catalyzed reporter deposition and its application in double immunostaining. J Histochem Cytochem 44:1353–1362
22. King G, Payne S, Walker F et al (1997) A highly sensitive detection method for immunohistochemistry using biotinylated tyramine. J Pathol 183:237–241
23. van Gijlswijk RP, Zijlmans HJ, Wiegant J et al (1997) Fluorochrome-labeled tyramides: use in immunocytochemistry and fluorescence in situ hybridization. J Histochem Cytochem 45:375–382
24. Yeon S, Bell F, Shultz M et al (2017) Dual-color, multiplex analysis of protein microarrays for precision medicine. Methods Mol Biol 1550:149–170
25. Laemmli UK (1970) Cleavage of structural proteins during the assembly of the head of bacteriophage T4. Nature 227:680–685
26. Luo S, Wehr NB, Levine RL (2006) Quantitation of protein on gels and blots by infrared fluorescence of Coomassie blue and Fast Green. Anal Biochem 350:233–238
27. Dsouza A, Scofield RH (2015) Protein stains to detect antigen on membranes. Methods Mol Biol 1314:33–40
28. Stillman BA, Tonkinson JL (2000) FAST slides: a novel surface for microarrays. BioTechniques 29:630–635

Chapter 10

Enhanced Protein Profiling Arrays for High-Throughput Quantitative Measurement of Cytokine Expression

Ruochun Huang, Chun-Hui Gao, Wenjuan Wu, and Ruo-Pan Huang

Abstract

The antibody array has become a powerful technology in recent years and is widely used to detect the expression levels of various proteins such as cytokines, growth factors, chemokines, and angiogenic factors, some of which are involved in cancer progression. In this chapter, we describe a protein array technology called enhanced protein profiling array, which can simultaneously and quantitatively measure the expression levels of a few proteins in hundreds or thousands of samples, and an example of its use is presented.

Key words Enhanced protein array, Antibody array, Throughput array, Quantitative array, Cytokine antibody array

1 Introduction

Cytokines play important roles in many aspects of cell physiology and pathology [1–3]. Multiple cytokine expression levels have been simultaneously determined using sandwich ELISA-based antibody array technology [4, 5]. Previously, these developed antibody array technologies have also been applied to analyze human diseases [6–9]. However, when comparing a limited number of factors from large sample sizes, it is much easier to array the samples in the same matrix and test for one or several factors at a time. Furthermore, arraying the samples in the same matrix requires much less sample volume (0.5 μL) and is more efficient for measuring the cytokine expression levels.

Tissue microarrays have become a powerful means for high-throughput molecular profiling of tumor specimens [10, 11]. Equally important is the detection of hundreds and even thousands of serum, plasma, conditioned media, tissue lysate, cell lysate, and other fluid samples quantitatively. Current major difficulties of simultaneous, quantitative measurement of protein levels from large sample groups are low detection sensitivity and specificity issues. Precoating a surface, like a nitrocellulose

Kelly C. Whittaker and Ruo-Pan Huang (eds.), *Antibody Arrays: Methods and Protocols*, Methods in Molecular Biology, vol. 2237, https://doi.org/10.1007/978-1-0716-1064-0_10,

membrane, with a specific antibody before printing the samples/analytes onto the surface can help overcome these problems. In this chapter, a protein array technology called enhanced protein profiling array [12], which can simultaneously and quantitatively measure the expression levels of a few proteins in hundreds or thousands of samples is discussed, and an example of its use is presented.

2 Materials

1. Antibody pairs and corresponding antigens: EGF and PDGF capture antibodies (500 μg/mL), biotin-conjugated detection antibodies (250 μg/mL), and recombinant protein (*see* **Note 1**).
2. Coating buffer: 0.1 M Na_2HPO_4, pH 9.0.
3. Hybond enhanced chemiluminescence (ECL) membranes (*see* **Note 2**).
4. Pipetman (0.1–2 μL).
5. Blocking buffer: 5% bovine serum albumin (BSA)/1× TBS.
6. Orbital shaker.
7. Tris-buffered saline (TBS): 0.01 M Tris–HCl, pH 7.6, 0.15 M NaCl.
8. TBS/0.1% Tween-20: 0.01 M Tris–HCl, pH 7.6, 0.15 M NaCl, 0.1% Tween-20.
9. Horseradish peroxidase (HRP)-conjugated streptavidin.
10. ECL reagents A and B (Amersham).
11. Small plastic boxes or containers.
12. Densitometer.
13. Sigma plot or similar software.
14. Human plasma sample (*see* **Note 3**).
15. Forceps.
16. Plastic sheet.
17. Kodak X-OMAT film and film processor.

3 Methods (Fig. 1)

1. Dilute the anti-human EGF and PDGF capture antibodies to 20 μg/mL with the coating buffer.
2. Incubate each membrane (Hybond enhanced chemiluminescence (ECL) membranes) with 10 mL of the prepared 20 μg/mL capture antibody (either anti-human EGF or PDGF) in

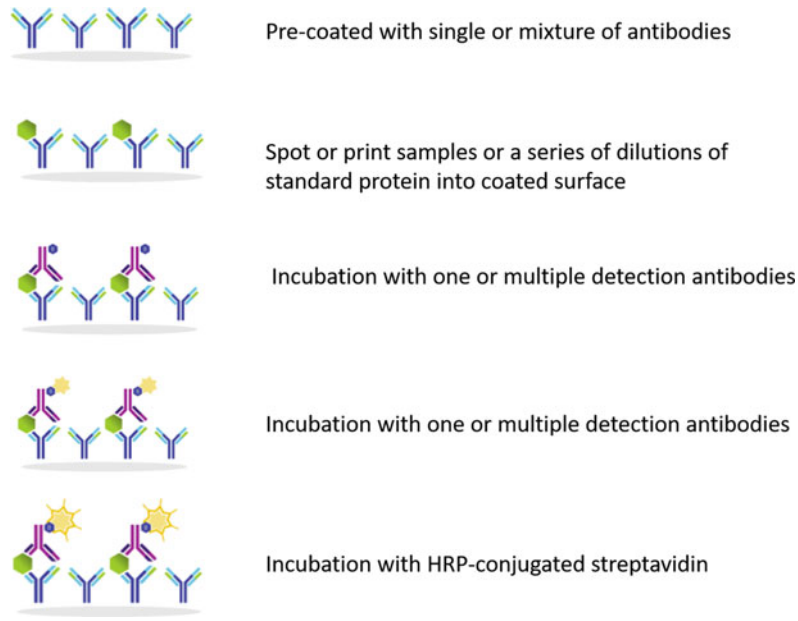

Fig. 1 Schematic of enhanced protein profiling array protocol

small plastic boxes or containers overnight at 4 °C using an orbital shaker.

3. Air-dry the membranes for 10–30 min at room temperature.
4. Dilute the EGF and PDGF antigens using Blocking buffer to the following concentrations: EGF: 625, 125, 25, 5, 1, and 0.20 ng/mL. PDGF: 315, 78.75, 19.69, 4.922, 1.230, 0.308 ng/mL (*see* **Note 4**).
5. Spot 0.2 μL of each of the prepared antigen solutions and the human plasma sample onto the membranes in duplicate using a Pipetman (0.1–2 μL). Air-dry the membranes for 10–30 min.
6. Block the membranes with 10 mL of blocking buffer for 30 min at room temperature (RT) with gentle shaking using an orbital shaker.
7. Remove the blocking buffer and incubate the membranes with 10 mL of EGF or PDGF biotin-conjugated detection antibody, respectively, with gentle shaking at RT for 2 h.
8. Remove the biotin-conjugated detection antibody and wash each membrane with 10 mL of TBS/0.1% Tween-20 three times (5 min each) with gentle shaking.
9. Remove the TBS/0.1% Tween-20 and wash with 10 mL of TBS twice (5 min each) with gentle shaking.
10. Remove the TBS and incubate the membranes with 10 mL of 200 ng/mL horseradish peroxidase (HRP)-conjugated streptavidin at RT for 1 h with gentle shaking.

11. Repeat the wash steps (**steps 8** and **9**).
12. For each membrane, add 5 mL of the ECL reagent A and 5 mL of the ECL Reagent B together to make a detection buffer mix.
13. Remove the TBS and pipette 10 mL of the detection buffer mix on to each membrane and incubate at room temperature for 2 min with gentle shaking.
14. Gently place the membrane with forceps (antibody side up) on a plastic sheet and cover the membrane with another plastic sheet. Gently smooth out any air bubbles. Avoid using pressure on the membrane.
15. The signal can be detected directly from the membrane by exposing the array to X-ray film (Kodak X-Omat™ AR film) with subsequent development. Expose the membranes for 40 s. Then re-expose the film according to the intensity of signals (*see* **Note 5**).
16. Determine the signal intensities using a densitometer. Generate standard curves of the antigens using Sigma plot or similar software (Figs. 2, 3 and 4).

4 Notes

1. In this chapter we present using EGF and PDGF as the protein targets. However, this technology is suitable for use with most all protein targets. To successfully develop enhanced protein profiling arrays, using a good antibody pair and standard antigen is the key. The antibody pairs should have high specificity and sensitivity. Although some antibodies have high affinity and specificity to their targets, most antibodies can also recognize additional proteins beside their target molecule. Therefore, it is critical to select antibody pairs with high specificity. Monoclonal antibodies, which usually have higher specificity should be the first choice. Polyclonal antibodies, on the other hand, usually have high affinity and are easy to produce, but the supply is limited, and it is difficult to set up the standardization of assay technique for a large quantity of samples and future applications [7].
2. Using a suitable substrate is one of the most important factors for performing successful experiments with enhanced protein profiling arrays. The best substrates must meet the following criteria: (1) high binding capacity, (2) uniform binding to the surface, (3) maintenance of the active form of the protein, (4) low background, (5) ease of performance and storage, and (6) cost effectiveness [13]. A number of solid supports can be used in the development of enhanced protein profiling arrays: glass slides, membranes, and plates. We recommend

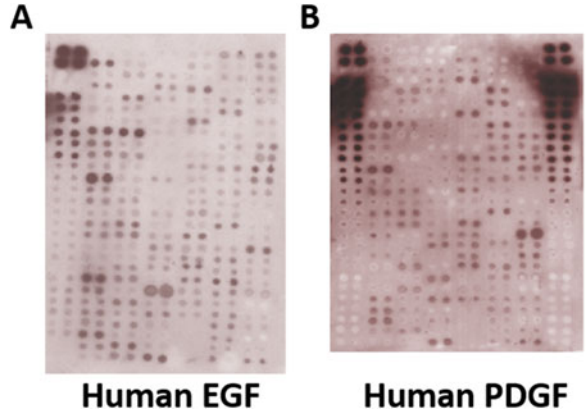

Fig. 2 Raw images of epidermal growth factor (EGF) (**a**) and platelet-derived growth factor (PDGF) (**b**) expression levels detected by enhanced protein profiling arrays

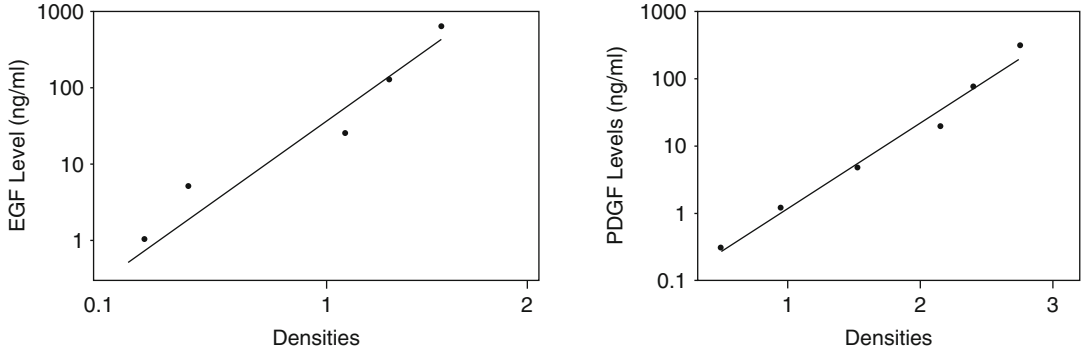

Fig. 3 The intensities of signals derived from standard Human EGF or human PDGF were determined by densitometry and were plotted against known concentrations of EGF or PDGF

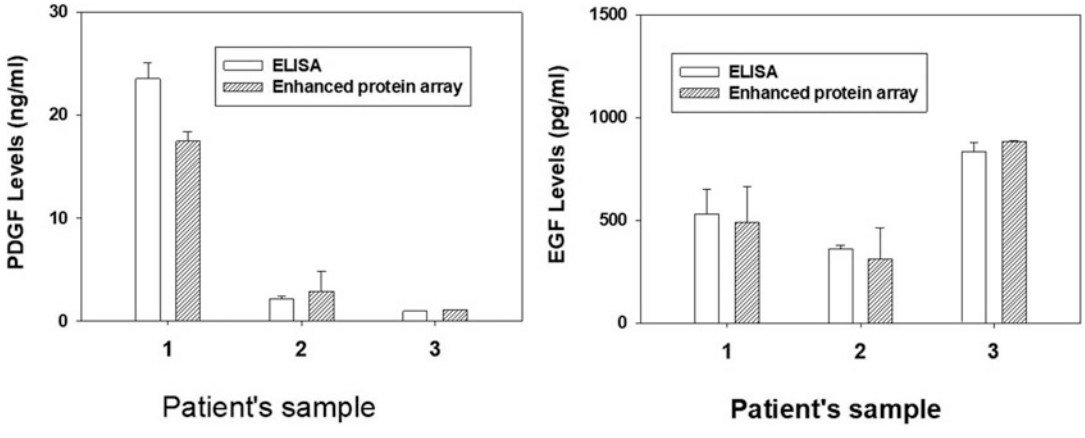

Fig. 4 Comparison of expression levels of PDGF and EGF by ELISA and enhanced protein profiling arrays. In general, the expression levels are similar between the two approaches

using Hybond ECL membranes for their low background and high sensitivity.

3. Serum should be stored at −80 °C and aliquoted to avoid a repeat thaw of samples. Serum and plasma can be directly spotted onto coated membranes.
4. The antigen concentrations to print on the array can vary and each researcher should empirically determine the optimal concentrations for their samples and antibody pairs.
5. The best detection approach should have (1) high sensitivity, (2) a large dynamic range, (3) low background noise, and (4) a low CV. One of the most sensitive approaches to detect protein is chemiluminescence, which can be quite quantitative and have reasonable dynamic ranges. However, alternative detection systems can be used. Fluorescence detection offers multiple channel detection capacity and long-lasting signals. This is an advantage compared with chemiluminescence. Since low autofluorescence in glass slides, protein arrays are normally constructed on glass slides when using fluorescence detection.

References

1. MacEwan DJ (2002) TNF receptor subtype signaling: differences and cellular consequences. Cell Signal 14:477–492
2. Vitkovic L, Maeda S, Sternberg E (2001) Anti-inflammatory cytokines: expression and action in the brain. Neuroimmunomodulation 9:295–312
3. Lotem J, Sachs L (2002) Cytokine control of developmental programs in normal hematopoiesis and leukemia. Oncogene 21:3284–3294
4. Huang RP (2003) Protein arrays, an excellent tool in biomedical research. Front Biosci 8: D559–D576
5. Huang RP (2003) Cytokine antibody arrays: a promising tool to identify molecular targets for drug discovery. Comb Chem High Throughput Screen 6:769–775
6. Huang RP (2001) Detection of multiple proteins in an antibody-based protein microarray system. J Immunol Methods 255:1–13
7. Huang RP, Huang R, Fan Y, Lin Y (2001) Simultaneous detection of multiple cytokines from conditioned media and patient's sera by an antibody-based protein array system. Anal Biochem 294:55–62
8. Huang R, Lin Y, Wang CC, Gano J, Lin B, Shi Q, Boynton A, Burke J, Huang RP (2002) Connexin 43 suppresses. human glioblastoma cell growth by down-regulation of monocyte chemotactic protein 1, as discovered using protein array technology. Cancer Res 62:2806–2812
9. Lin Y, Huang R, Santanam N, Liu Y, Parthasarathy S, Huang R (2002) Profiling of human cytokines in healthy individuals with vitamin E supplementation by antibody array. Cancer Lett 187:17–24
10. Kononen J, Bubendorf L, Kallioniemi A et al (1998) Tissue microarrays for high-throughput molecular profiling of tumor specimens. Nat Med 4:844–847
11. Simon R, Nocito A, Hubscher T et al (2001) Patterns of her-2/neu amplification and overexpression in primary and metastatic breast cancer. J Natl Cancer Inst 93:1141–1146
12. Huang R, Lin Y, Shi Q et al (2004) Enhanced protein profiling arrays with ELISA-based amplification for high-throughput molecular changes of tumor patients' plasma. Clin Cancer Res 10:598–609
13. Fung E (ed) (2004) Protein arrays, cytokine protein arrays, Methods in molecular biology, vol 264. Humana Press Inc., Totowa, NJ, p 215

Chapter 11

Methods for Membranes and Other Absorbent Surfaces

Jarad J. Wilson, Yun Xi, Ruochun Huang, and Ruo-Pan Huang

Abstract

Membrane arrays are a unique array platform option for the detection of multiple analytes or materials simultaneously. Their naturally absorptive properties and near universal use in various laboratory methods make it an excellent source with which to probe multiple factors simultaneously. Any liquid sample type can be probed, from bacterial strains, tissue lysates, secreted proteins, to DNA aptamers. Below, we will describe some considerations in how to print a membrane array and then a specific usage of the membrane arrays as it relates to a sandwich-based antibody array technique for simultaneously detection of secreted proteins in a liquid sample.

Key words Membrane array, Antibody array, Dot blot array

1 Introduction

Membrane arrays have been used widely to study protein expression, glycosylation changes in samples, phosphorylation status of proteins, and even protein/protein interactions [1–4]. The absorptive nature of the membrane array makes it ideal for most anything to be probed, and most any liquid sample. The two most common types of membranes, polyvinylidene difluoride (PVDF) and nitrocellulose, are options to use as a printing surface. One advantage of using membrane arrays is that they do not possess any natural immunofluorescent coatings, which allows for detection through a variety of means (fluorescence, chemiluminescence, luminescence, and others), features that can be limiting with other array surface options and applications.

Starting any membrane assay begins with the printing/coating of the membranes themselves in preparation of the assay. The original printing method involved hand printing the targets onto a membrane surface, usually using some form of grid or stencil format. Manual pipetting is often limited to microliter drop sizes, making the spots on the membrane larger than would actually be needed by any array. Also, the variability at the extreme low range

Kelly C. Whittaker and Ruo-Pan Huang (eds.), *Antibody Arrays: Methods and Protocols*, Methods in Molecular Biology, vol. 2237, https://doi.org/10.1007/978-1-0716-1064-0_11,

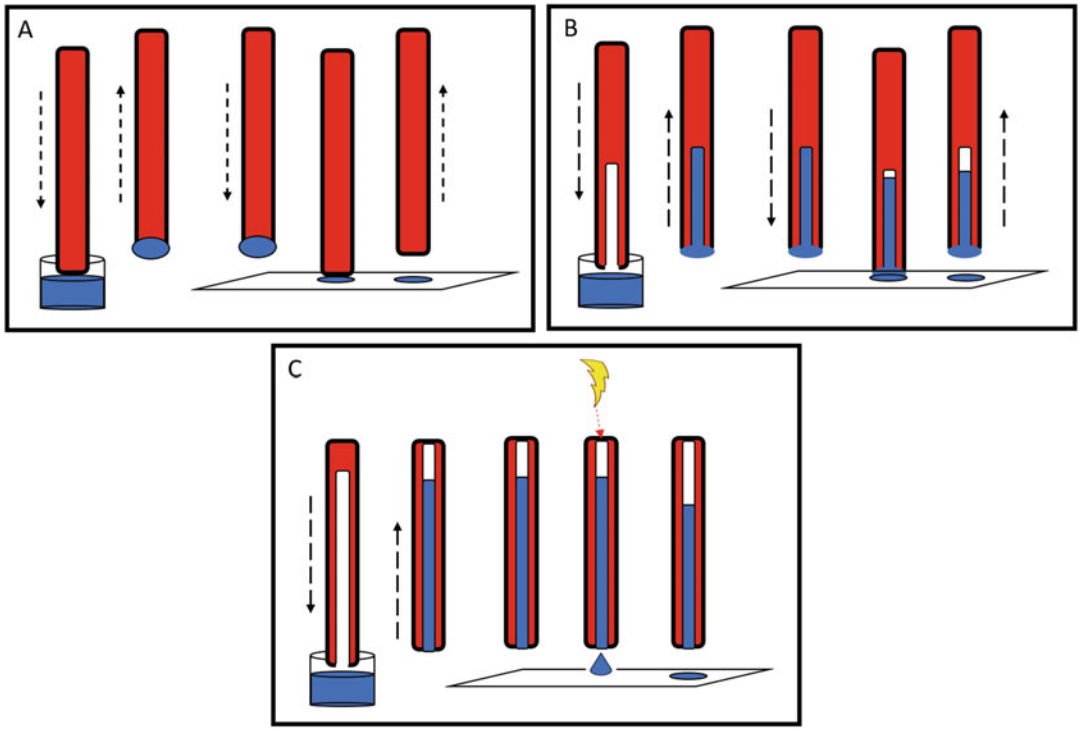

Fig. 1 Three types of common membrane printing technology. (**a**) Shows a solid contact printing pin, which requires volume loading onto a precisely tuned tip, which this deposits the liquid material onto the surface by adsorption. (**b**) Shows a contact quilled pin which loads up several spots worth of liquid via capillary action within the contact pin itself. This volume is printed sequentially as the volume is drawn out for each spot via capillary action. (**c**) Shows a noncontact quilled print pin which also draws up volume inside its reservoir inside the pin. However, this pin prints when a voltage change occurs on the pin itself

end of most pipettes means the precision and accuracy of the molecules being spotted is not sufficient. All of these limitations, and the need for scalability, began the discussion of technology that allows for speed, precision, and quality in regard to membrane printing.

The original form of printing is contact printing, where the material to be placed on the array is done onto the surface directly, whereby it comes into direct physical contact with the printed surface [5]. Direct deposition of printing materials onto a surface is usually done either through a solid pin design or a quill type pin (Fig. 1). Solid pin designs are built to specifically "draw" up a defined volume onto the surface of the pin (Fig. 1a). These designs are precisely machined to only allow liquid retention on a defined region of the pin surface, and not further up the base of the pin. One drawback to this design is that the throughput is limited, as for each target spot to be placed, the pin must dip into a solution, move to the printing surface, deposit the material, and then returned for a

Table 1
Pros and cons of each printing method

Contact printing; solid pin	Contact printing; quilled pin	Noncontact; quilled pin
Pros		
Consistent print volumes	Printing volume can be changed to meet design	Printing volume can be changed on the fly
Low maintenance	Reservoir allows for multiple arrays to be printed	Larger reservoir amounts
Fast and reliable option	Faster and reliable option	Larger selection of array spot sizes
		Fastest and reliable option
Cons		
Nozzles have a defined print volume	Contact time can change coating amount	Humidity effects can change direction of droplets
Slower printing	Adsorption varies from surface to surface	Droplets are exposed to environment
Limiting cleaning of pins	Reservoir can create a noncircular shape	Rebound of droplet on surface can change spot shape
Additional wash volume required		

repeat dip or rinse every time. The quilled design on the other hand (Fig. 1b) draws up more fluid through the inside of the pin, allowing a reservoir of printing material over the course of multiple depositions onto the array surface. This allows for continuous printing without additional rinse needs, minimizing down time of the printer. Noncontact, piezo style printers also utilize a quill type nozzle for printing material on a surface. However, these "shoot" a droplet of precise volume onto the printing surface (Fig. 1c). This print format provide the highest throughput currently as there is no "down" time for the nozzle, as it does not require contacting the printing surface, nor reloading at each spot. Pros and cons of each method are outlined in Table 1, and additional details of printing methods and technology will be covered elsewhere. This chapter will describe how to perform a printed membrane-based array, focusing on a sandwich-based method from blocking, incubation, and detection options for membrane arrays.

2 Materials

The Materials required herein are for a common sandwich antibody-based membrane array being read via chemiluminescent detection.

1. Human Cytokine Array C3, AAH-CYT-3 (RayBiotech) (*see* **Note 1**).
2. Human Serum Sample (*see* **Notes 2** and **3**).
3. Triton X-100 Lysis Buffer: 50 mM Tris–HCl, pH 8.5, 150 mM NaCl, 1% Triton X-100 (*see* **Notes 4** and **5**).
4. Protease inhibitors (*see* **Note 6**).
5. Blocking buffer 1: 0.01 M Tris–HCl, pH 7.6, 0.15 M NaCl, 5% bovine serum albumin (*see* **Note 7**).
6. Sample buffer: 1× phosphate buffered saline, 5% bovine serum albumin, 1% Casein (*see* **Note 7**).
7. Wash Buffer I: 2% Tween 20, 100 mM Tris–HCl, pH 7.6, 150 mM NaCl.
8. Wash Buffer II: 100 mM Tris–HCl, pH 7.6, 150 mM NaCl (*see* **Note 8**).
9. Biotinylated Detection Antibody Cocktail (*see* **Note 9**): 1:1000 dilution of biotinylated detection reagents added to a total volume of 2 mL to create a ready to use 1× concentration detection reagent or antibody.
10. A 1000-fold dilution of HRP-streptavidin solution (*see* **Note 10**).
11. Peroxidase conjugate stabilizer (Pierce).
12. Detection reagent (1 mL needed per membrane): 1:1000 dilution of concentrated HRP-streptavidin solution containing a 200× dilution of peroxidase conjugate stabilizer (*see* **Note 10**).
13. Detection Solution 1 and Detection Solution 2: 2-part horseradish peroxidase substrate for enhanced chemiluminescent (ECL) detection (Amersham/GE, RPN2106).
14. 4–8 well incubation tray for membranes.
15. Tweezers.
16. High quality MilliQ 18 MΩ cm or similar reverse osmosis/deionized water.
17. Orbital shaker and/or oscillating rocker.
18. Blotting paper.
19. Chemidoc-it Chemiluminescent blot detection system (*see* **Note 10**).

20. Transparent plastic or saran wrap sheets cut to 2× the size of the membrane used (for membrane detection). Larger pieces can be made for multiple membranes.
21. Pipettes: 200 μL.
22. Microcentrifuge tubes.

3 Methods

1. Remove the membrane array, blocking buffer, sample buffer, wash buffers I and II, and samples from storage and equilibrate to room temperature for at least 1 h, or until the buffers are thawed.
2. Remove the membranes from any packaging and place them array side up in the incubation tray (*see* **Notes 11**, **25** and **26**).
3. Add 2 mL of Blocking Buffer to cover the array in buffer, being careful not to touch the array.
4. Incubate for 30 min at room temperature on top of an oscillating rocker (low speed setting so as not to slosh the fluid in the incubation tray).
5. Carefully aspirate the blocking buffer from the incubation tray.
6. Pipette 2 mL of Human Serum Sample into each well and incubate for 1.5–5 h at room temperature OR overnight at 4 °C (*see* **Note 12**).
7. Aspirate samples using a standard 200 μL pipette tip from each well, being careful to change pipette tips to avoid well-to-well contamination.
8. Pipette 2 mL of Wash Buffer I into each well and incubate for 5 min at room temperature (*see* **Note 13**).
9. Aspirate Wash Buffer I from each well, being careful to change pipette tips to avoid well to well contamination.
10. Repeat Wash Buffer I incubation and aspiration (**steps 8** and **9**) two additional times for a total of 3 washes, completely removing the Wash Buffer I at each incubation.
11. Pipette 2 mL of Wash Buffer II into each well and incubate for 5 min at room temperature.
12. Aspirate Wash Buffer II from each well, being careful to change pipette tips to avoid well to well contamination.
13. Repeat Wash Buffer II incubation and aspiration (**steps 11** and **12**) one additional time for a total of 2 washes, completely removing the Wash Buffer II at each incubation.
14. Pipette 2 mL of the Biotinylated Detection Antibody Cocktail into each well and incubate for 2 h (*see* **Note 14**).

15. Carefully aspirate the Biotinylated Detection Antibody Cocktail from each well, being careful to change pipette tips to avoid well to well contamination.
16. Wash membranes with Wash Buffer I and Wash Buffer II exactly as indicated above (**steps 8–13**).
17. Pipette 2 mL of the Detection Reagent into each well and incubate for 2 h (*see* **Note 15**).
18. Carefully aspirate the Detection Reagent from each well, being careful to change pipette tips to avoid well-to-well contamination.
19. Wash membranes with Wash Buffer I and Wash Buffer II exactly as indicated above (**steps 8–13**).
20. Transfer the membrane(s), printed side up, onto a sheet of blotting paper on a flat surface (*see* **Note 16**).
21. Remove excess Wash Buffer II by tilting the membrane and blotting the membrane edges with another piece of blotting paper.
22. Transfer the membrane(s) onto the saran wrap sheet laid on a flat surface.
23. Per membrane, add 250 μL of Detection Solution I to a clean tube, then add 250 μL of Detection Solution II, and mix well (*see* **Note 17**).
24. Add 500 μL of the Detection Buffer Mix made in **step 23** onto the top of each membrane, being careful to cover the top of each membrane, and incubate for 2 min at room temperature (*see* **Note 18**).
25. Place another sheet of saran wrap on top of the membranes and, using a pipette or similar, roll out any bubbles present from top to bottom. This should create a sandwich of the membrane between two saran wrap sheets without any bubbles present (*see* **Notes 18** and **19**).
26. Transfer the sandwiched membrane(s) to the Chemidoc-it chemiluminescence imaging system (*see* **Note 10**).
27. Using multiple exposures, expose membranes for 10 s, 30 s, 1 min, 2 min, and 5 min (*see* **Notes 20** and **21**).
28. Typical results from an exposure of 1 min are similar to Fig. 2.
29. Using the onboard Vision Works software, extract the signals from each spot on the membrane array, and export to Microsoft Excel (*see* **Note 22**).
30. Normalize all membranes by comparing the signals of positive controls minus background from each membrane using the below formula (*see* **Notes 23** and **24**):

$$X(Ny) = X(y) * \mathrm{P1} / \mathrm{P(y)}$$

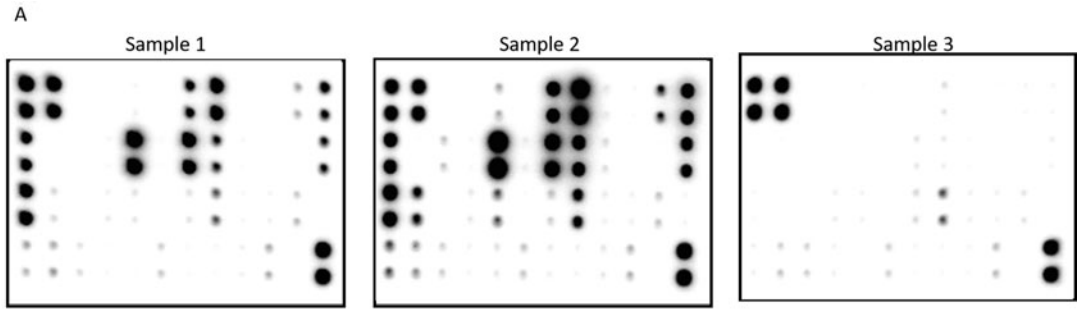

B

Each antibody is spotted in duplicate vertically	A	B	C	D	E	F	G	H	I	J	K	L
	1	POS	POS	NEG	NEG	ENA-78 (CXCL5)	GCSF	GM-CSF	GRO a/b/g	GRO alpha (CXCL1)	I-309 (TCA-3/CCL1)	IL-1 alpha (IL-1 F1)	IL-1 beta (IL-1 F2)
	2												
	3	IL-2	IL-3	IL-4	IL-5	IL-6	IL-7	IL-8 (CXCL8)	IL-10	IL-12 p40/p70	IL-13	IL-15	IFN-gamma
	4												
	5	MCP-1 (CCL2)	MCP-2 (CCL8)	MCP-3 (CCL7)	M-CSF	MDC (CCL22)	MIG (CXCL9)	MIP-1 delta	RANTES (CCL5)	SCF	SDF-1	TARC (CCL17)	TGF beta 1
	6												
	7	TNF alpha	TNF beta	EGF	IGF-1	Angiogenin	OSM	TPO	VEGF-A	PDGF-BB	Leptin	NEG	POS
	8												

Fig. 2 (**a**) Shows an image of 3 Sandwich-based Membrane Arrays. Sample 1 is an untreated conditioned media sample, while Sample 2 shows a treated sample's conditioned media. A media only blank is shown in Sample 3. You can note the positive control spots in each membrane as the same location highlighted in Red. (**b**) Shows a map of the antibody array performed which can be used to determine the analyte name of the spot being evaluated

where:

$P1$ = mean signal density of Positive Control spots on reference array

$P(y)$ = mean signal density of Positive Control spots on Array "y"

$X(y) = X(Ny)$ = normalized signal intensity for spot "X" on Array "y"

31. Compare fold-change signals from one membrane to any other after this normalization to determine if any increases/decreases in proteins in the samples are present.
32. Please see Notes 27–30 for other array types, processing, detection methodologies, and other considerations.

4 Notes

1. This array is a duplicate-spotted sandwich antibody array with known positive control spots and negative control spots. Although, most any common sandwich antibody-based membrane array will be suitable for this protocol.
2. In general, most liquid samples are suitable for use on this array. However, samples should be clarified to avoid interference from any debris. This can be best accomplished by mixing the samples, and then centrifuging them for 2 min at $>2500 \times g$.

3. Sample dilution should be determined empirically for each array of interest, but the following general guidelines have been found to work well:
   (a) Serum and plasma: twofold to tenfold dilution.
   (b) Cell and tissue lysates: load 50–500 μg of total protein. Lysates should have at least a five-fold to ten-fold dilution to minimize the effects of any detergent (therefore, original lysate concentration should be 1–5 mg/mL).
   (c) Other bodily fluids: Neat to fivefold dilution (heavily array and sample dependent).
   (d) Cell cultured media: Neat (no dilution needed) although conditioned media samples containing Fetal Bovine Serum (FBS) could contain proteins that are sufficiently homologous and/or interfering as to affect the array.

   It is recommended to remove this if possible from the sample to be run. If not possible, it is critical to perform needed media only controls containing FBS. 1–2 mL of final ready to use sample is recommended and covers the majority of arrays up to 5 cm × 2.5 cm in dimension.
4. Recommended lysis buffers for membrane-based arrays meet these criteria:
   (a) Avoid >0.1% SDS or other strongly denaturing detergents.
   (b) Non-ionic detergents such as Triton X-100 or NP-40 are best, although zwitterionic detergents such as CHAPS, or mild ionic detergents such as sodium deoxycholate will work.
   (c) Use no more than 2% v/v total detergent.
   (d) Avoid the use of sodium azide.
   (e) Avoid >10 mM reducing agents, such as dithiothreitol or mercaptoethanols.
5. Another example lysis buffer using a RIPA formulation, 50 mM Tris–HCl, pH 7.6, 150 mM NaCl, 5 mM Na_2EDTA, 1% NP-40, 0.5% sodium deoxycholate, brought up in PBS is suitable. Addition of less than 0.1% sodium dodecyl sulfate (SDS) is optional.
6. It is recommended to add protease inhibitors to most samples to preserve the sample (Example: Pierce Protease Inhibitor Tablets). Addition of phosphatase or other inhibitors may also be considered.
7. It is best to determine the best blocking buffer and sample buffer for your array and your samples. Some alternatives can include 5% BSA, with or without 1% Casein, as well as 5–10% non-fat dry milk, all brought up in 1× phosphate buffered saline.

8. If large numbers of arrays are to be used, or to be used often, larger 10× solutions of washer buffers can be created and stored, then reconstituted as needed.
9. The membrane array outlined above is for a sandwich-based antibody array, used to evaluate protein levels in a sample. Other methodologies could incorporate lectins, glycans, aptamers, small molecules, and other detection reagents specific to the purpose of the array.
10. The detection method above utilizes streptavidin HRP chemiluminescent detection. Infrared (IR) dyes, Fluorescent Cy3 or Cy5 conjugates, and other techniques could also work. Please note that a detection system capable of detecting these dyes would be required for the final data acquisition (*see* **steps 26–29**).
11. Most membrane arrays will be marked or notched to show which side of the array is the "top." The top is the face of the membrane with antibodies printed on it and must be facing to the top for all incubation and washing steps for best results.
12. Sample incubation time varies between membrane array methods and the samples being used. Shorter incubation times are best for concentrated samples, while longer incubation times can bring out lesser present proteins in a sample. However, additional incubation time can also bring up the inherent background in a sample.
13. Volumes of buffer indicated are specific to the arrays being run, and more or less may be required for differently sized arrays.
14. Detection antibody incubation times here are specific for sandwich-based antibody arrays. Aptamer, glycan, lectin, or small molecule detection reagents may require more/less time than indicated.
15. Different HRP-streptavidin or different detection methods may require more or less dilution and incubation times of this reagent. This is a critical step, and empirical determination of best amounts and times is recommended.
16. This step is for removing as much buffer as possible from the array without drying it out completely. Do not let the membrane dry out completely.
17. This volume is specific to the array being run. It is recommended to add just enough detection buffers to the top of the array which covers the array completely. This keeps all the detection reagent on the array for the entire detection duration period, until it is removed.
18. Exposure of the array should begin within 5 min of the completion of the 2-min Detection Buffer Mix incubation step (**step 24**), and no later than 15 min after, as the

chemiluminescent signals will fade. If too much time has passed, you can repeat the incubation of HRP-Streptavidin, followed by the Detection Buffers incubation (**steps 19–24**).

19. Direct exposure of the membrane is also possible if saran wrap is not available or desired.
20. Exposure timing is best done as a multi-staged capture of the arrays over specific set times to avoid trial and error of single exposure times.
21. Membranes may often be stored in the sandwich for future use by taping the saran wrap sandwiched membrane closed and placing this at −20 °C until needed.
22. Other common tools/software can be used to extract the density measurements of the spots including ImageJ, Western Vision, and Image Studio.
23. Controlled amount of printed material, so-called positive control spots, are often used to normalize array to array exposure deviation on arrays run at the same time. These can be seen in figure Y. The average of all 6 in this example will be taken and used as a comparison from array to array.
24. Negative control spots, or local background spots, can be used to subtract out any nonspecific background signal from actual target spot data.
25. Membranes should only be handled by tweezers at the very edge of the arrays to avoid directly touching any printed area.
26. Multiple membranes can be incubated simultaneously with slightly more volume than required for a single array.
27. If using Infrared or fluorescent dyes, use caution when marking your membrane with a permanent marker as the ink in these markers can be naturally fluorescent in the channel of interest. Detergents in buffers can also solubilize and smear this ink as well.
28. Most membrane arrays cannot be stripped and reprobed, as the process of stripping often removes the printed material from the membrane surface directly. Depending on the printed surface and chemistry of the printed material, this is not always the case, but should be determined empirically before use.
29. Larger or smaller arrays may require differently size incubation plates, or buffer volumes.
30. Optical densities (ODs) of the indicated spot being evaluated cannot directly be compared to the ODs of other target spots, as the sensitivity, specificity, and affinity of other antibodies or binding markers varies from spot to spot.

References

1. Huang RP, Huang R, Fan Y, Lin Y (2001) Simultaneous detection of multiple cytokines from conditioned media and patient's sera by an antibody-based protein array system. Anal Biochem 294:55–62. ISSN: 0003-2697 (Print)
2. Ivanov SS, Chung AS, Yuan Z-I, Guan Y-J, Sachs KV, Reichner JS, Chin YE (2004) Antibodies immobilized as arrays to profile protein post-translational modifications in mammalian cells. Mol Cell Proteomics 3:788–795. ISSN: 1535-9476 (Print)
3. Rodriguez M, Li SS-C, Harper JW, Songyang Z (2004) An oriented peptide array library (OPAL) strategy to study protein-protein interactions. J Biol Chem 279:8802–8807. ISSN: 0021-9258 (Print)
4. Rosenfeld R, Bangio H, Gerwig GJ, Rosenberg R, Aloni R, Cohen Y, Amor Y, Plaschkes I, Kamerling JP, Maya RB-Y (2007) A lectin array-based methodology for the analysis of protein glycosylation. J Biochem Biophys Methods 70(3):415–426. ISSN: 0165-022X (Print)
5. Gershon D (2002) Microarray technology: an array of opportunities. Nature 416:885–891. ISSN: 0028-0836 (Print)

Chapter 12

Precise Chip-to-Chip Reagent Transfer for Cross-Reactivity-Free Multiplex Sandwich Immunoassays

François Paquet-Mercier, David Juncker, and Sébastien Bergeron

Abstract

Common multiplex sandwich immunoassays suffer from cross-reactivity due to the mixing of detection antibodies and the combinatorial, undesired interaction between all reagents and analytes. Here we present the snap chip to perform antibody colocalization microarrays that eliminates undesirable interactions by running an array of singleplex assays realized by sequestering detection antibodies in individual nanodroplets. When detecting proteins in biological fluids, the absence of cross-reactivity allows a higher level of multiplexing, reduced background, increased sensitivity, and ensures accurate and specific results. The use of the snap chip is illustrated by measuring highly related analytes such as proteins isoforms and phosphoproteins, both particularly prone to cross-reactivity, in a single experiment. The main steps of the protocol are preparation of sample, incubation on an assay slide harboring the microarrayed capture antibodies, transfer of the microarrayed detection antibodies on their cognate spots, and measurement of the assay results by fluorescence.

Key words Antibody microarray, Snap chip, Cross-reactivity free, Multiplex, Sandwich immunoassay, ELISA, Chip-to-chip

1 Introduction

Enzyme-linked immunosorbent assays (ELISA) is the gold standard method to detect specific proteins in biological fluids. Although ELISA assays are relatively fast and simple, their main limitation is that it can only be performed on one analyte at a time. This is particularly problematic when the volume of samples is limited, or the reagents are expensive. Multiplexed sandwich immunoassays are powerful techniques to measure multiple protein

Electronic supplementary material The online version of this chapter (https://doi.org/10.1007/978-1-0716-1064-0_12) contains supplementary material, which is available to authorized users.

Kelly C. Whittaker and Ruo-Pan Huang (eds.), *Antibody Arrays: Methods and Protocols*, Methods in Molecular Biology, vol. 2237, https://doi.org/10.1007/978-1-0716-1064-0_12,

concentrations simultaneously. Despite a great initial excitement, its global adoption and a progressive abandon of the common singleplex ELISA, they were hampered by cross-reactivity resulting in false positive signals. Cross-reaction occurs when the detection antibodies are mixed together and applied to the whole array, causing each individual detection antibody to interact with every single analyte. The likelihood of an undesirable reaction occurring rapidly increase with the level of multiplexing (*i.e.*, the number of analytes), and it is sometimes impossible to combine all your preferred analytes, and more likely impossible to study protein isoforms and their respective phospho-proteins in the same assay due to incompatibility [1–3].

The Antibody Colocalization Microarrays (ACM) for multiplex sandwich assays eliminates this problem [4]. Indeed, the detection antibodies are not mixed but rather precisely delivered to their cognate spots only in a second spotting round. To eliminate the need for a microarray spotter during the assay and make it accessible to non-specialized laboratories, the snap chip technology has been developed and commercialized by Parallex BioAssays Inc. under the trade name SnapChip. In addition to a common assay slide pre-spotted with capture antibodies, a transfer slide with pre-spotted arrays of nanodroplets containing the detection antibodies is prepared. After incubating the assay slide with sample, rinsing, and drying, the detection antibodies can be delivered by snapping the two slides together, so that each spot is covered by a nanodroplet containing the cognate detection antibody. The snap chip platform represents a simple and innovative alignment setup for simple chip-to-chip transfer. The nanodroplets act as nanocompartments, and every individual analyte of the multiplex is physically isolated, which eliminates undesirable interactions among the reagents. The colocalization of the capture and detection antibodies in nanodroplets reproduces the conditions of the common ELISA by replacing the microwells of a microtiter plate with nanodroplets. The absence of cross-reactivity is highly desirable to reduce multiplex assay development time and cost, ensure accurate results, and study highly related analytes [5–7]. Using the snap chip approach, one can benefit from the high-throughput and sample economy of multiplex assays without compromising on assay sensitivity or specificity. Moreover, standard glass slides can serve as assay slides, and through the availability of the hand-held Snap alignment tool, it represents an attractive solution for scientists to conduct multiplex immunoassays without need for a microarray spotter and other expensive equipment.

The assay process flow using the snap chip is highly similar to an ELISA and regular multiplexed sandwich assay on planar microarrays (Fig. 1). The assay begins with the incubation of the samples on the assay slide. During this step, the target proteins are bound by their respective capture antibody immobilized on spots in the

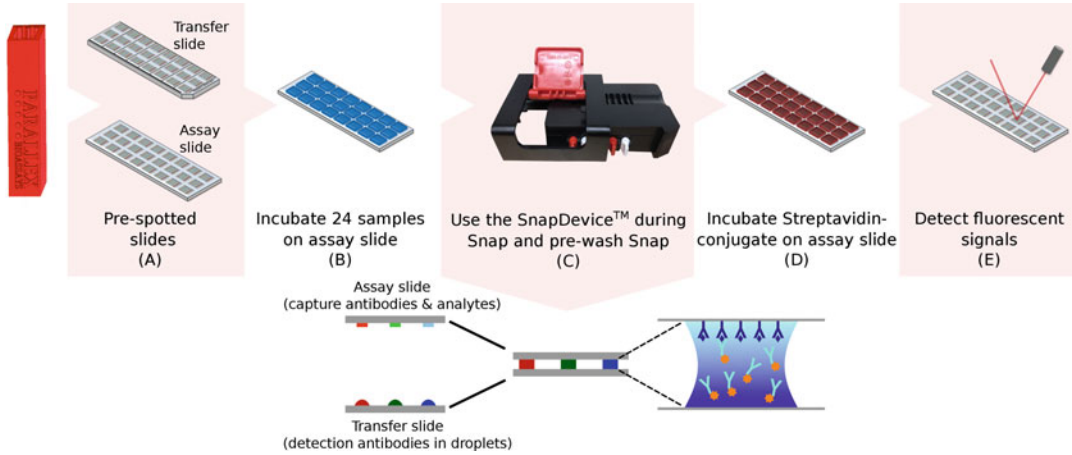

Fig. 1 Assay process flow for the snap chip assay. (**a**) Assay and transfer slides respectively pre-spotted with capture and detection antibodies. (**b**) Incubation of the samples for 1 h on assay slide. (**c**) Precise delivery of biotinylated detection antibodies contained on transfer slide to their cognate spots using the SnapDevice™ (after washing and drying of the assay slide). (**d**) Incubation with fluorescently-labelled streptavidin. (**e**) Detection of signals with fluorescence scanner

arrays. Following washing, the SnapDevice™ is used to precisely transfer biotinylated detection antibodies contained in nanodroplets from the transfer slide to their cognate spots on the assay slide. An incubation then allows the biotinylated detection antibodies to bind the antigens already immobilized on the capture antibodies, forming the sandwich assay. Next, the transfer slide is separated from the assay slide, and after washing, the slide is incubated with a fluorescently labelled streptavidin, and the binding results revealed using a fluorescence microarray scanner.

2 Materials

Material, equipment, and solutions are from Parallex BioAssays Inc., St-Basile-le-Grand, QC, Canada, unless stated otherwise.

2.1 Buffers and Solutions

1. Nondenaturing lysis buffer: Prepare 1 L of PBS buffer (add 800 mL of ddH_2O to a 1 L volumetric flask. Add 8 g of NaCl, 0.2 g of KCl, 1.44 g of Na_2HPO_4 and 0.24 g of KH_2PO_4. Adjust pH to 7.4. and complete volume to 1 L). Add 1% NP40 or 1% Triton X-100 (*see* **Note 1**).
2. Protease inhibitors (cOmplete™ mini protease inhibitor cocktail (Roche)) and phosphatase inhibitors 100× (1 M NaF and 200 mM Na_3VO_4) (*see* **Note 2**).
3. Blocking buffer and sample diluent buffer (PBS buffer with 1% BSA and 0.1% Tween-20).

4. Wash buffer (PBS buffer with 0.1% Tween-20).
5. Streptavidin-conjugate: Add 10 mL of blocking buffer to 1 μL of 1 mg/mL of streptavidin-conjugate solution and vortex for 20 s (*see* **Note 3**).

2.2 Material and Specialized Equipment

1. Assay slide: Take the slides out from the fridge and leave the package at room temperature for 30 min before opening (*see* **Note 4**).
2. Transfer slide: Incubate at least 30 min at ambient humidity before assay.
3. Absorbent slide.
4. PARAwell™ incubation system.
5. SnapDevice™.
6. Slide washing plate.
7. Sealing film.
8. Microarray centrifuge.
9. Microarray scanner for fluorescence detection: Set excitation at 650 nm and emission at 665 nm.
10. Orbital shaker.

3 Methods

3.1 Sample Preparation and Incubation

1. Equilibrate all kit's components for ≥30 min to room temperature before opening the bag.
2. Prepare tissues or cells lysates with nondenaturing lysis buffer freshly supplemented with protease and phosphatase inhibitors (*see* **Note 5**).
3. Determine the concentration of protein for each sample (e.g., BCA or Bradford), and adjust all samples to the same concentration with blocking buffer supplemented with protease and phosphatase inhibitors. Refer to Table 1 to determine the best concentration for your samples (*see* **Note 6**).
4. Fix the assay slide in a PARAwell™ incubation system (*see* **Note 7**).
5. Add 100 μL of blocking buffer in each well (*see* **Note 8**).
6. Incubate at room temperature for 20 min on an orbital shaker at 450 RPM.
7. Dilute samples with the block/sample diluent buffer at a pre-determined concentration.
8. Discard the blocking buffer from the wells by inverting the microchip and tap it forcefully on an absorbent paper (on a flat surface or in your hand) to remove any residual fluid.

Table 1
Recommended protein concentration for different types of cells or tissues

Tissue/cells	Species	Recommended total protein concentration range (μg/mL)
Liver	M	500–2000
White adipose tissue (epididymal)	M	250–750
Sk. muscle (gastrocnemius)	M	750–2000
HepG2	H	500–1500

9. Add samples (45–100 μL) and cover with a sealing film.
10. Incubate at room temperature for 2 h on an orbital shaker at 450 RPM (*see* **Notes 9** and **10**).
11. Discard the samples by pipetting or by inverting the microchip (*see* **Note 11**).
12. Wash three times for 5 min with wash buffer (*see* **Note 12**).
13. Disassemble the PARAwell™ incubation system.
14. Transfer the assay slide to the slide washing plate.
15. Wash once for 1 min with 5 mL of ddH_2O at room temperature on an orbital shaker at 450 RPM.
16. Dry the assay slide using a microarray centrifuge or a nitrogen stream.

3.2 SNAP: Precisely Deliver the Detection Antibodies to Their Cognate Spots

For more detailed information on how the use the SnapDevice™, refer to Video 1 presented in the Electronic Supplementary Materials on the chapter's webpage on link.springer.com.

1. Incubate the transfer slide for ≥30 min at ambient temperature and humidity.
2. On the SnapDevice™ (Fig. 2), pull and rotate all knobs by 90° to lock them in the open position.
3. Position the transfer slide into the holder, aligning the clipped corners of the transfer slide and the foam pad together (Fig. 3).
4. Release the red knobs (attached to Pogo pins) in order to push the transfer slide against the fixed alignment pins (*see* **Note 13**).
5. Put the assay slide upside down (Parallex logo facing down and on the same side of the clipped corners) sitting on the four pogo pins (Fig. 3).
6. Release the white knobs (attached to mobile pins) in order to push the assay slide against the fixed alignment pins.
7. Gently assemble the top shell (Fig. 4) (*see* **Note 14**).

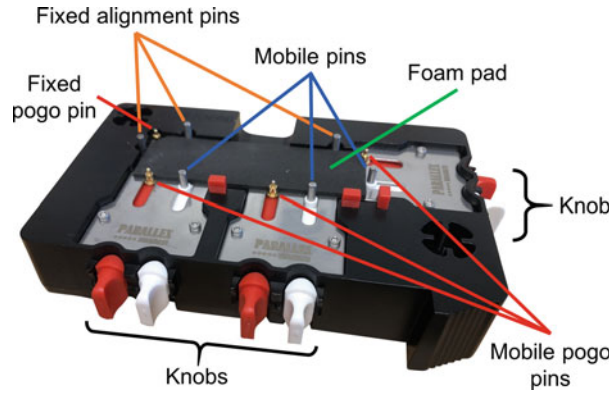

Fig. 2 SnapDevice™ from Parallex BioAssays Inc. Important parts of the device for this protocol are highlighted in the figure

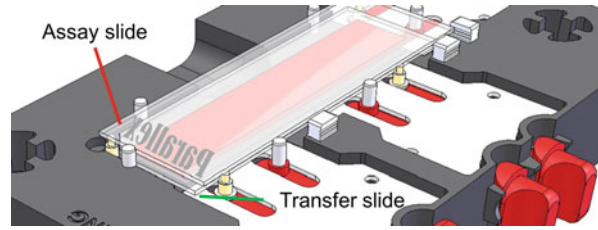

Fig. 3 Transfer slide and assay slides positioned in the SnapDevice™. The transfer slide must sit on the foam pad facing up. Clipped corners of the foam and the slide should align. The assay slide must be facing down suspended over the transfer slide, sitting on the 4 pogo pins, with the engraved logo aligned with the clipped corners

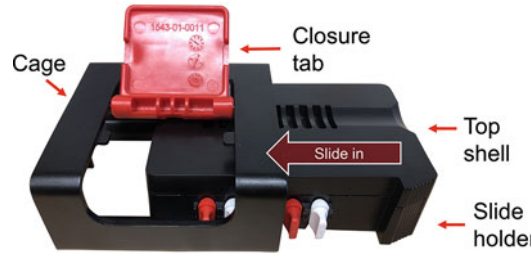

Fig. 4 Complete SnapDevice™ with top shell over slides holder. Before pushing the closure tab, the SnapDevice™ needs to be slid in the cage in the indicated direction

8. Lift the closure tab and insert the SnapDevice™ into its cage.
9. Push the closure tab down and wait 1 min.
10. Take the assay slide out and incubate it for 2 h at 65% relative humidity. Discard the transfer slide.

3.3 Pre-wash SNAP

1. Pull and rotate all knobs on the SnapDevice™ to lock them in the open position.
2. Insert the absorbent slide, aligning the clipped corners of the absorbent slide and the foam pad together, and release the red knobs.
3. Insert the assay slide upside down and release the white knobs.
4. Gently assemble the top shell (*see* **Note 14**).
5. Lift the closure tab and insert the SnapDevice™ into its cage.
6. Push the closure tab down and wait 1 min.
7. Take the assay slide out. Discard the absorbent slide.

3.4 Measuring the Assay Signals

1. Put the assay slide in the slide washing plate and wash 3 times for 5 min with 5 mL of wash buffer at room temperature, on an orbital shaker at 450 RPM.
2. Discard the wash buffer and add 5 mL of streptavidin-conjugate (*see* **Note 3**).
3. Incubate the slide at room temperature for 30 min on an orbital shaker at 450 RPM.
4. Wash once for 1 min in 5 mL of ddH_2O at room temperature.
5. Dry the slide using a microarray centrifuge or a nitrogen stream.
6. Scan the slide with a microarray scanner (*see* **Note 15**) (Fig. 5).

4 Notes

1. The assay works with different nondenaturing lysis buffers compatible with ELISA. Avoid SDS in the lysis buffer.
2. Alternative protease and phosphatase inhibitors can be used.
3. The streptavidin-conjugate is light-sensitive. Protect from light until the end of the procedure.
4. Never touch the surface of the slides as they are very sensitive. They must only be held by the edges. To avoid contamination, slides should always be handled in a clean environment with powder free gloves. The presence of dust or debris can cause high background signal. Red and black permanent markers can significantly interfere with fluorescent signal detection. We recommend marking the slides with diamond scribes, or with green or blue ultra-fine point permanent marker after testing for autofluorescence.
5. Always use fresh or properly stored samples prepared with protease and phosphatase inhibitors. Degradation of the sample will result in weak signal and improper measurement of the analyte.

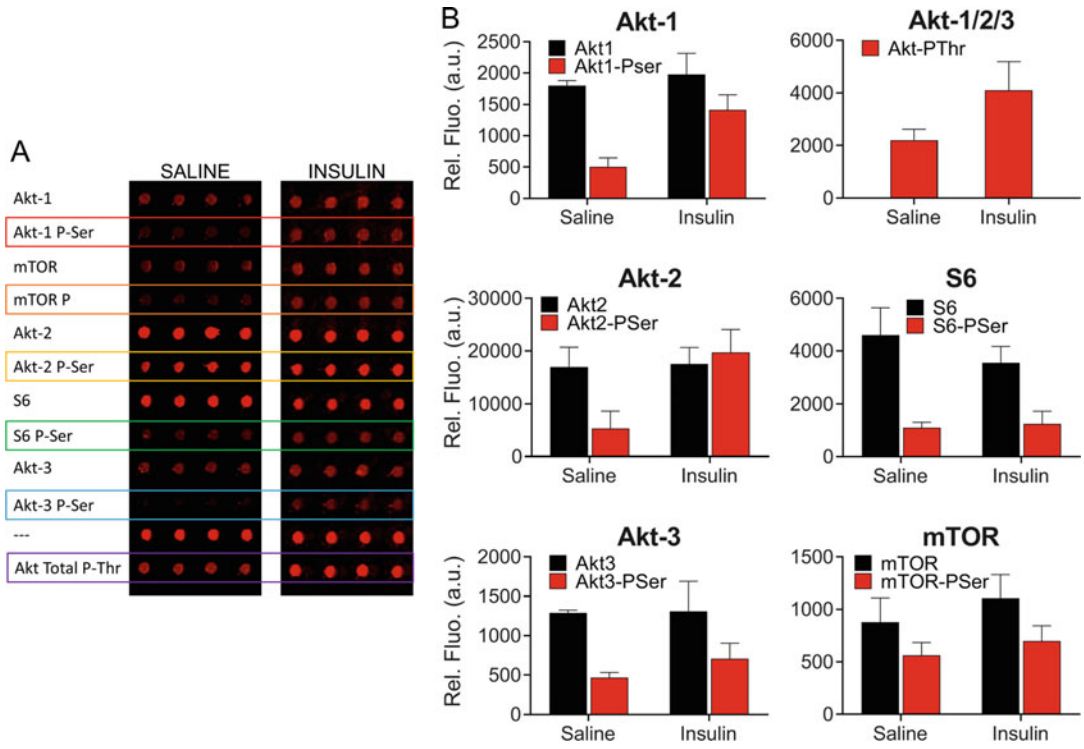

Fig. 5 Representative scan images (**a**) and corresponding bar graph representation (**b**) showing 4 replicate spots for 11 proteins and phospho-proteins involved in the activation of the insulin-stimulated Akt pathway in white adipose tissue. Epididymal fat pad lysates from 3 saline- and 7 insulin-stimulated mice were diluted at 1 mg/mL and analyzed with the snap chip. Results in (**b**) are averaged from 3 independent experiments. Error bars are standard deviations

6. We also recommend to experimentally determine the protein concentration that should be used for samples to ensure results fall in the linear portion of the assay. To do so, run a representative sample at different concentrations (1:2 dilution series). Weak or saturated signal can be caused by a too low or too high concentration of the sample, respectively.
7. The antibody arrays are on the side you can read the logo. Be sure to position the silicon gasket and create wells for samples incubation on this side.
8. Make sure to completely cover the bottom of each well with reagent or sample. Improperly covered arrays in the well will cause uneven signal.
9. We recommend preparing a 65% relative humidity chamber at this time, so it has time to equilibrate before it is needed.
10. If bubbles are formed before or during incubation, decrease shaking speed. Formation of bubbles during this step will result in an uneven signal. It is important to check for bubble formation and remove them.

11. Be careful not to contaminate wells with samples from adjacent wells. If discarding the samples by inverting, we recommend slapping the PARAwell™ system on an absorbent paper (on a flat surface or in your hand) to remove any residual liquid on its top surface.
12. Improper washing of the wells can cause high background in the signals. Make sure to completely remove wash buffer in each wash step. If necessary, increase wash time, number of washing cycles, and/or use more buffer. Avoid overflowing wash buffer or any other solution into neighboring well as this could cause cross-contamination.
13. Make sure that the slide does not sit on top of the pogo pin barrel. This could damage the slide when closing the SnapDevice™.
14. Do not apply pressure when assembling the top shell.
15. Weak or saturated signals can be the result of inadequate detection. If this is the case, readjust the scanning parameters.

Acknowledgments

This work was supported by Mitacs, MEDTEQ, and the Canadian National Research Council.
We thank Dr. André Marette and Noémie Daniel for fruitful discussions and access to biological samples. We thank Louisa Guignard for producing and editing the video (Supplementary Material).

References

1. Juncker D, Bergeron S, Laforte V, Li H (2014) Cross-reactivity in antibody microarrays and multiplexed sandwich assays: shedding light on the dark side of multiplexing. Curr Opin Chem Biol 18:29–37. https://doi.org/10.1016/j.cbpa.2013.11.012
2. Landegren U, Vänelid J, Hammond M, Nong RY, Wu D, Ullerås E, Kamali-Moghaddam M (2012) Opportunities for sensitive plasma proteome analysis. Anal Chem 84(4):1824–1830. https://doi.org/10.1021/ac2032222
3. Tighe PJ, Ryder RR, Todd I, Fairclough LC (2015) ELISA in the multiplex era: potentials and pitfalls. Prot Clin Appl 9(3–4):406–422. https://doi.org/10.1002/prca.201400130
4. Pla-Roca M, Leulmi RF, Tourekhanova S, Bergeron S, Laforte V, Moreau E, Gosline SJC, Bertos N, Hallett M, Park M, Juncker D (2012) Antibody colocalization microarray: a scalable technology for multiplex protein analysis in complex samples. Mol Cell Proteomics 11(4): M111.011460. https://doi.org/10.1074/mcp.M111.011460
5. Li H, Bergeron S, Annis MG, Siegel PM, Juncker D (2015) Serial analysis of 38 proteins during the progression of human breast tumor in mice using an antibody colocalization microarray. Mol Cell Proteomics 14(4):1024. https://doi.org/10.1074/mcp.M114.046516
6. Li H, Bergeron S, Juncker D (2012) Microarray-to-microarray transfer of reagents by snapping of two chips for cross-reactivity-free multiplex immunoassays. Anal Chem 84(11):4776–4783. https://doi.org/10.1021/ac3003177
7. Li H, Bergeron S, Larkin H, Juncker D (2017) Snap chip for cross-reactivity-free and spotter-free multiplexed sandwich immunoassays. J Vis Exp 129:e56230. https://doi.org/10.3791/56230

Chapter 13

Antibody Printing Technologies

Valentin Romanov and Benjamin D. Brooks

Abstract

Antibody microarrays are routinely employed in the lab and in the clinic for studying protein expression, protein-protein, and protein-drug interactions. The microarray format reduces the size scale at which biological and biochemical interactions occur, leading to large reductions in reagent consumption and handling times while increasing overall experimental throughput. Specifically, antibody microarrays, as a platform, offer a number of different advantages over traditional techniques in the areas of drug discovery and diagnostics. While a number of different techniques and approaches have been developed for creating micro and nanoscale antibody arrays, issues relating to sensitivity, cost, and reproducibility persist. The aim of this review is to highlight current state-of the-art techniques and approaches for creating antibody arrays by providing latest accounts of the field while discussing potential future directions.

Key words Antibodies, Affinity binding, Analyte capture, High throughput, Screening, Chip, Diagnostics, Proteomics, Drug discovery, Protein immobilization, Protein profiling, Detection, Ligand

1 Introduction

Protein arrays provide a powerful platform as antibody screening assays, for studying antibody specificity while also providing a means for identification and characterization of post-translation modifications [1]. Protein microarrays are important tools in the fields of disease diagnosis and therapies, protein-protein interaction analysis, vaccine development, biochemical pathway mapping, enzyme-substrate profiling, immunoprofiling, proteomics, and drug discovery [2, 3]. While protein microarray techniques for affinity identification evolved from analytical immunoassays and are functionally similar, the microarray format provides several advantages over traditional techniques, including lower reagent consumption, ability to multiplex protein detection on a single platform that can be fabricated rationally by design, improved specificity, sensitivity, and higher throughput. Miniaturization of reaction and capture zones allows for the study of system-wide biochemical activity. Thousands of tiny, densely packed array spots provide the perfect platform for simultaneous screening of many

Kelly C. Whittaker and Ruo-Pan Huang (eds.), *Antibody Arrays: Methods and Protocols*, Methods in Molecular Biology, vol. 2237, https://doi.org/10.1007/978-1-0716-1064-0_13,

protein-protein, protein-lipid, and protein-nucleic acid interactions [4]. The vision of protein microarrays has been and continues to create "multiplexed and ultrasensitive assays that reliably target several specific analytes in a biological complex milieu without amplification or purification" [2].

Antibody and protein microarray technology and methodology evolved in parallel [5]. Antibody arrays are similar functionally to protein arrays, where instead of protein, arrays of spotted antibodies are utilized for detection and characterization of antigens within a complex solution (serum, plasma, lysate, etc.). In such fashion, it is possible to identify either the proteins of interest or novel antibody-antigen interactions. For instance, two differing biological samples, containing 500 different proteins, can be loaded onto a chip containing 500 monoclonal antibodies for direct binding comparisons [6]. Antibody arrays may be built from a variety of sources including antibodies, antibody fragments, affibodies, or aptamers [5]. A primary function of an antibody array is detection. Detection is driven by antibody specificity or the ability to bind specific active partners. Antibody arrays can be used for identifying and tracking changes in overall protein expression, post-translation modification, protein-protein, and protein-drug interactions and for the detection of toxins. A number of factors determine the quality and reproducibility of the array [2, 3]. Consideration should be given to the designing and optimizing of antibody arrays including how the antibody is produced, immobilization, and any potential cross-reactivity. For example, polyclonal antibodies, while a cheaper source of antibodies than monoclonal antibodies, may interact with more than one epitope on the same antigen. Conversely, monoclonal antibodies are highly homogenous and interact with a specific epitope on the antigen.

While regularly utilized, as a whole, adoption of arrays for both antibody and protein discovery has been limited [2]. Issues with adoption stem from a number of sources including poor or aberrant spot morphology and reproducibility, low signal-to-noise ratios, and poor target-surface binding or compatibility [2, 3]. For example, adoption of microarrays within translational research, where biomarker discovery and validation are used for diagnosis and treatment of patients has been slow due to the need for large quantities of purified protein, the associated costs, flexibility, sensitivity, and reproducibility of the format [7]. Specifically, slow adoption of antibody microarrays for biomarker discovery is due to limitations in detection (sensitivity) and the need for high-quality antibodies (highly specific with no cross-reactivity). For instance, in some cases, polyclonal antibodies have proven more sensitive and selective than monoclonal antibodies [8]. Nevertheless, improvements in printing technologies coupled with inline automation of sampling handling, processing, and collection may help with some of these limitations while also reducing experimental errors that

arise from the different modes of antibody immobilization, bias in sample preparation, and general issues relating to array handling and processing [9].

Microarray design strategies can typically be divided into three categories: functional, analytical, and reverse phase assays [10]. Functional arrays provide a platform for studying and screening molecular interactions [11]. Analytical microarrays are pull-down assays, that is, they capture molecules found within the solution by utilizing antibodies or aptamers and are used for studying binding affinities and protein expression levels [12]. Reverse-phase arrays use whole-cell extract for immunochemical detection of proteins [13]. They can also be used for studying tissue samples, lysate, serum, or bodily fluids [14]. This tool is useful for studying time- and dose-dependent protein dynamics. Compared to standard Western blots, this technique has the potential to create 1000 times more data using 10,000 times less volume [13].

The type of design strategy may inform the choice of printing technology. A number of different solutions have been developed for creating micro and nanoscale protein and antibody arrays. Each technique comes with its own set of advantages and disadvantages, with some limitations easier to surmount than others. Postulated in 2011 and still true to this day is the sentiment that no single array method exists to meet the needs of all microarray users [15]. However, glancing in the direction of industry [16] and overall literature referral popularity as an indicator, pin (contact), and jet (noncontact) printing remain in widespread use owing to their ease-of-use and automation [17, 18]. Here we outline some of the more popular techniques utilized for printing protein and antibody arrays. Specifically, this overview separates printing styles based on technique. We discuss contact, noncontact, lithography, and atomic force microscopy (AFM)-based array techniques. We do not aim to cover every single method, for instance, we do not discuss cell-free printing techniques; however, we direct the reader to an excellent recent review discussing advances in this field [19]. We present a general overview while discussing the advantages and disadvantages of each technique. Further, we provide the latest examples from the literature with the goal of showcasing progress and potential future directions.

2 Contact Printing

2.1 Pin Printing

Pin printing is the quintessential contact printing technique. A rigid pin comes into direct contact with a clean or pre-functionalized surface depositing a minute (picoliter-nanoliter) amount of solution, translating to spots that vary from tens to hundreds of micrometers in diameter (Fig. 1a). Pins come in a variety of styles (solid, split, and quill) and materials (stainless steel, silicone, tungsten, and

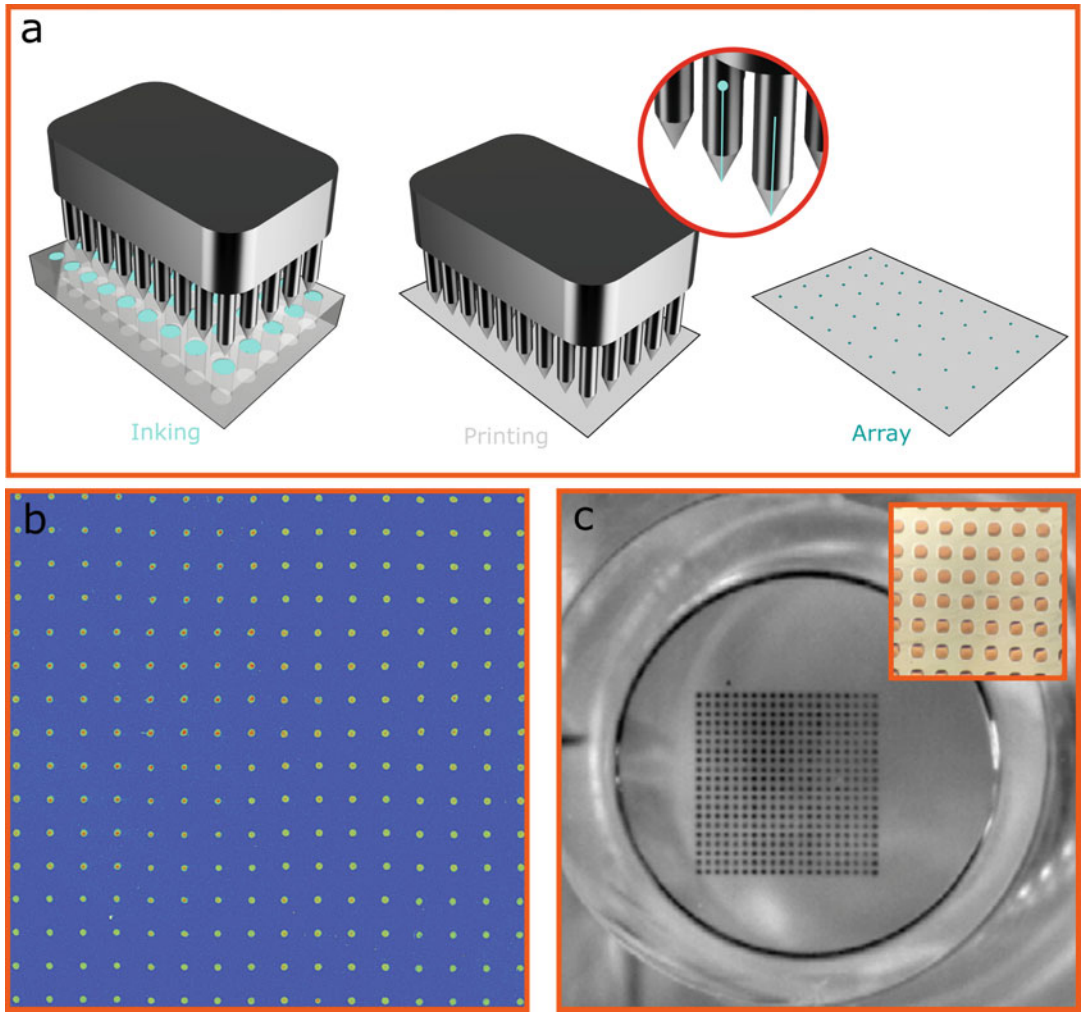

Fig. 1 (**a**) Schematic of pin printing. Inset, close up of different pin configurations (quill and split pin). (**b**) Solid tip pins of 150 μm in diameter. Printed spots are of Cy3-labeled anti-rabbit IgG onto poly(L-lysine) slides [138]. (Adapted with permission from ref. 138. Copyright 2003 American Chemical Society). (**c**) 20 × 20 quill pin (slit width 60 μm) printed microarray with a 96-wellplate, with 150 μm spacing between adjacent spots. Printed spots are of bovine serum albumin with rhodamine dye for visualization [139]. (Reprinted from ref. 139, with permission from Elsevier)

titanium) [20]. A typical operational workflow of a pin arrayer includes (1) dipping of pins into dispensing solution and (2) depositing a known amount of solution by light surface tapping.

While conceptually simple, a myriad of variables determine overall arraying quality, including surface energetics (i.e., surface-liquid interactions), surface functionalization, temperature, humidity, printing speed, sample viscosity, and evaporation rates [15, 21]. Experimental needs drive pin-style selection, for example,

quill pins are able to hold more sample through an embedded reservoir, increasing throughput, but are prone to breaking and clogging. While spots can be deposited onto any flat surface, whether a glass slide (Fig. 1b) or inside of 96-well plate (Fig. 1c), specialized, sometimes proprietary formulations are needed for reducing nonspecific binding. The density of microarrays depends on the size of deposited droplets, throughput of which strongly depends on capillarity (the volume of solution attached to the pin) and surface adhesion [21]. Pin style, material properties, and axial movement of the microarray head that houses the pins are just some of the considerations in overall throughput. Automation, while certainly a strength also comes with limitations. Microarray head movement between sample, deposition, and cleaning sites increases throughput time, while the contact nature of the technique gives rise to pin breakage [2].

The inherent challenges associated with pin printing provide a platform for future innovation. Numerous methods have been developed for improving array sensitivity (reducing signal-to-noise ratios), ranging from SERS (surface-enhanced ramen scattering) label-free detection [22] to signal amplification using quantum dots [23] and plasmonic nanogratings [24]. Other innovations include coupling of a standard pin printed microarray with mass spectrometry for high-throughput evaluation of small molecule binding [25] and computational techniques for improving data processing in the hopes of reducing the complexity and associated time costs [26, 27].

2.2 Microstamp Printing

Microstamping (μCP), originally described as a method for patterning 1 μm electrically conductive gold structures on silicone [28] quickly found application in protein research [29]. Microstamping is performed with an elastic stamp typically made from polydimethylsiloxane (PDMS), although other materials can also be used [30] (Fig. 2a). Stamp features are limited by the resolution of lithography tools available to the user. Stamp fabrication is typically performed using microfabrication techniques within a cleanroom environment. Significantly, once the master mask is fabricated, it can be used and reused multiple times. Changes to the patterning array will require the fabrication of a new master; however, after the initial investment, PDMS stamps can be made quickly and at low cost. The finished elastomeric stamp conforms to surface topology, can be functionalized (to make it either hydrophobic or hydrophilic), and is reusable [31]. Typical workflow for microstamping includes (1) surface coating ("inking") with the desired printing solution and (2) direct stamp contact with the substrate (with either a wet or a dry stamp) [32, 33]. Stamping is a parallel process and can be performed several times before reinking. Successful transfer of protein onto the surface of interest is determined by the wettability of both the stamp and the surface [34].

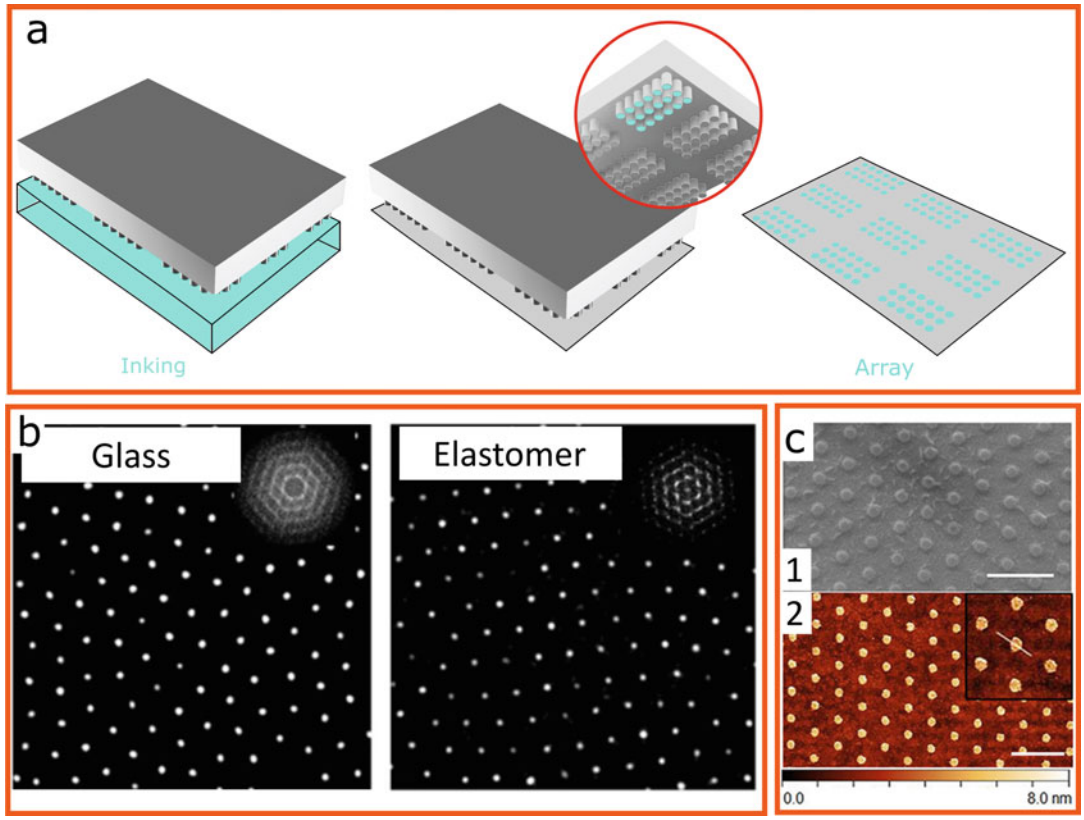

Fig. 2 (**a**) Schematic of microstamping. Inset, close up of the inking features with an inked array. (**b**) Nanocontact printing of biotynalited BSA-Texas Red from a glass stamp to an elastomeric surface (Sylgard-184, 10:1 cross-linker ratio). Glass surface is patterned by first covering the surface of the glass with a monolayer of micrometer particles, followed by silane/pluronic blocking and finished with addition of the target protein. Spot size ~400 nm [45]. (Adapted with permission from ref. 45. Copyright 2017 American Chemical Society). (**c**) SEM images of, (1) fabricated nanostamp and (2) an array of BSA protein on a coated coverslip. Nanostamp spot diameter 300 nm with average spot height ~4 nm [46]. (Image adapted from original)

Spot uniformity depends on a number of factors including stamping pressure, Young's modulus of the material (a measure of stiffness), stamp detachment speed, and stamp surface functionalization [18]. Of significant concern is contamination, which either arises from uncured PDMS or from cross-contamination between successive inking. Beyond simple discarding of stamps after each use, a number of strategies have been developed to address contamination concerns including surface treatment of PDMS [35] and new stamp designs [36].

A variety of innovations have been reported since the initial description of the technique. To overcome stamp deformation and feature collapse often observed on minimally patterned PDMS stamps [37], a harder material may be used (such as PMMA

[38]). Multilayer stamps, for sequential pressure-based deposition, have also been developed [39]. Alternatively, an altogether different patterning strategy can be adopted in the form of the "stamp-off" technique where a topographically featureless stamp (with pre-patterned protein regions) is used for transfer [40, 41]. Recently, a technique termed indirect microstamping was developed to overcome limitations relating to protein transfer from stamp to surface [42]. Antibodies arrayed by this approach demonstrated improved functionality over traditional μCP techniques. Rather than depositing the target of interest, the indirect μCP technique deposits the blocking agent first (BSA (bovine serum albumin)) followed by target incubation.

Advances in patterning techniques have led to improvements in array density and throughput by reducing pattern size. By reducing the size of the features on the rigid mask, nanoscale features can be fabricated for subsequent inking and protein transfer. One of the very first examples of nanocontact printing demonstrated protein feature sizes down to 40 nm covering an area of 9 mm^2 [43]. One of the main challenges with nanocontact printing is damage to either the stamp or the substrate during loading and unloading of the stamp [44]. One way to overcome this limitation is by creating a sacrificial template from PVA (polyvinyl alcohol) that can be used for patterning and subsequently removed by hydration in PBS (phosphate-buffered saline) [44]. This technique, along with others [45] (Fig. 2b), allows for direct patterning of soft substrates. Another way to overcome this limitation is to develop stronger elastomeric materials. A formulation of PDMS called X-PDMS has been used to create an elastomeric stamp for printing protein patterns down to 80 nm [46] (Fig. 2c).

2.3 Stencil Lithography

Stencils are masks, used to block parts of the substrate while exposing others for patterning. In contrast to microstamping where the protein array features are transferred from the pattern found on the stamp, in stencil arrays, cutouts in the stamp act as zones for protein deposition. Protein patterning by stencils is easy and straightforward. A typical workflow includes (1) adhering of an elastomeric stencil onto the surface of a substrate and (2) filling of the stencil with protein solution [47] (Fig. 3a, b).

Stencils made from PDMS are able to conformally seal to a number of different topologically smooth substrates. Since the base material is typically PDMS, stencils tend to suffer from the same drawbacks as stamps, namely, deformation and tearing during stencil loading and unloading. One strategy to reduce mechanical failure is to introduce a rigid backbone while maintaining an elastomeric seal. Hybrid elastomeric-metal stencils (HEMS) are steel stencils covered with a thin layer of a UV-sensitive, photocurable elastomer resulting in a flexible and tough stencil with good sealing properties to smooth surfaces [48]. UV curable polymers readily

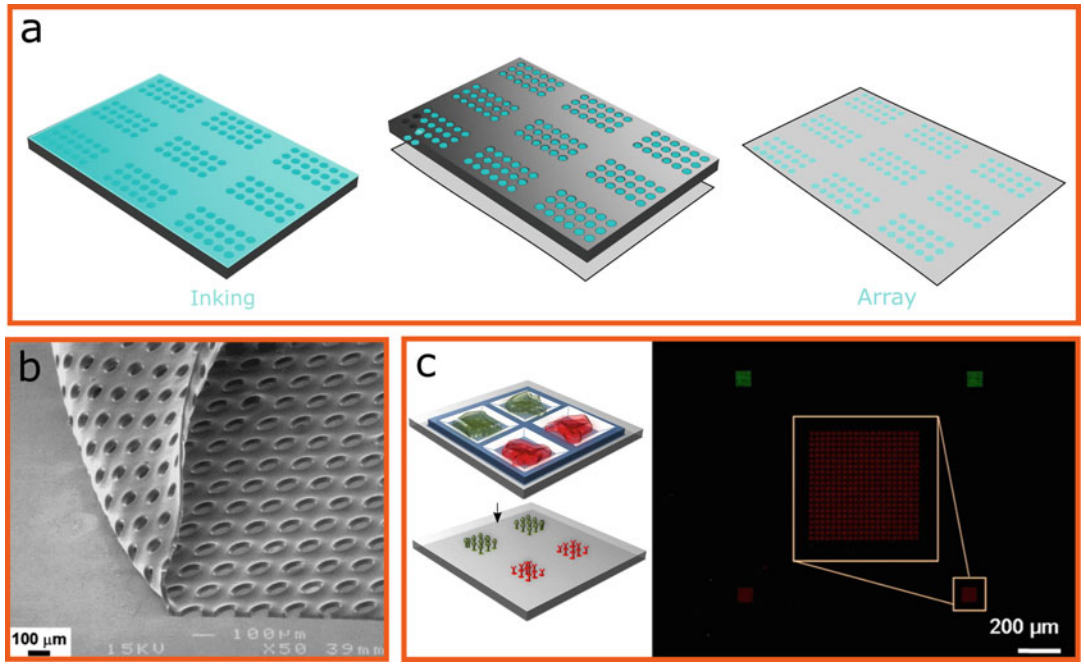

Fig. 3 (**a**) Schematic of the stencil patterning process. (**b**) SEM image of an elastomeric stencil [47]. Hole diameter, 100 µm, stencil thickness, 50 µm. (Adapted with permission from ref. 47. Copyright 2000 American Chemical Society). (**c**) A rigid, silicon nitride (SiNx) on silicon wafer stencil is attached to a PDMS substrate [51]. Printed nanoarrays consist of antimouse IgG-TRITC and antimonkey IgG-FITC antibodies. A variety of pattern sizes were demonstrated ranging from 100 to 900 nm on an equivalently sized stencil. (Adapted with permission from ref. 51. Copyright 2012 American Chemical Society)

cross-link to form well-defined patterns with a variety of possible stiffnesses (Young's modulus). Stencils made entirely from UV curable polymers have been demonstrated [49]. Other material strategies include the use of Parylene-C which forms a rigid, reusable stencil [50]. A limitation of stencil arrays is that protein delivery to the surface is driven by diffusion, presenting a challenge when speed is desired.

Innovations in single-molecule patterning spurred the development of nanostencil lithography. The first application of nanostencil lithography to protein patterning utilized a rigid, silicon nitride membrane as the stencil. The stencil, containing many truncated, pyramidal reservoirs with feature patterning down to 100 nm, can conformally bind to a functionalized PDMS slab for protein deposition [51] (Fig. 3c). Recently, hole-mask colloidal lithography (HCL) was adapted as a method for creating rigid stencils with feature sizes down to 15 nm [52]. An initial layer of PMMA and PDDA (poly(diallyldimethylammonium chloride)) masked by a layer of randomly distributed polystyrene nanospheres is etched all the way through to the base material (glass), creating wells. These wells are then used as stencils and are removed once sufficient protein surface coverage is obtained.

2.4 Microfluidic Printing

Microfluidics is the manipulation and processing of fluids at the micro or nanoscale. The distinct advantage of microfluidic platforms is small reagent consumption, increased surface-area-to-volume ratios, reduced diffusion distances, and, as such, reaction times and increased sensitivity within a potentially low-cost format [53]. Protein and antibody patterning is typically carried out within enclosed microfluidic networks (μFNs). Microfluidic networks are elastomeric guides, used to direct biomolecules to reaction areas on top of pre-functionalized surfaces [54] (Fig. 4a). Elastomeric guides are usually bonded with pre-treated surfaces, forming closed fluidic circuits, as such, necessitating the use of pliable and elastic materials, typically PDMS. Channel features, such as height and width, are determined by the negative structures found on the microfabricated mask, where sub-micrometer features can be readily attained [54, 55]. At this scale, channels are filled by capillary action. A typical protein array formation workflow includes (1) bonding of microfluidic guides to a pre-functionalized surface (whether glass, gold, or other chemistries of interest) and (2) channel filling by capillary action via addition of the sample to one end of the open fluidic circuit [56] (Fig. 4b). A major advantage of this approach is also its weakness and relates to molecular adsorption. The hydrophobic nature of PDMS leads to protein loss by adsorption, necessitating surface passivation or functionalization [57].

Several techniques have been developed that take advantage of microfluidic flow-based printing. The microfluidic network printing workflow is typically limited to unidirectional protein deposition due to permanent bonding of the elastomeric guide to the functionalized surface. Reversable bonding means a variety of different patterns can be created [56]. A number of recent research efforts have merged the simplicity and predictability of pin printing with fluidic networks, allowing for high-throughput target discovery and binding analysis. This approach combines the high-throughout, small reagent consumption of pin microarrays with an elastomeric guide that delivers reagents via fluidic circuits to the microarray for analysis [58, 59]. The same fluidic network principle can be applied to channels of varying geometries. The continuous flow microspotter (CFM) is in essence a multichannel microfluidic network. Rather than employing long, straight channels, the CFM utilizes an elastomeric microfluidic printhead that directly docks (reversibly) with a pre-functionalized surface [60] (Fig. 4c). Once docked, the printhead creates 48 distinct, addressable spots. Printheads with 96 spots have also been developed [61]. As each spot is a unique fluidic circuit, 96 different protein or drug combinations can be tested simultaneously. Combined with SPR (surface plasmon resonance), this platform provides a high-throughput format for antibody profiling through fluorescent and binding affinity measurements [61].

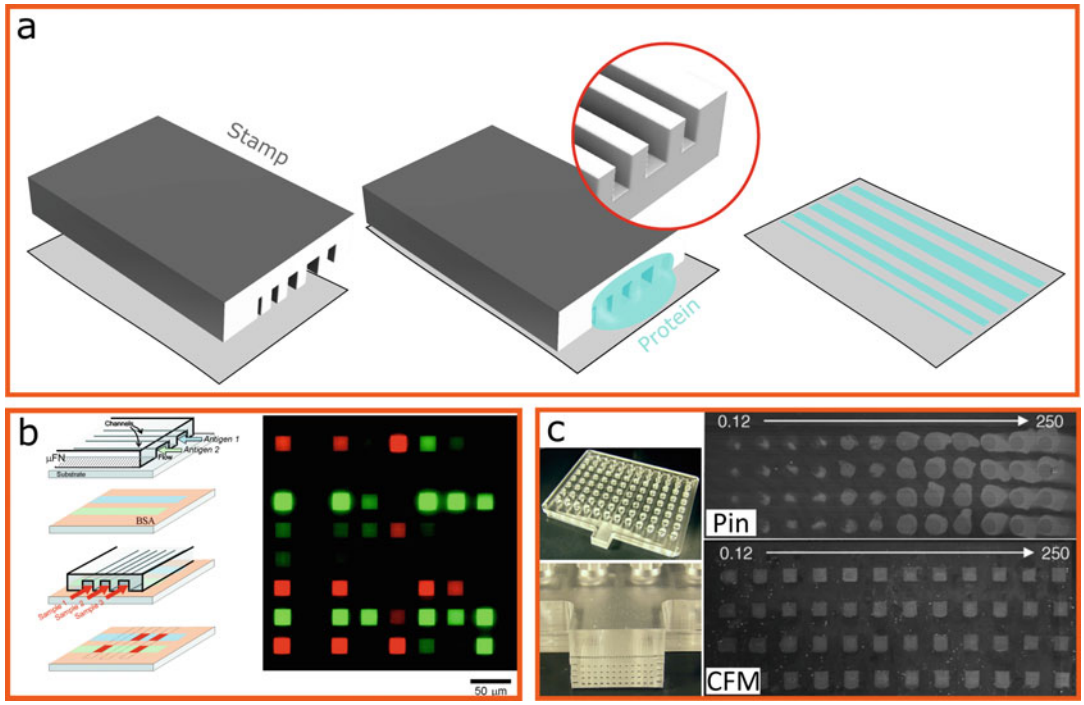

Fig. 4 (**a**) Schematic of a typical microfluidic network. An elastomeric stamp is bound to a substrate, forming distinct, patternable areas. Blue indicates protein solution. Inset, close up of the channels. (**b**) Creation of a microfluidic mosaic. Left, antigens are deposited on a functionalized surface, followed by BSA blocking and exposure of patterned areas to multiple samples of various antibodies. Right, an 8 × 8 mosaic consisting of human, bovine, mouse, chicken, dog, and guinea pig antibodies labeled with either FITC (green) or TRITC (red) [56]. (Adapted with permission from ref. 56. Copyright 2001 American Chemical Society). (**c**) Image of the print head used in the CFM with an image of the 4 × 12 microfluidic array fabricated in PDMS. Right, comparison of pin spotted arrays of protein A to those created using the CFM. Dilutions varied from 0.12 to 250 μg/mL [60]. (Reprinted from ref. 60, with permission from Elsevier)

3 Noncontact Printing

3.1 *Inkjet Printing*

Inkjet printing relies on the ejection of small droplets from a larger, moving reservoir (Fig. 5a). A distinct advantage of this printing technique is contactless array formation, eliminating the need for sealing (microfluidics) or mechanical touching (pins). Inkjet printing techniques can be separated into two distinct areas, continuous inkjet (CIJ) printing and drop-on-demand (DOD) printing [62]. Both techniques are capable of printing sub-100 μm diameter droplets which translates to pico-nanoliter droplet volumes. Droplet formation with the CIJ technique occurs as a result of Rayleigh instability, where a jet of pressure-driven liquid through an orifice of pre-defined size, breaks up into smaller droplets. By keeping the nozzle at an electrical potential, a small electrical charge is imparted on the droplets allowing for droplet stream steering and deflection

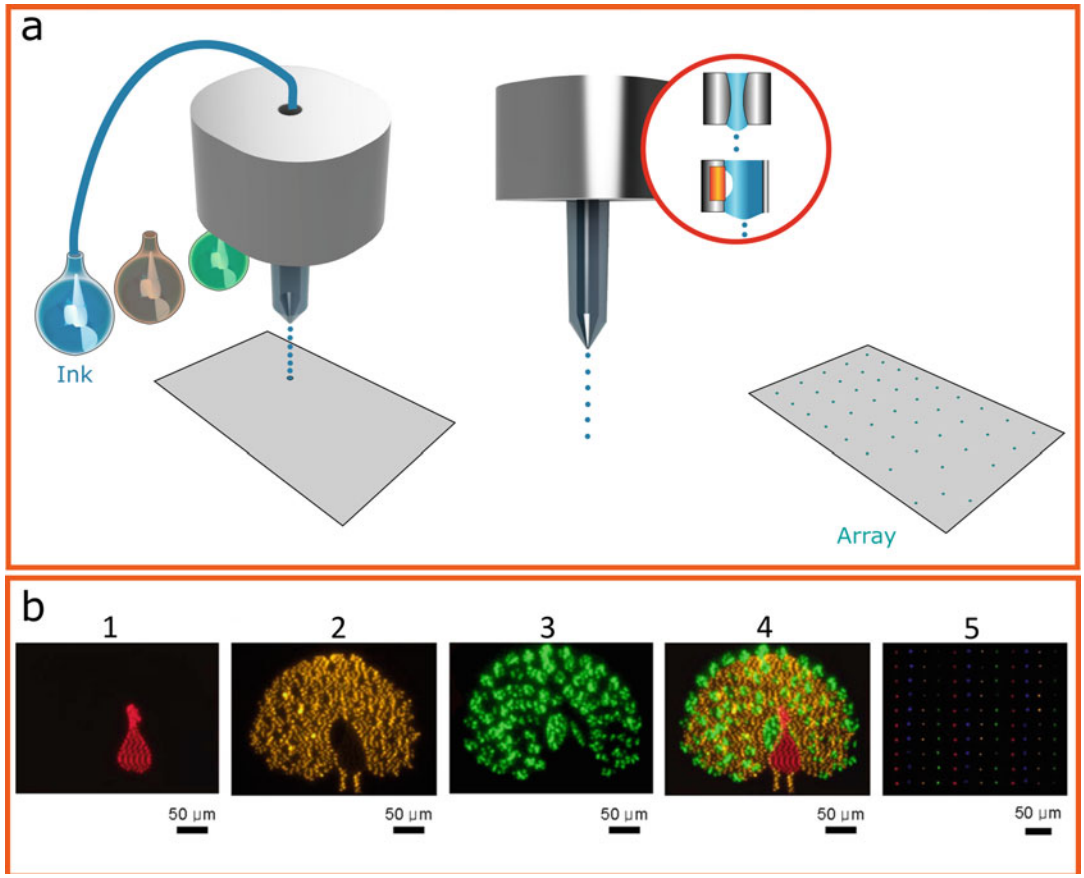

Fig. 5 (**a**) Schematic of inkjet printing. Inset, close up of different liquid ejection strategies (piezo and thermal). (**b**) Electrohydrodynamic printing of, (1) Cy5-Streptavidin (1 μm nozzle, spot size ~1.1 μm), (2) Alexa 546—Goat antirabbit IgG (1 μm nozzle, spot size ~1.6 μm), (3) Fluorescein-Streptavidin (1 μm nozzle, spot size ~1.9 μm), (4) Composite image of 1–3, (5) Alternating dot array of the aforementioned proteins (2 μm nozzle, spot size ~3.4 μm) [70]. (Adapted with permission from ref. 70. Copyright 2012 American Chemical Society)

[63]. Alternatively, the DOD technique relies on mechanical or thermal actuation for droplet dispensing. The protein mixture, loaded within the printing cartridge, is dispensed by either mechanical actuation (the opening and closing of a reservoir valve) [64] or by rapid pressure changes within the reservoir induced by either thermal [65] or volumetric changes (piezo actuation) [66].

The need for droplet selection during CIJ printing arises from satellite droplet formation. Satellite droplets may either recombine with other droplets or contaminate other parts of the array. This particular defect depends on the ejection pressure and liquid properties [62]. The limitation of DOD-based techniques relate to ink rheology, namely, intrinsic liquid properties such as liquid viscosity, density, and surface tension [67]. Inkjet printing, similar to other techniques mentioned in this chapter, suffers from protein accumulation at the point of ejection but can be addressed with careful

control over environmental conditions and liquid properties [2]. In order to address nozzle clogging due to rheologically varying inks, a laser system called BA-LIFT (blister-actuated laser-induced forward transfer) was recently developed [68]. Femtoliter droplets are created when single-laser pulses, focused onto a carrier substrate, create areas of expanding gas within a thin polyimide film pre-coated with a semi-viscous solution. Droplets can be patterned with high spatial control devoid of the coffee-ring effect (analyte accumulation on the periphery of a deposited spot [69]). Even greater droplet size control (droplet diameters of ~100 nm) has been demonstrated by electrohydrodynamic jet printing techniques. Electrohydrodynamic flows form when an electric field is generated between a metallic nozzle and a substrate [70, 71] (Fig. 5b). A technique that forgoes the use of nozzles and high-voltage circuits and electrodes has also been developed, where droplets are created using the pyroelectric effect [72]. The pyroelectric effect takes advantage of material properties where electric fields are established under thermal loads [73].

Microfluidic alternatives have also been developed in an effort to overcome some of the limitations found in inkjet printing, specifically relating to surface spot uniformity and dehydration [74]. This technique is referred to as "open-space" [75] microfluidics whereby fluid is hydrodynamically shaped and constrained above the printing surface. By eliminating the need for surface contact but by continuously flowing protein solution over the target area, a dense, highly uniform, continuously hydrating array can be readily created. Analyte recirculation reduces reagent waste and deposition time while increasing surface density and homogeneity [76]. To improve throughput and reduce printing time, multiple arrays can be engineered on a single microfluidic probe for selective delivery of proteins [77].

4 Lithography

4.1 Photolithography

Photolithography is the process by which a light-sensitive material is exposed and developed to form highly uniform, microscale, and/or nanoscale features. A typical workflow for patterning and depositing proteins includes (1) coating a carrier substrate (usually silicone or glass) with a photosensitive material (resist), (2) exposing the resist to UV or electron beam irradiation through a selectively etched chrome mask, and (3) chemical development of exposed or unexposed areas (Fig. 6a). At this stage, proteins may be directly bound to the processed surface or further exposure, and development cycles can be employed to create selective regions for binding both target and blocking proteins [78]. Photosensitive materials fall into two categories: positive and negative. Positive resists degrade under irradiation and are dissolved away, while negative

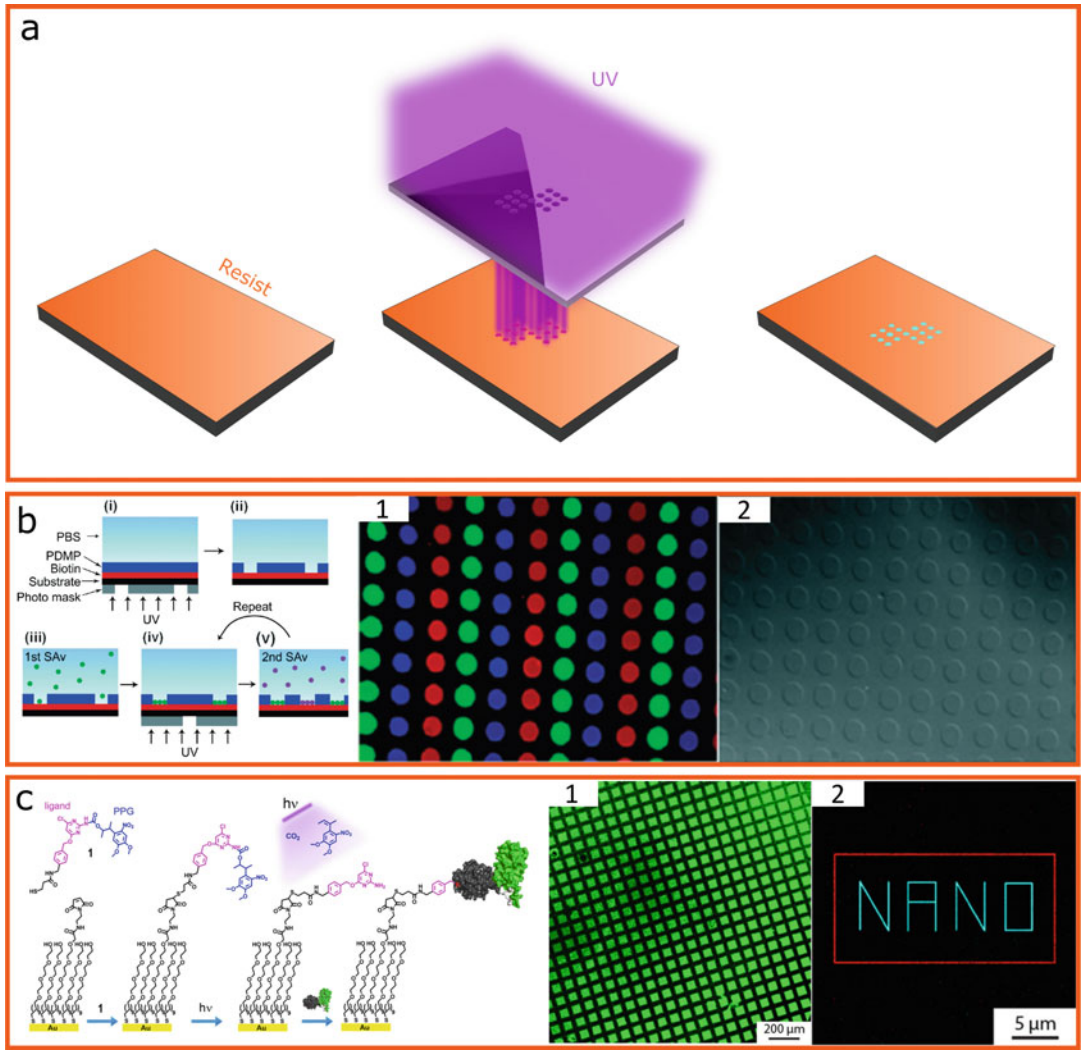

Fig. 6 (**a**) Schematic of the photolithographic process. (**b**) Immobilization of multiple streptavidin molecules. Left, areas of PDMP (poly(2,2-dimethoxy nitrobenzyl methacrylate-r-methyl methacrylate-r-poly(ethylene glycol) methacrylate) exposed to UV are dissolved away, revealing an underlaying region of biotin. Streptavidin is then used to bind biotin. In similar fashion, other areas on the substrate can be exposed and probed. Right, (1) an overlay of multiple labeled streptavidin proteins bound to biotin, and (2) brightfield image of the same area, showing the underlaying structure [82]. (Adapted with permission from ref. 82. Copyright 2010 American Chemical Society). (**c**) A ligand on the surface of a functionalized surface is used to bind SnapTag fusion proteins. PPG initially blocks ligand-fusion protein interaction until UV exposure resulting in covalent capture of proteins in illuminated areas. Right, (1) capture of mVenus-SnapTag protein and (2) capture of mCerulean-SnapTag and mCherry-SnapTag proteins. Linewidths of 420 nm [88]. (Adapted with permission from ref. 88. Copyright 2018 American Chemical Society)

resists cross-link and form solid structures while unexposed areas are removed. Resist chemistry and the irradiation source will ultimately determine structure resolution and binding efficiency of biological molecules [79]. Proteins are bound to the surface by

either physical adsorption, including electrostatic, ionic, or hydrophobic/philic interactions, covalent attachment to functional groups such as amines, thiols, and epoxies or affinity interactions [80]. Sub-micrometer, accurate, and intricate patterns that span the diameter of the wafer can be readily fabricated. However, changes to the underlaying array pattern require changes to the mask, increasing processing time, and cost. Consistent protein coverage depends on surface cleanliness, while bound-protein activity and functionality depend on the type of resist, processing steps, and functional groups used to prepare the surface [81].

Arrays prepared by this technique are typically used for probing single protein species at a time. Advancements in microscope projection photolithography (where a microscope is utilized for mask alignment and resist exposure) and developments in biocompatible photoresists with complimentary processing steps have been demonstrated for multiprotein species deposition with feature size down to 20 μm [82] (Fig. 6b). Research efforts in developing environmentally friendly, nontoxic solvents are also underway [83, 84]. Fluoropolymers are an especially interesting class of materials exhibiting good chemical resistance, stability, and good electrical properties [85]. This material is inert and thermally stable. Hydrofluoroether solvent readily dissolves fluorinated polymers and has been shown to be relatively gentle to deposited macromolecules [83]. Surfaces can also be readily patterned with photoactivatable chemistries [86]. For example, the self-assembly of a maleimide-presenting alkanethiolate monolayer on a gold substrate, coated with benzyl chloropyrimidine ligand, can be used to capture a Snap-tag [87] fusion protein from solution [88]. The photosensitive nitrophenyl photoprotecting group bound to the ligand is utilized to block protein binding. The photoprotecting group can be removed with either UV or laser irradiation. In this way, multiple Snap-tag fusion proteins can covalently attach, in a site-specific fashion, to photomasked irradiated regions on the surface, characterized by regions devoid of nitrophenyl photoprotecting groups exposing the capture ligand [88] (Fig. 6c).

4.2 Electron Beam Patterning

Electron beam lithography (E-beam) is similar to the standard photolithographic process but with a few marked differences. First, E-beam lithography does not require the generation of a mask; rather, the pattern can be programmed on a computer. Second, electrons bombarding the surface can be used to either ablate polymeric materials or modify their properties [89] with subsequent resist dissolution. E-beam patterning modifies resist properties in a similar fashion to the standard photolithographic process, where the resist is either cross-linked (negative resist) or degraded (positive) at pre-programmed locations (Fig. 7a). Resist composition plays a significant role in attaining patterns of desired size, as resists vary in sensitivity, contrast, and dissolution rates

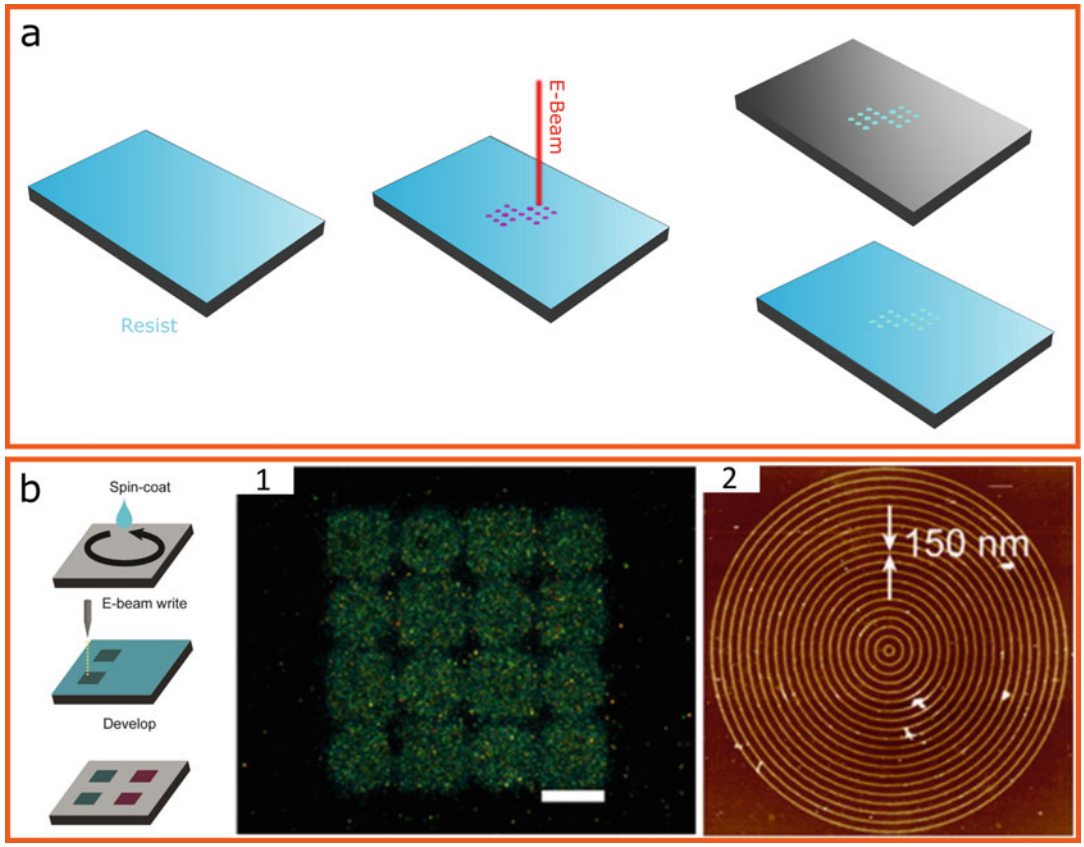

Fig. 7 (**a**) Schematic of electron beam lithography. (**b**) E-beam lithography is used to irradiate a solution containing protein, ascorbic acid, and Polyprotek, spin coated onto a pre-functionalized substrate. Cross-linked areas remain, while non-cross-linked areas are removed. Right, (1) Capture of two proteins, TNFα and IL-6. Silver-enhanced gold nanoparticles are used to enhance signal. Scale bar, 20 μm. (2) A close-up of one of the circles from (IL-6) (1). Line width, 150 nm [93]. (Adapted with permission from ref. 93. Copyright 2016 American Chemical Society)

[90]. For instance, the sensitivity of a PMMA (Polymethyl methacrylate) positive resist along with its resolution is greater than the standard SU-8 (Epoxy base) negative resist [90]. Maskless exposure adds flexibility to the design process, reducing costs associated with design iteration and opening the door for both two- and three-dimensional protein immobilization. A distinct advantage of E-beam lithography is a feature patterning on substrates with nanometer spatial resolution (~10 nm features are readily attainable) [91]. Molecules can be adsorbed to the prepared surface via a number of different processes once the pattern has been etched or new regions of the substrate are exposed and developed. A significant drawback of E-beam lithography is cost. Electron beam equipment is expensive, with patterning typically performed under ultra-vacuum conditions within a cleanroom environment. E-beam patterning is a slow process when compared to the aforementioned techniques.

The ability to pattern at the nanoscale opens up a number of exciting opportunities including tighter array packing stemming from smaller, denser feature patterning. To this end, efforts are being made to push the resolution limits well into the single nanometer range. The electron column, along with the electromagnetic lenses, electron energy, and a number of other factors, affects electron behavior (scattering phenomenon) before reaching the resist. One way to enhance resolution is to reduce the size of the electron beam (spot size) by reducing aberrations [92]. Features down to 1.7 nm have been demonstrated [92]. Rather than relying on diffusive processes for protein-binding post-fabrication, direct patterning of preformed protein films has also been demonstrated. One strategy for protecting antibodies from irradiation and pressures within the E-beam chamber is to protect them within a hydrogel matrix. By combining antibodies with ascorbic acid (which protects protein from irradiation) and polymers with trehalose side chains (PolyProtek) a protective resist can be created [93] (Fig. 7b). Electron irradiation cross-links the trehalose polymer to a pre-deposited PEG (polyethylene glycol) layer forming a hydrogel that protects and stabilizes the protein within its matrix. Several rounds of resist deposition and irradiation can yield multiprotein covered surfaces. Other research efforts are focused on reducing E-beam writing times by developing multibeam arrays [94].

5 AFM Nanoscale Patterning Techniques

5.1 Dip-Pen Lithography

Originally demonstrated as a technique for writing alkanethiols with linewidth resolution down to 30 nm [95], dip-pen lithography (DPL) has since been adopted by a large number of laboratories around the world [96]. Dip-pen lithography is performed using an AFM tip, where nanoscale arrays are written by capillary transport of molecules from the inked tip to the substrate (Fig. 8a). The size and density of individual array spots depend on the size of the probe, the chemical affinity of the ink, and its interaction with the functionalized substrate [95]. The ink and its underlaying properties play a fundamental role in the overall resolution and deposition of molecules from the tip to the surface [97]. A variety of different molecules have been printed using this technique including lipids [98–100] and an assortment of proteins [101–103] (Fig. 8b).

An often-cited criticism of using an AFM tip for spotting arrays is the lack of throughput. One way to circumvent this limitation is by tip parallelization, where multiple tips are fabricated on a substrate following attachment to the scanning head. Using standard photolithography techniques, an array of 55,000 cantilevered tips has been demonstrated [104]. The gravity-driven alignment system, coupled with many small pyramidal tips, resulted in the formation of 55,000 duplicates on the underlaying substrate. An

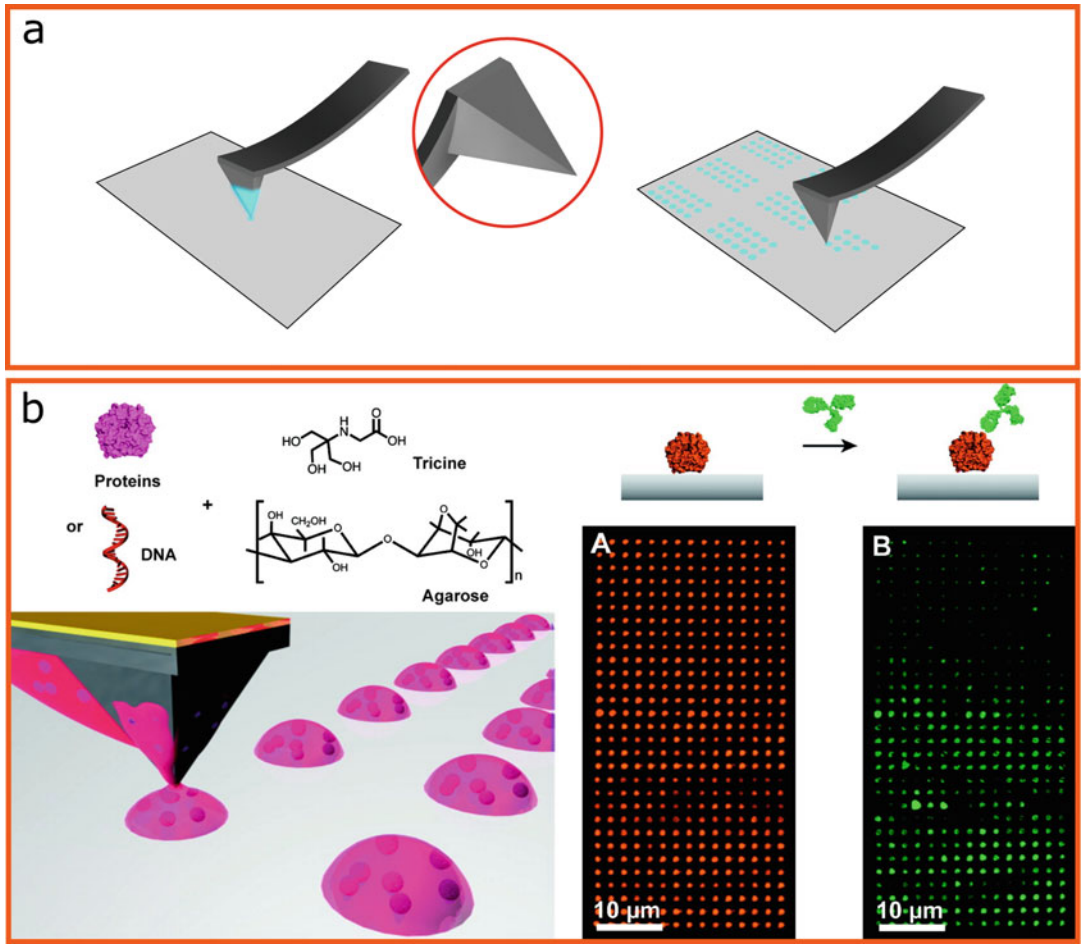

Fig. 8 (**a**) Schematic of the dip-pen process. Inset, close up of the AFM tip. (**b**) A schematic of the ink and matrix complex alongside the dip-pen deposition process. Right, an array of CTβ-Alexa 594 proteins inked onto a substrate followed by incubation with an anticholera toxin-Alexa 488 [103]. (Adapted with permission from ref. 103. Copyright 2009 American Chemical Society)

alternative, relatively low-cost, cantilever-free approach is to utilize elastomeric tips, termed polymer pen lithography (PPL). The underlaying principle is similar to nanocontact printing; however, rather than manually applying a stamp to the substrate, the pen array is mounted to a piezo scanner. The first demonstration of PPL reported an elastomeric array consisting of 11 million pens [105]. Feature size in PPL is a function of both the probe residence time in direct contact with the substrate and the subsequent contact force [106]. Multiplexed protein array patterns as small as 100 nm have been demonstrated [106]. Furthermore, pen arrays fabricated from PDMS can be further processed to add extra functionality. A variety of different strategies have been developed for functionalizing PDMS, from click chemistries for enhancing hydrophilocity

[107] to salinization [108] and plasma functionalization [109]. In similar fashion, PPL pens can also be functionalized with surface chemistries enabling fabrication of complex arrays [110]. Interestingly, it is possible to reverse the PPL deposition workflow, that is, a pen array can be used to remove material from a substrate. By combining chemical lift-off lithography with polymer pen lithography (PPCLL), it is possible to remove layers of self-assembling monolayers through direct surface contact using elastomeric pens [111]. Polymer pens with sub-20 nm tips were used to pattern alkanethiols with sub 50 nm linewidths. Regions devoid of SAMs can be used for attaching molecules of interest [112, 113].

While DLP is not strictly a contact printing technique, the inking solution which forms a meniscus between the tip and the substrate must be regenerated for subsequent spotting. One way to overcome this limitation is to constantly deliver the inking solution to the tip via an integrated conduit. Nanofountain pen lithography (FPL) was originally developed as a means of delivering chromium etchant through a cantilevered micropipette [114]. Driven by capillary pressure, a droplet formed at the tip of the micropipette can be used for direct patterning of the underlaying substrate. Capillary aperture size can vary from tens of nanometers to as large as needed. Recently, printed features down to 15 nm have been demonstrated using metallic inks [115] with a 200 nm capillary aperture. This approach has been used extensively for printing protein and antibody arrays [115–118]. Protein array spots as small as 200 nm using a 100 nm aperture have been demonstrated [119]. In order to gain greater control over dispensing/injection cycles and as a way to track tip-to-surface proximity, a new technique called fluidFM (fluid force microscopy) was developed. A sub-micrometer aperture in the AFM tip, coupled with a nanofluidic channel that spans the length of the cantilever can be used for both force sensing and for localized patterning of reagents [120, 121] and cellular extracts [122].

5.2 Nanoshaving

Nanoshaving is based on the same principles as DLP; that is, it utilizes a scanning probe microscope to pattern surfaces. At its simplest, nanoshaving uses an AFM tip to shave or mechanically remove molecules from the surface of the substrate. In its earliest form, nanoshaving was used to generate arrays of dots and lines on photoresist or gold surfaces, with periodicities down to 35 nm and linewidths down to 50 nm [123]. Fabrication of micro and nanoarrays typically involves the following steps: (1) deposition of a masking, self-assembling monolayer (SAM) on the surface of the substrate, (2) direct etching of the SAM layer with an AFM tip, and (3) incubation of the target molecule with the patterned surface. For instance, antibody arrays can be fabricated by trenching an alkyl-thiol SAM, acting as the mask, and by subsequently incubating antibodies to bind within the trenches [124]. In this case, the

height of the SAM layer was 10 nm with trench dimensions 400 nm by 4 μm. Nanoshaving has been used extensively to study antibody-antigen interactions using a variety of masking agents and patterning profiles [125, 126]. Nanoshaving can be used as a direct patterning tool for mask generation. For example, it can be combined with soft lithography techniques for creating elastomeric stamps for subsequent array formation, with linewidth down to 200 nm [127]. Similarly, nanoshaving has been used in conjunction with bovine serum albumin (BSA) as the blocking agent to define 55 nm lines that act as trenches, for subsequent building of stable lipid bilayers [128]. Increasing experimental throughput by reducing the number of processing steps can be accomplished via the nanografting technique, an extension of nanoshaving. Nanografting consists of two steps performed simultaneously. First, an AFM tip, submersed in one type of molecule, is used to scan and remove material from the surface of the substrate. Second, trenches created with the AFM tip are subsequently filled with the reactive molecules present within the solution [129, 130]. Nanografting has been used extensively for creating protein and antibody arrays [131, 132].

6 Summary

Antibody micro and nano array technologies will continue evolving in complexity and throughput. These are powerful platforms regularly used in the fields of diagnostics, drug testing, and discovery. Antibody arrays provide a number of advantages over enzyme-linked immunosorbent assays (ELISA) and Western blots in terms of reagent consumption, sensitivity, and throughput [9]. Nevertheless, adoption of antibody arrays for experimental and clinical applications has historically been slow. Often cited challenges relating to sensitivity, detection, and reproducibility are being tackled from a number of different directions. Quantum dot and nanoparticle assays have been shown to effectively increase sensitivity and the dynamic range of fluorescence antibody arrays [133]. While a number of different techniques have been developed for spotting antibodies and proteins onto functionalized surfaces, no one technique can currently meet the needs of every user. A logical step forward is the coupling of existing techniques in order to enhance functionality and throughput and improve user experience. Examples of integrated technologies include immobilization of molecules via pin spotted arrays combined with microfluidic fluid networks for sample interrogation and microfluidic spot printing of antibodies coupled to an SPR platform for measuring real-time kinetics [134]. Progress is being made on antibody microarrays; however, the progress is limited in many regards.

In our last review, we noted "as much as improved surfaces and protein stability are critical to microarray advances, two major technical hurdles related to printing must also be overcome before microarrays can attain their promise. These are the development of (1) high-throughput methods for producing high-affinity, high-stability, high-specificity proteins engineered for use as microarray capture reagents, and (2) a robust, consistent, high-throughput printing technology that survives storage and multiple assay conditions and lab-lab variations" [2]. Since that time, science has made significant strides in individual areas, especially protein production methods. Thus, we are seeing isolated successes such as those noted above. However, these strides are not broadly applicable and still remain in the research (i.e., drug discovery) realms.

Contact printing techniques remain as popular tools for patterning large amounts of samples on a variety of substrates. These techniques are typically coupled with robotic automation, reducing handling requirements. New innovations in printing and detection are coming from combining instrumentation to perform several functions in either series or parallel, promising higher density arrays at lower costs. For example, the advent of 3D printing has enabled the translation of conceptual ideas into direct actionable items, leading to new innovations, such as the integration of antibody arrays with smartphone-based detection [135, 136] or for masking substrates [137]. Innovations in lithographic techniques have led to the development of smaller, finer feature arrays resulting in higher-density patterns. A number of new techniques and approaches have been developed for either boosting or enhancing functionality of elastomeric-based array methods. Each printing approach comes with its own set of advantages and challenges, with the final choice of arrayer depending on the experimental needs of the user.

References

1. Pandey A, Mann M (2000) Proteomics to study genes and genomes. Nature 405(6788):837–846. https://doi.org/10.1038/35015709
2. Romanov V, Nikki Davidoff S, Miles AR, Grainger DW, Gale BK, Brooks BD (2014) A critical comparison of protein microarray fabrication technologies. Analyst 139(6): 1303–1326. https://doi.org/10.1039/C3AN01577G
3. MacBeath G (2002) Protein microarrays and proteomics. Nat Genet 32(4):526–532. https://doi.org/10.1038/ng1037
4. Bertone P, Snyder M (2005) Advances in functional protein microarray technology. FEBS J 272(21):5400–5411. https://doi.org/10.1111/j.1742-4658.2005.04970.x
5. Angenendt P (2005) Progress in protein and antibody microarray technology. Drug Discov Today 10(7):503–511. https://doi.org/10.1016/S1359-6446(05)03392-1
6. Pavlickova P, Schneider EM, Hug H (2004) Advances in recombinant antibody microarrays. Clin Chim Acta 343(1):17–35. https://doi.org/10.1016/j.cccn.2004.01.009
7. Yu X, Petritis B, LaBaer J (2016) Advancing translational research with next-generation protein microarrays. Proteomics 16(8): 1238–1250. https://doi.org/10.1002/pmic.201500374

8. Lian W, Wu D, Lim DV, Jin S (2010) Sensitive detection of multiplex toxins using antibody microarray. Anal Biochem 401(2):271–279. https://doi.org/10.1016/j.ab.2010.02.040
9. Chen Z, Dodig-Crnković T, Schwenk JM, Tao S (2018) Current applications of antibody microarrays. Clin Proteomics 15:7. https://doi.org/10.1186/s12014-018-9184-2
10. Stoevesandt O, Taussig MJ, He M (2009) Protein microarrays: high-throughput tools for proteomics. Expert Rev Proteomics 6(2): 145–157. https://doi.org/10.1586/epr.09.2
11. Berrade L, Garcia AE, Camarero JA (2011) Protein microarrays: novel developments and applications. Pharm Res 28(7):1480–1499. https://doi.org/10.1007/s11095-010-0325-1
12. Hall DA, Ptacek J, Snyder M (2007) Protein microarray technology. Mech Ageing Dev 128(1):161–167. https://doi.org/10.1016/j.mad.2006.11.021
13. Spurrier B, Ramalingam S, Nishizuka S (2008) Reverse-phase protein lysate microarrays for cell signaling analysis. Nat Protoc 3(11):1796–1808. https://doi.org/10.1038/nprot.2008.179
14. Mueller C, Liotta LA, Espina V (2010) Reverse phase protein microarrays advance to use in clinical trials. Mol Oncol 4(6): 461–481. https://doi.org/10.1016/j.molonc.2010.09.003
15. Austin J, Holway AH (2011) Contact printing of protein microarrays. In: Korf U (ed) Protein microarrays: methods and protocols, Methods in molecular biology. Humana Press, Totowa, NJ, pp 379–394. https://doi.org/10.1007/978-1-61779-286-1_25
16. Gupta S, Manubhai KP, Kulkarni V, Srivastava S (2016) An overview of innovations and industrial solutions in protein microarray technology. Proteomics 16(8):1297–1308. https://doi.org/10.1002/pmic.201500429
17. Clancy KFA, Dery S, Laforte V, Shetty P, Juncker D, Nicolau DV (2019) Protein microarray spots are modulated by patterning method, surface chemistry and processing conditions. Biosens Bioelectron 130:397–407. https://doi.org/10.1016/j.bios.2018.09.027
18. Pereiro I, Cors JF, Pané S, Nelson BJ, Kaigala GV (2019) Underpinning transport phenomena for the patterning of biomolecules. Chem Soc Rev 48(5):1236–1254. https://doi.org/10.1039/C8CS00852C
19. Yu X, Petritis B, Duan H, Xu D, LaBaer J (2018) Advances in cell-free protein array methods. Expert Rev Proteomics 15(1): 1–11. https://doi.org/10.1080/14789450.2018.1415146
20. Barbulovic Nad I (2006) Bio-microarray fabrication techniques—a review. Crit Rev Biotechnol 26(4):237. https://doi.org/10.1080/07388550600978358
21. Kong F, Yuan L, Zheng YF, Chen W (2012) Automatic liquid handling for life science a critical review of the current state of the art. J Lab Autom 17(3):169–185. https://doi.org/10.1177/2211068211435302
22. Knauer M, Ivleva NP, Liu X, Niessner R, Haisch C (2010) Surface-enhanced Raman scattering-based label-free microarray readout for the detection of microorganisms. Anal Chem 82(7):2766–2772. https://doi.org/10.1021/ac902696y
23. Finetti C, Plavisch L, Chiari M (2016) Use of quantum dots as mass and fluorescence labels in microarray biosensing. Talanta 147:397–401. https://doi.org/10.1016/j.talanta.2015.10.012
24. Liu C, Meng F, Wang B, Zhang L, Cui X (2018) Plasmonic nanograting enhanced fluorescence for protein microarray analysis of carcinoembryonic antigen (CEA). Anal Methods 10(1):145–150. https://doi.org/10.1039/C7AY02232H
25. Yao C, Wang T, Zhang B, He D, Na N, Ouyang J (2015) Screening of the binding of small molecules to proteins by desorption electrospray ionization mass spectrometry combined with protein microarray. J Am Soc Mass Spectrom 26(11):1950–1958. https://doi.org/10.1007/s13361-015-1221-z
26. Fishman D, Kuzmin I, Vilo J, Peterson H (2019) PAWER: protein array web ExploreR. bioRxiv 692905. https://doi.org/10.1101/692905
27. Da Gama Duarte J, Goosen RW, Lawry PJ, Blackburn JM (2018) PMA: protein microarray analyser, a user-friendly tool for data processing and normalization. BMC Res Notes 11(1):156. https://doi.org/10.1186/s13104-018-3266-0
28. Kumar A, Whitesides GM (1993) Features of gold having micrometer to centimeter dimensions can be formed through a combination of stamping with an elastomeric stamp and an alkanethiol "Ink" followed by chemical etching. Appl Phys Lett 63(1):2002–2004. https://doi.org/10.1063/1.110628

29. Bernard A, Delamarche E, Schmid H, Michel B, Bosshard HR, Biebuyck H (1998) Printing patterns of proteins. Langmuir 14(9):2225–2229. https://doi.org/10.1021/la980037l
30. Kaufmann T, Jan Ravoo B (2010) Stamps, inks and substrates: polymers in microcontact printing. Polym Chem 1(4):371–387. https://doi.org/10.1039/B9PY00281B
31. Kane RS, Takayama S, Ostuni E, Ingber DE, Whitesides GM (1999) Patterning proteins and cells using soft lithography. In: Williams DF (ed) The biomaterials: silver jubilee compendium. Elsevier Science, Oxford, pp 161–174. https://doi.org/10.1016/B978-008045154-1.50020-4
32. Hyun J, Zhu Y, Liebmann-Vinson A, Beebe TP, Chilkoti A (2001) Microstamping on an activated polymer surface: patterning biotin and streptavidin onto common polymeric biomaterials. Langmuir 17(20):6358–6367. https://doi.org/10.1021/la010695x
33. Renault JP, Bernard A, Juncker D, Michel B, Bosshard HR, Delamarche E (2002) Fabricating microarrays of functional proteins using affinity contact printing. Angew Chem Int Ed 41(13):2320–2323. https://doi.org/10.1002/1521-3773(20020703)41:13<2320::AID-ANIE2320>3.0.CO;2-Z
34. Tan JL, Tien J, Chen CS (2002) Microcontact printing of proteins on mixed self-assembled monolayers. Langmuir 18(2):519–523. https://doi.org/10.1021/la011351+
35. Zhang Z, Ma H, Hausner DB, Chilkoti A, Beebe TP (2005) Pretreatment of amphiphilic comb polymer surfaces dramatically affects protein adsorption. Biomacromolecules 6(6):3388–3396. https://doi.org/10.1021/bm050446d
36. Lin SC, Tseng FG, Huang HM, Chen Y-F, Tsai YC, Ho CE, Chieng CC (2004) Simultaneous immobilization of protein microarrays by a micro stamper with back-filling reservoir. Sens Actuators B Chem 99(1):174–185. https://doi.org/10.1016/S0925-4005(03)00554-9
37. Ruiz SA, Chen CS (2007) Microcontact printing: a tool to pattern. Soft Matter 3(2):168–177. https://doi.org/10.1039/B613349E
38. Wang Y, Goh SH, Bi X, Yang K-L (2009) Replication of DNA submicron patterns by combining nanoimprint lithography and contact printing. J Colloid Interface Sci 333(1):188–194. https://doi.org/10.1016/j.jcis.2009.02.010
39. Tien J, Nelson CM, Chen CS (2002) Fabrication of aligned microstructures with a single elastomeric stamp. Proc Natl Acad Sci 99(4):1758–1762. https://doi.org/10.1073/pnas.042493399
40. Desai RA, Khan MK, Gopal SB, Chen CS (2011) Subcellular spatial segregation of integrin subtypes by patterned multicomponent surfaces. Integr Biol 3(5):560–567. https://doi.org/10.1039/c0ib00129e
41. Rodriguez NM, Desai RA, Trappmann B, Baker BM, Chen CS (2014) Micropatterned multicolor dynamically adhesive substrates to control cell adhesion and multicellular organization. Langmuir 30(5):1327–1335. https://doi.org/10.1021/la404037s
42. Juste-Dolz A, Avella-Oliver M, Puchades R, Maquieira A (2018) Indirect microcontact printing to create functional patterns of physisorbed antibodies. Sensors 18(9):3163. https://doi.org/10.3390/s18093163
43. Li H-W, Muir BVO, Fichet G, Huck WTS (2003) Nanocontact printing: a route to sub-50-nm-scale chemical and biological patterning. Langmuir 19(6):1963–1965. https://doi.org/10.1021/la0269098
44. MacNearney D, Mak B, Ongo G, Kennedy TE, Juncker D (2016) Nanocontact printing of proteins on physiologically soft substrates to study cell haptotaxis. Langmuir 32(50):13525–13533. https://doi.org/10.1021/acs.langmuir.6b03246
45. Alameddine R, Wahl A, Pi F, Bouzalmate K, Limozin L, Charrier A, Sengupta K (2017) Printing functional protein nanodots on soft elastomers: from transfer mechanism to cell mechanosensing. Nano Lett 17(7):4284–4290. https://doi.org/10.1021/acs.nanolett.7b01254
46. Lindner M, Tresztenyak A, Fülöp G, Jahr W, Prinz A, Prinz I, Danzl JG, Schütz GJ, Sevcsik E (2019) A fast and simple contact printing approach to generate 2D protein nanopatterns. Front Chem 6:655. https://doi.org/10.3389/fchem.2018.00655
47. Ostuni E, Kane R, Chen CS, Ingber DE, Whitesides GM (2000) Patterning mammalian cells using elastomeric membranes. Langmuir 16(20):7811–7819. https://doi.org/10.1021/la000382m
48. Pla-Roca M, Leulmi RF, Djambazian H, Sundararajan S, Juncker D (2010) Addressable nanowell arrays formed using reversibly sealable hybrid elastomer-metal stencils. Anal Chem 82(9):3848–3855. https://doi.org/10.1021/ac100335d

49. Masters T, Engl W, Weng ZL, Arasi B, Gauthier N, Viasnoff V (2012) Easy fabrication of thin membranes with through holes. Application to protein patterning. PLoS One 7(8):e44261. https://doi.org/10.1371/journal.pone.0044261
50. Tan CP, Ri Seo B, Brooks DJ, Chandler EM, Craighead HG, Fischbach C (2009) Parylene peel-off arrays to probe the role of cell–cell interactions in tumour angiogenesis. Integr Biol 1(10):587–594. https://doi.org/10.1039/b908036h
51. Huang M, Galarreta BC, Artar A, Adato R, Aksu S, Altug H (2012) Reusable nanostencils for creating multiple biofunctional molecular nanopatterns on polymer substrate. Nano Lett 12(9):4817–4822. https://doi.org/10.1021/nl302266u
52. Lum W, Gautam D, Chen J, Sagle LB (2019) Single molecule protein patterning using hole mask colloidal lithography. Nanoscale. https://doi.org/10.1039/C9NR05630K
53. Whitesides GM (2006) The origins and the future of microfluidics. Nature 442(7101): 368–373. https://doi.org/10.1038/nature05058
54. Delamarche E, Bernard A, Schmid H, Michel B, Biebuyck H (1997) Patterned delivery of immunoglobulins to surfaces using microfluidic networks. Science 276(5313): 779–781. https://doi.org/10.1126/science.276.5313.779
55. Delamarche E, Bernard A, Schmid H, Bietsch A, Michel B, Biebuyck H (1998) Microfluidic networks for chemical patterning of substrates: design and application to bioassays. J Am Chem Soc 120(3):500–508. https://doi.org/10.1021/ja973071f
56. Bernard A, Michel B, Delamarche E (2001) Micromosaic immunoassays. Anal Chem 73(1):8–12. https://doi.org/10.1021/ac0008845
57. Huang B, Wu H, Kim S, Zare RN (2005) Coating of poly(Dimethylsiloxane) with n-dodecyl-β-d-maltoside to minimize nonspecific protein adsorption. Lab Chip 5(10):1005–1007. https://doi.org/10.1039/B509251E
58. Tong Z, Rajeev G, Guo K, Ivask A, McCormick S, Lombi E, Priest C, Voelcker NH (2018) Microfluidic cell microarray platform for high throughput analysis of particle–cell interactions. Anal Chem 90(7):4338–4347. https://doi.org/10.1021/acs.analchem.7b03079
59. Liu X, Li H, Jia W, Chen Z, Xu D (2017) Selection of aptamers based on a protein microarray integrated with a microfluidic chip. Lab Chip 17(1):178–185. https://doi.org/10.1039/C6LC01208F
60. Natarajan S, Katsamba PS, Miles A, Eckman J, Papalia GA, Rich RL, Gale BK, Myszka DG (2008) Continuous-flow microfluidic printing of proteins for array-based applications including surface plasmon resonance imaging. Anal Biochem 373(1):141–146. https://doi.org/10.1016/j.ab.2007.07.035
61. Boesch AW, Miles AR, Chan YN, Osei-Owusu NY, Ackerman ME (2017) IgG Fc variant cross-reactivity between human and rhesus macaque FcγRs. mAbs 9(3):455–465. https://doi.org/10.1080/19420862.2016.1274845
62. Martin GD, Hoath SD, Hutchings IM (2008) Inkjet printing—the physics of manipulating liquid jets and drops. J Phys Conf Ser 105:012001. https://doi.org/10.1088/1742-6596/105/1/012001
63. Derby B (2010) Inkjet printing of functional and structural materials: fluid property requirements, feature stability, and resolution. Annu Rev Mater Res 40(1):395–414. https://doi.org/10.1146/annurev-matsci-070909-104502
64. McWilliam I, Kwan MC, Hall D (2011) Inkjet printing for the production of protein microarrays. In: Korf U (ed) Protein microarrays: methods and protocols, Methods in molecular biology. Humana Press, Totowa, NJ, pp 345–361. https://doi.org/10.1007/978-1-61779-286-1_23
65. Setti L, Piana C, Bonazzi S, Ballarin B, Frascaro D, Fraleoni-Morgera A, Giuliani S (2004) Thermal inkjet technology for the microdeposition of biological molecules as a viable route for the realization of biosensors. Anal Lett 37(8):1559–1570. https://doi.org/10.1081/AL-120037587
66. Klenkar G, Valiokas R, Lundström I, Tinazli A, Tampé R, Piehler J, Liedberg B (2006) Piezo dispensed microarray of multivalent chelating thiols for dissecting complex protein−protein interactions. Anal Chem 78(11):3643–3650. https://doi.org/10.1021/ac060024+
67. Delaney JT, Smith PJ, Schubert US (2009) Inkjet printing of proteins. Soft Matter 5(24): 4866–4877. https://doi.org/10.1039/B909878J
68. Hecht L, Rager K, Davidonis M, Weber P, Gauglitz G, Dietzel A (2019) Blister-actuated LIFT printing for multiparametric functionalization of paper-like biosensors. Micromachines 10(4):221. https://doi.org/10.3390/mi10040221

69. Deng Y, Zhu X-Y, Kienlen T, Guo A (2006) Transport at the air/water interface is the reason for rings in protein microarrays. J Am Chem Soc 128(9):2768–2769. https://doi.org/10.1021/ja057669w
70. Shigeta K, He Y, Sutanto E, Kang S, Le A-P, Nuzzo RG, Alleyne AG, Ferreira PM, Lu Y, Rogers JA (2012) Functional protein microarrays by electrohydrodynamic jet printing. Anal Chem 84(22):10012–10018. https://doi.org/10.1021/ac302463p
71. Park J-U, Lee JH, Paik U, Lu Y, Rogers JA (2008) Nanoscale patterns of oligonucleotides formed by electrohydrodynamic jet printing with applications in biosensing and nanomaterials assembly. Nano Lett 8(12):4210–4216. https://doi.org/10.1021/nl801832v
72. Ferraro P, Coppola S, Grilli S, Paturzo M, Vespini V (2010) Dispensing nano–pico droplets and liquid patterning by pyroelectrodynamic shooting. Nat Nanotechnol 5(6):429–435. https://doi.org/10.1038/nnano.2010.82
73. Bourim EM, Moon C-W, Lee S-W, Kyeong Yoo I (2006) Investigation of pyroelectric electron emission from monodomain lithium niobate single crystals. Phys B Condens Matter 383(2):171–182. https://doi.org/10.1016/j.physb.2006.02.034
74. Juncker D, Schmid H, Delamarche E (2005) Multipurpose microfluidic probe. Nat Mater 4(8):622–628. https://doi.org/10.1038/nmat1435
75. Kaigala GV, Lovchik RD, Delamarche E (2012) Microfluidics in the "open space" for performing localized chemistry on biological interfaces. Angew Chem Int Ed 51:11224–11240. https://doi.org/10.1002/anie.201201798
76. Autebert J, Cors JF, Taylor DP, Kaigala GV (2016) Convection-enhanced biopatterning with recirculation of hydrodynamically confined nanoliter volumes of reagents. Anal Chem 88(6):3235–3242. https://doi.org/10.1021/acs.analchem.5b04649
77. Taylor DP, Zeaf I, Lovchik RD, Kaigala GV (2016) Centimeter-scale surface interactions using hydrodynamic flow confinements. Langmuir 32(41):10537–10544. https://doi.org/10.1021/acs.langmuir.6b02983
78. Douvas A, Argitis P, Diakoumakos CD, Misiakos K, Dimotikali D, Kakabakos SE (2001) Photolithographic patterning of proteins with photoresists processable under biocompatible conditions. J Vac Sci Technol B 19(6):2820–2824. https://doi.org/10.1116/1.1408954
79. Petrou PS, Chatzichristidi M, Douvas AM, Argitis P, Misiakos K, Kakabakos SE (2007) A biomolecule friendly photolithographic process for fabrication of protein microarrays on polymeric films coated on silicon chips. Biosens Bioelectron 22(9):1994–2002. https://doi.org/10.1016/j.bios.2006.08.036
80. Lam CN, Chang D, Olsen BD (2016) Protein nanopatterning. In: Zhang M, Naik RR, Dai L (eds) Carbon nanomaterials for biomedical applications, Springer series in biomaterials science and engineering. Springer International Publishing, Cham, pp 445–480. https://doi.org/10.1007/978-3-319-22861-7_14
81. You C, Piehler J (2016) Functional protein micropatterning for drug design and discovery. Expert Opin Drug Discov 11(1):105–119. https://doi.org/10.1517/17460441.2016.1109625
82. Kim M, Choi J-C, Jung H-R, Katz JS, Kim M-G, Doh J (2010) Addressable micropatterning of multiple proteins and cells by microscope projection photolithography based on a protein friendly photoresist. Langmuir 26(14):12112–12118. https://doi.org/10.1021/la1014253
83. Machairioti F, Petrou P, Oh H-T, Lee J-K, Kakabakos S, Argitis P, Chatzichristidi M (2019) Bio-orthogonal fluorinated resist for biomolecules patterning applications. Colloids Surf B Biointerfaces 178:208–213. https://doi.org/10.1016/j.colsurfb.2019.03.006
84. Zakhidov AA, Lee J-K, Fong HH, DeFranco JA, Chatzichristidi M, Taylor PG, Ober CK, Malliaras GG (2008) Hydrofluoroethers as orthogonal solvents for the chemical processing of organic electronic materials. Adv Mater 20(18):3481–3484. https://doi.org/10.1002/adma.200800557
85. Dhara MG, Banerjee S (2010) Fluorinated high-performance polymers: poly(arylene ether)s and aromatic polyimides containing trifluoromethyl groups. Prog Polym Sci 35(8):1022–1077. https://doi.org/10.1016/j.progpolymsci.2010.04.003
86. Hengsakul M, Cass AEG (1996) Protein patterning with a photoactivatable derivative of biotin. Bioconjug Chem 7(2):249–254. https://doi.org/10.1021/bc960007z
87. Keppler A, Gendreizig S, Gronemeyer T, Pick H, Vogel H, Johnsson K (2003) A general method for the covalent labeling of fusion proteins with small molecules in vivo. Nat Biotechnol 21(1):86–89. https://doi.org/10.1038/nbt765

88. Zhou S, Metcalf KJ, Bugga P, Grant J, Mrksich M (2018) Photoactivatable reaction for covalent nanoscale patterning of multiple proteins. ACS Appl Mater Interfaces 10(47): 40452–40459. https://doi.org/10.1021/acsami.8b16736
89. Schmidt RC, Healy KE (2009) Controlling biological interfaces on the nanometer length scale. J Biomed Mater Res A 90A(4): 1252–1261. https://doi.org/10.1002/jbm.a.32501
90. Chen Y (2015) Nanofabrication by electron beam lithography and its applications: a review. Microelectron Eng 135:57–72. https://doi.org/10.1016/j.mee.2015.02.042
91. Kolodziej CM, Maynard HD (2012) Electron-beam lithography for patterning biomolecules at the micron and nanometer scale. Chem Mater 24(5):774–780. https://doi.org/10.1021/cm202669f
92. Manfrinato VR, Stein A, Zhang L, Nam C-Y, Yager KG, Stach EA, Black CT (2017) Aberration-corrected electron beam lithography at the one nanometer length scale. Nano Lett 17(8):4562–4567. https://doi.org/10.1021/acs.nanolett.7b00514
93. Lau UY, Saxer SS, Lee J, Bat E, Maynard HD (2016) Direct write protein patterns for multiplexed cytokine detection from live cells using electron beam lithography. ACS Nano 10(1):723–729. https://doi.org/10.1021/acsnano.5b05781
94. Spallas JP, Silver CS, Muray LP (2006) Arrayed miniature electron beam columns for mask making. J Vac Sci Technol B 24(6): 2892–2896. https://doi.org/10.1116/1.2395955
95. Piner RD, Zhu J, Xu F, Hong S, Mirkin CA (1999) "Dip-Pen" nanolithography. Science 283(5402):661–663. https://doi.org/10.1126/science.283.5402.661
96. Salaita K, Wang Y, Mirkin CA (2007) Applications of dip-pen nanolithography. Nat Nanotechnol 2(3):145–155. https://doi.org/10.1038/nnano.2007.39
97. Liu G, Hirtz M, Fuchs H, Zheng Z (2019) Development of dip-pen nanolithography (DPN) and its derivatives. Small 15(21): 1900564. https://doi.org/10.1002/smll.201900564
98. Sekula-Neuner S, Maier J, Oppong E, Cato ACB, Hirtz M, Fuchs H (2012) Allergen arrays for antibody screening and immune cell activation profiling generated by parallel lipid dip-pen nanolithography. Small 8(4):585–591. https://doi.org/10.1002/smll.201101694
99. Sekula S, Fuchs J, Weg-Remers S, Nagel P, Schuppler S, Fragala J, Theilacker N, Franzreb M, Wingren C, Ellmark P et al (2008) Multiplexed lipid dip-pen nanolithography on subcellular scales for the templating of functional proteins and cell culture. Small 4(10):1785–1793. https://doi.org/10.1002/smll.200800949
100. Navikas V, Gavutis M, Rakickas T, Valiokas R (2019) Scanning probe-directed assembly and rapid chemical writing using nanoscopic flow of phospholipids. ACS Appl Mater Interfaces 11(31):28449–28460. https://doi.org/10.1021/acsami.9b07547
101. Wilson DL, Martin R, Hong S, Cronin-Golomb M, Mirkin CA, Kaplan DL (2001) Surface organization and nanopatterning of collagen by dip-pen nanolithography. Proc Natl Acad Sci 98(24):13660–13664. https://doi.org/10.1073/pnas.241323198
102. Lee SW, Oh B-K, Sanedrin RG, Salaita K, Fujigaya T, Mirkin CA (2006) Biologically active protein nanoarrays generated using parallel dip-pen nanolithography. Adv Mater 18(9):1133–1136. https://doi.org/10.1002/adma.200600070
103. Senesi AJ, Rozkiewicz DI, Reinhoudt DN, Mirkin CA (2009) Agarose-assisted dip-pen nanolithography of oligonucleotides and proteins. ACS Nano 3(8):2394–2402. https://doi.org/10.1021/nn9005945
104. Salaita K, Wang Y, Fragala J, Vega RA, Liu C, Mirkin CA (2006) Massively parallel dip–pen nanolithography with 55 000-pen two-dimensional arrays. Angew Chem Int Ed 45(43):7220–7223. https://doi.org/10.1002/anie.200603142
105. Huo F, Zheng Z, Zheng G, Giam LR, Zhang H, Mirkin CA (2008) Polymer pen lithography. Science 321(5896):1658–1660. https://doi.org/10.1126/science.1162193
106. Zheng Z, Daniel WL, Giam LR, Huo F, Senesi AJ, Zheng G, Mirkin CA (2009) Multiplexed protein arrays enabled by polymer pen lithography: addressing the inking challenge. Angew Chem Int Ed 48(41): 7626–7629. https://doi.org/10.1002/anie.200902649
107. Zhang J, Chen Y, Brook MA (2013) Facile functionalization of PDMS elastomer surfaces using thiol-ene click chemistry. Langmuir 29(40):12432–12442. https://doi.org/10.1021/la403425d

108. Wipff P-J, Majd H, Acharya C, Buscemi L, Meister J-J, Hinz B (2009) The covalent attachment of adhesion molecules to silicone membranes for cell stretching applications. Biomaterials 30(9):1781–1789. https://doi.org/10.1016/j.biomaterials.2008.12.022
109. Kurkuri MD, Al-Ejeh F, Yan Shi J, Palms D, Prestidge C, Griesser HJ, Brown MP, Thierry B (2011) Plasma functionalized PDMS microfluidic chips: towards point-of-care capture of circulating tumor cells. J Mater Chem 21(24):8841–8848. https://doi.org/10.1039/C1JM10317B
110. Hosford J, Valles M, Krainer FW, Glieder A, Shin Wong L (2018) Parallelized biocatalytic scanning probe lithography for the additive fabrication of conjugated polymer structures. Nanoscale 10(15):7185–7193. https://doi.org/10.1039/C8NR01283K
111. Xu X, Yang Q, Cheung KM, Zhao C, Wattanatorn N, Belling JN, Abendroth JM, Slaughter LS, Mirkin CA, Andrews AM et al (2017) Polymer-pen chemical lift-off lithography. Nano Lett 17(5):3302–3311. https://doi.org/10.1021/acs.nanolett.7b01236
112. Cao HH, Nakatsuka N, Liao W-S, Serino AC, Cheunkar S, Yang H, Weiss PS, Andrews AM (2017) Advancing biocapture substrates via chemical lift-off lithography. Chem Mater 29(16):6829–6839. https://doi.org/10.1021/acs.chemmater.7b01970
113. Chen C-Y, Wang C-M, Li H-H, Chan H-H, Liao W-S (2018) Wafer-scale bioactive substrate patterning by chemical lift-off lithography. Beilstein J Nanotechnol 9(1):311–320. https://doi.org/10.3762/bjnano.9.31
114. Lewis A, Kheifetz Y, Shambrodt E, Radko A, Khatchatryan E, Sukenik C (1999) Fountain pen nanochemistry: atomic force control of chrome etching. Appl Phys Lett 75(17):2689–2691. https://doi.org/10.1063/1.125120
115. Yeshua T, Layani M, Dekhter R, Huebner U, Magdassi S, Lewis A (2018) Micrometer to 15 nm printing of metallic inks with fountain pen nanolithography. Small 14(1):1702324. https://doi.org/10.1002/smll.201702324
116. Ramiya Ramesh Babu HK, Gheber LA (2018) Rapid assaying of miniaturized protein microarray. Sens Actuators B Chem 268:55–60. https://doi.org/10.1016/j.snb.2018.04.074
117. Tsarfati-BarAd I, Sauer U, Preininger C, Gheber LA (2011) Miniaturized protein arrays: model and experiment. Biosens Bioelectron 26(9):3774–3781. https://doi.org/10.1016/j.bios.2011.02.030
118. Tsarfati-BarAd I, Gier K, Sauer U, Gheber LA (2019) An improved approach to use protein A for signal enhancement of miniaturized immunoarrays. Sens Actuators B Chem 284:289–295. https://doi.org/10.1016/j.snb.2018.12.153
119. Taha H, Marks RS, Gheber LA, Rousso I, Newman J, Sukenik C, Lewis A (2003) Protein printing with an atomic force sensing nanofountainpen. Appl Phys Lett 83(5):1041–1043. https://doi.org/10.1063/1.1594844
120. Meister A, Gabi M, Behr P, Studer P, Vörös J, Niedermann P, Bitterli J, Polesel-Maris J, Liley M, Heinzelmann H et al (2009) FluidFM: combining atomic force microscopy and nanofluidics in a universal liquid delivery system for single cell applications and beyond. Nano Lett 9(6):2501–2507. https://doi.org/10.1021/nl901384x
121. Saftics A, Türk B, Sulyok A, Nagy N, Gerecsei T, Szekacs I, Kurunczi S, Horvath R (2019) Biomimetic dextran-based hydrogel layers for cell micropatterning over large areas using the FluidFM BOT technology. Langmuir 35(6):2412–2421. https://doi.org/10.1021/acs.langmuir.8b03249
122. Guillaume-Gentil O, Rey T, Kiefer P, Ibáñez AJ, Steinhoff R, Brönnimann R, Dorwling-Carter L, Zambelli T, Zenobi R, Vorholt JA (2017) Single-cell mass spectrometry of metabolites extracted from live cells by fluidic force microscopy. Anal Chem 89(9):5017–5023. https://doi.org/10.1021/acs.analchem.7b00367
123. Wendel M, Kühn S, Lorenz H, Kotthaus JP, Holland M (1994) Nanolithography with an atomic force microscope for integrated fabrication of quantum electronic devices. Appl Phys Lett 65(14):1775–1777. https://doi.org/10.1063/1.112914
124. Nuraje N, Banerjee IA, MacCuspie RI, Yu L, Matsui H (2004) Biological bottom-up assembly of antibody nanotubes on patterned antigen arrays. J Am Chem Soc 126(26):8088–8089. https://doi.org/10.1021/ja048617u
125. Zhao Z, Matsui H (2007) Accurate immobilization of antibody-functionalized peptide nanotubes on protein-patterned arrays by optimizing their ligand–receptor interactions. Small 3(8):1390–1393. https://doi.org/10.1002/smll.200700006
126. Zhao Z, Banerjee IA, Matsui H (2005) Simultaneous targeted immobilization of anti-human IgG-coated nanotubes and anti-mouse IgG-coated nanotubes on the

complementary antigen-patterned surfaces via biological molecular recognition. J Am Chem Soc 127(25):8930–8931. https://doi.org/10.1021/ja051053p

127. Tutkus M, Rakickas T, Kopustas A, Ivanovaitė Š, Venckus O, Navikas V, Zaremba M, Manakova E, Valiokas R (2019) Fixed DNA molecule arrays for high-throughput single DNA–protein interaction studies. Langmuir 35(17):5921–5930. https://doi.org/10.1021/acs.langmuir.8b03424
128. Shi J, Chen J, Cremer PS (2008) Sub-100 nm patterning of supported bilayers by nanoshaving lithography. J Am Chem Soc 130(9):2718–2719. https://doi.org/10.1021/ja077730s
129. Xu S, Liu G (1997) Nanometer-scale fabrication by simultaneous nanoshaving and molecular self-assembly. Langmuir 13(2):127–129. https://doi.org/10.1021/la962029f
130. Garcia R, Martinez RV, Martinez J (2006) Nano-chemistry and scanning probe nanolithographies. Chem Soc Rev 35(1):29–38. https://doi.org/10.1039/B501599P
131. Bano F, Fruk L, Sanavio B, Glettenberg M, Casalis L, Niemeyer CM, Scoles G (2009) Toward multiprotein nanoarrays using nanografting and DNA directed immobilization of proteins. Nano Lett 9(7):2614–2618. https://doi.org/10.1021/nl9008869
132. Wadu-Mesthrige K, Xu S, Amro NA, Liu G (1999) Fabrication and imaging of nanometer-sized protein patterns. Langmuir 15(25):8580–8583. https://doi.org/10.1021/la991196n
133. Sevenler D, Daaboul GG, Ekiz Kanik F, Ünlü NL, Ünlü MS (2018) Digital microarrays: single-molecule readout with interferometric detection of plasmonic nanorod labels. ACS Nano 12(6):5880–5887. https://doi.org/10.1021/acsnano.8b02036
134. Awasthi S, Hook LM, Swaminathan G, Cairns TM, Brooks B, Smith JS, Ditto NT, Gindy ME, Bett AJ, Espeseth AS et al (2019) Antibody responses to crucial functional epitopes as a novel approach to assess immunogenicity of vaccine adjuvants. Vaccine 37(29):3770–3778. https://doi.org/10.1016/j.vaccine.2019.05.068
135. Ludwig SKJ, Tokarski C, Lang SN, van Ginkel LA, Zhu H, Ozcan A, Nielen MWF (2015) Calling biomarkers in milk using a protein microarray on your smartphone. PLoS One 10(8):e0134360. https://doi.org/10.1371/journal.pone.0134360
136. Li Z, Li Z, Zhao D, Wen F, Jiang J, Xu D (2017) Smartphone-based visualized microarray detection for multiplexed harmful substances in milk. Biosens Bioelectron 87:874–880. https://doi.org/10.1016/j.bios.2016.09.046
137. Guo S, Lin X, Wang Y, Gong X (2019) Fabrication of paper-based enzyme immobilized microarray by 3D-printing technique for screening α-glucosidase inhibitors in mulberry leaves and lotus leaves. Chin Med 14(1):13. https://doi.org/10.1186/s13020-019-0236-y
138. Angenendt P, Glökler J, Konthur Z, Lehrach H, Cahill DJ (2003) 3D protein microarrays: performing multiplex immunoassays on a single chip. Anal Chem 75(17):4368–4372. https://doi.org/10.1021/ac034260l
139. Wu D, Song L, Chen K, Liu F (2012) Modelling and hydrostatic analysis of contact printing microarrays by quill pins. Int J Mech Sci 54(1):206–212. https://doi.org/10.1016/j.ijmecsci.2011.10.010

Chapter 14

Self-Assembling Peptide Hydrogels for 3D Microarrays

Greta Bergamaschi, Alessandro Strada, Roberto Frigerio, Marina Cretich, and Alessandro Gori

Abstract

Recent advances in biosensing analytical platforms have brought relevant outcomes for novel diagnostic and therapy-oriented applications. In this context, hydrogels have emerged as appealing matrices to locally confine biomolecules onto sensing surfaces under solution mimetic conditions, preserving their structural integrity and function. Here, we describe the application of a self-assembling peptide hydrogel as a suitable matrix for 3D microarray bioassays. The hydrogel is printable and self-adhesive and allows for fast analyte diffusion. As a showcase example, we describe its application in a diagnostic immunoassay for the detection of arbovirus infection.

Key words Self-assembly peptide hydrogels, 3D bioassays, Supramolecular nanostructures, Microarrays

1 Introduction

The performances of analytical platforms strictly rely on the functional integrity of molecular bioprobes upon surface immobilization [1–3]. In this sense, different chemical approaches for bioprobe immobilization and complementary surface modification (e.g., polymeric coatings) have been investigated toward the goal of optimal bioprobe surface display [4–8]. In this scenario, hydrogels represent ideal 3D microenvironments to locally entrap biomolecules on analytical surfaces under solution mimetic conditions (Fig. 1). Along with providing a suitable matrix to preserve bioprobe structure and function, additional advantages of these systems include increased loading capacity, decreased nonspecific binding, and an enhanced signal-to-noise ratio [9–11].

An alternative to the classic polymeric and biopolymeric (e.g., polyacrylamide, alginate, agarose, polyethylenglycol) gel matrices [12–14], self-assembling peptide hydrogels have gained widespread interest thanks to their peculiar properties [15–19]. These gels are formed through the establishment of noncovalent interactions

Kelly C. Whittaker and Ruo-Pan Huang (eds.), *Antibody Arrays: Methods and Protocols*, Methods in Molecular Biology, vol. 2237, https://doi.org/10.1007/978-1-0716-1064-0_14,

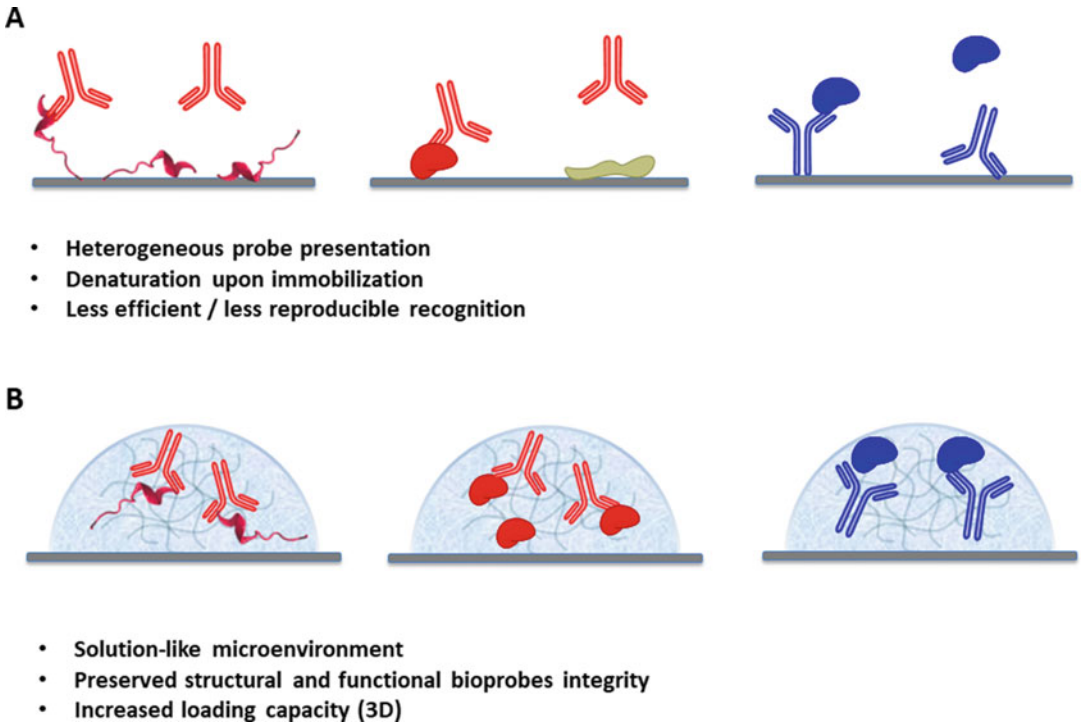

Fig. 1 Graphical representation of surface-bound (panel **a**) vs. hydrogel-confined (panel **b**) bioprobes. While direct surface binding, either by covalent immobilization or adsorption, can result in heterogeneous bioprobe exposure to the analytes or in probe denaturation (panel **a**), hydrogels represent favorable microenvironments where structural and functional features are preserved

between peptide monomers leading to the formation of highly ordered supramolecular structures, which can be easily manipulated to afford virtually unlimited possibilities for material properties design.

Here we describe the use of a self-assembled peptide hydrogel based on the YF-Q11 monomer (Ac-YFQQKFQFQFEQQ-conh2) as a matrix for 3D microarray immunoassays [20] (Fig. 2). Of relevance, thanks to its noncovalent nature, the hydrogel has favorable rheologic properties that make it directly printable with a piezoelectric microarray spotter, therefore avoiding multistep, laborious strategies for chip fabrication. Moreover, the material is self-adhesive onto a variety of surfaces, including silicon and poly(methyl methacrylate) (PMMA) slides, and in selected monomer concentration, the hydrogel is freely permeable to biomolecules. Using this strategy, we developed a bioanalytic microarray platform that enabled us to perform fluorescence immunoassays under solution-like conditions within an ultrashort timeframe (<10 min) and a pM detection limit [20]. In the present chapter, we describe in detail the experimental procedures concerning the synthesis of the YF-Q11 monomer, the hydrogel formation process, and the scheme for microarray immunoassays for the detection of arbovirus infections (Fig. 3).

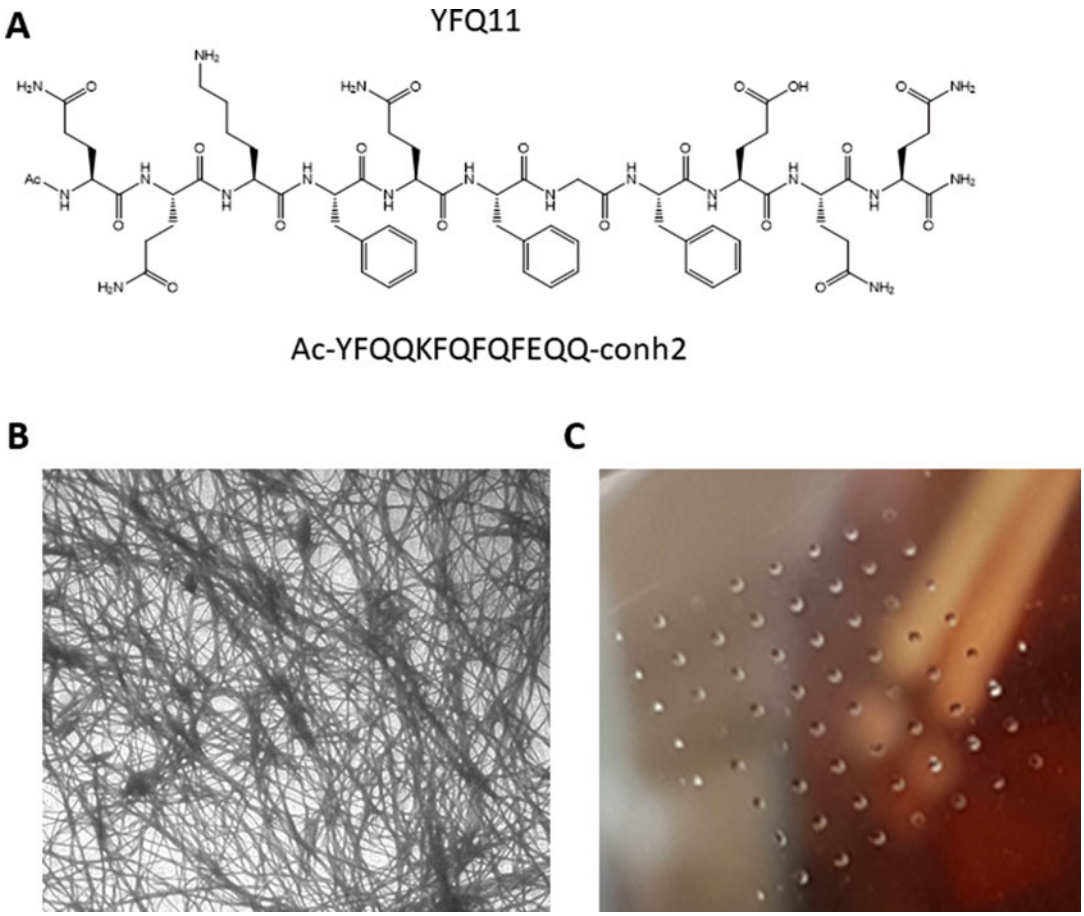

Fig. 2 Full amino acid sequence and structure for self-assembling peptide YFQ11 (panel **a**). TEM image of nanofibrils formed upon YF-Q11 self-assembly (panel **b**). Hydrogel 3D spots (panel **c**). Spots rapidly dry out of a solution environment but promptly rehydrate when immersed in water or a buffer solution

2 Materials

All the organic reagents and solvents, unless stated otherwise, should be of high purity. All solvents for solid-phase peptide synthesis (SPPS) are used without further purification. HPLC grade acetonitrile (ACN) and ultrapure 18.2 Ω water (Millipore-MilliQ) were used for the preparation of all buffers for liquid chromatography. Prepare and store all reagents at room temperature (unless indicated otherwise). Diligently follow all waste disposal regulations when disposing waste materials.

2.1 Peptide Synthesis and Purification: Resin Loading

1. Rink amide resin.
2. *N*-α-Fmoc-L-amino acids.
3. *N,N′*-dimethylformamide (DMF).
4. Dichloromethane (DCM).

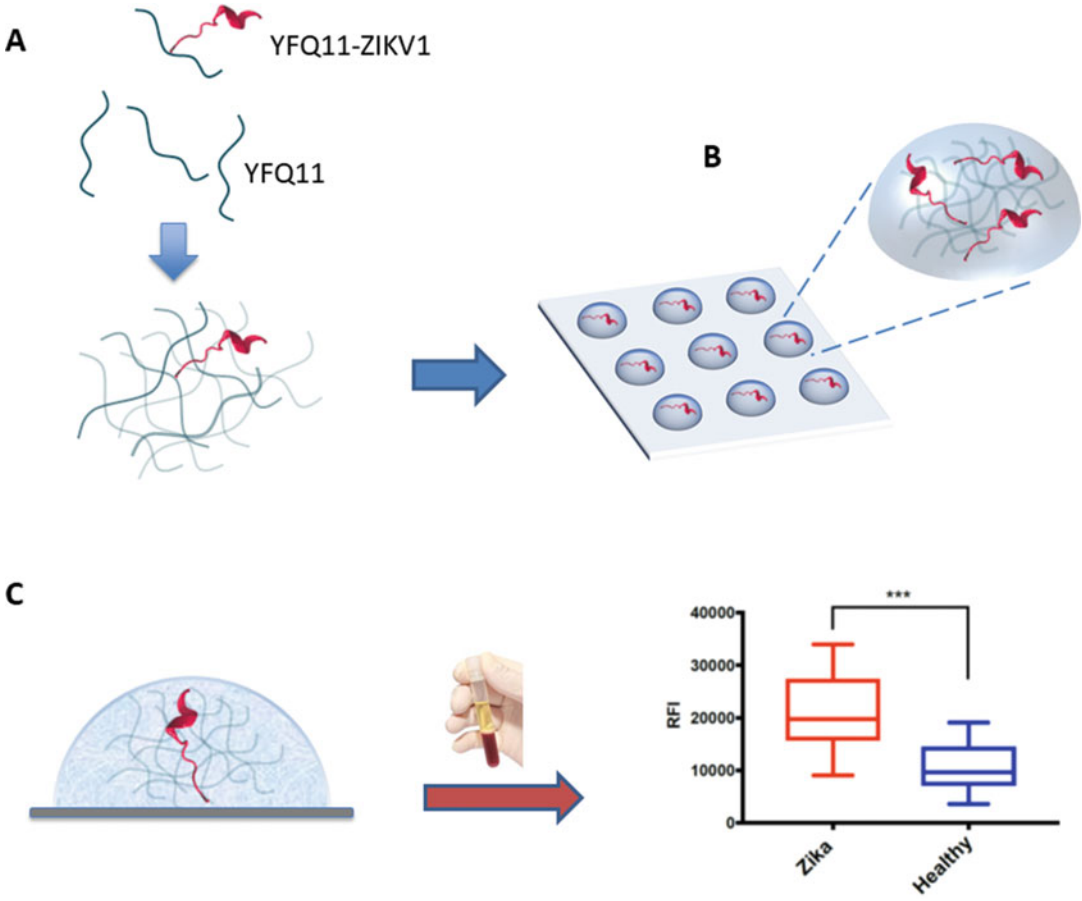

Fig. 3 Overview of hydrogel bioassay strategy. YFQ11 is incubated with YFQ11-ZIKV1 to rapidly self-organize into a soft co-assembled hydrogel (panel **a**). The hydrogel is then deposited onto microarray slides by a noncontact spotting technology to obtain 3D arrays (panel **b**) that are probed with serum samples to distinguish infected individuals and healthy controls (panel **c**)

5. Ethyl cyanoglyoxylate-2-oxime (Oxyma).
6. *N*,*N*′-diisopropylcarbodiimide (DIC).
7. 4-Dimethylaminopyridine (DMAP)
8. *N*-Methyl-2-pyrrolidone (NMP).
9. Hexafluorophosphate benzotriazole tetramethyl uronium (HBTU).
10. *N*,*N*-Diisopropylethylamine (DIEA).
11. Entering Fmoc-amino acid: Fmoc-amino acid, HBTU and DIEA (1:1:2.5 eq. over resin loading) in NMP (4 mL) (*see* **Note 1**).
12. Capping solution: acetic anhydride/DIEA 1/1 in DCM (4 mL) (*see* **Note 2**).
13. Fmoc-deprotection: 20% piperidine solution in DMF (4 mL).

2.2 Peptide Coupling

1. *N*-α-Fmoc-L-amino acids.
2. Ethyl cyanoglyoxylate-2-oxime (Oxyma).
3. *N*,*N*′-diisopropylcarbodiimide (DIC).
4. *N*,*N*′-dimethylformamide (DMF).
5. Coupling solution: Fmoc-amino acid, DIC and Oxyme (1:1:1, 4 eq. over resin loading) (*see* **Note 3**).
6. ALSTRA Initiator+ peptide synthesizer for microwave-assisted, fully automated synthesis (Biotage).

2.3 Cleavage from the Resin

1. Trifluoroacetic acid (TFA).
2. Triisopropylsilane (TIS).
3. Thioanisole.
4. MilliQ water.
5. Cleavage solution: TFA, TIS, water, thioanisole mixture (90:5:2.5:2.5 v/v/v/v) (*see* **Note 4**).

2.4 Work-Up, RP-HPLC Analysis, and Purification

1. MilliQ water.
2. Acetonitrile (ACN).
3. Diethyl ether (*see* **Note 5**).
4. Analytical HPLC system equipped with UV or diode-array detector (Shimadzu).
5. Semipreparative HPLC system equipped with UV detector (Shimadzu).
6. HPLC phase A solution: 97.5% H_2O, 2.5% ACN, 0.7% TFA.
7. HPLC phase B solution: 30% H_2O, 70% ACN, 0.7% TFA.
8. Centrifuge.

2.5 Microarrays

1. Noncontact microarray spotter (sciFLEXARRAYER S12, Scienion).
2. PMMA slides (microfluidic ChipShop GmbH, Jena, Germany).
3. 1% w/v milk powder solution in PBS.
4. Incubation buffer: 0.05 M Tris/HCl, pH 7.6, 0.15 M NaCl, 0.02% v/v Tween 20.
5. Washing buffer: 0.05 M Tris/HCl, pH 9, 0.25 M NaCl, 0.05% v/v Tween 20.
6. Cy3-labeled Goat antihuman IgG.
7. A panel of positive ZIKV serum samples.
8. A panel of human serum samples from healthy donors (*see* **Note 6**).

3 Methods

Peptide sequences to be used in the assay are reported in Table 1 (*see* **Note 7**).

3.1 Peptide Synthesis

1. *Resin loading*. Swell the resin (0.5 mmol/g loading) in NMP/DCM 1/1 mixture (4 mL) for 30 min and then wash with DMF (3 × 3 mL). Add the loading solution of entering Fmoc-amino acid and shake the resin at room temperature (rt) for 4 h. Wash the resin with DMF (2 × 3 mL) and perform the capping step with the acetic anhydride/DIEA in DCM mixture (1 × 3 mL) at rt for 30 min. Then, wash the resin with DMF (2 × 3 mL), CH_2Cl_2 (2 × 3 mL), and then DMF (2 × 3 mL). Perform Fmoc-deprotection with 20% piperidine solution in DMF (4 mL) at rt for 10 min. Wash the resin with DMF (5 × 3 mL) and submit the resin to fully automated iterative peptide assembly (Fmoc-SPPS).
2. *Peptide assembly via iterative fully automated microwave-assisted SPPS*. Assemble peptide sequence by stepwise microwave-assisted Fmoc-SPPS operating in a 0.1 mmol scale. Perform the activation of entering Fmoc-protected amino acids (0.3 M solution in DMF) using 0.5 M Oxyma in DMF/0.5 M DIC in DMF (1:1:1 molar ratio), with a 5 eq. excess over the initial resin loading. Perform the coupling step for 7 min at 75 °C and then wash peptidyl resin with DMF (2 × 3.5 mL). Perform the Fmoc-deprotection step by treatment with a 20% piperidine solution in DMF at rt (1 × 10 mL) and then wash peptidyl resin with DMF (4 × 3.5 mL). Upon complete assembly, wash the resin with DCM (5 × 3.5 mL) and perform the capping of the N-terminal with acetic anhydride/DIEA in DCM mixture (1 × 3 mL) at rt for 30 min (*see* **Note 8**).
3. *Cleavage from the resin*. Treat the resin-bound peptide with an ice-cold TFA cleavage solution. Gently shake the resin for 2 h at room temperature (1 × 4 mL) (*see* **Note 9**).

Table 1
Peptide sequences to be realized for the assay

Code	Sequence
YFQ11	Ac-YFQQKFQFQFEQQ-NH2
YFQ11-N3	Ac-K(N3)-GG-YFQQKFQFQFEQQ-NH2
ZIKV1-Prg	Prg-(O2Oc)2-VNELPHGWKAWGKSYFVRAAKT-COOH
YFQ11-ZIKV1 conjugate	Ac-X-GG-YFQQKFQFQFEQQ-NH2 X-(O2Oc)2-VNELPHGWKAWGKSYFVRAAKT-COOH

4. *Work-up and purification*. Drop the cleavage mixture into ice-cold diethyl ether (40 mL) to precipitate the crude mixture. Collect the crude peptide by centrifugation and wash with further cold diethyl ether to remove scavengers (2 × 40 mL). Remove residual diethyl ether and dry the crude product by a gentle nitrogen flow.
5. *RP-HPLC analysis and purification*. Perform analytical RP-HPLC using a C18 column (5 μm, 4.6 mm i.d. × 150 mm). Elute using a binary gradient of mobile phase A and mobile phase B with the following chromatographic method: 10% B to 100% B in 14 min, flow rate, 1 mL/min. Perform preparative RP-HPLC using C18 column (10 μm, 21.2 mm i.d. × 250 mm) with the following chromatographic method: 30% B to 100% B in 45 min; floe rate, 14 mL/min (*see* **Note 10**). Quantify the collected peptide by UV spectroscopy (280 nm, $\xi = 1.48$) and aliquot in a plastic Eppendorf tube (*see* **Note 11**). Store the peptide fractions at −80 °C and then lyophilize just before use.
6. *Electrospray ionization mass spectrometry (ESI-MS)*. Perform electrospray ionization mass spectrometry (ESI-MS) to check the correct mass for the purified product.
7. *Synthesis of YFQ11 monomer-ZIKV1 epitope conjugate*. Dissolve YFQ11-N3 (1 eq.) in water. Immediately mix the resulting solution with a solution of ZIKV1-Prg (1.1 eq.) and then add $CuSO_4$ (2 eq.) and ascorbic acid (5 eq.). The reaction mixture is let to react under gentle shaking until full reagent conversion is obtained (RP-HPLC monitoring). Upon reaction completion, the conjugation product is isolated by preparative RP-HPLC and lyophilized.

3.2 Hydrogel Formation

1. *Empty control hydrogel*: dissolve freshly lyophilized YF-Q11 aliquots in milliQ water to a 250 μM concentration. Sonicate the resulting solution for 15 min and then dilute to the desired concentration and incubate at 40 °C for 2 h to accelerate gel formation. Freshly prepared hydrogels can be stored at rt and used up to 24 h from preparation.
2. *Bioprobe functionalized hydrogel*: to stably embed immunoreactive peptide epitopes within the hydrogel matrix, dissolve freshly lyophilized YF-Q11 aliquots in milliQ water to 250 μM concentration adding the covalent conjugate of ZKV1-YFQ11 at a 10% ratio in the YF-Q11 hydrogel matrix. Sonicate the resulting solution for 15 min and then dilute to a 25 μM concentration. Incubate at 40 °C for 2 h to accelerate gel formation. Freshly prepared hydrogels can be stored at rt and used up to 24 h from preparation.

3.3 Microarrays: General Procedure

1. PMMA slides are pre-treated with a 1% w/v milk powder solution in PBS for 1 h at room temperature, washed with distilled water and dried under nitrogen stream.
2. YF-Q11 hydrogel is spotted using a noncontact microarray spotter with an 80 μM nozzle; 20 droplets are deposited for each spot (approximately volume 8 nL).
3. Immediately after spotting, all slides are stored for 2 h in a sealed chamber, saturated with sodium chloride.
4. Before use slides are briefly rinsed with water, dried under a nitrogen stream and scanned to evaluate initial fluorescence intensity.
5. *Fluorescence analysis:* scan the dry slides with a TECAN power scanner using the Cy3 (Ex 550 nm; Em 570 nm) and Cy5 (Ex 650 nm; Em 670 nm) wavelengths.
6. Data are analyzed with the aid of the analysis software ScanArray Express from PerkinElmer. The software provides the mean fluorescence intensity of each spot corrected for spot-specific background.

3.4 3D Immunoassay Test

1. Freshly prepare both empty control hydrogel and ZIKV1 functionalized hydrogel.
2. Spot both hydrogels on powder milk-coated PMMA slides (at least 10 different spots each).
3. Store spotted slides into a sealed chamber, saturated with sodium chloride for 2 h.
4. Rinse in water for 1 min.
5. Incubate the slide with serum samples diluted 1:50 in incubation buffer for 5 min.
6. Wash in washing buffer for 2 min under gentle shaking.
7. Dry the slides under a gentle nitrogen stream.
8. Incubate slides for 2 min with 1 μg/mL Cy3-labeled antihuman IgG. secondary antibody in incubation buffer.
9. Wash in PBS for 2 min.
10. Rinse with water.
11. Dry slides under a gentle nitrogen stream.
12. Scan slides for fluorescence evaluation.
13. Laser power and photomultiplier gain are adjusted to avoid saturation of the fluorescence signal.
14. Fluorescence intensity on ZIKV1 functionalized hydrogel spots is quantified using ScanArray Express software from PerkinElmer.

15. Intensity values for replicate spots are averaged, and student unpaired *t*-test over the groups of ZIKV positive individuals and control samples is performed using Prism 7 from GraphPad to determine whether fluorescence intensity differences are statistically significant.

4 Notes

1. Fmoc-amino acid Rink Amide Resin preparation: weigh the entering Fmoc-amino acid at 5 eq. on the synthesis scale (e.g., 0.5 mmol/100 μmol resin scale). Weigh the coupling reagent HBTU at a 1:1 molar ratio with the entering Fmoc-amino acid. Dissolve in 4 mL of DMF. Add DIEA to the solution in a 2:1 molar ratio with the entering Fmoc-amino acid. Add the obtained loading solution to the swollen resin.
2. Prepare a 1/1 molar ratio Ac_2O/DIEA mixture in DCM (4 mL). Add the capping solution to the resin. Perform capping after the loading step and before the Fmoc deprotection.
3. Fmoc-amino acid coupling solution preparation: weigh the entering amino acid at 5 eq. on the synthesis scale (e.g., 0.5 mmol/100 μmol resin scale). Add 0.5 M Oxyme and 0.5 DIC solution in DMF at a 1:1:1 molar ratio with the entering amino acid. Wear a mask when weighing oxyme.
4. Cleavage solution preparation: to an ice-cold TFA solution, add 2.5% of TIS, 2.5% of water, and 2.5% of thioanisole (4 mL for 100/150 μmol resin). Add the prepared solution to the resin to perform final cleavage.
5. Use ice-cold Et_2O in this step.
6. Human sera from healthy donors used obtained from volunteries, which donated blood for transfusion purposes, and their use was permitted for research purposes only.
7. All reported peptide sequences are synthesized according to the same protocol described in Subheading 3.1. Standard amino acids are represented by conventional one letter code. K(N3): azidolysine, Prg: propargylglycine, (O2Oc): 8-amino-3,6-dioxaoctanoic acid, X–X: means triazole-bridge bound sequences.
8. Upon complete assembly, wash the resin with DCM (5 × 3.5 mL) and perform the capping of the terminal amine with acetic anhydride/DIEA in DCM mixture (1 × 3 mL) at rt for 30 min.
9. Wash the resin several times with DCM before the cleavage step to eliminate DMF traces. In order to obtain reproducible

samples, only a small amount of resin should be cleaved and purified. Optimal results can be obtained with treating 50 mg of the final resin-bound peptide.

10. Dissolve the crude product in 6 mL of DMSO. To avoid aggregation processes, add in each HPLC-tube 2 mL of ACN. Collect pure sample fractions every 10 s, in order to maintain a peptide concentration lower than 0.5 mM.
11. To avoid aging processes and the formation of insoluble aggregates, aliquot the pure peptide in 0.1/0.2 μmol fractions at a concentration lower than 0.5 mM. Store aliquots at −80 °C and lyophilize on demand.

Acknowledgments

Fondazione Cariplo and Regione Lombardia, project HYDROGEX are gratefully acknowledged for financial support (grant n. 2018-1720). This work was also partially funded by Project READY (Regione Lombardia, Grant ID 229472).

References

1. Gori A, Longhi R (2016) Chemoselective strategies to peptide and protein bioprobes immobilization on microarray surfaces. Methods Mol Biol (Clifton, N.J.) 1352:145–156
2. Cretich M, Damin F, Chiari M (2014) Protein microarray technology: how far off is routine diagnostics? Analyst 139:528–542
3. Peluso P, Wilson DS, Do D, Tran H, Venkatasubbaiah M, Quincy D, Heidecker B, Poindexter K, Tolani N, Phelan M, Witte K, Jung LS, Wagner P, Nock S (2003) Optimizing antibody immobilization strategies for the construction of protein microarrays. Anal Biochem 312:113–124
4. Chiari M, Cretich M, Damin F, Di Carlo G, Oldani C (2008) Advanced polymers for molecular recognition and sensing at the interface. J Chromatogr B:866, 89–103
5. Gori A, Sola L, Gagni P, Bruni G, Liprino M, Peri C, Colombo G, Cretich M, Chiari M (2016) Screening complex biological samples with peptide microarrays: the favorable impact of probe orientation via chemoselective immobilization strategies on clickable polymeric coatings. Bioconjug Chem 27:2669–2677
6. Gupta N, Lin BF, Campos LM, Dimitriou MD, Hikita ST, Treat ND, Tirrell MV, Clegg DO, Kramer EJ, Hawker CJ (2010) A versatile approach to high-throughput microarrays using thiol-ene chemistry. Nat Chem 2:138–145
7. Nimse SB, Song K, Sonawane MD, Sayyed DR, Kim T (2014) Immobilization techniques for microarray: challenges and applications. Sensors (Basel, Switzerland) 14:22208–22229
8. Gori A, Cretich M, Vanna R, Sola L, Gagni P, Bruni G, Liprino M, Gramatica F, Burastero S, Chiari M (2017) Multiple epitope presentation and surface density control enabled by chemoselective immobilization lead to enhanced performance in IgE-binding fingerprinting on peptide microarrays. Anal Chim Acta 983:189–197
9. Ikeda M, Ochi R, Hamachi I (2010) Supramolecular hydrogel-based protein and chemosensor array. Lab Chip 10:3325
10. Tanase CP, Albulescu R, Neagu M (2011) Application of 3D hydrogel microarrays in molecular diagnostics: advantages and limitations. Expert Rev Mol Diagn 11:461–462
11. Li H, Leulmi RF, Juncker D (2011) Hydrogel droplet microarrays with trapped antibody-functionalized beads for multiplexed protein analysis. Lab Chip 11:528–534
12. Zhang R, Liberski A, Khan F, Diaz-Mochon JJ, Bradley M (2008) Inkjet fabrication of hydrogel microarrays using in situ nanolitre-scale polymerisation. Chem Commun 1317

13. Pla-Roca M, Leulmi RF, Tourekhanova S, Bergeron S, Laforte V, Moreau E, Gosline SJC, Bertos N, Hallett M, Park M, Juncker D (2012) Antibody colocalization microarray: a scalable technology for multiplex protein analysis in complex samples. Mol Cell Proteomics 11:M111.011460–M111.011460
14. Charles PT, Goldman ER, Rangasammy JG, Schauer CL, Chen MS, Taitt CR (2004) Fabrication and characterization of 3D hydrogel microarrays to measure antigenicity and antibody functionality for biosensor applications. Biosens Bioelectron 20:753–764
15. Méndez-Ardoy A, Granja JR, Montenegro J (2018) pH-Triggered self-assembly and hydrogelation of cyclic peptide nanotubes confined in water micro-droplets. Nanoscale Horizons 3:391–396
16. Pizzi A, Pigliacelli C, Gori A, Nonappa N, Ikkala O, Demitri N, Terraneo G, Castelletto V, Hamley IW, Baldelli Bombelli F, Metrangolo P (2017) Halogenation dictates the architecture of amyloid peptide nanostructures. Nanoscale 9:9805–9810
17. Raymond DM, Nilsson BL (2018) Multicomponent peptide assemblies. Chem Soc Rev 47:3659–3720
18. Zhou J, Li J, Du X, Xu B (2017) Supramolecular biofunctional materials. Biomaterials 129:1–27
19. Hendricks MP, Sato K, Palmer LC, Stupp SI (2017) Supramolecular assembly of peptide amphiphiles. Acc Chem Res 50:2440–2448
20. Gagni P, Romanato A, Bergamaschi G, Bettotti P, Vanna R, Piotto C, Morasso CF, Chiari M, Cretich M, Gori A (2019) A self-assembling peptide hydrogel for ultrarapid 3D bioassays. Nanoscale Adv 1:490–497

Chapter 15

Surface Modification of Glass Slides with Aminosilanes for Microarray Use

Chris Stuart

Abstract

Glass serves as the solid support for a variety of array types; however, the chemical nature of glass makes it unsuitable for high-affinity binding to most biomolecules. In this chapter, we describe the activation and surface coating of glass with silane, a wide-ranging group of molecules that can covalently attach to the surface of glass and modify it with a variety of functional groups.

Key words Glass coating, Aminosilane, Silane, Surface modification, Microarray

1 Introduction

There are myriad types of array formats designed to detect just as many targets, including proteins [1], antibodies [2], lectins [3], glycans [4], small molecules [5], and DNA [6]. Despite the variety of detected targets and methods employed, all arrays require a way to spatially differentiate between each target. This is commonly achieved by immobilizing a capture molecule onto a solid surface, which results in a localization of the signal for a given target. In next-generation sequencing, the surface of the flow cell is coated with capture DNA, which captures genomic DNA or cDNA which has been appended with a library index sequence. The captured DNA can then be amplified into a discrete spot on the flow cell. This DNA spot is subsequently amplified using modified dNTPs which give off fluorescent signal when incorporated into the growing complementary DNA strand, which is monitored, and the sequence decoded based on the pattern of fluorescence given off during the amplification [6]. In bead-based arrays, the target is captured onto beads which are then detected either by flowing through a detector one at a time or by settling into microwells which are then imaged, and the targets are identified using bead size, fluorescence, or other methods [7]. Perhaps one of the most

Kelly C. Whittaker and Ruo-Pan Huang (eds.), *Antibody Arrays: Methods and Protocols*, Methods in Molecular Biology, vol. 2237, https://doi.org/10.1007/978-1-0716-1064-0_15,

commonly used arrays is slide-based arrays, where antibodies or proteins are printed onto the surface in a known pattern. The target of interest is then captured and detected, and the identity of the target can be identified by referring to the print map.

Despite the multitude of array options, they all require the capture of a biomolecule onto a solid surface. This can be accomplished very simply in some cases, such as binding antibodies to a polycarbonate or polystyrene using high pH carbonate buffers (as is commonly done in ELISA plate coating). However, plastics are often not an ideal material for array processing. Repeated thermal cycling, such as that experienced during next-generation sequencing, can result in warping and cracking of the array. Plastics also have high autofluorescence, which can decrease the sensitivity of the array. For most planar arrays, including NGS flow cells and many antibody and protein arrays, a glass substrate is the solid support of choice. It is thermally stable, has low auto fluorescence and opacity, and can be modified to work in a variety of assays.

Glass, however, is a term that encompasses a wide variety of materials. In general, and for the purposes of this chapter, glass is a solid structure with a lattice composed of interlocking Si–O–Si bonds. The arrangement of the Si–O–Si, whether randomly distributed and amorphous or ordered in a crystalline pattern, can also impart different physical properties to the glass. When the arrangement of the Si–O–Si bonding is crystalline, the structure is referred to as quartz. Quartz generally has more favorable optical qualities and more consistent surface structure than amorphous glass, but in our testing, the decreased opacity and autofluorescence are not significant enough to justify the increased cost, although in some applications this additional cost maybe justified, such as for atomic force microscopy or total internal reflection fluorescence microscopy [8, 9]. Additives to the glass can also alter its physical properties. Addition of low levels of sodium oxide, calcium oxide, alumina, boron trioxide, boric oxide, barium oxide, germanium dioxide, lead oxide, and others can all alter the refractive index, thermal expansion, opacity, and hardness [10, 11]. The exact assay specifications and requirements will dictate what type of glass is appropriate for the array. Beyond the chemical composition of the glass, the physical characteristics of how the glass was formed also plays a role in the use of the glass for array purposes. Two important characteristics are the amount of particulate and impurities in the glass, which will increase the opacity of the glass, and the surface of the glass where the array will be printed. In general, a smoother more uniform glass surface will result in a more uniform coating, decreasing deviations and background. However, glass in its natural state is generally unreactive to biomolecules such as proteins and DNA, requiring modification of the glass surface to enable its use in arrays.

While poly L-lysine can be coated onto the glass with a simple incubation and enables biomolecule adherence to the glass, the coating is not uniform or easily controlled, which does not lend itself to use in arrays. The primary way to modify the surface of the glass substrate to be used as the solid support in the array is through the use of silane coating [12, 13]. Silanes used for glass coatings are organosilanes which contain a silicon atom bound to up to three alkoxy groups of various lengths and up to three functional groups, with a total of four bonds to the silicon atom (e.g., three alkoxy groups, one functional group). The functional groups available on silanes number in the thousands, along with variations to the number of alkoxy groups and the length of the alkane chain on the silane. The bond between the silicon and alkoxy group of the silane can be hydrolyzed and readily react with free hydroxyls. Hydroxyls can be generated on the surface of glass through a variety of methods, two of the most popular of which are through plasma activation or submersion in "piranha solution," a mixture of concentrated sulfuric acid and hydrogen peroxide. In plasma activation, a high voltage is passed through an evacuated chamber with a low pressure of gas introduced by the operator (this can be oxygen, nitrogen, argon, or even air). The gas becomes ionized by the potential across the chamber resulting in the generation of plasma and free radicals, which can break the Si–O–Si bonds on the surface of the glass, resulting in free Si and OH. Plasma activation can also etch and modify the surface of the glass, depending on the gases used to generate the plasma. When "piranha solution" is used, the mixture of concentrated sulfuric acid and hydrogen peroxide results in the generation of hydronium ion and elemental oxygen. The hydronium ion reacts the Si–O bond of the glass, resulting in Si and OH on the surface. Both methods are also effective in cleaning the surface of the glass, which is also important for even coating of silanes. Regardless if the glass was activated via plasma or piranha solution, the free Si on the surface will readily reform the Si–O bonds with the adjacent OH that was formed during activation, and, because of this, the glass must be introduced to the silanes immediately after activation and should not be stored for later use.

When the silanes are introduced to the free Si on the glass surface, the alkoxy groups of the silane are displaced by the hydroxyl on the glass surface, releasing an alcohol in the process (formed by the alkoxy chain and hydrogen from the hydroxyl). This results in a new covalent bond between the Si of the silane and the oxygen on the glass surface. Because silanes can contain more than a single alkoxy group, multiple bonds can be formed between the silane and the glass. While this can result in a stronger bond between the coating and the glass, silanes with multiple alkoxy

groups can also polymerize and create a non-uniform surface. In this chapter, we will focus on the piranha solution method as this is readily achieved in any lab and does not require special equipment beyond a fume hood and the proper glass ware.

2 Materials

All solutions should be prepared fresh and with reagent grade materials. Follow all waste disposal regulations when disposing of waste.

1. 9″ × 12″ Pyrex dish.
2. Large glass container with at least 5× volume of the piranha solution to be used for collection, storage, and disposal.
3. Glass staining rack, 20 slide capacity recommended, with removable metal handle.
4. 7 4″ × 7″ Pyrex dishes with sufficient height to cover the slides.
5. Glass staining rack for slides, at least 3″ in height.
6. Oven, preheated to 90 °C.
7. 20 75 mm × 25 mm slides (*see* **Note 1**).
8. Fume hood.
9. Glass graduated cylinders.
10. Acetone, 750 mL.
11. Water, 3 L (*see* **Note 2**).
12. Xylene, 1.25 L.
13. Methanol, 1.5 L.
14. Sulfuric acid, 300 mL.
15. 30% hydrogen peroxide, 50 mL.
16. APTES, 1 mL (*see* **Note 3**).

3 Methods

1. All steps should be performed in a fume hood wearing proper PPE. Place 1 of the 4″ × 7″ Pyrex dishes in the 9″ × 12″ Pyrex container to serve as a secondary containment for the piranha solution. The 4″ × 7″ dish will be used to prepare the piranha solution and activate the slides (*see* **Note 4**).
2. Into another of the 4″ × 7″ Pyrex dishes, pour 500 mL of water and cover. This will be used to rinse the residual piranha solution off of the slides.

3. Into another of the 4″ × 7″ Pyrex dishes, place 500 mL of methanol and cover.
4. Into another of the 4″ × 7″ Pyrex dishes, pour 250 mL of acetone and 250 mL of xylene, mix and cover.
5. Into another of the 4″ × 7″ Pyrex dishes, pour 500 mL of xylene and cover.
6. Into another of the 4″ × 7″ Pyrex dishes, pour 500 mL of xylene and 1 mL of APTES, mix and cover.
7. Into another of the 4″ × 7″ Pyrex dishes, pour 500 mL of acetone and cover.
8. Load 20 slides into each of the slots of the staining rack holder (*see* **Note 5**) taking care that none of the slides are leaning onto each other as this will result in liquids being trapped and reducing the quality of the final coating.
9. Pour 300 mL of sulfuric acid into the 4″ × 7″ Pyrex dish inside the secondary glass container (*see* **step 1**), slowly to avoid splashing. Then add 50 mL of 30% hydrogen peroxide to the acid to generate the piranha solution (*see* **Note 6**).
10. Carefully lower the slides into the piranha solution made in **step 9**. Remove the metal handle from the glass staining rack. The introduction of the slides into the solution will result in additional gas evolution.
11. Allow the slides to incubate for 30 min.
12. After incubation, remove the slides from the piranha solution, allowing them to drain before transferring to the Pyrex dish with water. Dip the slides up and down in the water ten times to wash. Then pour the water out and refill with 500 mL of fresh water. Repeat this process four times to ensure complete removal of the acid from the slides.
13. Transfer the slides from the water dish the dish containing methanol and dip the slides ten times. Dispose of the methanol and add 500 mL of fresh methanol into the dish and repeat the dipping. Dispose of the methanol in the dish, add the final 500 mL of methanol, and repeat the dipping.
14. Transfer the slides to the Pyrex dish containing the acetone/xylene mixture. Submerge the slides into the solution and remove them slowly and then immediately place them in the dish containing only xylene.
15. Dip the slides five times in and out of the xylene.
16. Transfer the slides to the Pyrex dish containing the xylene/APTES mixture and dip up and down five times.
17. Drain the slides until most of the xylene/APTES mixture has been removed.

18. Transfer the slides to the Pyrex dish containing acetone, dip up and down five times, and then on the final time the slides are removed from the acetone, remove them very slowly (*see* **Note 7**).
19. Once the slides have been removed, place them in the pre-heated oven for 30 min to cure.
20. Once cured, the slides can be stored at room temperature until needed.
21. Allow the piranha solution to cool to room temperature, at least 1 h, before transferring to the large glass container for collection. The solution is highly acidic and should be discarded in compliance with your organization's procedures and local law.

4 Notes

1. This protocol also uses 75 mm × 25 mm × 1 mm slides as the substrate for modification, although other glass or quartz substrates may be used as well.
2. Water used for washing should be deionized and filtered with at least a 22 μm filter prior to use.
3. The procedure presented here utilizes APTES, a common aminosilane which can be used to bind proteins onto the surface of the array; however, other silanes could be substituted for altered functionalization on the glass surface with minimal alterations to the protocol.
4. Caution should be taken whenever working with piranha solution as the mixture of the two components is highly exothermic, evolves gas, and will quickly react with most organic compounds, including plastics, and can corrode metals quickly. Because of this, whenever piranha solution is generated, it should be done so under a fume hood with proper PPE (gloves, lab coat, face shield, or goggles), using only glassware rated for high-temperature use, such as Pyrex containers. Most chambers used for histological staining will break under the thermal shock and are not advised to be used.
5. Take care that none of the slides are leaning onto each other when placed in the glass staining rack, as this will result in liquids being trapped and reducing the quality of the final coating.
6. The mixture will be highly exothermic and evolve gas. Use caution and wear proper PPE whenever piranha solution is used.

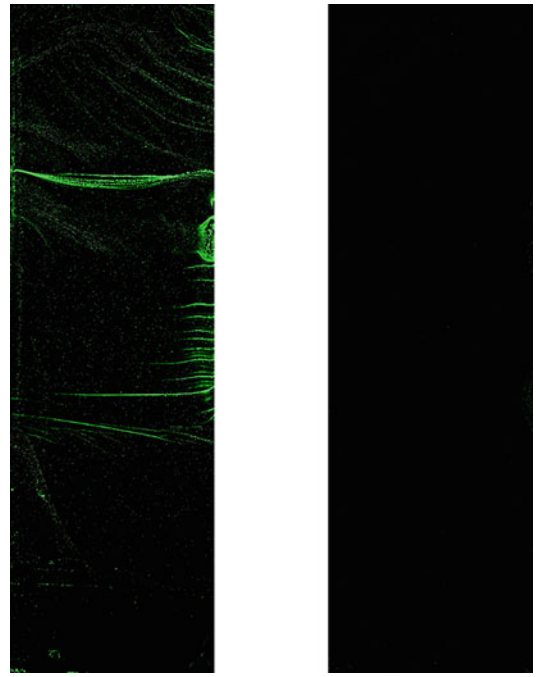

Fig. 1 Demonstrates the high fluorescent background caused by removing slides too quickly from acetone (left) vs. the background when removed slowly so that no acetone is left on the slide (right)

7. If the slides are removed slowly enough, no acetone should be left on the slides as they are pulled out of the acetone. If acetone is left on the slide after it has been removed, any impurities in the acetone can be deposited onto the slide and result in high fluorescent background (Fig. 1).

References

1. Sutandy F, Reymond X et al (2013) Overview of protein microarrays. Curr Protoc Prot Sci Chapter 27:Unit 27.1. https://doi.org/10.1002/0471140864.ps2701s72
2. Weisheng B et al (2019) Discovering endometriosis biomarkers with multiplex cytokine arrays. Clin Proteomics 16:28. https://doi.org/10.1186/s12014-019-9248-y
3. Benachour H et al (2018) Vitronectin (Vn) glycosylation patterned by lectin affinity assays—a potent glycoproteomic tool to discriminate plasma Vn from cancer ascites Vn. J Mol Recognit 31(5):e2690. https://doi.org/10.1002/jmr.2690
4. McCombs JE et al (2016) Glycan specificity of neuraminidases determined in microarray format. Carbohydr Res 428:31–40. https://doi.org/10.1016/j.carres.2016.04.003
5. Bradner JE et al (2006) A robust small-molecule microarray platform for screening cell lysates. Chem Biol 13(5):493–504. https://doi.org/10.1016/j.chembiol.2006.03.004
6. Bumgarner R (2013) DNA microarrays: types, applications and their future. In: Ausubel FM et al (eds) Current protocols in molecular biology, vol 22. Wiley, New York, p Unit 22.1. https://doi.org/10.1002/0471142727.mb2201s101
7. Elshal MF, McCoy JP (2006) Multiplex bead array assays: performance evaluation and comparison of sensitivity to ELISA. Methods 38(4):317–323. https://doi.org/10.1016/j.ymeth.2005.11.010
8. Anderson MS (2000) Locally enhanced Raman spectroscopy with an atomic force microscope.

Appl Phys Lett 76(21):3130–3132. https://doi.org/10.1063/1.126546

9. Ban T, Goto Y (2006) Direct observation of amyloid growth monitored by total internal reflection fluorescence microscopy. In: Methods in enzymology, vol 413. Academic Press, New York, pp 91–102. https://doi.org/10.1016/S0076-6879(06)13005-0
10. Wu Y-Q et al (2002) Effect of glass additives on the strength and toughness of polycrystalline alumina. J Eur Ceram Soc 22(2):159–164. https://doi.org/10.1016/S0955-2219(01)00253-9
11. Fujimoto Y et al (2007) Effect of GeO2 additive on fluorescence intensity enhancement in bismuth-doped silica glass. J Mater Res 22(3):565–568. https://doi.org/10.1557/jmr.2007.0073
12. Curran JM et al (2005) Controlling the phenotype and function of mesenchymal stem cells in vitro by adhesion to silane-modified clean glass surfaces. Biomaterials 26(34):7057–7067. https://doi.org/10.1016/j.biomaterials.2005.05.008
13. Rogers Y-H et al (1999) Immobilization of oligonucleotides onto a glass support via disulfide bonds: a method for preparation of DNA microarrays. Anal Biochem 266(1):23–30. https://doi.org/10.1006/abio.1998.2857

Chapter 16

Dried Blood-Based Protein Profiling Using Antibody Arrays

Kelly C. Whittaker, Ying Qing Mao, Siwei Zhu, Zhiqiang Lv, and Ruo-Pan Huang

Abstract

Dried blood samples have been increasingly considered for clinical applications in recent years. The main disadvantages that limit DBS utility in clinical applications are the small sample volume collected, area bias and homogeneity issues, and sample preparation requirements for the necessary sensitivity and reproducibility required for clinical assessment. The recent advances in antibody array technology overcome the common disadvantages of immunoassay approaches by increasing the multiplex capabilities and decreasing the sample volume requirements as well as minimizing the expense and technical expertise required with many alternative high-density approaches like mass spectrometry.

Key words Dried blood sample, Antibody array, Proteomics, Protein detection, Method protocol

1 Introduction

Dried blood sample (DBS) collection involves collecting capillary blood through a simple finger prick and applying it to filter paper. It was originally developed over 50 years ago for newborn screening but has expanded into many other clinical arenas including infection diagnosis [1, 2], clinical pharmacology [2], toxico- and pharmacokinetic studies [3], forensic toxicology [4], drug development and monitoring [5], metabolic profiling [1], environmental control and epidemiological disease surveillance [1, 6], etc. In particular, protein profiling and the quantitative analysis of proteins have been an increasingly popular focus for clinical diagnostics. Proteins perform most biological functions; thus, their measurement can inform not only on the normal functioning but also the malfunctioning of proteins that cause disease and can be used for disease diagnosis, assessment of disease risk, and monitoring of disease progression and therapeutic effectiveness. Single-target immunoassays like ELISAs were traditionally used to analyze protein expression in DBSs for clinical application [7–11]. However, the need for

Kelly C. Whittaker and Ruo-Pan Huang (eds.), *Antibody Arrays: Methods and Protocols*, Methods in Molecular Biology, vol. 2237, https://doi.org/10.1007/978-1-0716-1064-0_16,

analysis of multiple proteins has increased the application of multiplex technologies like mass spectrometry and antibody arrays.

The main disadvantages that limit DBS utility in clinical applications are the small sample volume collected as well as the area bias and homogeneity issues. The development of volumetric blood collection devices can overcome some of these issues. The next challenge for analyzing proteins from DBSs focused on preparing the samples and eluting the proteins to be able to obtain sufficiently sensitive and reliable results. Mass spectrometry approaches are robust, are mostly sensitive, have high multiplexing capabilities, and can be readily automated, all advantages that made it the prevailing technology for protein profiling of DBS in clinical applications for many years. However, many methods for using DBSs for clinical purposes were up to 20 times less sensitive than conventional immunoassay approaches [12] likely because of the limits in sample volume [13]. The limitations of high cost and required technical expertise, as well as the aforementioned sample requirements, sparked interest in antibody array approaches in recent years due to the technical advances in multiplexing, dynamic range, and high-throughput capabilities on this platform.

Considerable technological advances in proteomic analysis in recent years, specifically in quantitative immunoassay approaches, have enabled cost-effective assays with precise, high-throughput capabilities. While the majority of these assays have been designed for use in serum or plasma [14], a few have been validated for DBSs. Martin et al. validated the use of an enzyme-linked immunosorbent assay (ELISA) to quantify adiponectin in a large-scale multicenter trial [7, 8]. Commercially available ELISAs have also been evaluated and optimized for the detection of various proteins in DBSs, including CRP [9, 10], alpha 1-acid glycoprotein [10], IgA [11], HCV antibodies [15], biologic exenatide [16], and an anti-CD20 monoclonal antibody drug [17]. Recent studies have also validated multiplex immunoassay approaches with DBSs, further increasing their utility for clinical applications by expanding the breadth of analytes detected. Bead-based multiplex protein arrays [18–21], reverse-phase peptide arrays [22], and planar antibody arrays [23] have been similarly utilized. In this chapter, we will describe collection of a DBS using a volumetric sampling device, the extraction and processing procedures of this sample, and the quantification of proteins using an antibody array.

2 Materials

2.1 Blood Collection and Preparation

1. Alcohol swab.
2. Lancet: 1.5 mm blade.
3. Biohazard bag.

4. Desiccant.
5. Volumetric blood collection device (PanoHealth) (*see* **Note 1**).
6. Protease inhibitor cocktail.
7. 1× PBS: 1000 mL distilled water, 8 g of NaCl, 0.2 g of KCl, 1.44 g of Na_2HPO_4, 0.24 g of KH_2PO_4, pH 7.4.
8. Elution buffer: 10 mL of 1× PBS, 10 μL of Tween-20, protease inhibitor cocktail resuspended per manufacturer's instructions into the above volume.
9. Microcentrifuge tubes: clear and black.
10. Oscillating shaker.
11. Vortex.

2.2 Antibody Array Analysis

1. Antibody array (*see* **Note 2**).
2. Cytokine Antigen Mix: mix corresponding antigens to the antibodies printed on the antibody array in 1 mL of Cy3 Buffer (*see* **Note 3**).
3. Detection Antibody Mix: biotin-conjugated antibodies to the corresponding antibodies printed on the antibody array in 1 mL of Cy3 Buffer (*see* **Note 4**).
4. Distilled water (dH_2O).
5. Sample Diluent: 5 g of BSA, 1000 mL of 1× PBS. Stir slowly to dissolve completely.
6. 20× Wash Buffer I: 20 mL of Tween-20, 1 L of 20× Wash Buffer II.
7. 20× Wash Buffer II: 100 mL of 2 M Tris–HCl, pH 7.5, 600 mL of 5 M NaCl, 300 mL of dH_2O.
8. Cy3 Buffer: 10 mg of BSA, 10 mL of 1× PBS.
9. Cy3-Conjugated Streptavidin: 10 μL Cy3-Conjugated Streptavidin (1 mg/mL), 97 μL of Cy3 Buffer in a black microcentrifuge tube.
10. Laser microarray scanner.

3 Methods

3.1 DBS Collection

1. Clean finger with an alcohol swab and puncture the finger with a lancet.
2. Create a large drop of blood. Then, touch the blood collection device to the blood drop and allow blood to fill the device completely (*see* **Note 5**).
3. Set aside to dry for 2 h at room temperature.

4. Store samples at −20 °C sealed in a biohazard bag with a desiccant pack until proceeding to Subheading 3.2 (*see* **Note 6**).

3.2 DBS Preparation

1. Cut off the 10 mm × 5 mm filled strip of the blood collection device and place in a microcentrifuge tube using forceps cleaned with alcohol.
2. Add 250 μL of elution buffer to the microcentrifuge tube with the cut, filled strip. Incubate for 4 h at room temperature on an oscillating shaker, vortexing for 10 s every 30 min.
3. Transfer the liquid to a clean microcentrifuge tube leaving the filter paper behind.
4. Centrifuge at 16 × *g* for 10 min.
5. Collect the supernatant into a clean microcentrifuge tube (*see* **Note 7**).

3.3 Antibody Array Analysis

1. Dilute the DBS eluate 20-fold in elution buffer (*see* **Note 8**).
2. Add 10 μL of Cytokine Antigen Mix to 500 μL of Sample Diluent. Reconstitute at room temperature for 15–30 min with gentle agitation. Label as Standard 1 (*see* **Note 9**).
3. Label another six microcentrifuge tubes Standard 2–Standard 7. Add 200 μL of Sample Diluent to each tube.
4. Add 100 μL of Standard 1 into the tube labeled Standard 2 and mix gently. Perform five more serial dilutions by adding 100 μL of Standard 2 to the tube labeled Standard 3 and so on.
5. Add 100 μL of Sample Diluent to another tube and label that as Negative Control.
6. Add 100 μL of Sample Diluent to the antibody array and incubate at room temperature for 30 min to block the array.
7. Decant the Sample Diluent and add 100 μL of Standards 1–7, Negative Control, and diluted eluate on the array in the corresponding wells. Incubate overnight at 4 °C on an oscillating shaker.
8. Add 50 mL of 20× Wash Buffer I to 950 mL dH_2O to make 1× Wash Buffer I.
9. Decant the Samples and Standards and wash five times, 5 min each, with 150 μL of 1× Wash Buffer I in each well at room temperature on an oscillating shaker. Ensure complete removal of the wash buffer at every wash.
10. Add 50 mL of 20× Wash Buffer II to 950 mL dH_2O to make 1× Wash Buffer II.
11. Decant the Wash Buffer I and wash two times, 5 min each, with 150 μL of 1× Wash Buffer II in each well at room temperature

on an oscillating shaker. Ensure complete removal of the wash buffer at every wash.

12. Add 1.4 mL of Sample Diluent to the Detection Antibody Mix. Spin briefly.
13. Add 80 μL of the diluted Detection Antibody Mix to each well. Incubate at room temperature for 90 min (*see* **Note 10**).
14. Decant the Detection Antibody Mix and wash according to **steps 9** and **11**.
15. Add 1.4 mL of Cy3 Buffer to 5 μL of Cy3-Conjugated Streptavidin in a black microcentrifuge tube and mix gently.
16. Add 80 μL of the diluted Cy3-Conjugated Streptavidin to each well. Cover from light and incubate at room temperature for 1 h.
17. Decant the Cy3-Conjugated Streptavidin and wash five times, 5 min each, with 150 μL of 1× Wash Buffer I at room temperature on an oscillating shaker. Ensure complete removal of the wash buffer at every wash.
18. Decant the Wash Buffer I and immerse the entire antibody array slide in another 30 mL of 1× Wash Buffer I. Gently shake at room temperature for 15 min.
19. Decant the Wash Buffer I and add 30 mL of 1× Wash Buffer II and gently shake at room temperature for 5 min (*see* **Note 11**).
20. Decant the 1× Wash Buffer II and dry the array slide completely with a compressed N_2 stream.
21. Scan the array using a laser microarray scanner with a Cy3 wavelength (excitation, 555 nm; emission, 565 nm; resolution, 10 μm) (*see* **Note 12**).
22. Data extraction can be done with most microarray analysis software. A linear curve is recommended for low-abundant proteins, while a log-log curve is recommended for medium- to high-abundant proteins.

4 Notes

1. There are several volumetric sampling devices commercially available, PanoHealth, Neoteryx, etc., that can collect varying amounts. Collect the total final volume of blood needed for the downstream assays.
2. There are a number of antibody arrays available commercially that can be used with the DBS eluate prepared in Subheading 3.2. The array used here is a quantitative, glass-based array. Sample and buffer volume requirements if using a different array will need to be adjusted.

3. The amount of each antigen should be optimized such that the dynamic range of detection for all proteins included in the array should be suitable for a single sample dilution. Cross-reactivity with all antibodies and other antigens should also be tested for.
4. The detection antibodies used need to be appropriately paired to the array printed antibodies and checked for cross-reactivity to the panel.
5. Each volumetric sampling device will be slightly different, please follow the manufacturer's instructions to ensure a complete and proper collection.
6. Fresh samples after drying can be immediately processed. If not immediately processed, they should be stored at −20 °C.
7. Eluted samples should be stored at 4 °C for no more than 1 day. Any unused eluted samples should be aliquoted, labeled, and stored at −80 °C.
8. The optimal sample dilution of the eluate to run on the antibody array can vary. The background signals across the array, the amount of protein expression retained as the eluate dilution increases, and the total sample volume restriction, which would make quantification of a large number of proteins untenable at low eluate dilutions, should all be considered when determining the optimal eluate dilution to run on the antibody array.
9. Complete reconstitution of the lyophilized standard is critical for accurate protein concentration quantification. Be sure to spin down the Cytokine Antigen Mix to ensure the entire contents are reconstituted. After adding 500 μL of Sample Diluent to the tube, avoid vigorous vortexing to prevent protein denaturation. Reconstitute the Cytokine Antigen Mix within 1 h of usage.
10. Longer incubation times with the detection antibody will result in higher signals; however, the background noise will also increase. A 90-min incubation with the detection antibody is optimal and longer than 2 h will cause too high background signals.
11. The large bulk washes are necessary to remove any possible remaining dye. It can also help lower the nonspecific signals of the sample. A longer incubation of Wash Buffer I will lower the background. However, an incubation of more than 2 h can also remove true signals.
12. The signal intensity for different cytokines can differ greatly in the same array; in such cases, multiple scans are recommended, with a higher PMT for low-signal cytokines and a low PMT for high-signal cytokines.

References

1. Demirev PA (2013) Dried blood spots: analysis and applications. Anal Chem 85(2):779–789. https://doi.org/10.1021/ac303205m
2. Snijdewind IJ, van Kampen JJ, Fraaij PL, van der Ende ME, Osterhaus AD, Gruters RA (2012) Current and future applications of dried blood spots in viral disease management. Antivir Res 93(3):309–321. https://doi.org/10.1016/j.antiviral.2011.12.011
3. Barfield M, Spooner N, Lad R, Parry S, Fowles S (2008) Application of dried blood spots combined with HPLC-MS/MS for the quantification of acetaminophen in toxicokinetic studies. J Chromatogr B Anal Technol Biomed Life Sci 870(1):32–37. https://doi.org/10.1016/j.jchromb.2008.05.025
4. Versace F, Déglon J, Lauer E, Mangin P, Staub C (2013) Automated DBS extraction prior to HILIC/RP LC–MS/MS target screening of drugs. Chromatographia 76(19–20): 1281–1293
5. Xu Y, Woolf EJ, Agrawal NG, Kothare P, Pucci V, Bateman KP (2013) Merck's perspective on the implementation of dried blood spot technology in clinical drug development—why, when and how. Bioanalysis 5(3):341–350. https://doi.org/10.4155/bio.12.321
6. Downs JA, Corstjens PL, Mngara J, Lutonja P, Isingo R, Urassa M, Kornelis D, van Dam GJ (2015) Correlation of serum and dried blood spot results for quantitation of Schistosoma circulating anodic antigen: a proof of principle. Acta Trop 150:59–63. https://doi.org/10.1016/j.actatropica.2015.06.026
7. Kramer MS, Chalmers B, Hodnett ED, Sevkovskaya Z, Dzikovich I, Shapiro S, Collet JP, Vanilovich I, Mezen I, Ducruet T, Shishko G, Zubovich V, Mknuik D, Gluchanina E, Dombrovskiy V, Ustinovitch A, Kot T, Bogdanovich N, Ovchinikova L, Helsing E, PROBIT Study Group (Promotion of Breastfeeding Intervention Trial) (2001) Promotion of Breastfeeding Intervention Trial (PROBIT): a randomized trial in the Republic of Belarus. JAMA 285(4):413–420
8. Martin RM, Patel R, Oken E, Thompson J, Zinovik A, Kramer MS, Vilchuck K, Bogdanovich N, Sergeichick N, Foo Y, Gusina N (2013) Filter paper blood spot enzyme linked immunoassay for adiponectin and application in the evaluation of determinants of child insulin sensitivity. PLoS One 8(8): 24–26. https://doi.org/10.1371/journal.pone.0071315
9. Brindle E, Fujita M, Shofer J, O'Connor KA (2010) Serum, plasma, and dried blood spot high-sensitivity C-reactive protein enzyme immunoassay for population research. J Immunol Methods 362(1-2):112–120
10. Wander K, Brindle E, O'Connor KA (2012) Sensitivity and specificity of C-reactive protein and α(1)-acid glycoprotein for episodes of acute infection among children in Kilimanjaro, Tanzania. Am J Hum Biol 24(4):565–568
11. Borte S, Janzi M, Pan-Hammarström Q, von Döbeln U, Nordvall L, Winiarski J, Fasth A, Hammarström L (2012) Placental transfer of maternally-derived IgA precludes the use of guthrie card eluates as a screening tool for primary immunodeficiency diseases. PLoS One 7(8):e43419
12. Kehler J, Akella N, Citerone D, Szapacs M (2011) Application of DBS for the quantitative assessment of a protein biologic using on-card digestion LC-MS/MS or immunoassay. Bioanalysis 3:2283–2290
13. Leuenberger N, Saugy J, Mortensen RB, Schatz PJ, Giraud S, Saugy M (2011) Methods for detection and confirmation of hematide/peginesatide in anti-doping samples. Forensic Sci Int 213(9):15
14. McDade TW, Williams S, Snodgrass JJ (2007) What a drop can do: dried blood spots as a minimally invasive. Demography 44(4): 899–925. https://doi.org/10.1353/dem.2007.0038
15. Marques BLC, Brandão CU, Silva EF, Marques VA, Villela-Nogueira CA, Do Ó KMR, de Paula MT, Lewis-Ximenez LL, Lampe E, Villar LM (2012) Dried blood spot samples: Optimization of commercial EIAs for hepatitis C antibody detection and stability under different storage conditions. J Med Virol 84:1600–1607
16. Lin YQ, Khetarpal R, Zhang Y, Song H, Li SS (2011) Combination of ELISA and dried blood spot technique for the quantification of large molecules using exenatide as a model. J Pharmacol Toxicol Methods 64(2):124–128
17. Lin YQ, Zhang Y, Li C, Li L, Zhang K, Li S (2012) Evaluation of dry blood spot technique for quantification of an Anti-CD20 monoclonal antibody drug in human blood samples. J Pharmacol Toxicol Methods 65(1):44–48
18. Chase BA, Johnston SA, Legutki JB (2012) Evaluation of biological sample preparation for immunosignature-based diagnostics. Clin Vaccine Immunol 19(3):352–358

19. Kofoed K, Schneider UV, Scheel T, Andersen O, Eugen-Olsen J (2006) Development and validation of a multiplex add-on assay for sepsis biomarkers using xMAP technology. Clin Chem 52(7):1284–1293
20. Skogstrand K, Ekelund CK, Thorsen P, Vogel I, Jacobsson B, Nørgaard-Pedersen B, Hougaard DM (2008) Effects of blood sample handling procedures on measurable inflammatory markers in plasma, serum and dried blood spot samples. J Immunol Methods 336(1): 78–84
21. Skogstrand K, Thorsen P, Nørgaard-Pedersen B, Schendel DE, Sørensen LC, Hougaard DM (2005) Simultaneous measurement of 25 inflammatory markers and neurotrophins in neonatal dried blood spots by immunoassay with xMAP technology. Clin Chem 51(10): 1854–1866
22. Faucher S, Martel A, Sherring A, Ding T, Malloch L, Kim JE, Bergeron M, Sandstrom P, Mandy FF (2004) Protein bead array for the detection of HIV-1 antibodies from fresh plasma and dried-blood-spot specimens. Clin Chem 50(7):1250–1253
23. Jiang W, Mao YQ, Huang R, Duan C, Xi Y, Yang K, Huang RP (2014) Protein expression profiling by antibody array analysis with use of dried blood spot samples on filter paper. J Immunol Methods 403(1–2):79–86

Chapter 17

Profiling Glycoproteins on Functionalized Reverse Phase Protein Array

Ying Zhang, Liyuan Zhang, Anton Iliuk, and W. Andy Tao

Abstract

Reverse phase protein array (RPPA), a high-throughput, parallel immunoassay in a dot-blot format, is a powerful tool to quantitatively profile protein expression in multiple samples simultaneously using small amounts of material. Despite its success, analysis of post-translationally modified (PTM) proteins has been limited in RPPA assays, primarily due to relatively low availability of antibodies specific to proteins of PTMs, e.g., glycosylation. Moreover, the high matrix complexity, with tens of thousands of proteins in cell lysates or tissue extracts and the low abundance of proteins with PTMs, makes it extremely challenging to detect these proteins with PTMs. Therefore, there is an urgent need to fill this gap, which would greatly contribute to the analysis of a specific PTM by RPPA. In this chapter, we introduce a novel RPPA platform, termed polymer-based reverse phase glycoprotein array (polyGPA), to measure the variation of glycosylation patterns on a three-dimensionally functionalized RPPA. Without the need of specific antibody towards glycosylation, polyGPA represents a highly sensitive strategy to analyze protein glycosylation in multiple complex biological samples in parallel.

Key words Reverse phase protein array, Post-translational modification (PTM), Antibody, Glycosylation, Dendrimer

1 Introduction

The reverse phase protein array (RPPA) approach has been employed as a high-throughput technique to visually profile and assess the relative expression of proteins in biological samples for protein validation, biomarker discovery, and cancer diagnostics [1–4]. In a typical RPPA analysis, the microarray elements are comprised of a mixture of proteins from complex biological samples (in the form of cellular or whole tissue extract) which are then probed with specific antibodies for quantitative analysis of target proteins. In this format, RPPAs enable highly parallel profiling of target proteins from multiple samples. Moreover, due to the low

Ying Zhang and Liyuan Zhang contributed equally to this work.

Kelly C. Whittaker and Ruo-Pan Huang (eds.), *Antibody Arrays: Methods and Protocols*, Methods in Molecular Biology, vol. 2237, https://doi.org/10.1007/978-1-0716-1064-0_17,

sample volume requirement (sub-nL level), RPPAs show great advantage in the analysis of clinical samples. Glycosylation, one of the most structurally complex forms of post-translational modifications (PTMs), acts as an essential regulator in a wide variety of fundamental molecular and cell biology processes [5, 6]. Aberrant glycosylation has been highlighted in the development and progression of many diseases through cell signaling and communication, cell dissociation and invasion, cell immune modulation, and metastasis formation [6–8]. Most of the FDA-approved clinical cancer biomarkers are glycoproteins [9]. In addition, targeting the analysis of glycosylation patterns in early cancer detection may improve the detection sensitivity and specificity and thereby increase the overall survival rate [10–12]. However, the main obstacle remaining to be addressed prior to the routine application of RPPA in glycosylation analysis is the lack of glyco-specific antibodies. With most antibodies being glycosylated, there are technical challenges in developing high-quality glyco-specific antibodies. Furthermore, the requirement for the specificity of antibodies used in RPPA is much higher than in other immunoassays. To date, glyco-specific antibodies that can be used for RPPA are still not readily available. Recently, we introduced a novel RPPA platform, termed polymer-based reverse phase glycoprotein array (polyGPA) [3], to investigate the variation of glycosylation patterns with high sensitivity and selectivity without the requirement of glyco-specific antibodies (Fig. 1). First, multiple hydroxylamine groups are grafted on the surface of the branched dendrimer, polyamidoamine generation 4 (PAMAM G4). Second, the synthesized hydroxyamino-functionalized dendrimer (ONH_2-dendrimer) is coated on a nitrocellulose membrane to generate the three-dimensionally functionalized RPPA, polyGPA. Then, mildly oxidized protein samples were spotted on the membrane. In this process, the carbohydrate parts of glycoproteins are oxidized using sodium periodate to form aldehyde groups that form covalent oxime bonds with hydroxyamino groups on the polyGPA to specifically capture glycoproteins, while non-glycosylated proteins are washed away. Finally, the captured glycoproteins can be analyzed and visualized by their general antibodies.

As the coated membrane captures glycoproteins only, although no glyco-specific antibody is used, the polyGPA specifically reflects the glycosylation changes in different samples. The specificity of polyGPA is 99% for the oxidized form of glycoprotein (with aldehyde groups) over the control sample without oxidization (Fig. 2). With the subnL sample volume, polyGPA offers quantitative measurement of glycoproteins (α-1-acid was using as the standard) in the range of 0.2–20 pg/nL. Moreover, the polyGPA's sensitivity is over tenfold higher than regular PPA, which may be attributed to the fact that more epitopes on the glycoprotein have been exposed after the glycan portion binds to the 3D-polyGPA membrane.

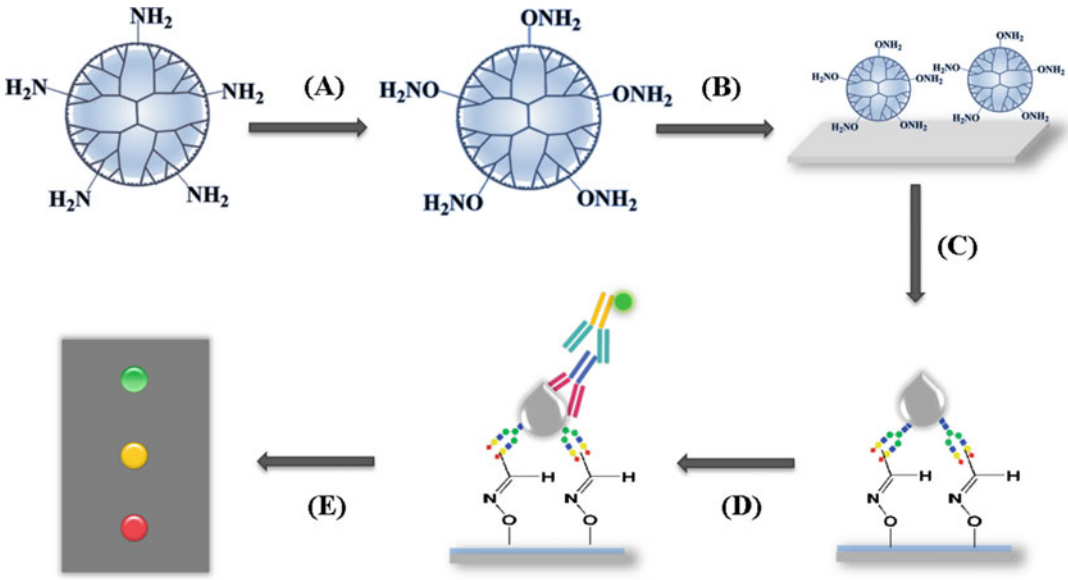

Fig. 1 The experimental workflow for polyGPA. (**a**) Synthesize ONH_2-PAMAM. (**b**) Coat nitrocellulose membrane to make polyGPA. (**c**) Spot oxidized samples. (**d**) Incubate first and second antibody. (**e**) Scan array

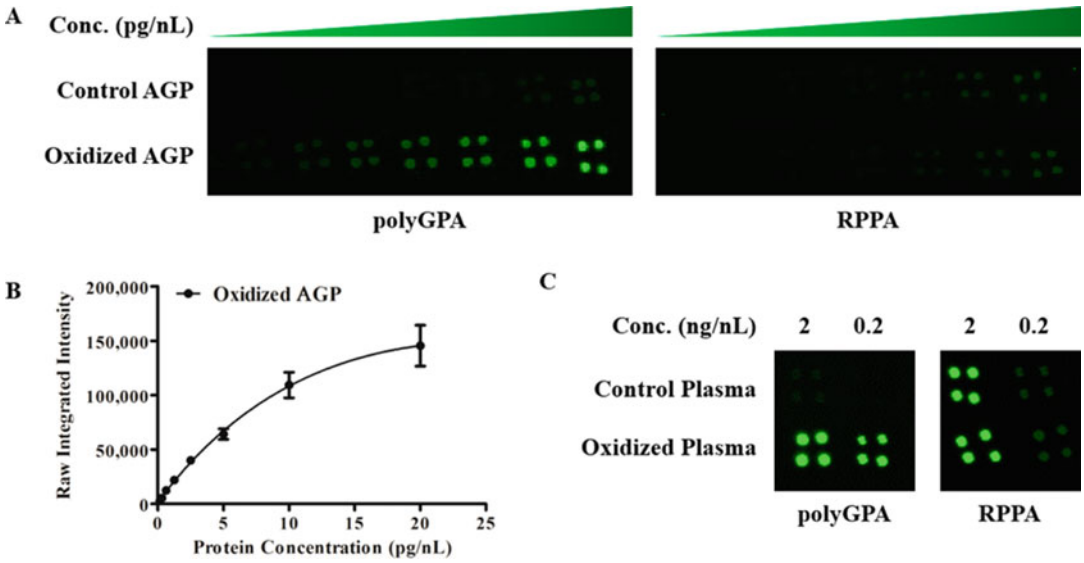

Fig. 2 (**a**) Specific capture and detection of standard AGP by polyGPA. (**b**) Quantification of fluorescent signals from oxidized AGP in panel A by polyGPA. (**c**) Detection of endogenous AGP in human plasma by polyGPA and RPPA. (Reproduced with permission from ref. [3])

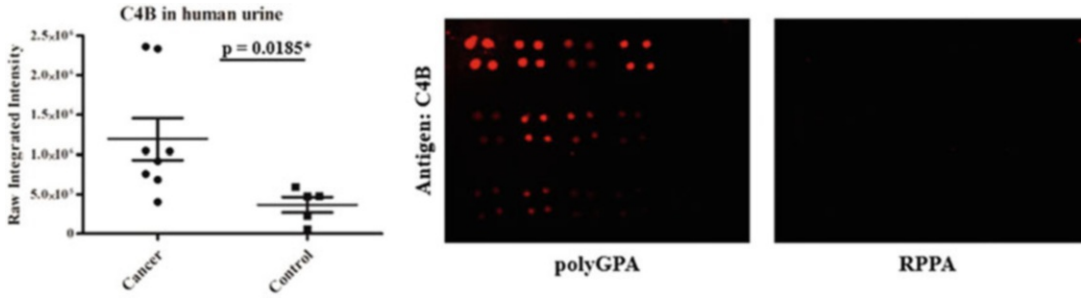

Fig. 3 Quantification of endogenous C4B in human urine. For each membrane, top two rows were printed with eight cancer patient samples, and bottom row was printed with five healthy control samples, four prints per individual sample. For quantitation of signals in polyGPA, mean intensity of four prints per individual was used. (Reproduced with permission from ref. [3])

The polyGPA platform has been used to analyze glycosylation changes in different types of samples. For example, using the polyGPA, we validated that the N-glycosylation of complement C4-B (C4B) significantly increased in urine of bladder cancer patients, suggesting that the glycosylation of urinary C4B might be a potential marker for bladder cancer (Fig. 3) [3]. In plasma-derived extracellular vesicles from breast cancer patients, the glycosylation of five biomarkers, including lymphocyte antigen 6 complex locus protein G6f (LY6G6F), von Willebrand factor (VWF), CD147/basigin (BSG), complement C1q subcomponent subunit A (C1QA), and angiopoietin-1 (ANGPT1/Ang1), was found to be significantly elevated using polyGPA [4]. These applications have demonstrated that this strategy could become a powerful technique for sensitive profiling of glycoproteins in a large number of clinical samples for both biomarker discovery and validation studies.

2 Materials

1. Polyamidoamine dendrimer generation 4 (PAMAM G4).
2. *N*,*N*′-diisopropylcarbodiimide (DIPCI).
3. (Boc-aminooxy) acetic acid.
4. Hydroxybenzotriazole.
5. Succinic anhydride.
6. 4-(Dimethylamino)pyridine.
7. Ninhydrin.
8. Trifluoroacetic acid.
9. Sodium dodecyl sulfate (SDS).
10. Tween 20.

11. Deionized water (18 MΩ cm at 25 °C).
12. Bovine serum albumin (BSA).
13. Hydrogen peroxide (H_2O_2).
14. Sodium sulfite.
15. Sodium periodate.
16. 2-Mercaptoethanol.
17. IRDye® 800 and IRDye® 680RD Streptavidin.
18. Biotinyl tyramide.
19. Secondary antibody linked with HRP for tyramide-based signal amplification.
20. Dimethylsulfoxide.
21. Nitrocellulose membranes (0.45 μm).
22. Sample printing pin (*see* **Note 1**).
23. SnakeSkin® pleated dialysis tubing (3500 MWCO, 22 mm dry diameter).
24. BCA Protein Assay Kit.
25. Sodium acetate buffer: 100 mM, pH 5.5.
26. Oxidation buffer: 10 mM sodium periodate in 100 mM sodium acetate, pH 5.5.
27. TBST buffer: 100 mM Tris/HCl, 150 mM NaCl, 0.1% (v/v) Tween 20, pH 7.4.
28. Borate buffer: 100 mM, pH 8.5.

3 Methods

Carry out all procedures at room temperature unless otherwise specified.

3.1 Synthesis of Hydroxylamine Functionalized-PAMAM

1. Dry the PAMAM G4 solution in methanol (100 μL, 40 μmol amino groups on surface).
2. Re-dissolve PAMAM G4 in 500 μL dimethylsulfoxide (DMSO).
3. Dissolve 9 μL *N*,*N*′-diisopropylcarbodiimide (DIPCI), 4.5 mg (Boc-aminooxy) acetic acid, and 6.3 mg hydroxybenzotriazole (HOBt) in 500 μL DMSO and incubate at room temperature for 30 min.
4. Mix the solution of **steps 2** and **3**, and incubate overnight at room temperature.
5. Add 20 mg succinic anhydride and 29 mg 4-(dimethylamino)pyridine (DMAP) to the above solution, and incubate at room temperature for 3 h to block any remaining amine groups on dendrimers.

6. Perform ninhydrin test after each incubation step to measure the residual amine groups on dendrimers (*see* **Note 2**).
7. Dilute and dialyze the reaction mixture in **step 5** against water using SnakeSkin® pleated dialysis tubing (3500 MWCO, 22 mm dry diameter) to remove excess chemicals. Concentrate and transfer the reaction mixture into a glass round bottom bottle.
8. Add one volume trifluoroacetic acid (TFA) to the reaction mixture of **step 7**, and incubate at room temperature for 1 h to remove the Boc groups on the dendrimers.
9. Concentrate the final solution by air blowing to reduce the TFA concentration and dialyze against water to obtain the hydroxylamine functionalized PAMAM.
10. Dilute the synthesized hydroxylamine functionalized PAMAM 1:3 with water and store at 4 °C for further use.

3.2 Periodate Oxidation of Samples

3.2.1 Standard Glycoprotein

1. Prepare 1 μg/μL standard glycoprotein in 100 mM sodium acetate (pH 5.5).
2. Add oxidation buffer to the protein solution and shake the sample in the dark at room temperature for 30 min.
3. Add sodium sulfite (final concentration of 50 mM) to the sample and shake in the dark for 15 min to quench the excess sodium periodate.
4. Denature the oxidized sample in 2% SDS and 2% 2-mercaptoethanol with boiling for 5 min.

3.2.2 Plasma

1. Dilute plasma to the concentration of 5 μg/μL with oxidation buffer.
2. Shake the sample in the dark at room temperature for 30 min.
3. Add sodium sulfite to the diluted plasma sample (final concentration of 50 mM) and shake in the dark for 15 min to quench the excess sodium periodate.
4. Denature the oxidized sample in 2% SDS and 2% 2-mercaptoethanol with boiling for 5 min.

3.2.3 Extracellular Vesicles of Plasma

1. Collect 1 mL plasma sample to an ethylenediaminetetraacetic acid (EDTA) containing tube.
2. Spin the tube at 1500 × *g* for 30 min to remove all cell debris and platelets.
3. Centrifuge the sample again at 20,000 × *g* at 4 °C for 1 h.
4. Collect the pellet and wash three times with cold PBS and collect the supernatant for further centrifugation.

5. Collect the pellet, these are the microvesicles.
6. To obtain the exosomes, further centrifuge the supernatant of the second centrifugation at 100,000 × *g* at 4 °C for 1 h.
7. Collect the pellet and wash it three times with cold PBS.
8. Collect the pellet, these are the exosomes.
9. Add 30 μL of 2% SDS in 100 mM sodium acetate (pH 5.5) to the pellet and heat for 10 min at 95 °C to lyse the microvesicles or exosomes.
10. Measure the protein concentration of the microvesicles or exosomes (**steps 5** and **6**) using bicinchoninic acid (BCA) assay.
11. Add oxidation buffer to the sample and shake in the dark at room temperature for 30 min.
12. Add sodium sulfite (final concentration of 50 mM) to the sample and shake in the dark for 15 min to quench the excess sodium periodate.
13. Denature the oxidized sample in 2% SDS and 2% 2-mercaptoethanol with boiling for 5 min.

3.2.4 Urine

1. Collect 10 mL of urine and centrifuge immediately at 1300 × *g* for 10 min at 4 °C.
2. Collect both color and clear supernatants to ensure there were no noticeable discrepancies.
3. Centrifuge the supernatant again at 4000 × *g* for 10 min at 4 °C.
4. Transfer the second supernatants (**step 3**) to Amicon Ultra-15 filters (MWCO 10 kDa).
5. Centrifuge the filters at 4000 × *g* for 20 min to concentrate the sample.
6. Add 10 mL of 50 mM Tris–HCl, pH 7.5, to the filter and centrifuge again at 4000 × *g* for 20 min to perform a buffer exchange.
7. Measure the protein concentration of the concentrated urine using a bicinchoninic acid (BCA) assay.
8. Add oxidation buffer to the sample and shake in the dark at room temperature for 30 min.
9. Add sodium sulfite to the sample (final concentration of 50 mM) and shake in the dark for 15 min to quench the excess sodium periodate.
10. Denature the oxidized sample in 2% SDS and 2% 2-mercaptoethanol with boiling for 5 min.

3.3 polyGPA Analysis

1. Incubate the nitrocellulose membranes with the diluted polyGPA reagent (Subheading 3.1, **step 10**) overnight at 4 °C (*see* **Note 3**)
2. Air-dry the coated membranes for further use.
3. Print the oxidized samples on membrane using a microarray printing pin. The sample volume is typically 10 nL.
4. Wash the membrane with 4% SDS in TBST three times and then in TBST alone one time, for 5 min per wash.
5. Block the membrane with 3% BSA in TBST for 1–4 h.
6. Probe with primary protein antibody.
7. Wash the membranes three times with TBST, for 5 min per wash.
8. Add the corresponding secondary antibody linked with HRP and incubate for 30 min to 1 h.
9. Incubate the membranes with 5 μM biotinyl tyramide in 0.003% H_2O_2 in 100 mM borate buffer (pH 8.5) for 10 min in the dark.
10. Wash with TBST three times, for 5 min per wash.
11. Probe with IRDye® 680RD Streptavidin for 1 h.
12. Wash the membranes three times with TBST, for 5 min per wash, and then two times with DI water.
13. Scan the membrane using an infrared imaging system (LI-COR Odyssey®) and record the fluorescent signals and quantify the signals using Image Studio (LI-COR Biosciences).

4 Notes

1. The microarray printing pin can be obtained from Arrayit® SMP15B.
2. Ninhydrin test is used for determine the residual amine groups on dendrimers. Briefly, sodium acetate (3.28 g) was dissolved in approximately 6 mL of water as a buffer. The pH of the resulting solution was adjusted to 5.2 using glacial acetic acid, and the final volume was diluted to 10 mL. The ninhydrin reagent was freshly prepared by adding 4 M sodium acetate buffer (1 mL-mg ninhydrin and 12 mg hydrindantin in 3 mL DMSO). For the assay, 50 mL of reagent was added to 100 mL of the sample in each well. The 96-well microplate was incubated at 80 °C for 30 min to allow the reaction to proceed. After incubation, 100 mL of a 50:50 mixture of ethanol and water was added to each well to oxidize the excess hydrindantin. The concentration of amine groups in the sample was determined at the wavelength of 570 nm based on the

calibration curve, which was established using pure PAMAM G4 of known concentrations.

3. PolyGPA only measures the overall glycosylation in a protein. For a glycoprotein with multiple glycosylation sites and different glycoforms, polyGPA may not be sensitive enough to a glycosylation change on a specific site and glycoform.

Acknowledgments

This work was supported by NIH grants 5R01GM088317, 1R01GM111788, and S10 RR025044 and NSF grant 1506752. Additional support was provided by the Purdue University Center for Cancer Research (P30 CA023168).

References

1. Li J, Zhao W, Akbani R et al (2017) Characterization of human cancer cell linesby reverse-phase protein arrays. Cancer Cell 31:225–239
2. Haugen MH, Lindgjaerde OC, Krohn M et al (2017) Proteomic response in breast cancer treated with neoadjuvant chemotherapy with and without bevacizumab: reverse phase protein array (RPPA) results from NeoAva—a randomized phase II study. Cancer Res 76 (14 Suppl):3268–3268
3. Pan L, Aguilar HA, Wang LN et al (2016) Three-dimensionally functionalized reverse phase glycoprotein array for cancer biomarker discovery and validation. J Am Chem Soc 138:15311–15314
4. Chen IH, Aguilar HA, Paez JSP et al (2018) Analytical pipeline for discovery and verification of glycoproteins from plasma-derived extracellular vesicles as breast cancer biomarkers. Anal Chem 90:6307–6313
5. Moremen KW, Tiemeyer M, Nairn AV (2012) Vertebrate protein glycosylation: diversity, synthesis and function. Nat Rev Mol Cell Biol 13:448–462
6. Pinho SS, Reis CA (2015) Glycosylation in cancer: mechanisms and clinical implications. Nat Rev Cancer 15:540–555
7. Ohtsubo K, Marth JD (2006) Glycosylation in cellular mechanisms of health and disease. Cell 126:855–867
8. Freeze HH (2013) Understanding human glycosylation disorders: biochemistry leads the charge. J Biol Chem 288:6936–6945
9. Fuzery AK, Levin J, Chan MM et al (2013) Translation of proteomic biomarkers into FDA approved cancer diagnostics: issues and challenges. Clin Proteomics 10:13
10. Nakagawa T, Miyoshi E, Yakushijin T et al (2008) Glycomic analysis of alpha fetoprotein L3 in hepatoma cell lines and hepatocellular carcinoma patients. J Proteome Res 7:2222–2233
11. Meany DL, Chan DW (2011) Aberrant glycosylation associated with enzymes as cancer biomarkers. Clin Proteomics 8:7–7
12. Gilgunn S, Conroy PJ, Saldova R et al (2013) Aberrant PSA glycosylation-a sweet predictor of prostate cancer. Nat Rev Urol 10:99–107

Chapter 18

Determining Protein Phosphorylation Status Using Antibody Arrays and Phos-Tag Biotin

Eiji Kinoshita, Emiko Kinoshita-Kikuta, and Tohru Koike

Abstract

We describe here a standard protocol for determining the phosphorylation status of protein multiplexes using antibody arrays and a biotinylated Phos-tag with a dodeca(ethylene glycol) spacer (Phos-tag Biotin). The procedure is based on an antibody microarray technique used in conjunction with an enhanced chemiluminescence system, and it permits the simultaneous and highly sensitive detection of multiple phosphoproteins in a cell lysate. By using this procedure, we have demonstrated the quantitative detection of the entire phosphorylation status of a target protein involved in intracellular signaling.

Key words Antibody array, Biotinylated Phos-tag, Enhanced chemiluminescence, Protein phosphorylation

1 Introduction

Protein phosphorylation is a well-characterized posttranslational modification that plays an important role in the control of a wide variety of cellular events. Abnormal phosphorylation has been implicated in various human diseases, including cancers [1], immune inflammation [2], and neurodegenerative disorders [3]. Therefore, effective analytical strategies for quantitative monitoring of changes in the phosphorylation status of certain proteins are essential tools in the field of the phosphoproteomics. Large-scale identification of phosphoproteins is now possible as a result of dramatic advancements in shotgun proteomics methods based on mass spectrometry (MS). However, these MS-based methods require expensive instrumentation, and they involve complicated procedures for sample preparation through enrichment of phosphopeptides by enzymatic digestion.

We have developed a technology known as Phos-tag that permits the analysis of phosphorylated biomolecules. Our Phos-tag technology utilizes a novel phosphate-binding tag molecule known as Phos-tag, which is capable of capturing phosphate monoester

Kelly C. Whittaker and Ruo-Pan Huang (eds.), *Antibody Arrays: Methods and Protocols*, Methods in Molecular Biology, vol. 2237, https://doi.org/10.1007/978-1-0716-1064-0_18,

dianions (R-OPO_3^{2-}) in aqueous solutions of neutral pH [4]. The Phos-tag technology has made contributions to the development of several procedures for research on the phosphoproteome, including an immobilized metal (zinc)-affinity chromatography technique for the separation and enrichment of phosphopeptides and phosphoproteins [5–10], as well as a phosphate-affinity electrophoresis technique for the detection of changes in the mobilities of phosphoproteins in comparison with those of their nonphosphorylated counterparts [11–30]. These techniques use various derivatives of the original Phos-tag molecule. Among these derivatives, biotin-labeled Phos-tag {Phos-tag Biotin; Phos-tag = 1,3-bis[bis(pyridin-2-ylmethyl)amino]propan-2-olato dizinc(II) complex} has been developed as a novel phosphate-affinity probe that has various applications in determining the phosphorylation status of a wide range of peptides and proteins (Fig. 1a) [30–37]. We have established several useful microarray-based techniques for the detection of phosphopeptides and phosphoproteins through the use of a biotin-labeled derivative of Phos-tag that contains an oligomer of 12 molecules of ethylene glycol [PEG12; dodeca(ethylene glycol)] as a long hydrophilic spacer between the biotin moiety and the Phos-tag moiety (Phos-tag Biotin BTL-111) (Fig. 1b) [33]. Because the long spacer confers greater flexibility to the phosphate-affinity Phos-tag moiety, Phos-tag Biotin BTL-111 can access phosphorylated targets more readily, thereby permitting a wider range of applications in the specific detection of protein phosphorylation [33–37]. Here, we introduce a standard protocol for determining the phosphorylation status of protein multiplexes using Phos-tag Biotin BTL-111 and a commercially available antibody array system [35].

2 Materials (*See* Note 1)

2.1 Lysate Samples

1. A commercially available lysate of Raw 264.7 cells (Santa Cruz Biotechnology, Santa Cruz, CA, USA) [35]. Store at −80 °C. Avoid repeated freeze–thaw cycles (*see* **Note 2**).
2. A commercially available lysate of Raw 264.7 cells treated with lipopolysaccharide (LPS) and phorbol 12-myristate 13-acetate (PMA) (Santa Cruz Biotechnology) [35]. Store at −80 °C. Avoid repeated freeze–thaw cycles (*see* **Note 2**).

2.2 Reactions on Arrays

1. Antibody array: Proteome Profiler Human Phospho-MAPK Array (R&D Systems, Minneapolis, MN, USA) (*see* **Note 3**). Store the array system at 2–8 °C (*see* **Note 4**).
2. TBS-T solution: 10 mM of Tris–HCl (pH 7.5) (*see* **Note 5**), 0.1 M NaCl, 0.1% (v/v) poly(oxyethylene) sorbitan monolaurate (Tween 20). Store at room temperature.

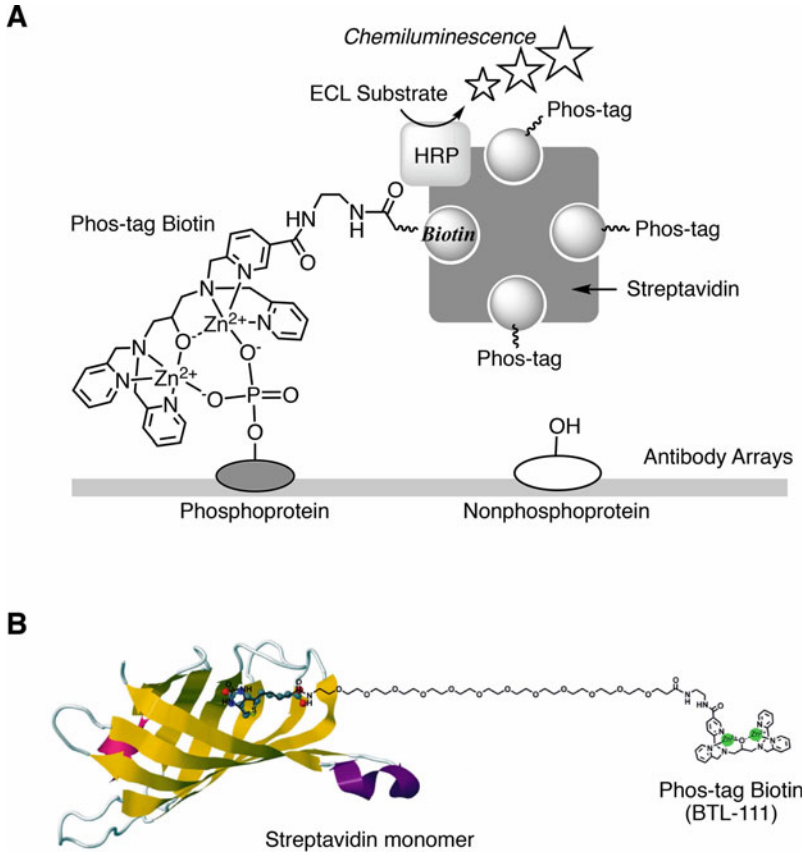

Fig. 1 (**a**) Schematic representation of ECL detection of phosphoproteins on an antibody array format by using Phos-tag Biotin. The phosphorylated targets were probed by using the complex of Phos-tag Biotin with HRP-conjugated streptavidin; the Phos-tag-bound targets were then detected by using an ECL system. (**b**) Superimposed images of the complex of a biotin moiety and a streptavidin monomer with Phos-tag Biotin (BTL-111)

3. Blocking buffer: TBS-T solution (made in **item 2**) containing 10% (w/v) bovine serum albumin (BSA). The solution should be prepared fresh as required.
4. Binding/washing buffer: TBS-T solution containing 1.0 M NaOAc and 1.0% (w/v) BSA. The solution should be prepared fresh as required.
5. Sample solution: Mix 40 μL (100 μg protein) of each lysate and 1460 μL of binding/washing buffer in a 2.0 mL microtube (final volume 1.5 mL). The solution should be prepared fresh as required. After preparation, store on ice and assay immediately.
6. 90-mm culture dishes.
7. Orbital shaker.

2.3 Phosphate-Affinity Probing with Phos-Tag

1. Solution A (TBS-T solution): **item 2** of Subheading 2.2.
2. Solution B: 1.0 mM Phos-tag Biotin BTL-111 solution (FUJIFILM Wako Pure Chemical Industries Ltd) (*see* **Note 6**). Store in a dark place at 4 °C. The Phos-tag Biotin solution is stable for at least 6 months under these conditions.
3. Solution C: 1.0 mM solution of $ZnCl_2$ (*see* **Note 7**). Store at room temperature.
4. Solution D: HRP-streptavidin-conjugated solution (GE Healthcare Bio-Sciences) (*see* **Note 6**). Store in a dark place at 4 °C.
5. Solution E: Mix 469 μL of Solution A, 10 μL of Solution B, 20 μL of Solution C, and 1 μL of Solution D in a 1.5-mL microtube (final volume 500 μL) (*see* **Note 8**) and then allow to stand for 30 min at room temperature.
6. Solution F: Transfer Solution E (500 μL) to a centrifugal filter device cup (e.g., a 30K Nanosep centrifuge, Pall Life Sciences, Ann Arbor, MI, USA) and centrifuge at 14,000 × *g* for 20 min at room temperature to remove the excess Zn(II)–Phos-tag Biotin complex (*see* **Note 8**). Dilute the remaining solution (<10 μL) in the cup with 3.0 mL of a binding/washing buffer solution. Solution F should be prepared fresh as required.
7. Centrifuge.
8. Plastic bag.

2.4 Enhanced Chemiluminescence Detection Reagent and Equipment

1. Enhanced chemiluminescence (ECL) detection reagent: Lumigen ECL Ultra (TMA-6, Lumigen, Southfield, MI, USA). Store in a dark place at 4 °C.
2. Image analyzer: LAS 3000 image analyzer (FUJIFILM, Tokyo, Japan).

3 Methods

3.1 Reactions on Arrays

1. To prevent nonspecific binding, block two antibody arrays with 10 mL of blocking buffer in a 90-mm culture dish overnight at room temperature with gentle shaking on an orbital shaker (*see* **Note 9** and Fig. 2a, left-hand panel).
2. Subject the arrays to three 10-min washes with 10 mL of binding/washing buffer solution in a 90-mm culture dish at room temperature on an orbital shaker.
3. After washing, independently incubate each array with 1.5 mL of the untreated or LPMS/PMA-treated sample solution in a plastic bag. Gently rock the bag on an orbital shaker overnight at 4 °C.

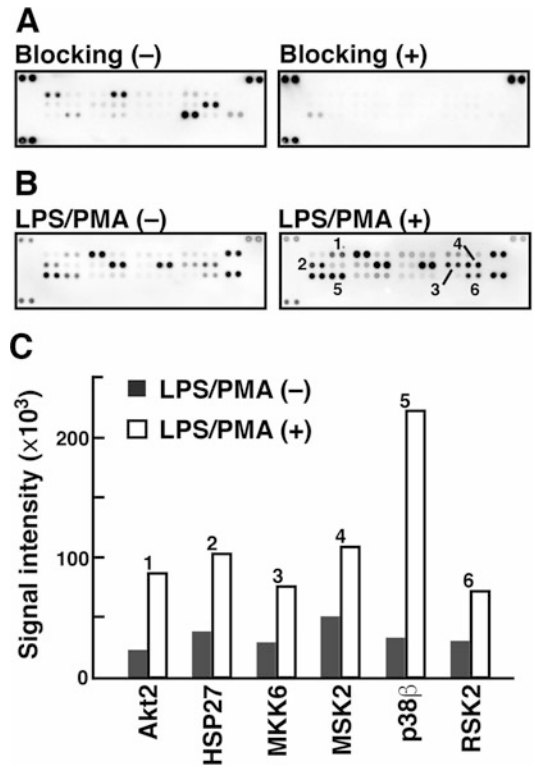

Fig. 2 Phosphorylation profiling of intracellular proteins by using an antibody array system. (**a**) Comparative data obtained by probing with HRP–SA before (left, −) and after (right, +) adding an original blocking treatment. (**b**) Profiling of multiplex protein phosphorylation involved in the LPS/PMA-signaling pathway of Raw 264.7 cells. Images of detections made using the lysates before and after LPS/PMA treatment are shown in the left-hand and right-hand panels, respectively. (**c**) Densitometric data from the images shown in (**b**). The reported values of signal intensity are means in duplicate. Proteins having signal intensities with values in excess of 20,000 that increased by more than a factor of two after LPS/PMA treatment are shown. As widely accepted on the basis of results of many other studies on LPS/PMA signaling, we confirmed the presence of significant increases in the levels of phosphorylation of several proteins, including Akt2, HSP27, and p38β, by using the antibody array system and Phos-tag Biotin. All the ECL images were obtained by using a LAS 3000 image analyzer, and the densitometric analysis was performed by using the Multi Gauge software associated with the analyzer. (Reproduced with permission from ref. 35 © (2013) Elsevier Inc.)

4. After incubation, carefully remove the array from the bag and subject it to three 10-min washes with 10 mL of binding/washing buffer solution in a 90-mm culture dish at room temperature on an orbital shaker.

3.2 Phosphate-Affinity Probing with Phos-Tag and Detecting Phosphoproteins

1. After washing, independently incubate each array with 1.5 mL of Solution F in a plastic bag. Gently rock the bag on an orbital shaker for 30 min at room temperature.
2. Carefully remove the array from the bag and subject it to three 10-min washes with 10 mL of binding/washing buffer solution in a 90 mm culture dish at room temperature on an orbital shaker.
3. For ECL detection, treat each array with an appropriate amount of the ECL reagent according to the manufacturer's instructions.
4. Detect the ECL signals using the LAS 3000 image analyzer (*see* Fig. 2b, c).

4 Notes

1. All reagents and solvents used are purchased at the highest commercial quality available and are used without further purification. All aqueous solutions are prepared using deionized and distilled water.
2. The lysate should be transferred into clean 1.5-mL microtubes, and each aliquot should be stored at −80 °C.
3. Each Human Phospho-MAPK Array consists of 52 individual antibody arrays spotted in duplicate on a nitrocellulose membrane; each capture antibody is a phosphorylation-independent antibody [35].
4. The manufacturer's instructions state that the arrays are stable for at least 3 months under these conditions. The array surface is stable under incubation conditions, but it is sensitive to mechanical stress and should not be touched or wiped.
5. Concentrated hydrochloric acid (HCl) is dangerously irritating to the skin, eyes, and mucous membranes. When handing this chemical, work in a chemical fume hood and wear gloves, eye protection, and a mask.
6. The commercially available Solution B and Solution D are used as received.
7. Zinc(II) nitrate solution [10 mM $Zn(NO_3)_2 \cdot 6H_2O$ in distilled water] is a suitable substitute. Because $ZnCl_2$ and $Zn(NO_3)_2$ are deliquescent salts, the solutions should be prepared by using fresh products from newly opened bottles. Aqueous solutions of $ZnCl_2$ or $Zn(NO_3)_2$ are stable for at least 6 months.
8. Because Phos-tag Biotin in Solution B (10 μL) is present in a large excess compared with HRP-conjugated streptavidin in Solution D (1 μL), we obtained the same result by using a

smaller amount of Phos-tag Biotin (e.g., 1 μL of Solution B). The volume of Solution B (1–10 μL) can be adjusted appropriately to obtain the required sensitivity or to reduce expense. If the volume of Solution B is decreased from 10 μL to 1 μL, there is no need to adjust the volumes of the other solutions.

9. If the blocking treatment is omitted, many false-positive ECL signals can be detected (*see* Fig. 2a, left-hand panel). Presumably, nonspecific interactions between some antibodies and the HRP-conjugated streptavidin are responsible for the false-positive signals.

Acknowledgments

This work was supported in part by KAKENHI Grants 19K07147 to E.K., 18K06596 to E.K.-K., and 17K08237 to T.K.

References

1. Singh V, Ram M, Kumar R et al (2017) Phosphorylation: implications in cancer. Protein J 36:1–16
2. Liu J, Qian C, Cao X (2016) Post-translational modification control of innate immunity. Immunity 45:15–30
3. Wang Y, Mandelknow E (2016) Tau in physiology and pathology. Nat Rev Neurosci 17:5–21
4. Kinoshita E, Takahashi M, Takeda H et al (2004) Recognition of phosphate monoester dianion by an alkoxide-bridged dinuclear zinc (II) complex. Dalton Trans 8:1189–1193
5. Kinoshita E, Yamada A, Takeda H et al (2005) Novel immobilized zinc(II) affinity chromatography for phosphopeptides and phosphorylated proteins. J Sep Sci 28:155–162
6. Kinoshita-Kikuta E, Kinoshita E, Yamada A et al (2006) Enrichment of phosphorylated proteins from cell lysate using a novel phosphate-affinity chromatography at physiological pH. Proteomics 6:5088–5095
7. Kinoshita-Kikuta E, Kinoshita E, Koike T (2009) Phos-tag beads as an immunoblotting enhancer for selective detection of phosphoproteins in cell lysates. Anal Biochem 389:83–85
8. Kinoshita-Kikuta E, Yamada A, Inoue C et al (2010) A novel phosphate-affinity bead with immobilized Phos-tag for separation and enrichment of phosphopeptides and phosphoproteins. J Integr OMICS 1:157–169
9. Tsunehiro M, Meki Y, Matsuoka K et al (2013) A Phos-tag-based magnetic-bead method for rapid and selective separation of phosphorylated biomolecules. J Chromatogr B Anal Technol Biomed Life Sci 925:86–94
10. Yuan ET, Ino Y, Kawaguchi M et al (2017) A Phos-tag-based micropipette-tip method for rapid and selective enrichment of phosphopeptides. Electrophoresis 38:2447–2455
11. Kinoshita-Kikuta E, Aoki Y, Kinoshita E et al (2007) Label-free kinase profiling using phosphate affinity polyacrylamide gel electrophoresis. Mol Cell Proteomics 6:356–366
12. Kinoshita E, Kinoshita-Kikuta E, Matsubara M et al (2008) Separation of phosphoprotein isotypes having the same number of phosphate groups using phosphate-affinity SDS-PAGE. Proteomics 8:2994–3003
13. Kinoshita E, Kinoshita-Kikuta E, Matsubara M et al (2009) Two-dimensional phosphate-affinity gel electrophoresis for the analysis of phosphoprotein isotypes. Electrophoresis 30:550–559
14. Kinoshita E, Kinoshita-Kikuta E, Ujihara H et al (2009) Mobility shift detection of phosphorylation on large proteins using a Phos-tag SDS-PAGE gel strengthened with agarose. Proteomics 9:4098–4101
15. Kinoshita E, Kinoshita-Kikuta E, Koike T (2009) Separation and detection of large phosphoproteins using Phos-tag SDS-PAGE. Nat Protoc 4:1513–1521
16. Kinoshita E, Kinoshita-Kikuta E (2011) Improved Phos-tag SDS-PAGE under neutral pH conditions for advanced protein phosphorylation profiling. Proteomics 11:319–323

17. Kinoshita E, Kinoshita-Kikuta E, Koike T (2012) Phos-tag SDS-PAGE systems for phosphorylation profiling of proteins with a wide range of molecular masses under neutral pH conditions. Proteomics 12:192–202
18. Kinoshita-Kikuta E, Kinoshita E, Koike T (2012) Separation and identification of four distinct serine-phosphorylation states of ovalbumin by Phos-tag affinity electrophoresis. Electrophoresis 33:849–855
19. Kinoshita-Kikuta E, Kinoshita E, Koike T (2012) A laborsaving, timesaving, and more reliable strategy for separation of low-molecular-mass phosphoproteins in Phos-tag affinity electrophoresis. Int J Chem (Mumbai, India) 4(5):1–8
20. Kinoshita E, Kinoshita-Kikuta E, Shiba A et al (2014) Profiling of protein thiophosphorylation by Phos-tag affinity electrophoresis: evaluation of adenosine 5′-O-(3-thiotriphosphate) as a phosphoryl donor in protein kinase reactions. Proteomics 14:668–679
21. Kinoshita-Kikuta E, Kinoshita E, Koike T (2014) Identification of two phosphorylated species of β-catenin involved in the ubiquitin-proteasome pathway by using two-dimensional Phos-tag affinity electrophoresis. J Electrophoresis 58:1–4
22. Kinoshita-Kikuta E, Kinoshita E, Matsuda A, Koike T (2014) Tips on improving the efficiency of electrotransfer of target proteins from Phos-tag SDS-PAGE gel. Proteomics 14:2437–2442
23. Kinoshita-Kikuta E, Kinoshita E, Eguchi Y et al (2015) Functional characterization of the receiver domain for phosphorelay control in hybrid sensor kinases. PLoS One 10:e0132598
24. Sugiyama Y, Katayama S, Kameshita I et al (2015) Expression and phosphorylation state analysis of intracellular protein kinases using Multi-PK antibody and Phos-tag SDS-PAGE. MethodsX 2:469–474
25. Kinoshita-Kikuta E, Kinoshita E, Eguchi Y, Koike T (2016) Validation of cis and trans modes in multistep phosphotransfer signaling of bacterial tripartite sensor kinases by using Phos-tag SDS-PAGE. PLoS One 11:e0148294
26. Kinoshita E, Kinoshita-Kikuta E, Kubota Y et al (2016) A Phos-tag SDS-PAGE method that effectively uses phosphoproteomic data for profiling the phosphorylation dynamics of MEK1. Proteomics 16:1825–1836
27. Kinoshita E, Kinoshita-Kikuta E, Karata K et al (2017) Specific glutamic acid residues in targeted proteins induce exaggerated retardations in Phos-tag SDS-PAGE migration. Electrophoresis 38:1139–1146
28. Kinoshita-Kikuta E, Kinoshita E, Ueda S et al (2019) Increase in constitutively active MEK1 species by introduction of MEK1 mutations identified in cancers. Biochim Biophys Acta Proteins Proteomics 1867:62–70
29. Uezato Y, Kameshita I, Morisawa K et al (2019) A method for profiling the phosphorylation state of tyrosine protein kinases. Biochim Biophys Acta Proteins Proteomics 1867:71–75
30. Kinoshita E, Kinoshita-Kikuta E, Takiyama K et al (2006) Phosphate-binding tag, a new tool to visualize phosphorylated proteins. Mol Cell Proteomics 5:749–757
31. Inamori K, Kyo M, Nishiya Y et al (2005) Detection and quantification of on-chip phosphorylated peptides by surface plasmon resonance imaging techniques using a phosphate capture molecule. Anal Chem 77:3979–3985
32. Nakanishi T, Ando E, Furuta M et al (2007) Identification on membrane and characterization of phosphoproteins using an alkoxide-bridged dinuclear metal complex as a phosphate binding tag molecule. J Biomol Tech 18:278–286
33. Kinoshita E, Kinoshita-Kikuta E, Sugiyama Y et al (2012) Highly sensitive detection of protein phosphorylation by using improved Phos-tag Biotin. Proteomics 12:932–937
34. Kinoshita E, Kinoshita-Kikuta E, Koike T (2013) Phos-tag-based microarray techniques advance phosphoproteomic. Proteomics Bioinf S6. https://doi.org/10.4172/jpb.S6-008
35. Kinoshita E, Kinoshita-Kikuta E, Koike T (2013) Sandwich assay for phosphorylation of protein multiplexes by using antibodies and Phos-tag. Anal Biochem 438:104–106
36. Kinoshita E, Kinoshita-Kikuta E, Koike T (2015) Advances in Phos-tag-based methodologies for separation and detection of the phosphoproteome. Biochim Biophys Acta Proteins Proteomics 1854:601–608
37. Kinoshita-Kikuta E, Kinoshita E, Koike T (2016) Phosphopeptide detection with biotin-labeled Phos-tag. Method Mol Biol 1355:17–29

Chapter 19

Analyzing Signaling Pathways Using Antibody Arrays

Hao Tang, Chaohui Duan, Zhizhou Kuang, and Ruo-Pan Huang

Abstract

Cell signaling is comprised of complex networks that regulate homeostasis and human diseases. The analyses of such pathways would improve our understanding of disease pathology and direct drug development. However, it remains a great challenge to study pathways using traditional methods. We developed a high-throughput sandwich-based antibody array technology for the simultaneous detection of multiple targets, capable of identifying the relative expression levels or phosphorylation levels of major signaling pathway proteins. This array-based system features a nitrocellulose membrane or glass slide solid support, spotted with antibodies targeting key proteins of major signaling pathways, including RTK, EGFR, MAPK, AKT, apoptosis, TGFb, JAK/STAT, NFkB, and insulin receptor pathways. We employed these antibody arrays to investigate how the anti-cancer drugs, camptothecin and phorbol 12-myristate 13-acetate (PMA), alter protein phosphorylation in Jurkat and HeLa cells, respectively. Our array data suggest that camptothecin treatment induced DNA double-strand breaks in Jurkat cells and activated the DNA damage pathways ATM and Chk2, which then further induced apoptosis through caspase 3 and PARP. PMA induced the MAPK pathway in HeLa cells through the activation of ERK, CREB, and RSK1. These array results are consistent with previous studies using traditional methods and were validated with Western blotting. Our studies demonstrate that pathway antibody arrays provide a rapid, efficient, and multiplexed approach for profiling phosphorylated proteins.

Key words Signaling pathway, Antibody array, MAPK, Apoptosis

1 Introduction

A cell signaling pathway is an essential mechanism that regulates all basic activities of cells and their responses to environmental changes. Many human diseases are related to errors of cell signaling pathways, and many signaling pathway components are effective pharmaceutical targets [1, 2]. Normally when a signal is initiated, like a ligand binding to its receptor, it will induce a cascade reaction which involves multiple players and steps and will transduce the signal from one part of cell to another or to other cells. The signal is often transduced through the regulation of the activities, location, and amount of key proteins. Our understanding of signaling

Kelly C. Whittaker and Ruo-Pan Huang (eds.), *Antibody Arrays: Methods and Protocols*, Methods in Molecular Biology, vol. 2237, https://doi.org/10.1007/978-1-0716-1064-0_19,

pathways has benefited enormously from genetic and biochemical analysis [1, 2].

Phosphorylation is the most important mechanism in directing both the activity and subcellular localization of many key signaling proteins. Protein phosphorylation plays a significant role in almost all cellular processes including cell growth, death, metabolism, and the stress response [3]. Protein phosphorylation and dephosphorylation, most commonly at a serine (S), threonine (T), or tyrosine (Y) residue, are regulated by kinases and phosphatases [3]. Accurately monitoring phosphorylated proteins at the cellular level is critical to decipher and understand cell signaling pathways [4, 5]. Protein phosphorylation is often detected by isotope labeling or by 2D gel and mass spectrometry analyses [6–8]. Both methods are highly sensitive [9]. However, because of the high equipment cost and labor required for mass spectrometry, and the special isotope handling and disposal required for radiolabeling, phospho-specific antibodies are generally the more preferred tool for detection of protein phosphorylation [10, 11]. Western blot or ELISAs can be designed to rapidly and inexpensively detect target protein levels and/or phosphorylation levels, allowing multiple samples to be tested in parallel. Alternatively, specific antibodies can be multiplexed into an array format, allowing the simultaneous detection of multiple target protein expression and/or phosphorylation levels. We developed a high-throughput sandwich-based antibody array system that features a nitrocellulose membrane or glass slide solid support, spotted with antibodies targeting more than 182 classical signaling pathway proteins, including RTK, EGFR, MAPK, AKT, Apoptosis, TGFb, JAK/STAT, NFkB, and insulin receptor pathways [12–15]. Here we demonstrate that multiple targets of MAPK and apoptosis signaling pathways can be analyzed spontaneously using antibody arrays. Capture antibodies of well-selected targets, 17 from the MAPK signaling pathway and 19 from the apoptosis signaling pathway, were printed on 2 nitrocellulose membranes, respectively (Tables 1 and 2). After incubation with cell lysates, these membranes were blotted with detection antibody mixes and HRP-conjugated goat anti-Rabbit IgG. Membranes were further developed using a chemiluminescent system, and spot signal intensities analyzed (Figs. 1 and 2).

Thus, through a single assay, we have identified multiple targets' change in phosphorylation status in response to each stimulation (Figs. 1 and 2), suggesting those targets are important to transduction of the stimulation signal. These data were further validated using Western blot (Fig. 3). Similar discoveries were reported previously using traditional methods [16–19]. Our studies demonstrate that by using antibody arrays, high-throughput detection of many related proteins and/or their phosphorylation status can be accomplished.

Table 1
Human apoptosis signaling pathway array map

	A	B	C	D	E	F	G	H
1 2	POS	POS	NEG	NEG	AKT (S473)	CREB (S133)	ERK1 (T202/ Y204) ERK2 (Y185/ Y187)	GSK3a (S21)
3 4	GSK3b (S9)	HSP27 (S82)	JNK (T183)	MEK (S217/ 221)	MKK3 (S189)	MMK6 (S207)	MSK2 (S360	mTOR (S2448)
5 6	p38 (T180/ Y182)	P53 (S15)	P70S6K (T421/ S424)	RSK1 (S380)	RSK2 (S386)	NEG	NEG	POS

POS positive control spot, *NEG* negative control spot

Table 2
Human/mouse MAPK phosphorylation array map

	A	B	C	D	E	F	G	H
1 2	POS	POS	NEG	AKT (S473)	ATM (S1981)	BAD (S112)	Casp3 (D175)	Casp7 (D198)
3 4	CHK1 (S296)	CHK2 (T68)	eIF2a (S51)	Erk1/2 (T202)	hsp27 (S82)	IkBa (S32)	JNK (T183)	NFKB (S536)
5 6	PARP (D214)	P27 (T198)	P38 (T180/ Y182)	P53 (S15)	SMAD2 (S245)	TAK1 (S412)	NEG	POS

POS positive control spot, *NEG* negative control spot

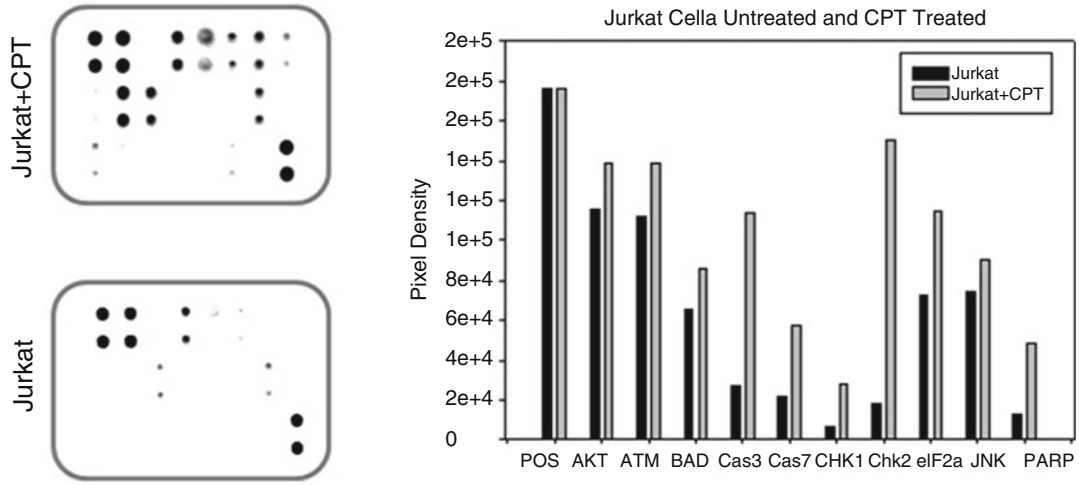

Fig. 1 Jurkat cells were either untreated (bottom panel) or treated (top panel) with camptothecin (CPT) for 16 h. Data shown are from a 20-s exposure using a chemiluminescence imaging system

2 Materials

1. DMEM, 1×.
2. RPMI 1640, 1×.
3. FBS.
4. Cell Lysis Buffer (RayBiotech).
5. Centrifuge.
6. 1 mM Phorbol 12-myristate 13-acetate (PMA) in DMSO.
7. 5 mM Camptothecin (CPT) in DMSO.

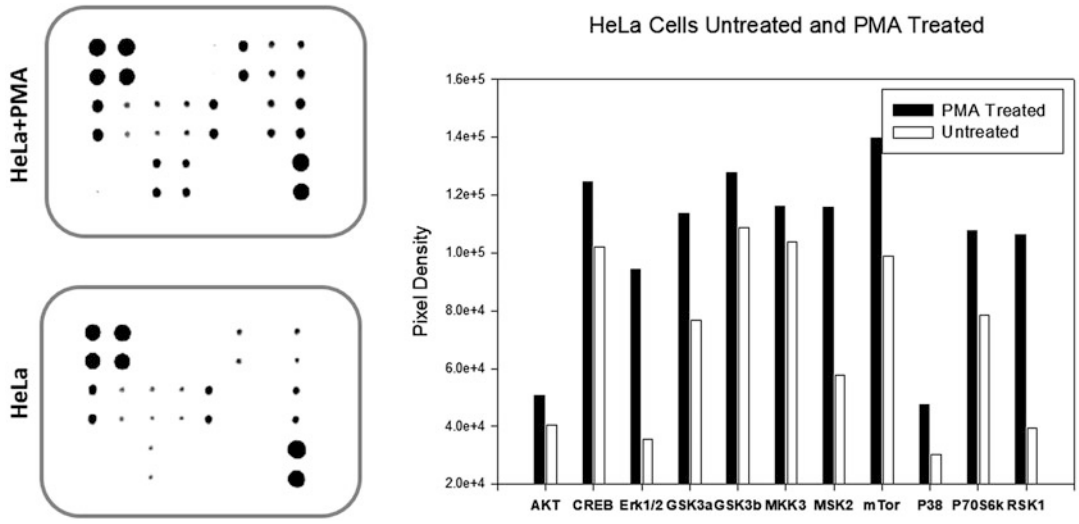

Fig. 2 HeLa cells were grown to 80% confluency and then serum starved overnight. Cells were either untreated (bottom panel) or treated (top panel) with 250 nM PMA for 20 min. Data shown are from a 20-s exposure using a chemiluminescence imaging system

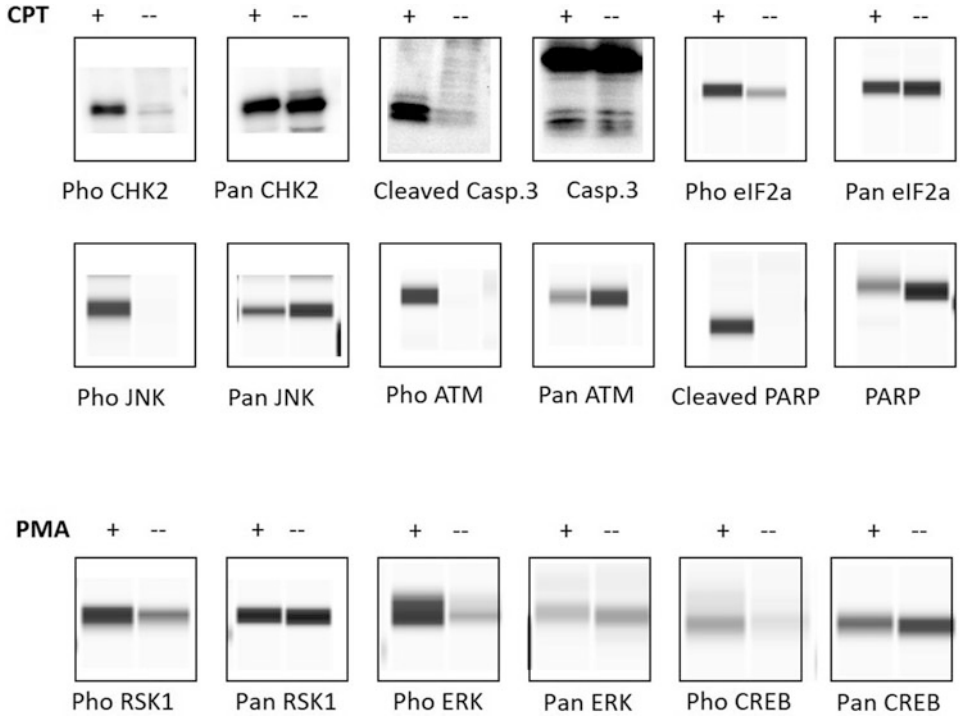

Fig. 3 Array results were further validated using Western blot. Antibodies against total protein and phosphorylated/cleaved protein of each were used following standard Western blot protocol

8. Antibody array: RayBio® C-Series Human Apoptosis Signaling Array C1 and Human/Mouse MAPK Phosphorylation Array.
9. Blocking Buffer: 0.01 M Tris–HCl, pH 7.6, 0.15 M NaCl, 5% bovine serum albumin.
10. Detection Antibody Cocktail: Mixture of 19 detection antibodies related to human apoptosis signaling pathway (*see* Table 1) or 17 detection antibodies related to human/Mouse MAPK signaling pathway (*see* Table 2).
11. HRP-Anti-Rabbit IgG Concentrate: HRP conjugated goat anti rabbit IgG, affinity purified.
12. Wash Buffer I: 2% Tween 20, 100 mM Tris–HCl, pH 7.6, 150 mM NaCl.
13. Wash Buffer II: 100 mM Tris–HCl, pH 7.6, 150 mM NaCl.
14. ECL Detection Buffer C (RayBiotech).
15. ECL Detection Buffer D (RayBiotech).
16. 8-Well Incubation Tray w/ Lid.
17. Protease Inhibitor Cocktail.
18. Phosphatase Inhibitor Cocktail.
19. Pipettors, 2, 20, 200 μL, 1 mL.
20. Pipet tips 2, 20, 200 μL, 1 mL,
21. Microfuge tubes, 1.5 mL.
22. Centrifuge.
23. BCA total protein assay kit.
24. Orbital shaker or oscillating rocker.
25. Tissue paper, blotting paper or chromatography paper.
26. Plastic sheet.
27. Adhesive tape or plastic wrap.
28. Distilled or de-ionized water.
29. EpiChemi3 Darkroom chemiluminescent imaging system.
30. GenePix software.

3 Methods

3.1 Sample Preparation (See Note 1)

1. Cell culture and stimulation: Grow HeLa cells to 80% confluence in DMEM medium with 10% FBS and then serum starve overnight.
2. Prepare 250 nM PMA: Add 2.5 μL of 1 mM PMA to 10 mL DMEM 1× medium.
3. Treat a population of HeLa cells with 250 nM PMA for 20 min and keep a population of HeLa cells untreated.

4. Grow Jurkat cells to 2×10^6 cells/mL in RPMI 1640 medium with 10% FBS.
5. Prepare 1 μM camptothecin (CPT): Add 2 μL of 5 mM CPT to 10 mL RPMI 1640 1× medium.
6. Treat a population of Jurkat cells with 1 μM camptothecin (CPT) for 16 h and keep a population of Jurkat cells untreated.
7. Remove the supernatant from the cell cultures and wash the cells twice with cold 1× PBS (for suspension cells, pellet the cells by spinning down the cells at 450 × *g* for 10 min) making sure to remove any remaining PBS before adding Lysis Buffer.
8. Solubilize the cells at 4×10^7 cells/mL in Cell Lysis Buffer containing Protease Inhibitor Cocktail and Phosphatase Inhibitor Cocktail (*see* **Note 2**). Pipette up and down to resuspend cells and rock the lysates gently at 2–8 °C for 30 min on an orbital shaker (*see* **Note 3**). Transfer extracts to microfuge tubes and centrifuge at 14,000 × *g* for 10 min. Save the supernatant as whole cell lysate and discard the pellet (*see* **Note 4**).
9. Determine the whole cell lysate protein concentrations using a BCA total protein assay kit. Lysates not used immediately should be aliquoted and stored at −70 °C. Lysates should be kept on ice prior to use (*see* **Note 5**).
10. Use Blocking Buffer to dilute whole cell lysates to a 0.2 mg/mL total protein concentration (*see* **Note 6**).

3.2 Array Assay

1. Take out antibody array and Blocking Buffer from storage and allow the components to equilibrate to room temperature (RT).
2. Carefully place each antibody array membrane (printed side up) into a well of the Incubation Tray (*see* **Note 7**). One membrane per well (*see* **Note 8**).
3. Pipette 2 mL of Blocking Buffer into each well (*see* **Note 9**) and incubate for 30 min at RT (*see* **Notes 10** and **11**).
4. Aspirate the Blocking Buffer from each well with a pipette.
5. Pipette 1 mL of the 0.2 mg/mL whole cell lysate from **step 10** of Subheading 3.1 into each well and incubate for 1.5–5 h at RT OR overnight at 4 °C (*see* **Notes 12** and **13**).
6. Aspirate samples from each well with a pipette.
7. Wash Buffer I Wash: Pipette 2 mL of 1× Wash Buffer I into each well and incubate for 5 min at RT. Repeat this two more times using fresh buffer for a total of three washes, aspirating out the buffer completely each time.
8. Wash Buffer II Wash: Pipette 2 mL of 1× Wash Buffer II into each well and incubate for 5 min at RT. Repeat this one more

time using fresh buffer for a total of two washes, aspirating out the buffer completely each time.

9. Pipette 2 mL of Blocking Buffer into the Detection Antibody Cocktail vial. Mix gently with a pipette. Pipette 1 mL of the prepared Detection Antibody Cocktail into each well and incubate for 1.5–2 h at RT OR overnight at 4 °C.
10. Aspirate the Detection Antibody Cocktail from each well.
11. Wash membranes as directed in **steps 7** and **8**.
12. Add 10 μL of HRP-Anti-Rabbit IgG Concentrate into 10 mL Blocking Buffer to make 1× HRP-Anti-Rabbit IgG. Pipette 2 mL of 1× HRP-Anti-Rabbit IgG into each well and incubate for 2 h at RT OR overnight at 4 °C.
13. Aspirate the HRP-Anti-Rabbit IgG from each well.
14. Wash membranes as directed in **steps 7** and **8**.
15. Transfer the membranes, printed side up, onto a sheet of chromatography paper, tissue paper, or blotting paper lying on a flat surface (such as a benchtop) (*see* **Note 14**).
16. Remove any excess wash buffer by blotting the membrane edges with another piece of paper.
17. Transfer and place the membranes, printed side up, onto a plastic sheet lying on a flat surface.
18. Into a single clean microcentrifuge tube, pipette equal volumes (1:1) of Detection Buffer C and Detection Buffer D to make the Detection Buffer mixture. Mix well with a pipette. For each membrane, use 250 μL of Detection Buffer C and 250 μL of Detection Buffer D.
19. Gently pipette 500 μL of the Detection Buffer mixture onto each membrane and incubate for 2 min at RT (*DO NOT ROCK OR SHAKE*). Immediately afterwards, proceed to **step 20**.
20. Place another plastic sheet on top of the membranes by starting at one end and gently "rolling" the flexible plastic sheet across the surface to the opposite end to smooth out any air bubbles. The membranes should now be "sandwiched" between two plastic sheets (*see* **Note 15**).
21. Transfer the sandwiched membranes to the EpiChemi3 Darkroom chemiluminescent imaging system and expose (Figs. 1 and 2) (*see* **Note 16**).

3.3 Data Extraction and Analysis

1. GenePix software should be used to extract spot signal densities from the array images.

2. For each array membrane, identify a single exposure that the exhibits a high signal-to-noise ratio (strong spot signals and low background response). Strong Positive Control Spot signals but not too strong that that they are "bleeding" into one another is ideal. The exposure time does not need to be identical for each array, but Positive Control signals on each array image should have similar intensities.
3. Measure the density of each spot using a circle that is roughly the size of one of the largest spots. Be sure to use the same extraction circle dimensions (area, size, and shape) for measuring the signal densities on every array for which you wish to compare the results.
4. For each spot, use the summed signal density across the entire circle (i.e., total signal density per unit area).
5. Once the raw numerical densitometry data is extracted, the background must be subtracted, and the data need to be normalized to the Positive Control signals.
6. Select values which you believe best represent the background. If the background is fairly even throughout the membrane, the Negative Control Spots (NEG) should be similar and are accurate for this purpose.
7. The intensity of the Positive Control signals can be used to normalize signal responses for comparison of results across multiple arrays, much like housekeeping genes and proteins are used to normalize results of PCR gels and Western blots, respectively. To normalize array data, one array is defined as the "Reference Array" to which the other arrays are normalized to. The choice of the Reference Array is arbitrary.
8. A simple algorithm can be used to calculate and determine the signal fold expression between like analytes (*see* **Note 17**).

$$X(Ny) = X(y) * \mathrm{P1} / \mathrm{P(y)}$$

where

$P1$ = mean signal density of Positive Control Spots on the reference array

$P(y)$ = mean signal density of Positive Control Spots on array "y"

$X(y)$ = mean signal density for spot "X" on array "y"

$X(Ny)$ = normalized signal intensity for spot "X" on array "y"

4 Notes

1. Optimal methods will need to be determined by each researcher empirically based on researched literature and knowledge of the samples.
2. It is strongly recommended to add a protease and phosphatase inhibitor cocktail to cell and tissue lysate samples.
3. Avoid sonication of 1 mL or less as this can quickly heat and denature proteins.
4. If not using fresh samples, freeze samples as soon as possible after collection.
5. Avoid multiple freeze-thaw cycles. If possible, sub-aliquot samples prior to initial storage. Always centrifuge the samples hard after thawing (~9,500 × *g* for 2–5 min) in order to remove any particulates that could interfere with detection.
6. A range of concentrations might be suitable, from 50 to 1000 μg of total protein (after at least a fivefold dilution to minimize the effect of any detergent(s)). Therefore, the original lysate concentration should be 250 μg to 5 mg/mL. Most samples will not need to be concentrated. If concentration is required, a spin column concentrator with a chilled centrifuge is recommended.
7. Mark the antibody printed side of each membrane using pencil in the upper left corner. Do not allow membranes to dry out during the experiment or they may become fragile and break OR high and/or uneven background may occur. Grasp membranes by the corners or edges only using forceps. DO NOT touch printed antibody spots.
8. All washes and incubations should be performed in the Incubation Tray, which can hold 10–20 mL buffer.
9. Avoid forceful pipetting directly onto the membrane; instead, gently pipette samples and reagents into a corner of each well.
10. Perform ALL incubation and wash steps under gentle rotation or rocking motion (~0.5 to 1 cycle/s) using an orbital shaker or oscillating rocker to ensure complete and even reagent/sample coverage. Rocking/rotating too vigorously may cause foaming or bubbles to appear on the membrane surface which should be avoided. Aspirate samples and reagents completely after each step by suctioning off excess liquid with a pipette. Tilting the tray so the liquid moves to a corner and then pipetting is an effective method.
11. Cover the incubation container with lid during all incubation steps to avoid evaporation and outside debris contamination. Ensure the membranes are completely covered with sufficient sample or reagent volume during each incubation.

12. Overnight incubations should be performed at 4 °C (also with gentle rocking/shaking). Longer incubations can help maximize the spot signal intensities. However, be aware that longer incubations can also increase the background response so complete liquid removal and washing are critical.
13. Optional overnight incubations may be performed for the following steps to increase overall spot signal intensities: **steps 5**, **9**, and **12** of Subheading 3.2.
14. Exposure should ideally start within 5 min after finishing **step 19** of Subheading 3.2 and be completed within 10–15 min as chemiluminescence signals will fade over time. If necessary, the membrane can be redeveloped after repeating washing, HRP-Anti-Rabbit IgG and Detection Buffer incubation (**steps 11–19** of Subheading 3.2). Multiple membranes can be placed next to each other and fit onto a single plastic sheet. Use additional plastics sheets if necessary.
15. Avoid "sliding" the top plastic sheet along the membranes' printed surface.
16. Optimal exposure times will vary, so performing multiple exposure times is strongly recommended. A few seconds to a few minutes is the recommended exposure time range, with 30 s to 1 min being suitable for most samples.
17. For example, let's determine the relative expression of AKT on two different arrays (Arrays 1 and 2). Let's assume that the duplicate signals for the AKT spots on each array are identical (or that the signal intensity used in the following calculation is the mean of the two duplicates spots). Also assume the following:

    $P1 = 2500$
    $P2 = 2700$
    $\mathrm{AKT}(1) = 300$
    $\mathrm{AKT}(2) = 455$
    Then $\mathrm{AKT}(N2) = 455 \times 2500/2700 = 421.30$

    The fold increase of $\mathrm{AKT}(N2)$ vs. $\mathrm{AKT}(1) = 421.3/300 = 1.40$-fold increase or a 40% increase in the signal intensity of AKT in Array 2 vs. Array 1.

References

1. Nair A, Chauhan P, Saha B, Kubatzky KF (2019) Conceptual evolution of cell signaling. Int J Mol Sci 20(13):3292. https://doi.org/10.3390/ijms20133292
2. Lemmon MA, Schlessinger J (2010) Cell signaling by receptor tyrosine kinases. Cell 141(7):1117–1134. https://doi.org/10.1016/j.cell.2010.06.011
3. Sefton BM (2001) Overview of protein phosphorylation. Curr Protoc Cell Biol Chapter 14: Unit 14.11. https://doi.org/10.1002/0471143030.cb1401s00
4. Ubersax JA, Ferrell JE Jr (2007) Mechanisms of specificity in protein phosphorylation. Nat Rev Mol Cell Biol 8(7):530–541. https://doi.org/10.1038/nrm2203

5. Ni Q, Titov DV, Zhang J (2006) Analyzing protein kinase dynamics in living cells with FRET reporters. Methods 40(3):279–286. https://doi.org/10.1016/j.ymeth.2006.06.013
6. Johnson SA, Hunter T (2005) Kinomics: methods for deciphering the kinome. Nat Methods 2(1):17–25. https://doi.org/10.1038/nmeth731
7. Mann M, Ong SE, Gronborg M, Steen H, Jensen ON, Pandey A (2002) Analysis of protein phosphorylation using mass spectrometry: deciphering the phosphoproteome. Trends Biotechnol 20(6):261–268. https://doi.org/10.1016/s0167-7799(02)01944-3
8. de Graauw M, Hensbergen P, van de Water B (2006) Phospho-proteomic analysis of cellular signaling. Electrophoresis 27(13):2676–2686. https://doi.org/10.1002/elps.200600018
9. Brill LM, Salomon AR, Ficarro SB, Mukherji M, Stettler-Gill M, Peters EC (2004) Robust phosphoproteomic profiling of tyrosine phosphorylation sites from human T cells using immobilized metal affinity chromatography and tandem mass spectrometry. Anal Chem 76(10):2763–2772. https://doi.org/10.1021/ac035352d
10. Ross AH, Baltimore D, Eisen HN (1981) Phosphotyrosine-containing proteins isolated by affinity chromatography with antibodies to a synthetic hapten. Nature 294(5842):654–656. https://doi.org/10.1038/294654a0
11. Czernik AJ, Girault JA, Nairn AC, Chen J, Snyder G, Kebabian J, Greengard P (1991) Production of phosphorylation state-specific antibodies. Methods Enzymol 201:264–283. https://doi.org/10.1016/0076-6879(91)01025-w
12. Al-Aidaroos AQ, Yuen HF, Guo K, Zhang SD, Chung TH, Chng WJ, Zeng Q (2013) Metastasis-associated PRL-3 induces EGFR activation and addiction in cancer cells. J Clin Invest 123(8):3459–3471. https://doi.org/10.1172/JCI66824
13. Bao X, Shi J, Xie F, Liu Z, Yu J, Chen W, Zhang Z, Xu Q (2018) Proteolytic release of the p75(NTR) intracellular domain by ADAM10 promotes metastasis and resistance to anoikis. Cancer Res 78(9):2262–2276. https://doi.org/10.1158/0008-5472.CAN-17-2789
14. Qiao L, Hu S, Liu S, Zhang H, Ma H, Huang K, Li Z, Su T, Vandergriff A, Tang J, Allen T, Dinh PU, Cores J, Yin Q, Li Y, Cheng K (2019) microRNA-21-5p dysregulation in exosomes derived from heart failure patients impairs regenerative potential. J Clin Invest 129(6):2237–2250. https://doi.org/10.1172/JCI123135
15. Poling HM, Wu D, Brown N, Baker M, Hausfeld TA, Huynh N, Chaffron S, Dunn JCY, Hogan SP, Wells JM, Helmrath MA, Mahe MM (2018) Mechanically induced development and maturation of human intestinal organoids in vivo. Nat Biomed Eng 2(6):429–442. https://doi.org/10.1038/s41551-018-0243-9
16. Lian JP, Huang R, Robinson D, Badwey JA (1999) Activation of p90RSK and cAMP response element binding protein in stimulated neutrophils: novel effects of the pyridinyl imidazole SB 203580 on activation of the extracellular signal-regulated kinase cascade. J Immunol 163(8):4527–4536
17. Prasad Tharanga Jayasooriya RG, Dilshara MG, Neelaka Molagoda IM, Park C, Park SR, Lee S, Choi YH, Kim GY (2018) Camptothecin induces G2/M phase arrest through the ATM-Chk2-Cdc25C axis as a result of autophagy-induced cytoprotection: implications of reactive oxygen species. Oncotarget 9(31):21744–21757. https://doi.org/10.18632/oncotarget.24934
18. Sanchez-Alcazar JA, Ault JG, Khodjakov A, Schneider E (2000) Increased mitochondrial cytochrome c levels and mitochondrial hyperpolarization precede camptothecin-induced apoptosis in Jurkat cells. Cell Death Differ 7(11):1090–1100. https://doi.org/10.1038/sj.cdd.4400740
19. Kim KW, Kim SH, Lee EY, Kim ND, Kang HS, Kim HD, Chung BS, Kang CD (2001) Extracellular signal-regulated kinase/90-KDA ribosomal S6 kinase/nuclear factor-kappa B pathway mediates phorbol 12-myristate 13-acetate-induced megakaryocytic differentiation of K562 cells. J Biol Chem 276(16):13186–13191. https://doi.org/10.1074/jbc.M008092200

Chapter 20

Using Antibody Arrays for Biomarker Discovery

Shuhong Luo, Yunbiao Ling, Li-Pai Chen, and Ruo-Pan Huang

Abstract

Biomarkers for diseases are important for the development of clinical diagnostic tests and can provide early intervention for cancer or cardiovascular patients. Over the past decade, antibody array technology has achieved significant technological improvement in the quantitative measurement of more than a thousand proteins simultaneously and has been utilized to screen and identify unique proteins as disease biomarkers. However, few biomarkers have been translated into clinical application. This chapter will discuss the protocol for the screening and validation of unique proteins that create a new avenue for biomarker discovery.

Key words Antibody array, Quantibody array, Biomarker

1 Introduction

In 2001, the National Institutes of Health defined the term "biomarker" as "a characteristic that is objectively measured and evaluated as an indicator of normal biological processes, pathogenic processes, or pharmacologic responses to a therapeutic intervention or other health care intervention." Biomarkers include protein, DNA, mRNA, cirRNA, single nucleotide polymorphisms (SNPs), metabolites, etc., which are produced by the diseased organ (e.g., tumor) or by the body in response to disease. Biomarkers are measurable indicators of a specific biological state, the presence, or the stage of disease. In health management, biomarkers could be used for the risk assessment of diseases. In diseases, biomarkers can be utilized for early diagnosis, determining staging and grading, selecting initial therapy, and monitoring therapy and the recurrence of disease [1].

Over the last two decades, proteins as biomarkers have manifested significant impact on the occurrence and development of diseases, and more and more proteins have been identified as biomarkers for the early detection of various fatal diseases such as cancer or autoimmune disorders. For example, carcinoembryonic

Kelly C. Whittaker and Ruo-Pan Huang (eds.), *Antibody Arrays: Methods and Protocols*, Methods in Molecular Biology, vol. 2237, https://doi.org/10.1007/978-1-0716-1064-0_20,

antigen (CEA) for colon cancer, prostate-specific antigen (PSA) for prostate cancer, or alpha-fetoprotein (AFP) for testicular and liver cancer, as well as identification of new drug and vaccine targets [2, 3]. The proteins encoded by these genes are responsible for mediating diseases, and direct proteomic determination of the protein expression changes could provide greater utility for monitoring disease, and it may have implications as a complementary strategy to histopathology [4]. However, many of the protein biomarkers used in the clinic still have a restricted diagnostic value. Therefore, there is a great need for proteomics research which can discover better and novel protein biomarkers possessing high predictive, diagnostic, and prognostic characteristics, which will enable development of high-quality multi-parameter assays with superior performance characteristics to guide diagnosis and management of patients. Proteomic technology for the discovery of biomarkers for diagnosis, prediction of disease course, guiding therapeutic selection, and monitoring response to therapy necessitates a robust, quantitatively accurate, and high-throughput analytical platform.

Although, judging from the decline in biomarker clearance in the past decades, better biomarkers are difficult to obtain, some technologies have been developed to allow for thousands of proteins to be identified and quantified in a single experiment. Mass spectrometry (MS) is a technique which involves measurements of mass-to-charge ratios of the ions formed when a sample is ionized. In recent years, mass spectrometry-based proteomics has developed into a powerful technology that is able to routinely study complex proteome samples. MS-based methods include surface-enhanced laser desorption/ionization (SELDI), time-of-flight mass spectrometry (TOF-MS), magnetic particle-assisted and matrix-assisted and matrix-assisted laser desorption/ionization (MALDI), two-dimensional gel electrophoresis (2D-GE)/MALDI MS, liquid chromatography (LC)-MS, and imaging by MALDI MS [5–10]. However, MS-based methods have poor reproducibility and lack of sensitivity [11], and reproducibility and sensitivity of detection techniques are key determining factors for successful biomarker discovery in biological fluids. Furthermore, multiplexed detection of low-abundance serum protein biomarkers is difficult for MS-based approaches, and the low-abundance serum proteins play a very important role in the etiopathogenesis of diseases, such as the interleukin family, tumor necrosis factors, interferons, and so on. Therefore, antibody array is an important technology for the discovery of disease biomarkers.

Antibody microarrays, on which numerous antibodies are printed at high density as capture agents for selective detection of target proteins, have been demonstrated as a promising approach for the protein profiling of biological samples. Due to high

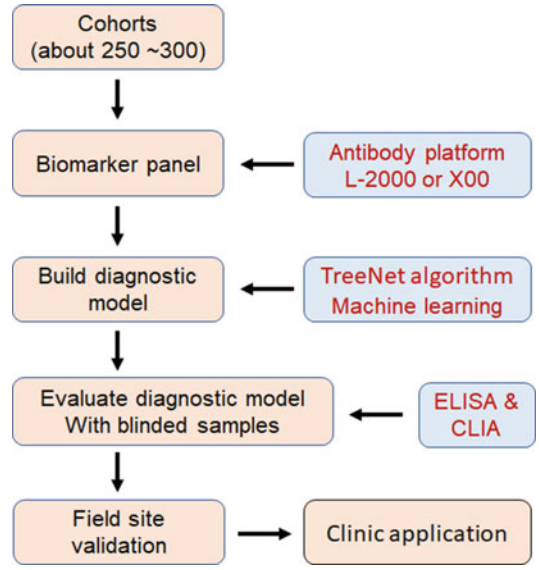

Fig. 1 Workflow for biomarker discovery. A discovery cohort ($N = 250–300$) comprising samples from individuals with disease or normal healthy controls was used to screen and identify a diagnostic biomarker panel using an antibody array platform and TreeNet machine learning. ELISA and CLIA were used to build diagnostic model using a new set of cohorts ($N = 300$). To validate the model and estimate performance, a blinded, fully independent cohort of samples ($N = 200–300$) were used to evaluate the diagnostic model. Finally, the field validation and clinic trail were performed

detection sensitivity, specificity, reproducibility, density, and throughput, antibody microarrays have emerged as a promising technology for multiplexed, quantitative, fast, and cost-effective protein expression profiling for biomarker discovery, diagnosis, prognosis, classification, phenotyping, evidence-based therapy selection, monitoring, and prediction of the risk of diseases. Furthermore, a single biomarker is not expected to capture the complexity of the diseases especially a heterogeneous disease like cancer [12], so the discovery of novel biomarkers for the early detection of disease, monitoring, therapy, and progression using antibody microarray technology is a major thrust of biomedical research. Figure 1 shows the standard procedure of biomarker discovery using antibody array technology. In this chapter, we will discuss how to test and prepare antibody pairs, how to test for cross-reactivity of those antibodies and corresponding antigens for suitability in an array, and the protocol for biomarker discovery using antibody array technology.

2 Materials

2.1 Antibody Pair Preparation

1. Intact monoclonal or polyclonal antibodies without conjugation can be used as capture antibodies on the arrays; biotinylated monoclonal or polyclonal antibodies are used as detection antibodies. The capture antibody and detection antibody measuring the same protein must be evaluated for matching ability (*see* **Note 1**).
2. PBS solution: 140 mM NaCl, 2.7 mM KCl, 10 mM sodium phosphate buffer, pH 7.4.
3. HRP-Streptavidin.
4. TMB reagent.
5. Stop solution: 2 M sulfuric acid.
6. 96-well plate.
7. Orbital shaker.

2.2 Printing of Antibody Microarrays

1. SciFlexarrayer 11 (Scienion).
2. Printing buffer: PBS solution.
3. Carboxyl coated microarray slides.
4. Positive control: Biotinylated bovine serum albumin (BSA) (*see* **Note 2**).
5. Negative control: PBS solution.
6. Multi-well incubation chamber: Chamber with 16 well silicone superstructure (RayBiotech, GA).
7. Standard glass slides.
8. Aluminum foil.

2.3 Clinical Sample Preparation

1. Collect blood samples, and centrifuge blood to separate serum using a standardized protocol, and store serum at −80 °C prior to use (*see* **Note 3**).

2.4 Antibody Array Performance

1. Blocking buffer: 1% (w/v) casein and 1% (v/v) Tween-20 in PBS.
2. Washing buffer I: 0.05% (v/v) Tween-20 in PBS.
3. Washing buffer II: PBS solution.
4. Cy3 equivalent dye-conjugated streptavidin.
5. 96-well plate washer.
6. Microarray Scanner equipped with a Cy3 wavelength.
7. Mapix or similar analysis software.

3 Methods

3.1 Preparation of Antibody Pairs

1. Dilute the antibodies to 0.2 mg/μL in PBS.
2. Add 100 μL of the diluted capture antibodies to each well of the 96-well plate, and incubate at room temperature with gentle shaking using the orbital shaker.
3. Remove the capture antibodies and add 200 μL of Washing buffer I to each well. Repeat three times for a total of four washes.
4. Remove Washing buffer I from the wells and add 100 μL of the corresponding protein to each well and incubate for 2 h at room temperature with gentle shaking using the orbital shaker.
5. Remove the corresponding protein and add 200 μL of Washing buffer I to each well. Repeat three times for a total of four washes.
6. Remove Washing buffer I from the wells and add 100 μL of the diluted detection antibodies into the appropriate wells and incubate for 2 h at room temperature with gentle shaking.
7. Remove the detection antibodies from the wells and add 100 μL of HRP-Streptavidin and incubate for 45 min at room temperature with gentle shaking.
8. Remove the HRP-Streptavidin from the wells and add 200 μL of Washing buffer I to each well. Repeat three times for a total of four washes.
9. Remove Washing buffer I from the wells and add 100 μL of TMB reagent to each well. Incubate for 30 min at room temperature in the dark with gentle shaking.
10. Remove the TMB reagent from the wells and add 50 μL of Stop solution to each well. Read at 450 nm immediately.

3.2 Printing of Antibody Arrays

1. Spin-down the antibodies and positive and negative controls.
2. Dilute the antibodies (*see* **Note 4**) and the positive control (10 μg/μL) with PBS (*see* **Note 5**).
3. Design the print layout (*see* **Note 6**).
4. Print the arrays using a microarray printer (*see* **Note 2**).
5. Dry the slides at room temperature.

3.3 Exclusion of Cross-Reactivity

1. Mount the slide in the multi-well incubation chamber.
2. Add 100 μL of Blocking buffer into each well and incubate at room temperature for 30 min to block the slides.
3. Decant the buffer from each well. Add 100 μL of detection antibody to each well (*see* **Note 9**). Incubate the arrays at room temperature for 2 h.

4. Decant the detection antibody from each well and wash five times (5 min each) with 150 μL of Washing buffer I at room temperature with gentle shaking. Completely remove the Washing buffer in each wash step. Dilute 20× Wash Buffer I with H2O.
5. Decant the 1× Wash Buffer I from each well, wash two times (5 min each) with 150 μL of 1× Wash Buffer II at room temperature with gentle shaking. Completely remove wash buffer in each wash step.
6. Add 100 μL of Cy3 equivalent dye-conjugated streptavidin (1 μg/μL) to each well. Cover the slide with aluminum foil to avoid exposure to light or incubate in a dark room. Incubate at room temperature for 1 h.
7. Decant the Cy3 equivalent dye-conjugated streptavidin from each well. Wash five times (5 min each) with 150 μL of Washing buffer I at room temperature with gentle shaking. Completely remove the wash buffer in each wash step.
8. Wash two times (5 min each) with 150 μL of Washing buffer II at room temperature with gentle shaking. Completely remove the wash buffer in each wash step.
9. Disassemble the multi-well incubation chamber by pushing clips outward from the slide side. Carefully remove the slide from the multi-well incubation chamber.
10. Remove droplets completely by gently applying suction with a pipette. Do not touch the array, only the sides.
11. Scan the slides using the microarray scanner equipped with a Cy3 wavelength (green channel) and analyze the cross-reactivity using Mapix or similar software (*see* **Note 7**).

3.4 Sample Detection

1. Dilute serum samples with Blocking buffer at 1:1.
2. Add 100 μL Blocking buffer into each well of an array printed slide and incubate at room temperature for 30 min to block slides.
3. Decant the Blocking buffer from each well. Add 100 μL of diluted serum to each well. Incubate the arrays at room temperature for 1–2 h.
4. Decant the serum from each well. Wash five times (5 min each) with 150 μL of Washing buffer I at room temperature with gentle shaking. Completely remove the wash buffer in each wash step.
5. Decant the Washing buffer I from each well and wash two times (5 min each) with 150 μL of Washing buffer II at room temperature with gentle shaking. Completely remove the wash buffer in each wash step.

6. Add 100 μL of detection antibody to each well (*see* **Note 8**). Incubate arrays at room temperature for 2 h.
7. Decant the detection antibody from each well. Wash five times (5 min each) with 150 μL of Washing buffer I at room temperature with gentle shaking. Completely remove the wash buffer in each wash step.
8. Decant the Washing buffer I from each well. Wash two times (5 min each) with 150 μL of Washing buffer II at room temperature with gentle shaking. Completely remove the wash buffer in each wash step.
9. Add 100 μL 1 μg/μL Cy3 equivalent dye-conjugated streptavidin to each well. Cover the device with aluminum foil to avoid exposure to light or incubate in dark room. Incubate at room temperature for 1 h.
10. Decant the Cy3 equivalent dye-conjugated streptavidin from each well. Wash five times (5 min each) with 150 μL of Washing buffer I at room temperature with gentle shaking.
11. Decant the Washing buffer I from each well. Wash two times (5 min each) with 150 μL of Washing buffer II at room temperature with gentle shaking. Completely remove the wash buffer in each wash step.
12. Disassemble the multi-well incubation chamber by pushing clips outward from the slide side. Carefully remove the slide from the multi-well incubation chamber.
13. Remove droplets completely by gently applying suction with a pipette. Do not touch the array, only the sides.
14. Scan the slides using the microarray scanner equipped with a Cy3 wavelength (green channel) and analyze the cross-reactivity using Mapix or similar software (*see* **Note 9**).

3.5 Data Analysis

1. Perform slide-to-slide normalization by the values of the positive control from each array.
2. The signal intensity values represent the protein expression profile, indicating which proteins are present and at what relative level.
3. Comparison of protein expression profiles for different sample cohorts, e.g., healthy versus disease, can be done using an ANOVA. The ability to classify two groups can be estimated using support vector machine (SVM) in R and be described by a receiver operating characteristic (ROC) curve.

4 Notes

1. The capture antibody and detection antibody from the same protein must simultaneously recognize the protein, a hallmark of the sandwich detection principle, which has higher specificity for the protein detection compared with single antibody approaches.
2. Dyes can be used as positive control as well. We used biotinylated BSA as a positive control.
3. The blood sample is centrifuged at 2000 × *g* for 10 min at 4 °C, and the supernatant is collected as the serum sample. The serum sample should be aliquoted and rapidly frozen at −80 °C. Repeated freeze-thaws should be avoided.
4. The spotting concentration depends on the affinity of the antibody. This will have to be optimized for each antibody. We use an antibody concentration of 0.2 mg/μL as the starting concentration.
5. The concentration of the positive control depends on the suggestion of the manufacturer.
6. Antibodies and positive and negative controls in an array are printed with quadruplicate spots. Four spots of each individual antibody/control are arranged in the same row. Sixteen identical arrays are printed on a slide.
7. The cross-reactivity will be considered negative if there is not any signal visible on the array.
8. The concentration of the detection antibody depends on its affinity.
9. The signal intensity values are read using the fixed circle method, and the median values of the spots are adopted.

References

1. Atkinson A J et al, NCI-FDA Biomarkers Definitions Working Group (2001) Biomarkers and surrogate endpoints: preferred definitions and conceptual framework. Clin Pharmacol Ther 69:89–95
2. Hanash S (2003) Disease proteomics. Nature 422:226–232
3. Moseley FL, Bicknell KA, Marber MS, Brooks G (2007) The use of proteomics to identify novel therapeutic targets for the treatment of disease. J Pharm Pharmacol 59:609–628
4. Petricoin EF, Zoon KC, Kohn EC, Barrett JC, Liotta LA (2002) Clinical proteomics: translating benchside promise into bedside reality. Nat Rev Drug Discov 1:683–695
5. Petricoin EF III, Liotta LA (2004) SELDI-TOF-based serum proteomic pattern diagnostics for early detection of cancer. Curr Opin Biotechnol 15:24–30
6. Villanueva J, Philip J, Entenberg D, Chaparro CA, Tanwar Mk, Holland EC, Tempst P (2004) Serum peptide profiling by magnetic particle-assisted, automated sample processing and MALDI-TOF mass spectrometry. Anal Chem 76:1560–1570
7. Bergman AC, Benjamin T, Alaiya A, Waltham M, Sakaguchi K, Franzen B, Linder S, Bergman T, Auer G, Appella E, Wirth PJ, Jornavall H (2000) Identification of gel-separated tumor marker proteins by mass spectrometry. Electrophoresis 21:679–686

8. Govorukhina NI, Keizer-Gunnink A, van der Zee AGJ, de Jong S, de Bruijin HWA, Bischoff R (2003) Sample preparation of human serum for the analysis of tumor markers-comparison of different approaches for albumin and gamma-globulin depletion. J Chromatogr A 1009:171–178
9. Neuhoff N, Kaiser T, Wittke S, Krebs R, Pitt A, Burchard A, Sundmacher A, Schlegelberger B, Kolch W, Mischak H (2004) Mass spectrometry for the detection of differentially expressed proteins: a comparison of surface-enhanced laser desorption/ionization and capillary electrophoresis/mass spectrometry. Rapid Commun Mass Spectrom 18:149–156
10. Chaurand P, Schwartz SA, Caprioli RM (2004) Assessing protein patterns in disease using imaging mass spectrometry. J Proteome Res 3:245–252
11. Baggerly KA, Morris JS, Coombes KR (2004) Reproducibility of SELDI-TOF protein patterns in serum: comparing datasets from different experiments. Bioinformatics 20:777–785
12. Anderson KS, LaBaer J (2005) The sentinel within: exploiting the immune system for cancer biomarkers. J Proteome Res 4:1123–1133

Chapter 21

Immune Cell Isolation from Murine Intestine for Antibody Array Analysis

Joshua A. Owens and Rheinallt M. Jones

Abstract

Gut mucosal immune cells play an essential role in health due to their ability to orchestrate host signaling events in response to exogenous antigens. These antigens may originate from microorganisms including viruses, commensal or pathogenic bacteria, or single-celled eukaryotes, as well as from dietary foodstuff-derived proteins or products. A critical technological capacity to understand host responses to antigens is the ability to efficiently isolate and functionally characterize immune cells from intestinal tissues. Additionally, after characterization, it is of paramount importance to understand the exact functions of these immune cells under different disease states or genetic variables. Here, we outline methods for immune cell isolation from murine small and large intestines with the goal of undertaking a functional analysis of isolated cell types using antibody array platforms.

Key words Intestine, Lamina propria lymphocytes, Intraepithelial lymphocytes, Peyer's patch, Antibody array

Abbreviations

IEL	Intraepithelial lymphocytes
LI	Large intestine
LPL	Lamina propria lymphocytes
PP	Peyer's patch
SI	Small intestine

1 Introduction

Immune cells in the intestinal mucosa continually sample and confront antigens released by microorganisms or foodstuff in the gut lumen [1, 2]. This luminal sampling and subsequent immune response is tightly regulated to maintain a balance between host defenses against pathogens while at the same time avoiding the onset of chronic inflammatory conditions [3–5]. Failure to resolve

Kelly C. Whittaker and Ruo-Pan Huang (eds.), *Antibody Arrays: Methods and Protocols*, Methods in Molecular Biology, vol. 2237, https://doi.org/10.1007/978-1-0716-1064-0_21,

inflammation can lead to a disruption of repair processes. Therefore, the inability to resolve inflammation is an underlying cause of conditions such as chronic inflammatory bowel disease [6–11]. Antigen-presenting cells (APCs), especially macrophages and dendritic cells (DCs), function at the frontline of microbial surveillance where they process foreign substances and present them to other immune cells, initiating an immune response involving T-cells, B-cells, innate lymphoid cells, and other cell types [12–15]. Structurally, the gut epithelial layer forms a selectively permeable barrier separating the luminal contents from sub-epithelial compartments through the generation of a mucus layer on the epithelium and by the expression of tight junction proteins that connect the epithelial cells together and maintain a tight barrier across the epithelial layer [16, 17]. The sub-epithelial compartment, known as the lamina propria (LP), harbors a substantial number of APCs and adaptive immune cells and is therefore perfectly situated to sample and respond to gut luminal contents that penetrate the epithelial layer [18–21]. This surveillance by APCs is essential for shaping community balance within the microbiota, for preserving the health of the intestinal tissue, and for orchestrating efficient responses against invading pathogens [22–26]. Paramount to understanding the mechanisms whereby these immune cells perform their tasks is the ability to efficiently isolate APCs and adaptive immune cells from a complex tissue. Several studies have outlined methodologies to isolate these cells; however, standardization of techniques is essential, especially when comparing immune activities under either steady-state, inflammatory, or specific genetic ablation conditions [27–30]. Here, we outline methodology for the efficient isolation of immune cell types from gut tissue including lamina propria lymphocytes (LPLs), intraepithelial lymphocytes (IELs), and cells within the Peyer's patches (PPs). Isolated cell types may be subsequently analyzed by multiplex ELISA antibody array platforms to identify critical chemokines or cytokines secreted by specific cell types under healthy or disease conditions.

2 Materials

2.1 Equipment

1. FACS Aria II or another FACS sorter.
2. MaxQ 4450 benchtop orbital shaker or any orbital shaker with sufficient capacity and temperature control.
3. (Optional) LS MACS Columns and MidiMACS Separator (Miltenyi Biotec).

2.2 Reagents and Solutions

1. 1× Hank's Balanced Salt Solution (HBSS), without phenol red, Ca^{2+}- and Mg^{2+}-free.
2. 1× PBS, Ca^{2+}- and Mg^{2+}-free.
3. Complete RPMI-1640 Medium: RPMI-1640 medium with 10% FBS.
4. Epithelial Digestion Buffer: 1× HBSS with 5% FBS, 5 mM EDTA, 10 mM HEPES.
5. LPL Digestion Buffer: RPMI-1640 medium with 10% FBS, 1 mg/mL collagenase type VIII, 50 μg/mL DNAse I.
6. 90% Percoll Solution: Mix 9 parts 100% Percoll with 1 part 10× HBSS, without phenol red, Ca^{2+}- and Mg^{2+}-free.
7. 30% Percoll Solution: Mix 2 parts 90% Percoll Solution with 1 part complete RPMI medium.
8. FACS Buffer: 1× PBS with 5% FBS and 0.5 mM EDTA.

2.3 Antibody and Staining Reagents

1. Ice-Cold Staining Buffer: 1× PBS with 5% FBS.
2. LIVE/DEAD Fixable Near-IR Dead Cell Stain Kit: use at a 1:1000 dilution.
3. Desired antibodies: for this protocol, we isolated activated CD4 T-cells with CD3-APC mAb (17A2) at 1:100 dilution, CD4-PerCP mAb (GK1.5) at a 1:100 dilution, CD8a-Brilliant Violet 605 mAb (53-6.7) at a 1:100 dilution, and CD45RB-FITC mAb (MB4B4) at a 1:100 dilution (*see* **Note 1**).
4. Cells can be extracted via MACS separation if a FACS sorter is unavailable (*see* **Note 2**).

2.4 Disposable Reagents

1. 50 mL conical tubes.
2. Small weigh boats.
3. 70 μm cell strainer.
4. 40 μm cell strainer flow cap.
5. 5 mL polystyrene round-bottom tubes.
6. Plastic 18 G × 38 mm gavage tube.
7. 1 mL syringe.

3 Methods

3.1 Dissection and Preparation of Small and Large Intestines

1. Warm the 1× PBS and Epithelial Digestion Buffer to room temperature, and warm the orbital shaker to 37 °C.
2. Euthanize mice according to approved IACUC guidelines.
3. Spray the mouse abdomen with 70% ethanol, make a horizontal incision with scissors, peel the back skin, and cut open the peritoneum.

4. Cut the intestine at the pyloric sphincter to separate the stomach from the proximal small intestine.
5. Carefully remove the small intestine while teasing away from the mesentery, and cut at the ileocecal valve to separate the small intestine from the large intestine.
6. Carefully remove the large intestine from the mesentery, and make a cut at the anal verge.
7. With the removed small and large intestine, push the luminal contents out by inserting an 18 G × 38 mm plastic gavage tube attached to a 1 mL syringe filled with PBS so that luminal contents flow out the other end of the intestine. Repeat this twice or until flow-through is no longer clouded. Alternatively, the intestine can be placed in a petri dish filled with PBS and moved rapidly around the dish so that luminal contents are emptied and dish is clouded. Repeat until dish is no longer clouded, about three to four times.
8. Take the small intestine and remove all Peyer's patches (PP). To isolate immune cells from the PP, push all PP through a 70-μm filter using a stopper from a 3 mL syringe to crush the PP and push the cells through.
9. Add 4–5 mL of ice-cold media, and push the media through the filter. Flow-through of PP cells should be placed in a 15 mL conical tube and can be stored on ice until done processing the intestine (*see* **Note 3**).
10. Open the small intestine longitudinally, and then cut into small pieces around 1 cm and place into a 50 mL tube with 30 mL of pre-warmed Epithelial Digestion Buffer.
11. Open the large intestine longitudinally, and then cut into small pieces around 1 cm, and place in a 50 mL tube with 30 mL of pre-warmed Epithelial Digestion Buffer (*see* **Notes 4** and **5**).

3.2 Removal of the Epithelial Layer

1. Place each 50 mL conical tube horizontally into an orbital shaker, and tape down to secure. Shake at 250 rpm for 20 min at 37 °C in order to remove the epithelium and intraepithelial lymphocytes (IELs).
2. Pour the contents of each 50 mL tube through a wire mesh strainer to recover the small pieces of tissue while allowing the epithelium and IELs pass through. If analyses of epithelial cells and IELs are desired, then place a 50 mL conical tube under the strainer during this step and place on ice.
3. Repeat these two steps one additional time for a total of 40 min of shaking.
4. After the last digestion, rinse the tissue in the strainer with 1× PBS to remove trace amounts of EDTA before proceeding (*see* **Note 6**).

3.3 Digestion of Intestinal Tissue

1. Warm the LPL Digestion Buffer and the orbital shaker to 37 °C.
2. Transfer the pieces of intestinal tissue from the strainer to the dissection board, and mince using sharp dissection scissors or a clean razor blade.
3. Transfer the minced intestine tissue to a 50 mL conical tube containing 20 mL of the LPL Digestion Buffer (*see* **Note 7**).
4. Place the conical tubes horizontally on the orbital shaker, and secure with tape, and digest at 200 rpm for 15 min at 37 °C.
5. Vortex for 5 s and then filter through a 70-μm cell strainer; use a stopper from a 3 mL syringe to help push the cells through. Add an additional 3–5 mL of media to push through remaining cells.
6. Add enough media to top off each 50 mL tube, and then centrifuge at 300 × *g* for 5 min at 4 °C (*see* **Note 8**).
7. Pour off the supernatant, and resuspend in 1 mL of complete RPMI = 1640 medium.

3.4 Isolation of Immune Cells

1. For isolating immune cells from each sample, fill a 50 mL conical tube with 10 mL of 30% Percoll solution. Then, using a glass pipette, add 5 mL of 90% Percoll below the 30% Percoll (*see* **Note 9**).
2. Layer cells on top of the 30% Percoll using a 1 mL pipette, pipetting along the side of the tube.
3. Centrifuge at 670 × *g* for 30 min at room temperature, and set the brakes and acceleration to slow.
4. After centrifugation, carefully remove the conical tubes and aspirate to the 7 mL line. Immune cells should be at the 30:90 interface in a small band. Add cold, complete RPMI-1640 medium to fill the conical tube.
5. Centrifuge at 300 × *g* for 5 min at 4 °C to pellet cells. Additionally, PP cells can be spun down at this point (*see* **Notes 10** and **11**).
6. At this point, if total immune cell analysis is desired, proceed to the antibody array protocol. If specific immune cells are desired, continue with Subheading 3.5.

3.5 FACS Sorting of Immune Cell Populations

1. Make Antibody Master Mix by combining 100 μL of ice-cold FACS buffer per sample with 1 μL of antibody per sample. Then add LIVE/DEAD Fixable Near-IR at a 1:1000 dilution. (*See* Subheading 3.6 Optional Protocol: MACS Separation if FACS sorting is unavailable.)

2. Resuspend each pellet with 100 μL of the Antibody Master Mix, and transfer from the conical tube to a 96-well round-bottom plate.
3. Incubate the samples in the dark at 4 °C for 30–40 min (*see* **Note 12**).
4. Centrifuge cells at 300 × *g* for 5 min at 4 °C to pellet, and flick off supernatant.
5. Wash cells by adding 200 μL of ice-cold FACS buffer, and repeat **step 4**. Wash for three times total.
6. Resuspend in 200 μL–1 mL depending on cell density. Density should be around 1×10^8 cells/mL, but a lower density is acceptable.
7. Transfer to a FACS tube with a 40-μm flow cap by placing pipette tip on the filter and slowly pushing the cells through. The cells are now ready for FACS sorting (Fig. 1, *see* **Note 13**).
8. After sorting, cells are ready to be analyzed by antibody array analysis according to the manufacturer's instructions. Typically, protein concentrations of between 200 and 500 μg/mL in a working volume of 100 μL are sufficient for faithful quantitative analysis of cytokines and chemokines within sorted immune cells using the antibody array platform.

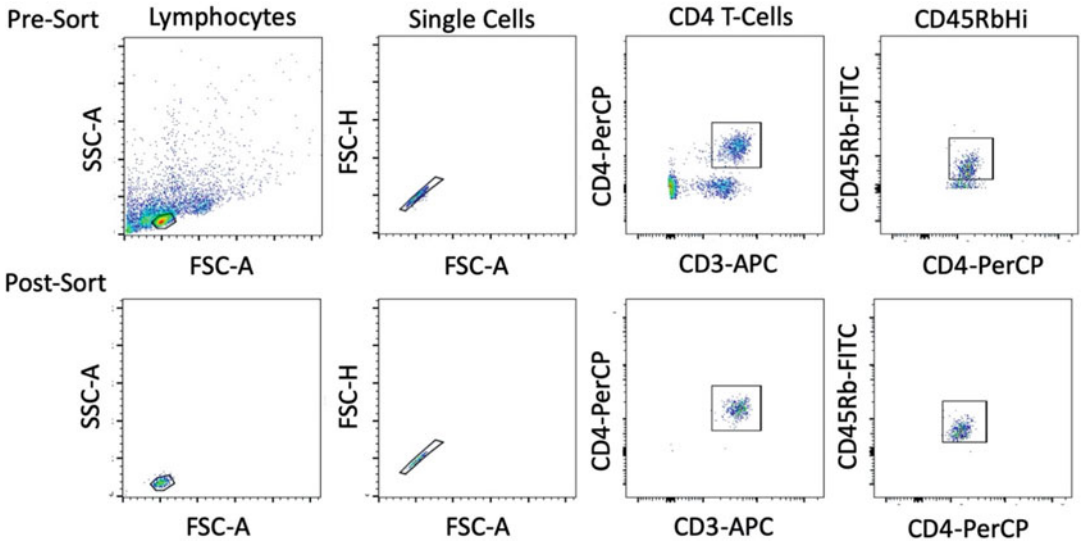

Fig. 1 FACS gating strategy for isolation of activated CD4 T-cells. First, gate by forward and side scatter for T-cells. Innate immune cells are the next population to the right and up for T-cells/B-cells. Next, gate by forward scatter area and height. This will ensure single cells. Next, gate by expression of CD4 and CD3. Finally, activated CD4 T-cells express high levels of CD45Rb, so draw the gate above a set threshold. This results in greater than 99% purity of the desired population and greater than 99% viability by trypan blue or LIVE/DEAD Near-IR staining

9. If antibody array analysis cannot be done immediately or if samples need to be shipped, immediately freeze down cells to preserve proteins for subsequent analysis, or immediately extract proteins and freeze down samples.

3.6 Optional: MACS Separation

1. Incubate the cells after Percoll separation with the desired MACS microbeads according to the manufacturer's instructions.
2. Wash the cells with ice-cold FACS buffer followed by centrifugation at 300 × *g* for 5 min at 4 °C.
3. Discard the supernatant, and pass the cells through a 40-μm filter.
4. Enrich for magnetic bead-attached cells by positive selection using a MidiMACS Separator and an LS magnetic column according to the manufacturer's instructions.
5. Either freeze cells down immediately or immediately extract protein as per standard methodologies for subsequent antibody array analysis.

4 Notes

1. The antibodies chosen in this protocol are for the explicit purpose of isolating CD4 T-cells from the intestine. If total immune cell populations are preferred, then this can be done after the Percoll separation step.
2. The use of a FACS sorter is the preferred sorting method, as this produces greater than 99% pure populations of the specific cells of interest. If FACS sorting is unavailable, MACS separation can give >90% pure populations of general immune cell subsets.
3. **Steps 1–10** of Subheading 3.1 should be performed as quickly as possible to ensure adequate cell yield and viability.
4. Peyer's patches can be difficult to see, but they will be a lighter tone compared to adjacent intestine tissue and will be slightly raised. To help distinguish PP from the surrounding tissue, move the darker luminal contents in the ileum toward the jejunum and duodenum to help distinguish the lighter PP. There should be around 8 PP in a healthy, adult mouse. They are mostly evenly spaced which can aid in finding all PP.
5. Each small and large intestine after being cut into 1 cm pieces should be placed into individual conical tubes. When isolating intestines from more than one animal, it is important to not

place more than one tissue sample per conical tube. This prevents increased cell death. If samples need to be pooled for adequate numbers, do so just before antibody array analysis.

6. EDTA is used during the epithelial digestion step. EDTA is an inhibitor of collagenase. We routinely wash the tissue in the strainer with PBS or medium to remove trace amounts of EDTA as to not inhibit the collagenase digestion.
7. We have had success with both type VIII and type IV collagenase from Sigma-Aldrich. In our hands, type IV collagenase is optimal for digestion of the large intestine.
8. Sometimes, a solid pellet for the large intestine samples is not observed. Either invert the sample several times and centrifuge again or remove supernatant until close to pellet and fill with fresh medium and centrifuge again. This is mostly due to high levels of fat in the sample.
9. This ensures a clean line of separation between the 90% Percoll and the 30% Percoll. Adding 90% Percoll and then adding 30% Percoll on top create too much mixing of the solutions and will not allow proper separation of immune cells in the Percoll gradient.
10. At this point, there should be small intestine IELs, large intestine IELs, small intestine LPLs, large intestine LPLs, and PP. These cells can be frozen down at −80 °C in complete RPMI medium with 10% DMSO and stored for 3–6 months. Freezing cells will decrease cell viability and should be avoided if possible, and some immune cells such as neutrophils will not survive freezing down.
11. If total immune cell population is desired, then combine the IEL population with the LPL population.
12. It is possible to overstain cells. Maximum time for incubation is around 1 h 30–40 min is preferred but may need to be adjusted depending on the specific antibodies chosen.
13. For all FACS staining, unstained intestinal cells can be used as a negative control to assist in gating. Additionally, compensation beads can be used.

Acknowledgments

R.M.J. is supported, in part, by NIH Grant R01DK098391.

References

1. Backhed F, Ley RE, Sonnenburg JL, Peterson DA, Gordon JI (2005) Host-bacterial mutualism in the human intestine. Science 307(5717):1915–1920. https://doi.org/10.1126/science.1104816
2. Jones RM (2016) The influence of the gut microbiota on host physiology: in pursuit of mechanisms. Yale J Biol Med 89(3):285–297
3. Artis D (2008) Epithelial-cell recognition of commensal bacteria and maintenance of immune homeostasis in the gut. Nat Rev Immunol 8(6):411–420. https://doi.org/10.1038/nri2316
4. Denning TL, Wang YC, Patel SR, Williams IR, Pulendran B (2007) Lamina propria macrophages and dendritic cells differentially induce regulatory and interleukin 17-producing T cell responses. Nat Immunol 8(10):1086–1094. https://doi.org/10.1038/ni1511
5. Coombes JL, Siddiqui KR, Arancibia-Carcamo CV, Hall J, Sun CM, Belkaid Y, Powrie F (2007) A functionally specialized population of mucosal CD103+ DCs induces Foxp3+ regulatory T cells via a TGF-beta and retinoic acid-dependent mechanism. J Exp Med 204(8):1757–1764. https://doi.org/10.1084/jem.20070590
6. Gong Y, Lin Y, Zhao N, He X, Lu A, Wei W, Jiang M (2016) The Th17/Treg immune imbalance in ulcerative colitis disease in a Chinese Han population. Mediat Inflamm 2016:7089137. https://doi.org/10.1155/2016/7089137
7. Xavier RJ, Podolsky DK (2007) Unravelling the pathogenesis of inflammatory bowel disease. Nature 448(7152):427–434. https://doi.org/10.1038/nature06005
8. Matthews JD, Owens JA, Naudin CR, Saeedi BJ, Alam A, Reedy AR, Hinrichs BH, Sumagin R, Neish AS, Jones RM (2019) Neutrophil-derived reactive oxygen orchestrates epithelial cell signaling events during intestinal repair. Am J Pathol 189(11):2221–2232. https://doi.org/10.1016/j.ajpath.2019.07.017
9. Jones RM, Desai C, Darby TM, Luo L, Wolfarth AA, Scharer CD, Ardita CS, Reedy AR, Keebaugh ES, Neish AS (2015) Lactobacilli modulate epithelial cytoprotection through the Nrf2 pathway. Cell Rep 12(8):1217–1225. https://doi.org/10.1016/j.celrep.2015.07.042
10. Alam A, Leoni G, Wentworth CC, Kwal JM, Wu H, Ardita CS, Swanson PA, Lambeth JD, Jones RM, Nusrat A, Neish AS (2014) Redox signaling regulates commensal-mediated mucosal homeostasis and restitution and requires formyl peptide receptor 1. Mucosal Immunol 7(3):645–655. https://doi.org/10.1038/mi.2013.84
11. Alam A, Leoni G, Quiros M, Wu H, Desai C, Nishio H, Jones RM, Nusrat A, Neish AS (2016) The microenvironment of injured murine gut elicits a local pro-restitutive microbiota. Nat Microbiol 1:15021. https://doi.org/10.1038/nmicrobiol.2015.21
12. Liu LM, MacPherson GG (1993) Antigen acquisition by dendritic cells: intestinal dendritic cells acquire antigen administered orally and can prime naive T cells in vivo. J Exp Med 177(5):1299–1307. https://doi.org/10.1084/jem.177.5.1299
13. Van Wilsem EJ, Van Hoogstraten IM, Breve J, Scheper RJ, Kraal G (1994) Dendritic cells of the oral mucosa and the induction of oral tolerance. A local affair. Immunology 83(1):128–132
14. Masopust D, Soerens AG (2019) Tissue-resident T cells and other resident leukocytes. Annu Rev Immunol 37:521–546. https://doi.org/10.1146/annurev-immunol-042617-053214
15. Brown EM, Kenny DJ, Xavier RJ (2019) Gut microbiota regulation of T cells during inflammation and autoimmunity. Annu Rev Immunol 37:599–624. https://doi.org/10.1146/annurev-immunol-042718-041841
16. Van der Sluis M, De Koning BA, De Bruijn AC, Velcich A, Meijerink JP, Van Goudoever JB, Buller HA, Dekker J, Van Seuningen I, Renes IB, Einerhand AW (2006) Muc2-deficient mice spontaneously develop colitis, indicating that MUC2 is critical for colonic protection. Gastroenterology 131(1):117–129. https://doi.org/10.1053/j.gastro.2006.04.020
17. Farquhar MG, Palade GE (1963) Junctional complexes in various epithelia. J Cell Biol 17:375–412. https://doi.org/10.1083/jcb.17.2.375
18. Hume DA, Robinson AP, MacPherson GG, Gordon S (1983) The mononuclear phagocyte system of the mouse defined by immunohistochemical localization of antigen F4/80. Relationship between macrophages, Langerhans cells, reticular cells, and dendritic cells in lymphoid and hematopoietic organs. J Exp Med 158(5):1522–1536. https://doi.org/10.1084/jem.158.5.1522
19. Egan CE, Maurer KJ, Cohen SB, Mack M, Simpson KW, Denkers EY (2011) Synergy

between intraepithelial lymphocytes and lamina propria T cells drives intestinal inflammation during infection. Mucosal Immunol 4(6): 658–670. https://doi.org/10.1038/mi.2011.31

20. Eisenbarth SC (2019) Dendritic cell subsets in T cell programming: location dictates function. Nat Rev Immunol 19(2):89–103. https://doi.org/10.1038/s41577-018-0088-1
21. Jones RM, Neish AS (2017) Redox signaling mediated by the gut microbiota. Free Radic Biol Med 105:41–47. https://doi.org/10.1016/j.freeradbiomed.2016.10.495
22. Round JL, Mazmanian SK (2009) The gut microbiota shapes intestinal immune responses during health and disease. Nat Rev Immunol 9(5):313–323. https://doi.org/10.1038/nri2515
23. Frank DN, St Amand AL, Feldman RA, Boedeker EC, Harpaz N, Pace NR (2007) Molecular-phylogenetic characterization of microbial community imbalances in human inflammatory bowel diseases. Proc Natl Acad Sci U S A 104(34):13780–13785. https://doi.org/10.1073/pnas.0706625104
24. van Wilgenburg B, Scherwitzl I, Hutchinson EC, Leng T, Kurioka A, Kulicke C, de Lara C, Cole S, Vasanawathana S, Limpitikul W, Malasit P, Young D, Denney L, Consortium S-H, Moore MD, Fabris P, Giordani MT, Oo YH, Laidlaw SM, Dustin LB, Ho LP, Thompson FM, Ramamurthy N, Mongkolsapaya J, Willberg CB, Screaton GR, Klenerman P (2016) MAIT cells are activated during human viral infections. Nat Commun 7:11653. https://doi.org/10.1038/ncomms11653
25. Schreiber HA, Loschko J, Karssemeijer RA, Escolano A, Meredith MM, Mucida D, Guermonprez P, Nussenzweig MC (2013) Intestinal monocytes and macrophages are required for T cell polarization in response to Citrobacter rodentium. J Exp Med 210(10): 2025–2039. https://doi.org/10.1084/jem.20130903
26. Jung S, Unutmaz D, Wong P, Sano G, De los Santos K, Sparwasser T, Wu S, Vuthoori S, Ko K, Zavala F, Pamer EG, Littman DR, Lang RA (2002) In vivo depletion of CD11c+ dendritic cells abrogates priming of CD8+ T cells by exogenous cell-associated antigens. Immunity 17(2):211–220
27. Tyagi AM, Yu M, Darby TM, Vaccaro C, Li JY, Owens JA, Hsu E, Adams J, Weitzmann MN, Jones RM, Pacifici R (2018) The microbial metabolite butyrate stimulates bone formation via T regulatory cell-mediated regulation of WNT10B expression. Immunity 49(6): 1116–1131, e1117. https://doi.org/10.1016/j.immuni.2018.10.013
28. Tanoue T, Morita S, Plichta DR, Skelly AN, Suda W, Sugiura Y, Narushima S, Vlamakis H, Motoo I, Sugita K, Shiota A, Takeshita K, Yasuma-Mitobe K, Riethmacher D, Kaisho T, Norman JM, Mucida D, Suematsu M, Yaguchi T, Bucci V, Inoue T, Kawakami Y, Olle B, Roberts B, Hattori M, Xavier RJ, Atarashi K, Honda K (2019) A defined commensal consortium elicits CD8 T cells and anticancer immunity. Nature 565(7741):600–605. https://doi.org/10.1038/s41586-019-0878-z
29. van Unen V, Li N, Molendijk I, Temurhan M, Hollt T, van der Meulen-de Jong AE, Verspaget HW, Mearin ML, Mulder CJ, van Bergen J, Lelieveldt BP, Koning F (2016) Mass cytometry of the human mucosal immune system identifies tissue- and disease-associated immune subsets. Immunity 44(5): 1227–1239. https://doi.org/10.1016/j.immuni.2016.04.014
30. Li JY, Chassaing B, Tyagi AM, Vaccaro C, Luo T, Adams J, Darby TM, Weitzmann MN, Mulle JG, Gewirtz AT, Jones RM, Pacifici R (2016) Sex steroid deficiency-associated bone loss is microbiota dependent and prevented by probiotics. J Clin Invest 126(6):2049–2063. https://doi.org/10.1172/JCI86062

Chapter 22

Database Development for Antibody Arrays

Zhaowei Xu, Likun Huang, and Sheng-Ce Tao

Abstract

Antibody arrays have been widely applied in both basic research and clinical studies. Data analysis, archiving, and sharing of resulting data are very important for exploring and expanding the power of antibody microarray studies. The protein microarray database (PMD) has provided standards tailored for the management of protein microarray data and constructed an automated pipeline for array data analysis. In this chapter, we will describe the framework design, platform construction, and analysis tool integration of the PMD.

Key words Antibody array, Database, Data analysis, Data archiving and Data sharing

1 Introduction

Antibody array is a miniaturized and high-throughput analysis system and is a specific type of protein microarray[1]. As a powerful technology of proteomics, antibody arrays have already been applied in a wide range of biological or clinical studies, such as the investigations of the serum antigen and the fast comparison of the levels of a defined set of proteins in a pair or among a group of related samples [2, 3]. Because it is a high-throughput and highly efficient analysis platform, a large amount of data have already been generated by antibody microarray analysis, and more data could be expected in the near future. The question now is how to organize and store these valuable data in a central place, facilitating free access and aiding other researchers to make full use of these data. Thus, a database specifically designed for protein/antibody microarray data is needed. To address this need, we have constructed a database, i.e., the protein microarray database (PMD: http://www.proteinmicroarray.cn/), which is specifically designed for archiving and analyzing protein microarray data [4]. In the PMD, users can easily browse and search the entire database by experimental name, protein microarray type, and sample information. Additionally, the PMD integrates several data analysis tools and provides an

Kelly C. Whittaker and Ruo-Pan Huang (eds.), *Antibody Arrays: Methods and Protocols*, Methods in Molecular Biology, vol. 2237, https://doi.org/10.1007/978-1-0716-1064-0_22,

automated data analysis pipeline for anyone who is interested in protein microarray data.

In this protocol, we will briefly describe the detailed steps, required software/hardware, and some special points worth noting for database development of antibody arrays.

2 Materials

1. The server and database in Alibaba cloud.
2. PHP: Hypertext Preprocessor.
3. Joomla!
4. R.
5. Antibody array raw data.

3 Methods

3.1 Design the Database Framework

1. The protein microarray database is composed of three parts: experiment data, array information, and analysis tools (Fig. 1).
2. Define the storage elements for the experiment data.
   (a) Project name.
   (b) Description.
   (c) Provider.
   (d) The array information.
   (e) Sample annotation.
   (f) Raw data.

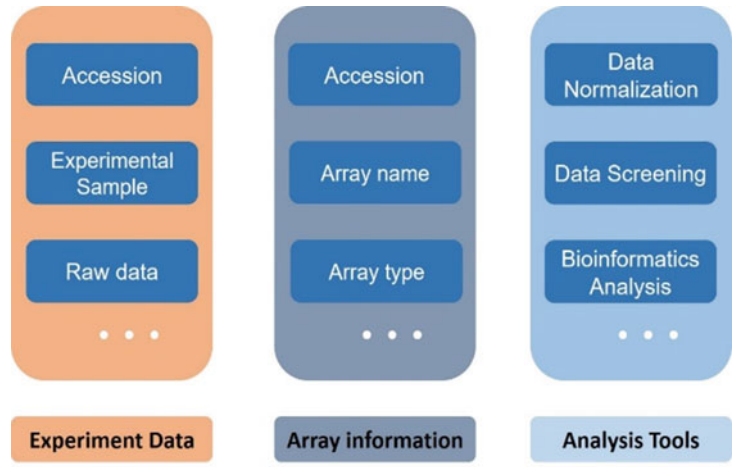

Fig. 1 The structure of antibody array database. The database consists of three parts, i.e., experiment data, array information, and analysis tools

3. Define the storage elements for the array information.
   (a) Array name.
   (b) Array type.
   (c) Species.
   (d) Provider.
   (e) Array annotation.
   (f) The array description.

3.2 Construct the Database in Alibaba Cloud

1. Apply the server with 100 G capacity and database with MySQL 5.5 in Alibaba cloud.
2. Select Ubuntu as the system and create user accounts with different permissions.
3. Install underlying dependency components, Apache2, PHP7.2, libapache2-mod--php7.2, php7.2-mysql, php-cli, php-common, php-mbsring, php-gd, php-intl, php-xml, php-mysql, php-zip, php-curl, and php-xmlrpc (*see* **Notes 1** and **2**): e.g., `sudo apt-get install apache2`.
4. Download the Joomla! from http://www.joomla.org.
5. Unzip the Joomla! package to the website directory, such as /var/www/html, and set the username and group of all files under the folder to Apache (CentOs is apache; Ubuntu is www-data):

```
unzip Joomla_*-Stable-Full_Package.zip
     chown -R www-data:www-data /var/www/html
```

6. Open the website with the browser (such as http://www.localhost), and enter Joomla! installation page. Fill in the website information, database IP, account, and password.
7. Check whether the dependent components have been installed and the PHP settings are correct. Select the initial template to install.
8. Delete the installation folder after installation.

3.3 Fill in Composition of Database Structure

1. According to the database framework, the database structure is composed of model, view, and controller (Fig. 2) (*see* **Note 3**).
2. Fill the Internal Function Library Files in components/com_A/models.
   (a) Add the codes for unloading the experiment data or array information in components/com_A/models/add.php.
   (b) Add the codes for browsing the database in components/com_A/models/browse.php.

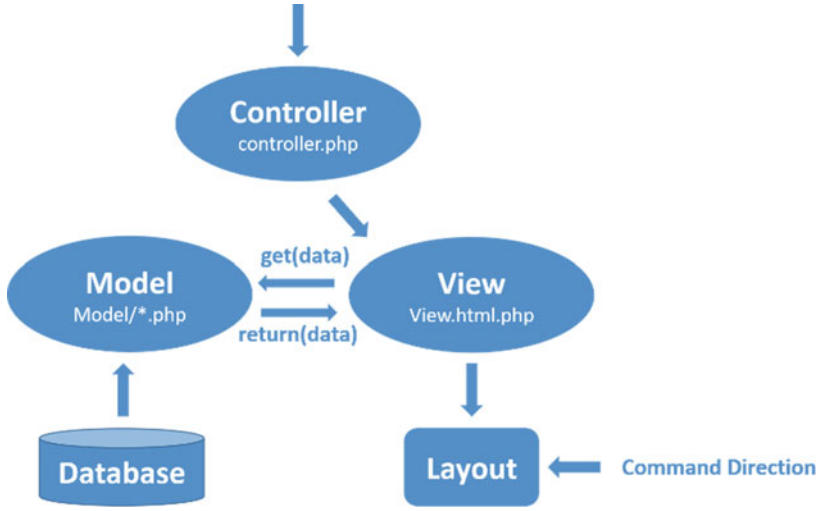

Fig. 2 The operation principle of antibody array database

(c) Add the codes for browsing the experiment data or array information in components/com_A/models/detail.php.

3. Fill the View Function Files in components/com_A/views.
4. Fill the codes of Controller Function in components/com_A/controller.php.

3.4 Construct the Analysis Tools

1. Take the array raw data from web page to a temporary folder named by time using PHP.
2. Transfer the array raw data to R using PHP (*see* **Note 4**).
3. Normalize the raw data by MASS and limma:

```
backgroundCorrect(RG,method="normexp")
normalizeBetweenArrays(RG.bgcorrect)
```

4. Merge the data of the repeated antibodies and calculate the differential signal:

```
data.all = RG.bgcorrect$E
 group=paste(RG.bgcorrect$genes[,"Block"],RG.
bgcorrect$genes[,"Name"],sep=":")
group = RG.bgcorrect$genes[,"Name"]
data = NULL
for(i in 1:ncol(data.all)) {
 data = cbind(data,tapply(data.all[,i],group,
mean))
}
colnames(data) = colnames(RG$E)
```

```
Fold change = log2(x/y)
p <- 1 - pnorm(x, y)
fisher.test(m, alternative = "less")$p.value
fisher.test(m, alternative = "greater")$p.value
```

5. Return the results to the web page.

4 Notes

1. Ensure that all dependent packages are installed successfully. If an error is encountered, such as php-cli not found, please reinstall the php-cli package.
2. When using version control software, it is necessary to retain the old version code for bug fixing.
3. Please strictly abide by Joomla! class and function naming rules.
4. The R should be installed on the server.

References

1. Zhou S, Cheng L, Guo S, Zhu H, Tao S (2012) Functional protein microarray: an ideal platform for investigating protein binding property. Front Biol 7:336–349
2. Chen Z, Dodig-Crnkovic T, Schwenk JM, Tao S-C (2018) Current applications of antibody microarrays. Clin Proteomics 15:7. https://doi.org/10.1186/s12014-018-9184-2
3. Kennedy PJ, Oliveira C, Granja PL, Sarmento B (2018) Monoclonal antibodies: technologies for early discovery and engineering. Crit Rev Biotechnol 38:394–408. https://doi.org/10.1080/07388551.2017.1357002
4. Xu Z et al (2016) PMD: a resource for archiving and analyzing protein microarray data. Sci Rep 6:19956. https://doi.org/10.1038/srep19956

Chapter 23

Data Analysis for Antibody Arrays

Huihua Zhang, Ying Qing Mao, Brianne Petritis, and Ruo-Pan Huang

Abstract

When obtaining high-throughput data from antibody arrays, researchers have to face a couple of questions: How and by what means can they get reasonable results significant to their research from these data? Similar to a gene microarray, the classical statistical pipeline of an antibody array includes data preprocessing transformation, differential expression analysis, classification, and biological annotation analysis. In this chapter, we will provide a pipeline of statistical approaches suitable for antibody arrays to facilitate better understanding of the results gained from each of these steps.

Key words Data preprocess, Differential expression analysis, Supervised classification, Unsupervised classification, Gene ontology, KEGG

1 Introduction

High-throughput technologies have become widely used in biological and clinical research. Most high-throughput data statistical analysis schemes are also suitable for data obtained from antibody arrays. Figure 1 illustrates a routine of data analysis scheme for an antibody array. Briefly, data analysis for antibody arrays begins with the acquisition of signal intensity or protein concentrations after background correction and normalization. Once a profile of comparable values is obtained, we can process a series of statistical analyses: (1) identification of differential expression analysis between two groups of samples under different conditions or with different phenotypes or experimental treatments, (2) classification or predicted visualization of expression profiles for each group of samples, and (3) determination of biological associations among proteins to facilitate better understanding of protein-protein interaction or mechanisms during disease or treatment progression. Indeed, there might be a number of approaches for each of step, and there will never be a "best" approach or a single technique that will allow us to find all the relationships in the data [1]. In this

Kelly C. Whittaker and Ruo-Pan Huang (eds.), *Antibody Arrays: Methods and Protocols*, Methods in Molecular Biology, vol. 2237, https://doi.org/10.1007/978-1-0716-1064-0_23,

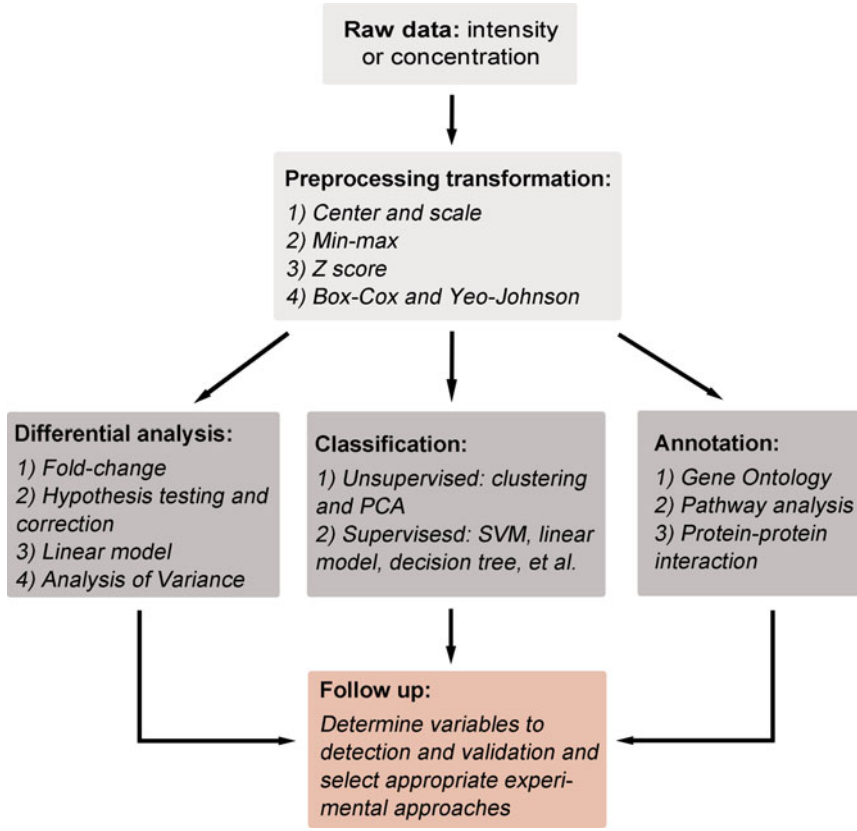

Fig. 1 Statistical analysis flow chart for antibody arrays. The flow chart represents the guidelines for each step of an antibody array

chapter, we will cover each of these steps and introduce some useful statistical approaches.

2 Data Preprocessing Transformation

Before comparing measured expression levels between different conditions, data preprocessing must be carried out to adjust the measured intensities or protein concentrations to facilitate comparisons and to select differentially expressed proteins between classes of samples [2]. In this section, data preprocessing mainly focuses on data transformation and data quality assessment.

There are several reasons why data must be preprocessed. The first reason is to remove distributional skewness. Most proteins, especially non-secreted proteins, are expressed at very low levels; few proteins are expressed at high concentration, indicating that the distribution of array data is often skewed to the right. Secondly, in microarray experiments, there are many sources of systematic variation [3]. Transformation attempts to remove variations such as

systematic biases, technical variations, and batch effects, allow the data to be comparable in order to find actual biological changes [4], and balance the individual intensities of the antigen-antibody binding reaction appropriately so that meaningful biological comparisons can be made. Data with different scales and outliers often lead to difficulties in visualization and degrade the predictive performance of many subsequent analyses, including differential expression analysis, clustering, principle component analysis, and other machine learning algorithms [5].

There are common transformation approaches suitable to antibody arrays:

- *Center and scale normalization*
- *Min-max transformation*
- *Z-score normalization* [6]
- *Power transformation* [5]*: Box-Cox* [7] *and Yeo-Johnson* [8] *transformation*

Center and scale are the most straightforward and common transformation approaches. "Center" subtracts the mean of the predictor's data from the predictor values, while "scale" divides the predictor's data by the standard deviation of the predictor values [9]. Z-score normalization, also called standardization, is calculated by subtracting the overall average intensity from the raw intensity data for each variance and dividing that result by the standard deviation of all of the measured intensities [6]. Z-score normalization transforms the data such that the resulting distribution has a mean of 0 and a standard deviation of 1. The Box-Cox transformation was developed for transforming the response variable. However, the Box-Cox method is simpler, is more computationally efficient, and is equally effective at estimating power transformations. The Yeo-Johnson transformation is similar to the Box-Cox transformation but can accommodate predictors with zero and/or negative values [9]. Other approaches, such as quantile transformation [10], range, PCA (principle component analysis), spatial sign [11], and TMM [12] (weighted trimmed mean of M-values), are also used for antibody array data [9]. Note that there is not a "perfect" normalization method, because expression data can significantly vary between different normalization procedures [3]. Which and how many transformation methods to choose depend on the data.

Prior to data analysis, post-normalization quality should be assessed to detect outliers and systematically wrong appliance of normalization methods [13]. Two useful plots directly reflect data quality after normalization: (1) MA plot [14], which is usually used to visualize the log2 fold change attributable to a given variable over the mean/median of normalized intensities for all the samples after preprocessing transformation, and (2) Box plot for all the samples (Fig. 2a).

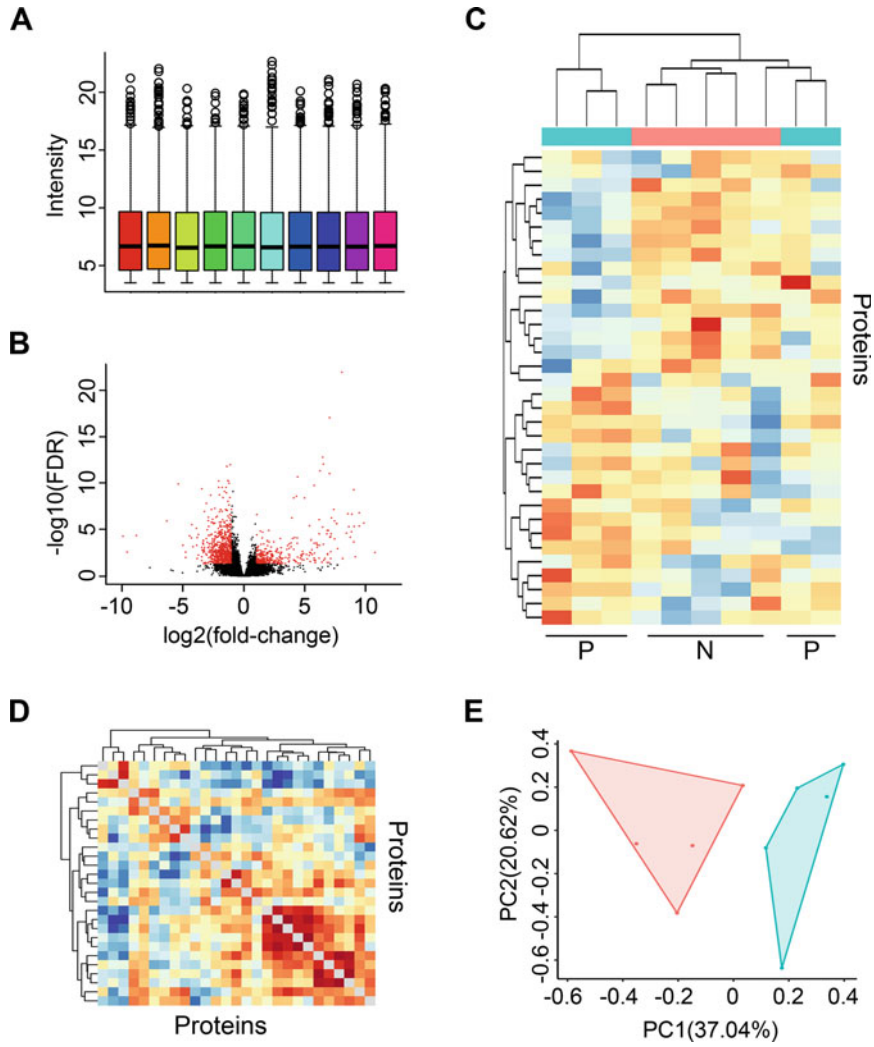

Fig. 2 Visualization of results for protein arrays. (**a**) Box plots after Yeo-Johnson transformation. Each color represents one sample, and the *y*-axis represents intensities after normalization. The central line of each box indicates the median value of each sample data. (**b**) A volcano plot is used to visualize fold change and statistical significance. The *x*-axis is the fold change between the two groups (often on a log2 scale), and the *y*-axis represents the *p*-value or FDR of differences between samples (often on a negative log10 scale). Red points present variables that show both statistical significance and fold change meeting the thresholds. (**c**) Clustering heatmap with Euclidean and complete distance of both samples and proteins. Rows indicate different individual samples, while columns represent proteins of similar expression values. (**d**) Clustering heatmap with Pearson correlation and complete distance between protein pairs. Proteins with high correlation are defined as a cluster. Red color presents positive correlation between pairs, whereas blue color presents negative correlation. (**e**) PCA plot shows clusters of samples based on their similarity. PCs on the *x*- and *y*-axis describe variation and account for the effects of the proteins

Outliers are defined as an observation that deviates too much from other observations [15]. Outliers can cause unexpectedly large deviations and "noise" in a dataset, and unsatisfactory analysis results because most analysis approaches are unable to

accommodate the unavoidable presence of "noise" [16]. Some approaches, like clustering and principle component analysis (PCA), are used to detect outliers. These are also classification approaches that will be discussed further in the next section. Sometimes, however, outliers are not only "outliers." They may have potential diagnostic or other significant biological utility, leading us in the direction of discovery [16].

3 Differential Expression Analyses

Similar to other high-throughput proteomic approaches, an antibody array can be used to identify changes in protein expression in response to an experimental treatment or clinical conditions, such as the response to therapy, disease phenotypes, diagnostic or prognostic biomarkers, disease classification, and determination of disease mechanisms [17]. Differential analysis is an important and basic tool for the deeper analysis of expression data. Next, we briefly discuss several approaches for differential expression analyses.

3.1 Fold Change

With gene microarrays, the fold change between two conditions was first used to identify differentially expressed genes [17, 18]. Antibody arrays can use the same principle, and fold change is also suitable for protein expression. Although, in statistics, there is no firm theoretical basis for selecting a post-normalization cutoff of fold-change increase or decrease to define differential expression [1], Chen et al. provided confidence intervals that can be used to identify differentially expressed genes [19]. Some proteins, such as phosphorylated proteins, transcription factors, and transmembrane proteins, which generally have altered levels of 1.5-fold or less, could have important biological effects. At this point, the fold-change method does not take into account the variance of the protein expression measured.

3.2 Hypothesis Testing

Hypothesis testing is required to identify differentially expressed proteins. There are two classifications: parametric and nonparametric tests. The parametric test, which often utilizes a Student's *t*-test for antibody array data, rests on the normal distribution of data where the mean is known or assumed to be known (difference in means between groups divided by the standard deviation) [17, 20]. In this case, data should be transformed to a normal distribution using the transformation methods mentioned above. A nonparametric test is used when the data is skewed. This approach often utilized a Wilcoxon signed-rank test, which eliminates the need for normality assumptions [19].

When the *p*-value exceeds a certain value in a single hypothesis test, e.g., *p*-value <0.05 or 0.01, the protein expression between the two groups of samples is considered to be different. However,

when we try to analyze many proteins at one time (multiple statistical tests), proteins expressed at similar levels exhibit similar variance and appear to be significantly different [21], increasing the incidence of a Type I error (false positive) [22]. For example, consider 2000 null hypothesis testing for 2 groups of samples for antibody array data, a *p*-value level of 0.05 would generate 100 false discoveries. For this reason, there are two approaches developed to combat this multiple test problem: controlling the family-wise error rate (FWER) and controlling the false discovery rate (FDR) [22, 23]. The most common way to control the FWER is with the Bonferroni correction [24], which is mainly useful for a fairly small number of multiple testing. But in large numbers of multiple testing, the Bonferroni correction is unsuitable and may lead to a very high rate of false negatives [20]. The alternative approach is to control the FDR. The FDR is the rate that significant features are truly null [25], which is defined as the expected percentage or proportion of rejected hypotheses that have been wrongly rejected [26]. The Benjamini and Hochberg (BH) method guarantees an upper bound for the FDR by a step-up or step-down procedure applied to the individual *p*-values [27]. Take the example above, array data for 2000 proteins with the control FDR of 0.05. If 500 differentially expressed proteins are identified, then the false positives are less than $500 \times 0.05 = 25$. On the other hand, an unfortunate by-product of multiple testing correction is an increase in false negatives, which may mask true events that are not statistically significant. Therefore, most researchers seem willing to accept false-positive errors so as not to miss findings that may be significant to their research [14]. In addition, due to its nonstatistical character of fold change, researchers tend to combine fold change and *p*-value/FDR approaches to screen for differential expressed variables, which are normally presented by a Volcano plot [28] (Fig. 2b).

3.3 Linear Model

In array experiments, small sample size populations are still very common. High-dimensional variables and a small sample size produce non-normally distributed data and leads to poor estimates of variance, posing challenging statistical problems. To combat these problems, linear models are developed to microarray data in a flexible and statistically rigorous way [29]. Two popular linear models, the empirical Bayes (eBayes) and generalized linear model (GLM, used for RNA sequencing data), can make the analyses stable even for experiments with a small sample size [10]. The empirical Bayes approach is equivalent to shrinkage of the estimated sample variances toward a pooled estimate [30]. It capitalizes on the parallel nature of microarrays to improve variance estimates and increase statistical power [14]. In controlled experiments, the empirical Bayes approach has been shown to give better estimates of standard deviations of expression than hypothesis testing

[21]. The basic statistic used for significance analysis is the moderated *t*-statistic, which has the same interpretation as an ordinary *t*-statistic from hypothesis tests but is computed for each probe and for each contrast. It also has increased degrees of freedom and moderated the standard errors across variables [31]. Limma [10] is a popular R/Bioconductor package containing the empirical Bayes model that is used to analyze antibody array and RNA sequencing data and to assess evidence for differential expression.

3.4 Analysis of Variance

The approaches for determining differentially expressed proteins mentioned above are suitable for two-group comparisons. However, sometimes comparison of the differences between three or more situations or some criterion for selecting proteins that are differentially regulated among groups is desirable. In this instance, the use of analysis of variance (ANOVA) [20, 32] or the Kruskal-Wallis test [33] is suitable. ANOVA calculates a consensus estimate of variability within groups, based on all of the groups, meaning each source of variance is accounted for [20]. It is easy to distinguish between interesting variations, such as the regulation between transcription factors and treatments.

4 Classification Analysis

When possible sets of differentially expressed proteins are identified, a classification analysis can be done to try to determine if these proteins achieved the expected treatment effect or predictive performance (e.g., tumors with good vs. bad prognoses, cell lines treated with or without drugs, and mechanisms during disease progress) [34]. Classification analyses involve supervised classification and unsupervised classification. Supervised classification defines that all objects are labeled and the algorithms learn to predict the output from the input data, while unsupervised classification entails unlabeled objects, and the algorithms learn the inherent structure from the input data [35]. Many classification algorithms have been widely used in antibody array research.

4.1 Unsupervised Classification

Unsupervised classification, such as clustering and principle component analysis, was one of the first machine learning algorithms to be applied to microarray analysis because of its simplicity and ease [36].

The most common clustering algorithm used in the antibody array field is hierarchical clustering [37]. With this approach, one simply obtains a clustering of proteins and any biological validity associated with the clustering, irrespective of sample size, data quality, or experimental design [14]. There are two important metrics to use to quantify the distance or similarity among proteins/samples: distance and the clustering method. The distance

metric includes Euclidean distance, Manhattan distance, Maximum distance, Pearson/rank correlation coefficient, etc. The clustering method entails single linkage, complete linkage, average linkage, and centroid linkage [37] (Fig. 2c, d). Relationships among the proteins and/or samples are represented by a tree (dendrogram), whose branch lengths reflect the degree of similarity between the proteins or samples [36]. Furthermore, proteins in the same cluster are defined as being involved in the same biological pathway and/or having the same biological function [38]. Nonhierarchical clustering methods can also be used for antibody array data, including partitioning methods (e.g., *k*-means), density-based methods (e.g., density-based spatial clustering of applications with noise (DBSCAN)), and grid-based methods (e.g., statistical information grid) [39].

It is important to determine if experiments have independent information or if the variables from clustering are highly correlated, and principal component analysis (PCA), another widely used unsupervised classification method, is an exploratory multivariate statistical approach used to emphasize variation and simplify visualization of multidimensional data [40, 41]. In the case of antibody arrays, PCA can summarize the ways in which variables change under different conditions or environments and search for outlier variables/samples [42] (Fig. 2e). For example, consider x samples with d variables. Through PCA analysis, k new variables are generated, where k is less than d. These k variables represent the principle components (PC). Each principal component is a linear combination of the original variables [43] that can effectively explain the variation of expression and is uncorrelated and orthogonal [42].

4.2 Supervised Classification

In clinical applications, a reliable and precise classification of cancers is essential for the successful diagnosis and treatment of cancers and the identification of previously unrecognized and clinically significant subclasses of cancers [34]. Compared to unsupervised classification approaches, supervised classification approaches are more accurate and reliable and have been widely used with antibody array data.

Supervised classification typically entails training on a subset of data with prior given labels, testing of another subset with known labels, and then assessment of the prediction accuracy on an unknown subset [44]. They are suitable for both binary and multi-classifications. The most popular models in biological and clinical research include decision trees, logistic regression, neural networks, support vector machine, random forest, generalized linear models, etc. In order to ensure independency among different subsets of data and validation of the classification model under similar conditions, samples should be preferentially collected and analyzed at different time points [45].

However, there are two challenges in microarray data analysis that classification algorithms have to face: a low number of samples and a high-dimensional data (variables or features) [46]. This leads many of the machine learning algorithms to enhance their generalizations to reduce overfitting and biases [47]. To solve this problem, we can (1) train with more data (increase sample number), (2) reduce dimensionality, (3) include cross-validation (CV), and (4) use regularization and ensembling (bagging and boosting) [5, 47]. Dimensionality reduction involves feature extraction and feature selection [46]. Feature extraction is a process of extracting a subset of new features/variables from the original ones, such as PCA and multidimensional scaling (MDS). Feature selection means reducing or finding the most meaningful variables, like filter methods, wrapper methods, and embedded methods [46]. In cross-validation, also called k-fold CV, the training set is split into k smaller sets, then a model is trained using $k - 1$ of the folds as training data, and validated on the remaining part of the data [5]. For example, Sandip et al. enrolled a total of 259 archived plasma samples with presymptomatic to late-stage Alzheimer's disease and from various controls and measured 120 signaling proteins. Using a shrunken centroid algorithm prediction analysis for microarrays (PAM) with tenfold cross-validation [48], they found 18 proteins that could be used to classify blinded samples from Alzheimer's and control individuals with close to 90% accuracy and to identify patients who had mild cognitive impairment that progressed to Alzheimer's disease 2–6 years later [49].

Once a classification model (binary classification model) is constructed, several metrics to assess the model's performance, sensitivity, specificity, accuracy, and their confident intervals (95% CI) [47], formulated in a 2×2 confusion matrix, can be used. Sensitivity (also called the true positive rate) measures the proportion of actual positives correctly identified as such, e.g., the percentage of actual Alzheimer's patients who are correctly identified as Alzheimer's patients, while specificity (also called the true negative rate) measures the proportion of actual negatives correctly identified as such [50]. Another assessment approach is receiver operating characteristic (ROC) analysis, which is used for assessing the overall performance of a classification model. In ROC analysis, area under curve (AUC) is a measure of the model's performance that depicts relative tradeoffs between sensitivity and 1-specificity [47, 50].

5 Biological Annotation Analyses

The results obtained from the above steps, including differential analysis and classification, are distributed for researchers to identify functional roles of respective proteins and mechanisms underlying biological processes and disease progression. Functional enrichment analyses involve gene ontology (GO) and signaling pathways.

GO annotations are created by associating a gene product (proteins and functional RNAs) with a GO term, capturing statements about how a gene product functions at the molecular level, where in the cell it functions, and what biological processes it is involved in (pathways, programs) [51]. Moreover, experimental knowledge obtained in one organism is often applicable to other organisms, particularly if the organisms share the relevant gene products [52]. The GO database entails three distinct aspects of function: molecular function (the molecular activity of a gene product), cellular component (where the gene products are active), and biological process (the pathways and larger processes to which that gene product's activity contributes) [53, 54]. The association of a GO term and a gene product can be summarized as the gene product has an activity or a molecular role (MF term) and directly participates in a process (BP term) and its function takes place in a specific cellular localization (CC term) [55].

Another popular annotation analysis is pathway enrichment, a powerful method for understanding the specific biological functions and relationships between gene products. There are two common pathway analysis methods [56]: (1) analysis based on the number of gene products in a pathway or gene coexpression including overrepresentation analysis approaches (hypergeometric distribution, binomial distribution, and chi-square distribution) and functional class scoring approaches on competitive null hypothesis and self-contained null hypothesis and (2) pathway topology-based approaches, which provide additional information about interactions and relationships among gene products in a given pathway. Among a variety of public databases available, Kyoto Encyclopedia of Genes and Genomes (KEGG) is an effective resource for understanding high-level functions and utilities of the biological system from genomic- and molecular-level information [57, 58]. It provides information about the biological system, consisting of molecular building blocks of genes and proteins (genomic information), chemical substances (chemical information), molecular wiring diagrams of interactions, reaction and relation networks (systems information), and disease and drug information (health information) [59]. When performing pathway analysis using KEGG, one can also find the associations among proteins. Protein-protein interactions (PPI) control a large number of cellular processes (such as interactions of protein kinases, protein phosphatases, glycosyltransferases, and proteases) [60] and thus provide a valuable framework for many new insights of the functional organization of the proteome [61]. Some useful integrated tools have been developed to combine data consolidation, prediction, scoring, and retrieval with data analysis and visualization [62]: STRING (Search Tool for the Retrieval of Interacting Genes/Proteins) [63, 64], Cytoscape [65], VisANT [66], and R [67]/RStudio software [68] (Fig. 3).

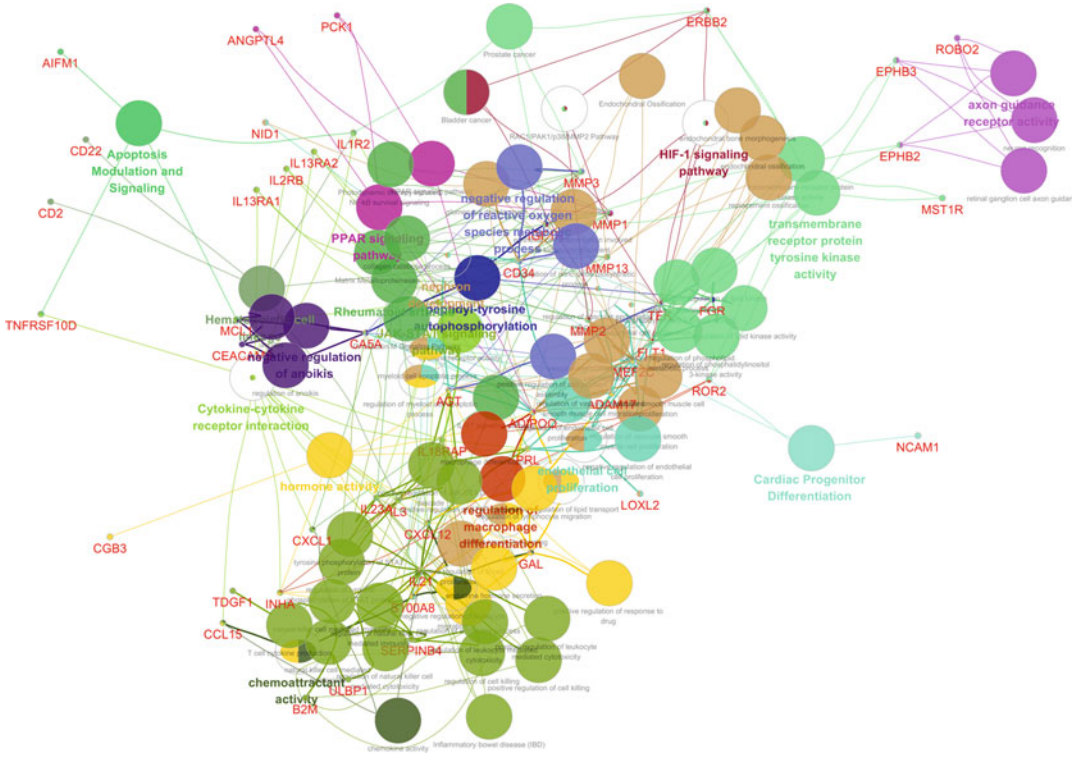

Fig. 3 Functional annotation enrichment analysis. Visualization the non-redundant biological terms for large clusters of gene products in a functionally grouped network by GlueGO [69], a Cytoscape plug-in. Functionally grouped network with terms as nodes linked based on their kappa score level. The size of the nodes reflects the enrichment significance of the terms

References

1. Quackenbush J (2001) Computational analysis of microarray data. Nat Rev Genet 2(6): 418–427
2. Quackenbush J (2002) Microarray data normalization and transformation. Nat Genet 32(Suppl):496–501. https://doi.org/10.1038/ng1032
3. Park T, Yi S-G, Kang S-H, Lee S, Lee Y-S, Simon R (2003) Evaluation of normalization methods for microarray data. BMC Bioinformatics 4:33–33. https://doi.org/10.1186/1471-2105-4-33
4. Fujita A, Sato JR, Rodrigues Lde O, Ferreira CE, Sogayar MC (2006) Evaluating different methods of microarray data normalization. BMC Bioinformatics 7:469. https://doi.org/10.1186/1471-2105-7-469
5. Pedregosa F, Varoquaux G, Gramfort A, Michel V, Thirion B, Grisel O, Blondel M, Prettenhofer P, Weiss R, Dubourg V, Vanderplas J, Passos A, Cournapeau D, Brucher M, Perrot M, Duchesnay É (2011) Scikit-learn: machine learning in Python. JMLR 12:2825–2830
6. Cheadle C, Vawter MP, Freed WJ, Becker KG (2003) Analysis of microarray data using Z score transformation. J Mol Diagn 5(2): 73–81. https://doi.org/10.1016/s1525-1578(10)60455-2
7. Box GEP, Cox DR (1964) An analysis of transformations. J R Stat Soc 26(2):211–243. https://doi.org/10.1111/j.2517-6161.1964.tb00553.x
8. Yeo IK, Johnson RA (2000) A new family of power transformations to improve normality or symmetry. Biometrika 87(4):954–959. https://doi.org/10.1093/biomet/87.4.954
9. Kuhn M, Johnson K (2013) Applied predictive modeling. Springer, New York
10. Smyth GK (2005) limma: linear models for microarray data. In: Gentleman R, Carey VJ, Huber W, Irizarry RA, Dudoit S (eds)

Bioinformatics and computational biology solutions using r and bioconductor. Springer, New York, pp 397–420. https://doi.org/10.1007/0-387-29362-0_23

11. Serneels S, Nolf E, Van Espen P (2006) Spatial sign preprocessing: a simple way to impart moderate robustness to multivariate estimators. J Chem Inf Model 46:1402–1409. https://doi.org/10.1021/ci050498u
12. Robinson MD, Oshlack A (2010) A scaling normalization method for differential expression analysis of RNA-seq data. Genome Biol 11(3):R25. https://doi.org/10.1186/gb-2010-11-3-r25
13. Koch M, Wiese M (2012) Quality visualization of microarray datasets using circos. Microarrays (Basel) 1(2):84–94. https://doi.org/10.3390/microarrays1020084
14. Allison DB, Cui X, Page GP, Sabripour M (2006) Microarray data analysis: from disarray to consolidation and consensus. Nat Rev Genet 7(1):55–65. https://doi.org/10.1038/nrg1749
15. Rao ACS, Somayajulu D, Banka H, Chaturvedi R (2012) Outlier detection in microarray data using hybrid evolutionary algorithm. Procedia Technol 6:291–298. https://doi.org/10.1016/j.protcy.2012.10.035
16. Pearson RK, Gonye GE, Schwaber JS (2003) Outliers in microarray data analysis. In: Johnson KF, Lin SM (eds) Methods of microarray data analysis III: papers from CAMDA' 02. Springer, Boston, MA, pp 41–55. https://doi.org/10.1007/0-306-48354-8_4
17. Tarca AL, Romero R, Draghici S (2006) Analysis of microarray experiments of gene expression profiling. Am J Obstet Gynecol 195(2):373–388. https://doi.org/10.1016/j.ajog.2006.07.001
18. Schena M, Shalon D, Davis RW, Brown PO (1995) Quantitative monitoring of gene expression patterns with a complementary DNA microarray. Science 270(5235):467–470. ISSN: 0036-8075 (Print)
19. Chen Y, Dougherty ER, Bittner ML (1997) Ratio-based decisions and the quantitative analysis of cDNA microarray images. J Biomed Opt 2(4):364–374, 311
20. Draghici S (2002) Statistical intelligence: effective analysis of high-density microarray data. Drug Discov Today 7(11):S55–S63. https://doi.org/10.1016/S1359-6446(02)02292-4
21. Hatfield GW, Hung SP, Baldi P (2003) Differential analysis of DNA microarray gene expression data. Mol Microbiol 47(4):871–877
22. Austin RS, Dialsingh I, Altman NS (2014) Multiple hypothesis testing: a review. J Indian Soc Agric Stat 68:303–314
23. Benjamini Y, Yekutieli D (2001) The control of the false discovery rate in multiple testing under dependency. Ann Stat 29(4):1165–1188. https://doi.org/10.1214/aos/1013699998
24. McDonald JH (2014) Multiple comparisons. In: Handbook of biological statistics, 3rd edn. Sparky House Publishing, Baltimore, MD
25. Storey JD, Tibshirani R (2003) Statistical significance for genomewide studies. Proc Natl Acad Sci U S A 100(16):9440–9445. https://doi.org/10.1073/pnas.1530509100
26. Benjamini Y, Hochberg Y (1995) Controlling the false discovery rate: a practical and powerful approach to multiple testing. J R Stat Soc 57(1):289–300. https://doi.org/10.1111/j.2517-6161.1995.tb02031.x
27. Tusher VG, Tibshirani R, Chu G (2001) Significance analysis of microarrays applied to the ionizing radiation response. Proc Natl Acad Sci U S A 98(9):5116–5121. https://doi.org/10.1073/pnas.091062498
28. Cui X, Churchill GA (2003) Statistical tests for differential expression in cDNA microarray experiments. Genome Biol 4(4):210. https://doi.org/10.1186/gb-2003-4-4-210
29. Ritchie ME, Phipson B, Wu D, Hu Y, Law CW, Shi W, Smyth GK (2015) limma powers differential expression analyses for RNA-sequencing and microarray studies. Nucleic Acids Res 43(7):e47–e47. https://doi.org/10.1093/nar/gkv007
30. Smyth GK (2004) Linear models and empirical Bayes methods for assessing differential expression in microarray experiments. Stat Appl Genet Mol Biol 3:3. ISSN: 1544-6115 (Electronic)
31. Phipson B, Lee S, Majewski IJ, Alexander WS, Smyth GK (2016) Robust hyperparameter estimation protects against hypervariable genes and improves power to detect differential expression. Ann Appl Stat 10(2):946–963. https://doi.org/10.1214/16-AOAS920
32. Kathleen Kerr M, Martin M, Churchill GA (2000) Analysis of variance for gene expression microarray data. J Comput Biol 7(6):819–837. https://doi.org/10.1089/10665270050514954
33. Olson NE (2006) The microarray data analysis process: from raw data to biological significance. NeuroRx 3(3):373–383. https://doi.org/10.1016/j.nurx.2006.05.005
34. Dudoit S, Fridlyand J (2003) Classification in microarray experiments. In: Statistical analysis of gene expression microarray data. CRC Press, Boca Raton, FL
35. Menjoge RS, Welsch RE (2008) Comparing and visualizing gene selection and classification methods for microarray data. In: Machine

learning in bioinformatics. Wiley, Hoboken, NJ, pp 47–68. https://doi.org/10.1002/9780470397428.ch2

36. Sebastiani P, Gussoni E, Kohane IS, Ramoni MF (2003) Statistical challenges in functional genomics. Stat Sci 18(1):33–70. https://doi.org/10.1214/ss/1056397486
37. Whitworth GB (2010) Chapter 2—An introduction to microarray data analysis and visualization. In: Methods in enzymology, vol 470. Academic Press, New York, pp 19–50. https://doi.org/10.1016/S0076-6879(10)70002-1
38. Basford KE, McLachlan GJ, Rathnayake SI (2012) On the classification of microarray gene-expression data. Brief Bioinform 14(4):402–410. https://doi.org/10.1093/bib/bbs056
39. Gulagiz F, Sahin S (2017) Comparison of hierarchical and non-hierarchical clustering algorithms. Int J Comput Eng Inform Technol 9(1):6–14
40. Bartenhagen C, Klein H-U, Ruckert C, Jiang X, Dugas M (2010) Comparative study of unsupervised dimension reduction techniques for the visualization of microarray gene expression data. BMC Bioinformatics 11:567–567. https://doi.org/10.1186/1471-2105-11-567
41. Cangelosi R, Goriely A (2007) Component retention in principal component analysis with application to cDNA microarray data. Biol Direct 2:2–2. https://doi.org/10.1186/1745-6150-2-2
42. Raychaudhuri S, Stuart JM, Altman RB (2000) Principal components analysis to summarize microarray experiments: application to sporulation time series. Pac Symp Biocomput 455–466. https://doi.org/10.1142/9789814447331_0043
43. Ma S, Dai Y (2011) Principal component analysis based methods in bioinformatics studies. Brief Bioinform 12(6):714–722. https://doi.org/10.1093/bib/bbq090
44. Brazma A, Vilo J (2000) Gene expression data analysis. FEBS Lett 480(1):17–24. https://doi.org/10.1016/s0014-5793(00)01772-5
45. Perez-Diez A, Morgun A, Shulzhenko N (2007) Microarrays for cancer diagnosis and classification. In: Mocellin S (ed) Microarray technology and cancer gene profiling. Springer, New York, pp 74–85. https://doi.org/10.1007/978-0-387-39978-2_8
46. Sánchez-Maroño N, Fontenla-Romero O, Pérez Sánchez B (2019) Classification of microarray data. In: Microarray bioinformatics. Springer Science+Business Media LLC, New York, pp 185–205. https://doi.org/10.1007/978-1-4939-9442-7_8
47. Kourou K, Exarchos TP, Exarchos KP, Karamouzis MV, Fotiadis DI (2015) Machine learning applications in cancer prognosis and prediction. Comput Struct Biotechnol J 13:8–17. https://doi.org/10.1016/j.csbj.2014.11.005
48. Tibshirani R, Hastie T, Narasimhan B, Chu G (2002) Diagnosis of multiple cancer types by shrunken centroids of gene expression. Proc Natl Acad Sci U S A 99(10):6567–6572. https://doi.org/10.1073/pnas.082099299
49. Ray S, Britschgi M, Herbert C, Takeda-Uchimura Y, Boxer A, Blennow K, Friedman LF, Galasko DR, Jutel M, Karydas A, Kaye JA, Leszek J, Miller BL, Minthon L, Quinn JF, Rabinovici GD, Robinson WH, Sabbagh MN, So YT, Sparks DL, Tabaton M, Tinklenberg J, Yesavage JA, Tibshirani R, Wyss-Coray T (2007) Classification and prediction of clinical Alzheimer's diagnosis based on plasma signaling proteins. Nat Med 13(11):1359–1362. https://doi.org/10.1038/nm1653
50. Fawcett T (2006) An introduction to ROC analysis. Pattern Recogn Lett 27(8):861–874. https://doi.org/10.1016/j.patrec.2005.10.010
51. Thomas PD (2017) The gene ontology and the meaning of biological function. In: Dessimoz C, Škunca N (eds) The gene ontology handbook. Springer, New York, pp 15–24. https://doi.org/10.1007/978-1-4939-3743-1_2
52. Ashburner M, Ball CA, Blake JA, Botstein D, Butler H, Cherry JM, Davis AP, Dolinski K, Dwight SS, Eppig JT, Harris MA, Hill DP, Issel-Tarver L, Kasarskis A, Lewis S, Matese JC, Richardson JE, Ringwald M, Rubin GM, Sherlock G (2000) Gene ontology: tool for the unification of biology. The Gene Ontology Consortium. Nat Genet 25(1):25–29. https://doi.org/10.1038/75556
53. The Gene Ontology Consortium (2018) The gene ontology resource: 20 years and still GOing strong. Nucleic Acids Res 47(D1):D330–D338. https://doi.org/10.1093/nar/gky1055
54. Smith B, Williams J, Schulze-Kremer S (2003) The ontology of the gene ontology. AMIA Annu Symp Proc 2003:609–613
55. Poux S, Gaudet P (2017) Best practices in manual annotation with the gene ontology. In: Dessimoz C, Škunca N (eds) The gene ontology handbook. Springer, New York, pp 41–54. https://doi.org/10.1007/978-1-4939-3743-1_4

56. Khatri P, Sirota M, Butte AJ (2012) Ten years of pathway analysis: current approaches and outstanding challenges. PLoS Comput Biol 8(2):e1002375. https://doi.org/10.1371/journal.pcbi.1002375
57. Ogata H, Goto S, Sato K, Fujibuchi W, Bono H, Kanehisa M (1999) KEGG: Kyoto encyclopedia of genes and genomes. Nucleic Acids Res 27(1):29–34. https://doi.org/10.1093/nar/27.1.29
58. Kanehisa M, Goto S (2000) KEGG: Kyoto encyclopedia of genes and genomes. Nucleic Acids Res 28(1):27–30. https://doi.org/10.1093/nar/28.1.27
59. Kanehisa M, Sato Y, Kawashima M, Furumichi M, Tanabe M (2016) KEGG as a reference resource for gene and protein annotation. Nucleic Acids Res 44(D1): D457–D462. https://doi.org/10.1093/nar/gkv1070
60. Phizicky EM, Fields S (1995) Protein-protein interactions: methods for detection and analysis. Microbiol Rev 59(1):94–123
61. Stelzl U, Worm U, Lalowski M, Haenig C, Brembeck FH, Goehler H, Stroedicke M, Zenkner M, Schoenherr A, Koeppen S, Timm J, Mintzlaff S, Abraham C, Bock N, Kietzmann S, Goedde A, Toksöz E, Droege A, Krobitsch S, Korn B, Birchmeier W, Lehrach H, Wanker EE (2005) A human protein-protein interaction network: a resource for annotating the proteome. Cell 122(6):957–968. https://doi.org/10.1016/j.cell.2005.08.029
62. Donaldson IM (2010) Chapter 170—Protein interaction data resources. In: Bradshaw RA, Dennis EA (eds) Handbook of cell signaling, 2nd edn. Academic Press, San Diego, CA, pp 1375–1385. https://doi.org/10.1016/B978-0-12-374145-5.00170-4
63. Snel B, Lehmann G, Bork P, Huynen MA (2000) STRING: a web-server to retrieve and display the repeatedly occurring neighbourhood of a gene. Nucleic Acids Res 28(18): 3442–3444. https://doi.org/10.1093/nar/28.18.3442
64. Szklarczyk D, Gable AL, Lyon D, Junge A, Wyder S, Huerta-Cepas J, Simonovic M, Doncheva NT, Morris JH, Bork P, Jensen LJ, Cv M (2019) STRING v11: protein-protein association networks with increased coverage, supporting functional discovery in genome-wide experimental datasets. Nucleic Acids Res 47(D1):D607–D613. https://doi.org/10.1093/nar/gky1131
65. Shannon P, Markiel A, Ozier O, Baliga NS, Wang JT, Ramage D, Amin N, Schwikowski B, Ideker T (2003) Cytoscape: a software environment for integrated models of biomolecular interaction networks. Genome Res 13(11):2498–2504. https://doi.org/10.1101/gr.1239303
66. Hu Z, Mellor J, Wu J, DeLisi C (2004) VisANT: an online visualization and analysis tool for biological interaction data. BMC Bioinformatics 5:17–17. https://doi.org/10.1186/1471-2105-5-17
67. R-Core-Team (2019) R: a language and environment for statistical computing. R Foundation for Statistical Computing, Vienna
68. RStudio-Team (2015) RStudio: integrated development for R. RStudio, Inc., Boston, MA
69. Bindea G, Mlecnik B, Hackl H, Charoentong P, Tosolini M, Kirilovsky A, Fridman W-H, Pagès F, Trajanoski Z, Galon J (2009) ClueGO: a cytoscape plug-in to decipher functionally grouped gene ontology and pathway annotation networks. Bioinformatics (Oxford, England) 25 (8):1091–1093. https://doi.org/10.1093/bioinformatics/btp101

Chapter 24

Statistical Analysis Options for Antibody Array Data

Jingqiao Lu

Abstract

In this chapter, we introduce the application of R, a statistical programming language in the analysis of antibody array data. We start from a brief introduction of R itself and then cover data filtration and transformation, data visualization, differential expression analysis with/without variance correction, co-expression network, functional enrichment analysis, and statistical modeling.

Key words Antibody array, Data analysis, R

1 Introduction

The statistical analysis on data generated from an antibody array, like all data analysis, can be conducted with various statistical software/packages/tools, ranging from comprehensive statistical suits (like SAS, SPSS, and S-plus), dedicated tools focusing on specific analysis topics like GSEA (gene set enrichment analysis), to general computer languages like Python, Perl, and R. In this chapter, we will introduce the application of R, a statistical programming language [1], in the analysis of antibody array data. There are some reasons we choose R: (1) R is flexible. It is a programming language dedicated to statistics with great flexibility, including but not limited to various statistical distribution functions, easy-to-handle grammar, vivid data visualization, and script-based analysis procedures with great reproducibility. (2) R is free. It is an open-source language that can be acquired easily. (3) R is cutting-edge. There are active communities of statisticians who are using R in their research and developing/validating/publishing their algorithms in R consistently. Most of the algorithms/methods are released as R packages, which can be retrieved and installed in any computer. Accordingly, one can get access to the latest advances via R with minimal effort. Of course, the advantages and flexibility of R may come with the sacrifice of some conveniences like "button-

Kelly C. Whittaker and Ruo-Pan Huang (eds.), *Antibody Arrays: Methods and Protocols*, Methods in Molecular Biology, vol. 2237, https://doi.org/10.1007/978-1-0716-1064-0_24,

clicking" analysis. R also may require drafting of some analysis scripts which requires a bit of programming thinking, but it is not difficult.

2 A Brief Introduction of R

R is a cross-platform statistical programming language. It can be installed on Windows, macOS, and UNIX/Linux platforms. To download R, please go to https://cran.r-project.org/. The installation is quite easy: for Windows users, just double-click the downloaded .exe file, and R (both 64-bit and 32-bit versions) will be installed; for macOS, similar double-clicking will install it, but a few patches are required depending on the OS version; for Unix-like systems, generally R can be installed from default repositories via command line, like sudo apt install r-base in Ubuntu. For details about the installation on a particular operating system, please refer to https://cran.r-project.org/doc/manuals/r-release/R-admin.html.

R is an explanatory language. That means R scripts are run line by line without compiling. There are two ways to run R scripts: interactive and batch mode. Below is an example of the interactive mode in the R console:

```
print("Hello world.")
```

```
## [1] "Hello world."
```

We can write "print("Hello world")" into a file named "hello_world.r" and then run the script with source() function:

```
source("hello_world.r")
```

```
## [1] "Hello world."
```

It will give us the same result.

As a programming language, R covers arithmetic and logic calculations (*see* Tables 1 and 2). R also provides functions for calculations which cannot be expressed as a single operator, like exponential, log, and descriptive statistics (*see* Table 3). R supports various data structures, including single value (numeric, string, NA, etc.), vector (a group of values), data matrix (a two-dimensional matrix of same-type values), data frame (a two-dimensional matrix of mixed-type values), and list (a collection of named objects including single value, data frame, list, and so on). Below is an example of the data structures:

Table 1
Arithmetic operators in R

Operator	Description
+	Addition
-	Subtraction
*	Multiplication
/	Division
^ or **	Exponentiation
x %% y	Modulus (x mod y) 5%%2 is 1
x %/% y	Integer division 5%/%2 is 2

Table 2
Logical operators in R

Operator	Description
<	Less than
<=	Less than or equal to
>	Greater than
>=	Greater than or equal to
==	Exactly equal to
!=	Not equal to
!x	Not x
x | y	x OR y
x & y	x AND y
isTRUE(x)	Test if X is TRUE

Table 3
Some R functions

Function	Description
exp(x)	Exponential function with base of e, x is power
log(x, base=a)	Log function with base of a
log2(x)	Log function with base of 2
mean(x)	Average of a group of numeric values, x is a vector
var(x)	Variance of a group of numeric values, x is a vector
median(x)	Median of a group of numeric values, x is a vector
sum(x)	Summation of a group of numeric values, x is a vector
length(x)	Number of values in a vector x

```
# single value

a = 1;

print(paste("a =", a)) # paste serves as the glue among values

## [1] "a = 1"

b = 'Hello'

print(paste("Mrs. Kim says", b, 'world!'))

## [1] "Mrs. Kim says Hello world!"

# vector

a = c(1, 4, 5) # c is the abbreviation of 'concatenate'

print(a)

## [1] 1 4 5

print(a[2]) # locate the 2nd element in the ‘a’ vector by putting the index in []

## [1] 4


# data matrix

data_matrix = matrix(1:6, nrow=2, ncol=3)

colnames(data_matrix) = c("A", "B", "C")

rownames(data_matrix) = 3:4

print(data_matrix)

##   A B C## 3 1 3 5## 4 2 4 6
```

```
print(data_matrix[1,2:3]) # show part of the first row in data_matrix

## B C

## 3 5



# data frame

df = data.frame(7:9, c("A", "B", "C"))

colnames(df) = c("order", "value")

print(df)

##   order value

## 1     7     A

## 2     8     B

## 3     9     C

print(df[2, 'value']) # retrieve a single value in a data frame

## [1] B

## Levels: A B C

# we can apply a function to the first column of the data frame 'df'

print(var(df[,1])) # variance of the 'order' column/variable in the data frame ‘df’

## [1] 1
```

There are also flow control statements in R:

```
# if ... elseif ... else

if(1 < 0) {

   print("Yes! 1 is less than 0!")

} else if (1 == 0) {

    print("Actually 1 equals 0.")}

else {

   print("1 is greater than 0.")

}

## [1] "1 is greater than 0."

# for loop

x = c(1, 3, 5)

for(i in 1:length(x)) {

    print(x[i])

}

## [1] 1

## [1] 3

## [1] 5
```

R provides a family of 'read' and 'write' functions to import and export files:

```
write.table(df, 'data_frame.csv', row.names=FALSE, sep=',')

df1 = read.csv('data_frame.csv')

print(df1)
```

```
##   order value
## 1     7     A
## 2     8     B
## 3     9     C
```

With a few functions provided by the R base module, we are able to conduct basic statistical descriptions, as shown below:

```
df_imported = read.csv('data_frame.csv')
ord = df_imported[, 'order']
res = data.frame(c( mean(ord), var(ord), min(ord),  max(ord)))
rownames(res) = c("Mean", "Variance", "Minimum", "Maximum")
colnames(res) = 'value'
print(res)
##          value
## Mean         8
## Variance     1
## Minimum      7
## Maximum      9
```

3 Packages Outside the R Base Module

R is an open-source project supported by a great community of statisticians and computer scientists, as well as active users who are providing feedback. When a new algorithm is developed, the developer may draft customized functions and package them as plug-ins, called "packages," for R. By installing the packages, we can take the advantage of the latest statistical models, efficient algorithms, and save time on tedious, error-prone script drafting. There are two major R package resources suitable for antibody array data analysis. The first one is CRAN, the official repository of R packages. Any

package available on CRAN has passed several strenuous validation tests. The install.packages() function will install any of these packages available on CRAN:

```
install.packages("ggplot2", keep_outputs=TRUE)

## * installing *source* package ‘ggplot2’ …

## ** package ‘ggplot2’ successfully unpacked and MD5 sums checked## ** using staged

installation## ** R## ** data## *** moving datasets to lazyload DB## ** inst

## ** byte-compile and prepare package for lazy loading## ** help

## *** installing help indices## *** copying figures## ** building package indices

## ** installing vignettes## ** testing if installed package can be loaded from temporary location

## ** testing if installed package can be loaded from final location

## ** testing if installed package keeps a record of temporary installation path

## * DONE (ggplot2)
```

Another source for R packages is bioconductor (https://www.bioconductor.org/), which is a repository of open-source bioinformatics tools:

```
if (!requireNamespace("BiocManager", quietly = TRUE))

install.packages("BiocManager")

BiocManager::install("ComplexHeatmap", keep_outputs=TRUE)

## Bioconductor version 3.9 (BiocManager 1.30.4), R 3.6.0 (2019-04-26)

## Installing package(s) 'ComplexHeatmap'

## * installing *source* package ‘ComplexHeatmap’ …

## ** using staged installation
```

The library() function can be used to include the R packages in the antibody array analysis:

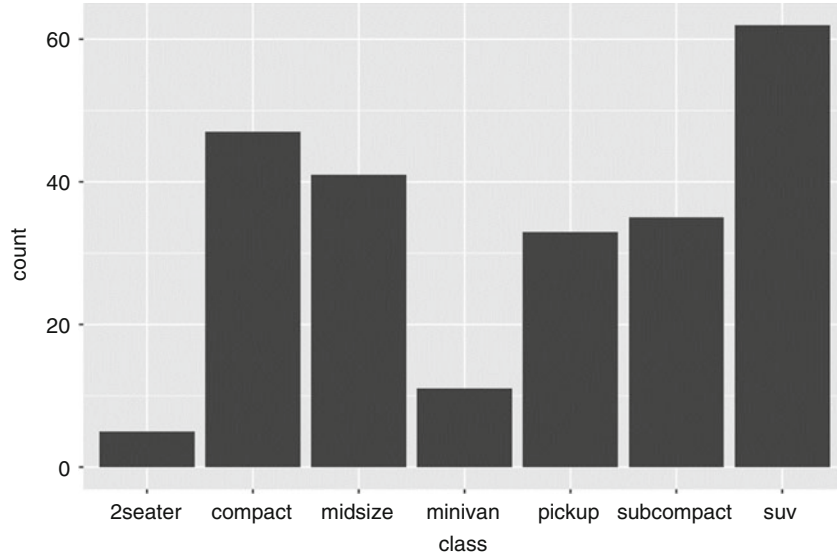

Fig. 1 An example of ggplot2: bar plot

```
library(ggplot2)
library(ComplexHeatmap)
## Loading required package: grid
## ========================================
## ComplexHeatmap version 2.0.0.
## ========================================
```

Once the packages are included, individual functions hiding within the R packages can be called directly (Fig. 1):

```
library(ggplot2)

ggplot(mpg, aes(class)) + geom_bar() # mpg is an automatically-loaded data frame in the ggplot2 package, and class is a column/variable in mpg.
```

4 Analysis of Antibody Array Data with R

As a high-throughput biomarker detection/measurement platform, the antibody array provides a powerful tool which is capable of reporting the expression levels of hundreds of proteins at the same time in an efficient manner. Such large-scale data requires a lot of data processing/statistical analysis, including (1) data cleanup and transformation; (2) visualization of the data profile; (3) differential expression analysis; (4) co-expression analysis; (5) enrichment analysis by integrating the findings in measured proteins and the

knowledge retrieved from other sources, like related signaling pathways and gene ontology; and (6) statistical modeling by developing models using the high-dimensional antibody array data to predict disease outcome, to classify patients, and to discover driving proteins.

4.1 Data Cleanup and Transformation

The data from an antibody array can be provided as concentrations or signal intensities. Sometimes, for a specific target, the value can be negative after removing background intensity, or the value can be missing if the signal is below the detection limit. R is able to easily handle the missing/negative values in a dataset:

```
data_set = read.csv('AAM-BLG-1_Results.csv')
head(data_set[,1:5]) # showing 4 columns/variables in the first 5 rows
in the dataset. Note the missing (NA) and negative values in the 3rd
row. NA means Not Available

##            Unnamed..1Sample.1   Sample.2  Sample.3Sample.4
## 1    Positive Control    42398 42398.00000 42398.00000 42398.000000
## 2                 Neg        1     1.00694     1.00687     1.004946
## 3              6Ckine        1     0.00000          NA   -36.680527
## 4           Activin A        1     1.00694     1.00687     1.004946
## 5            Activin C       1     1.00694     1.00687     8.542041
## 6 Activin RIB / ALK-4        1     1.00694     1.00687     1.004946
# replace the NA, 0 and negative values with 1
data_set[data_set <=0 | is.na(data_set)] = 1
head(data_set[, 1:5])
##            Unnamed..1 Sample.1    Sample.2    Sample.3     Sample.4
## 1    Positive Control    42398 42398.00000 42398.00000 42398.000000
## 2                 Neg        1     1.00694     1.00687     1.004946
## 3              6Ckine        1     1.00000     1.00000     1.000000
## 4           Activin A        1     1.00694     1.00687     1.004946
## 5            Activin C       1     1.00694     1.00687     8.542041
## 6 Activin RIB / ALK-4        1     1.00694     1.00687     1.004946
```

Sometimes, we can simply exclude the observations/variables with missing/negative values:

```
# Remove observations with missing/negative values
data_set_exclude_sample = data_set[, -c(4,5)]
head(data_set_exclude_sample[, 1:5])
##            Unnamed..1 Sample.1    Sample.2     Sample.5     Sample.6
## 1    Positive Control    42398 42398.00000 42398.000000 42398.000000
## 2                 Neg        1     1.00694     1.030028     1.046935
## 3              6Ckine        1     1.00000     1.000000   123.014812
## 4           Activin A        1     1.00694     2.060055    64.386476
```

```
## 5           Activin C        1     1.00694    32.960886    92.130242
## 6 Activin RIB / ALK-4        1     1.00694     1.030028    38.736579
# Remove targets with missing/negative values
data_set_exclude_target = data_set[-3,]
head(data_set_exclude_target[, 1:5])
##             Unnamed..1 Sample.1    Sample.2    Sample.3     Sample.4
## 1     Positive Control    42398 42398.00000 42398.00000 42398.000000
## 2                  Neg        1     1.00694     1.00687     1.004946
## 4           Activin A         1     1.00694     1.00687     1.004946
## 5            Activin C        1     1.00694     1.00687     8.542041
## 6  Activin RIB / ALK-4        1     1.00694     1.00687     1.004946
## 7 Adiponectin / Acrp30       31     1.00694     1.00687    14.069243
```

Data transformation is straight forward, too:

```
# Log2 transformation
data_set_log2 = log2(data_set[,2:ncol(data_set)])
rownames(data_set_log2) = data_set[,1]
head(data_set_log2[,1:4])
##                     Sample.1     Sample.2     Sample.3     Sample.4
## Positive Control    15.37171 15.371708591 15.371708591 15.371708591
## Neg                  0.00000  0.009977997  0.009877114  0.007117921
## 6Ckine               0.00000  0.000000000  0.000000000  0.000000000
## Activin A            0.00000  0.009977997  0.009877114  0.007117921
## Activin C            0.00000  0.009977997  0.009877114  3.094580762
## Activin RIB / ALK-4  0.00000  0.009977997  0.009877114  0.007117921
```

```
# Standardization - centering and scaling
# calculate the mean and standard deviation (SD) of each target
averages = apply(data_set_log2, 1, mean)
stdevs = apply(data_set_log2, 1, function(x) {sqrt(var(x))})
# Standardization by subtracting the mean and scaling with SD
data_set_log2_standardized = (data_set_log2 - averages)/stdevs
head(data_set_log2_standardized[,1:4])
##                       Sample.1   Sample.2   Sample.3   Sample.4
## Neg                 -1.1170657 -0.7410343 -0.7448362 -0.8488193
## 6Ckine              -0.8134752 -0.8134752 -0.8134752 -0.8134752
## Activin A           -0.5878568 -0.5838792 -0.5839194 -0.5850193
## Activin C           -0.9067482 -0.9030441 -0.9030815  0.2420566
## Activin RIB / ALK-4 -0.4182023 -0.4126504 -0.4127065 -0.4142418
```

4.2 Visualization of Data Profile: Heatmap of Antibody Array Data

Using a heatmap after data transformation can provide an intuitive way to visualize the relative expression of targets in multiple samples. We can also rearrange the positions of targets/samples based on distance in the heatmap and divide the targets/samples into subgroups by hierarchical clustering by linking with a dendrogram.

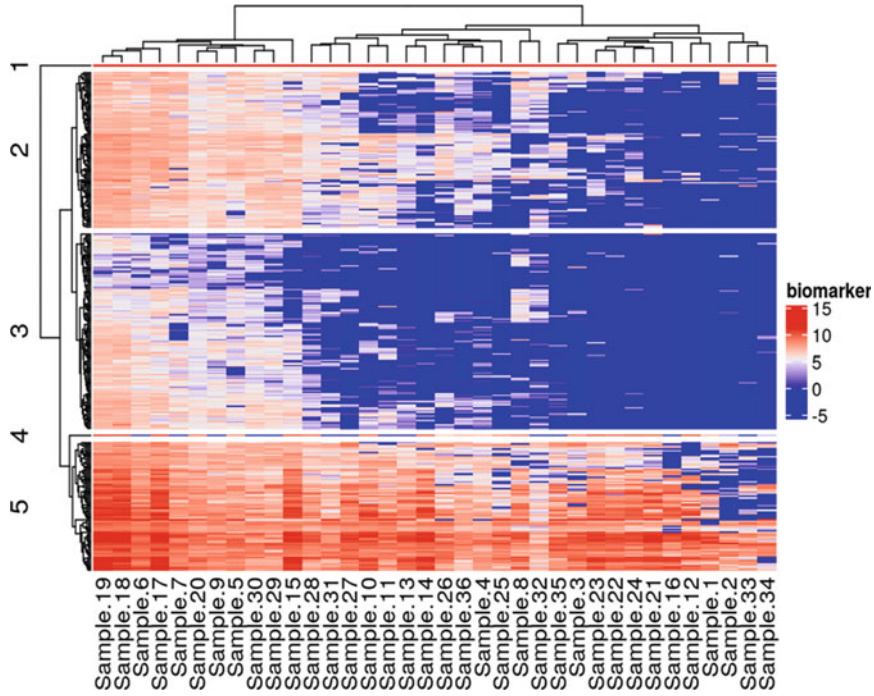

Fig. 2 An example of a heatmap with hierarchical clustering

A heatmap with hierarchical clustering with R package *ComplexHeatmap* is shown below (Fig. 2) [2]:

```
library(ComplexHeatmap)
# 5 biomarker clusters; suppress row names (biomarker)
ht = Heatmap(data_set_log2, name='biomarker', split=5, show_row_names=F)
ht
```

4.3 Principal Component Analysis and Visualization

The difference among samples originates from, or can be reflected by, the variation existing in the measurements. Intuitively, the measurements carrying the greatest variation may retain the power to classify samples and/or to represent the intrinsic data characteristics. Principal component analysis (PCA) treats the variation extraction from a different perspective. Rather than selecting the original measurements with the highest variation, PCA decomposes the whole variation from all the measurements and generates uncorrelated variables, named principal components (PCs), with each carrying some variation existing in the original data. Each PC is a linear combination of all the original measurements with specific weights/coefficients. By selecting PCs carrying the greatest variation, we can visualize the data profile of an antibody array with two or three PCs only while keeping most of

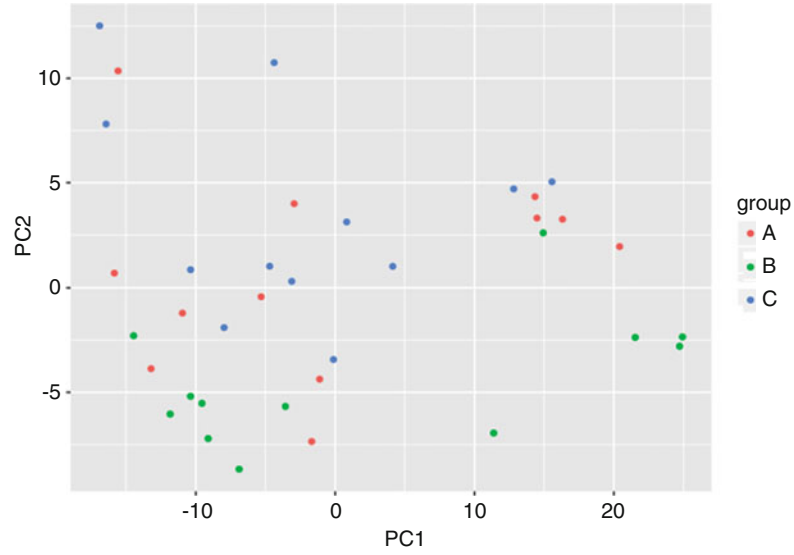

Fig. 3 An example of a PCA plot

the variations in the original dataset (Fig. 3). An example is shown below:

```
pcaObj = prcomp(scale(t(data_set_log2)))

pcs = data.frame(pcaObj$x)

#load ggplot2

library(ggplot2)

g = ggplot(pcs, aes(PC1, PC2, color=group))g + geom_point()
```

4.4 Differential Expression Analysis

4.4.1 Differential Expression Analysis by Target with Multiple Comparison Correction

The targets with differential expression between two groups can be detected with a classic t-test or with a Mann-Whitney-Wilcoxon test. An example of this analysis in R is shown below:

```
# two-sample t-test

t.test(data_set_log2[1:10, 1], data_set_log2[11:20, 1])

##  Welch Two Sample t-test

##  data:  data_set_log2[1:10, 1] and data_set_log2[11:20, 1]

## t = 0.12719, df = 17.346, p-value = 0.9003

## alternative hypothesis: true difference in means is not equal to 0
```

```
## 95 percent confidence interval:
##  -2.447491  2.762012
## sample estimates:
## mean of x mean of y
##  1.535294  1.378033


# two-sample, non-parametric Wilcoxon test
wilcox.test(data_set_log2[1:10, 1], data_set_log2[11:20, 1])
## Warning in wilcox.test.default(data_set_log2[1:10, 1],
## data_set_log2[11:20,1] : cannot compute exact p-value with ties
## Wilcoxon rank sum test with continuity correction
## data:  data_set_log2[1:10, 1] and data_set_log2[11:20, 1]
## W = 53, p-value = 0.8038
## alternative hypothesis: true location shift is not equal to 0
```

However, when multiple targets are compared between groups, the p-values have to be corrected to account for the false discovery rate [3]. The possibility of seeing a small p-value increases with the number of comparisons, even if there is no true difference between the groups.

```
pvalue = NULL
for(i in 4:20) {
  p_value = t.test(data_set_log2[1:10, i], data_set_log2[11:20, i])$p.value
  pvalue = c(pvalue, p_value)
}
```

```
fdr = p.adjust(pvalue, 'fdr')

head(data.frame(pvalue, fdr))

##       pvalue       fdr

## 1 0.07674305 0.7115943

## 2 0.80037580 0.8132305

## 3 0.45150852 0.7115943

## 4 0.58601883 0.7115943

## 5 0.55113015 0.7115943

## 6 0.51732824 0.7115943
```

4.4.2 Differential Expression Analysis Based on Permutation

The power of classical statistical comparison for differentially expressed targets may be limited by a small sample size in an antibody array dataset, which can lead to great sampling error and unstable variance estimation. Tusher et al. introduced a permutation-based approach for significant analysis in microarray (SAM) [4]. It permutes the samples to form varied group assignments and then calculates the signal-to-noise measurement (d) of each target under each permuted scenario with offset on standard deviations. The difference between the d observed in the actual experimental design against the average value across all the permutations is used to determine the differential expression, by comparing with the predefined criteria delta. The targets with larger/smaller d are considered as significant. An example is shown below (Fig. 4):

```
library(siggenes) # load R package

head(data_matrix[,1:5])

##            C01      C02      C03      C04      C05

## AR     57.52530  38.84040  43.64372  48.60113  41.46322

## Axl   331.62918 490.58897 418.80853 352.08540 345.74067

## CD27L   0.00000   0.00000   0.00000   0.00000   0.00000

## CD30    0.00000   0.00000   0.00000   0.00000   0.00000

## CD40  151.54535 413.73522 344.28913 156.33027 299.75342
```

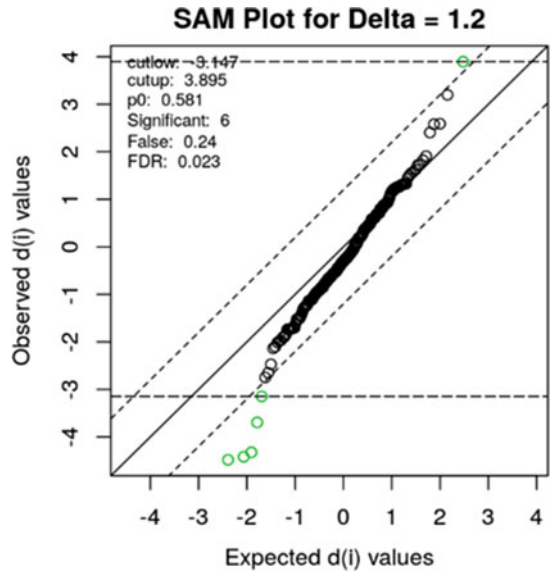

Fig. 4 An example of SAM plot. Significantly different targets are colored green

```
## CXCL16  47.06713  27.36741  29.75997  34.49295  35.39381

group = c(rep("A", 10), rep("B", 10))

sam.out = sam(data_matrix, group, rand=1234)

## Warning: Expected class labels are 0 and 1. A is set to 0, and B is set to1.

summary(sam.out, delta=1.2)@mat.sig

##          Row   d.value     stdev     rawp    q.value      R.fold

## IGFBP-3   13 -4.482097  57.49562 0.00015 0.005809724 1.071757e-80

## ICAM-1    49 -4.417786 250.65831 0.00015 0.005809724 0.000000e+00

## IL-6      57 -4.323980   2.90103 0.00015 0.005809724 8.206574e-07

## NOV      148  3.895335 581.60240 0.00035 0.010167017         Inf

## JAM-A    104 -3.694945 586.75162 0.00055 0.012781393 0.000000e+00

## G-CSF     47 -3.146907  13.45766 0.00280 0.046477794 3.718880e-15

plot(sam.out, 1.2)
```

4.4.3 Differential Expression Analysis Basing on Variance Estimated with Empirical Bayes Method

Smyth developed a method to handle the unstable target-wise variance based on the empirical Bayes method by borrowing information from other targets [5]. Assuming the variance of targets follows a distribution with prior information s0 and d0, a posterior estimation can be derived with the observed data by the empirical Bayesian method, which shrinks from the observed target-wise variance to s0. The moderated target variance leads to a more stable statistical inference under a linear model framework. The R package limma can accomplish this process with only a few statements, as shown below:

```
library(limma)

## Attaching package: 'limma

#limma requires a design matrix for analysis

group = factor(c(rep("A", 10), rep("B", 10)), levels=c("A", "B"))

design = model.matrix(~group)

rownames(design) = colnames(data_matrix)

design[c(1:3, 18:20),]

##     (Intercept) groupB

## C01           1      0

## C02           1      0

## C03           1      0

## C38           1      1

## C39           1      1

## C40           1      1

fit = lmFit(data_matrix, design) # fitting linear models for targets

fit = eBayes(fit) # adjusting the variance of targets

topTable(fit, adjust='BH') # report results with multiple test correction on p-values

## Removing intercept from test coefficients
```

```
##              logFC    AveExpr        t      P.Value  adj.P.Val       B
## IL-6      -20.21672   12.28301 -5.136268 6.359335e-05 0.01271867 -4.295531
## IGFBP-3   -265.65427 1028.35782 -4.679456 1.742973e-04 0.01693305 -4.321513
## ICAM-1    -1115.19390 3851.38957 -4.510748 2.539958e-04 0.01693305 -4.368513
## NOV        2272.44838 5237.97419  3.961587 8.736726e-04 0.04368363 -4.331873
## JAM-A     -2174.57164 2470.71958 -3.757689 1.384094e-03 0.05536378 -4.383234
## G-CSF       -47.93405   31.12796 -3.538806 2.265932e-03 0.07553108 -4.399673
## Galectin-1 1119.91000 5054.89606  3.259349 4.235442e-03 0.12101263 -4.421531
## IL-5       -17.59264   11.54497 -3.195746 4.878854e-03 0.12197134 -4.426628
## IL-13      -103.78452   86.10774 -2.914217 9.069025e-03 0.20153388 -4.449635
## TSLP         76.42316   91.50405  2.780571 1.211980e-02 0.24239601 -4.460757
```

4.5 Co-expression Network Analysis

The power of the antibody array comes from the high-throughput measurement of multiple target proteins. With antibody array data, the relations/connections among the proteins can be identified using co-expression analysis. The co-expression network analysis evaluates the protein relationships based on the correlation between pairs of proteins. Assuming the correlated proteins may be involved in the same biological pathway/mechanism, co-expression analysis can bring insight into the network of protein interactions. Co-expression network analysis can be conducted within *one* group of samples of specific interest. The key goal is finding the adjacency matrix derived from the pairwise correlation between targets. If the correlation coefficients, ranging from −1 to +1, are lacking good resolution, co-expression analysis may conduct transformation on the coefficients, like removing the sign of coefficients and raising them to a power no less than 1, to increase the sensitivity. The connections between multiple target pairs construct a network, and those with closer connections can be considered as one group, called a module. The modules can be linked to external information, like clinical traits or functional annotation of targets. Below is an analysis example with the R package WGCNA [6] (Fig. 5 and 6, data from https://wikis.utexas.edu/display/bioiteam/Clustering+using+WGCNA):

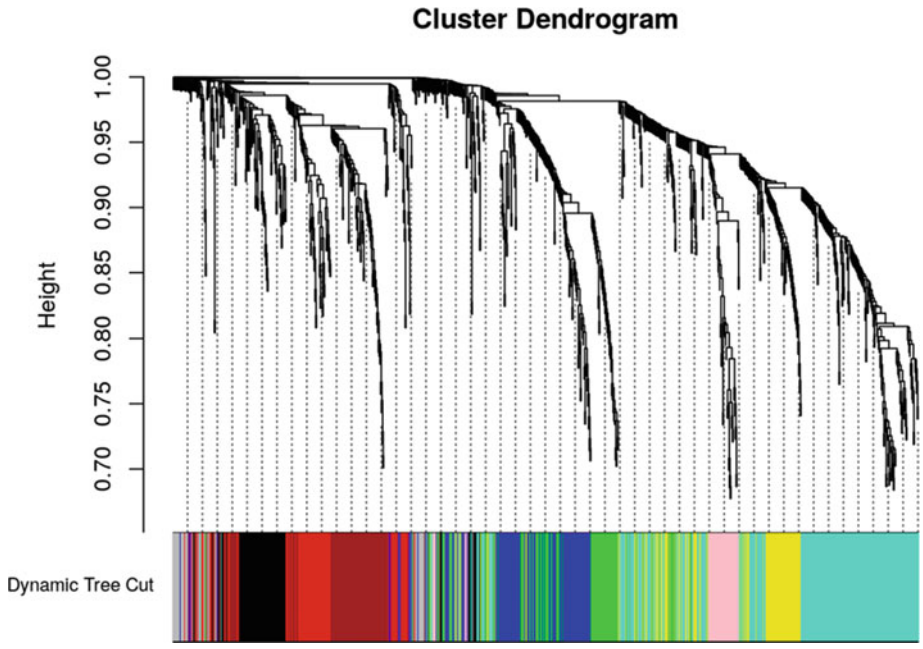

Fig. 5 Utexas modules from a weighted gene co-expression analysis

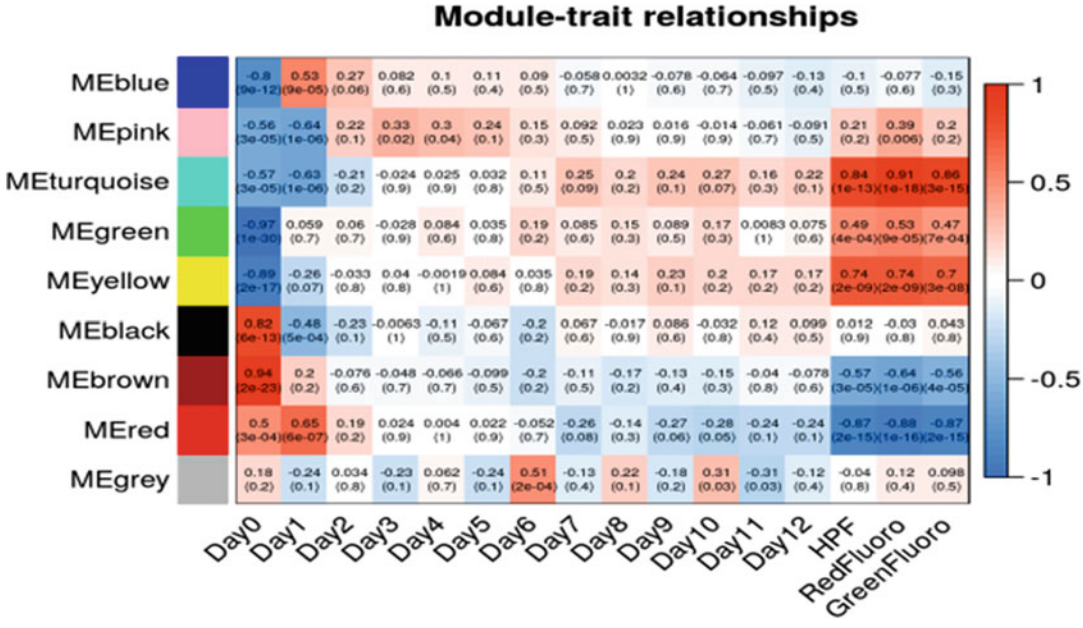

Fig. 6 An example of module-trait relationship heatmap

```
library(WGCNA)

library(flashClust)

# WGCNA requires targets as columns, and samples as rows

datExpr = read.csv("data/SampleTimeSeriesRLD.csv")

rownames(datExpr) = datExpr$XdatExpr = t(datExpr[,-1])

datTraits = read.csv("data/Traits_23May2015.csv")

rownames(datTraits) = datTraits$SampledatTraits = datTraits[,-1]
```

We can choose a soft threshold power for correlation coefficients analysis.

```
#constructing a set of soft-thresholding powers

powers = c(c(1:10), seq(from =10, to=30, by=1))

#call network topology analysis function

sft = pickSoftThreshold(datExpr, powerVector=powers, verbose =5, networkType="signed")

## pickSoftThreshold: will use block size 1000.

## pickSoftThreshold: calculating connectivity for given powers...

##    ..working on genes 1 through 1000 of 1000

##    Power SFT.R.sq  slope truncated.R.sq mean.k. median.k. max.k.

## 1      1    0.604  2.520        0.85600  524.00   543.000  609.0

## 2      2    0.177 -0.985       -0.00776  317.00   322.000  448.0

## 3      3    0.434 -1.180        0.28100  210.00   203.000  354.0

## 4      4    0.562 -1.190        0.55000  147.00   133.000  291.0

## 5      5    0.610 -1.160        0.68600  107.00    90.900  245.0

## 6      6    0.634 -1.180        0.77700   81.00    66.500  209.0

## 7      7    0.674 -1.180        0.81700   62.60    49.900  180.0
```

```
## 8     8  0.709 -1.210  0.85200  49.30  38.600  157.0
## 9     9  0.729 -1.240  0.87600  39.50  29.600  138.0
## 10   10  0.756 -1.240  0.90300  32.10  23.000  122.0
## 11   10  0.756 -1.240  0.90300  32.10  23.000  122.0
## 12   11  0.766 -1.290  0.90500  26.40  18.200  108.0
## 13   12  0.791 -1.300  0.92200  21.90  14.500   96.5
## 14   13  0.792 -1.350  0.91400  18.30  11.500   86.5
## 15   14  0.811 -1.360  0.92600  15.50   9.210   77.8
## 16   15  0.829 -1.380  0.93600  13.20   7.520   70.3
## 17   16  0.861 -1.350  0.95100  11.30   6.250   63.6
## 18   17  0.874 -1.370  0.95900   9.71   5.060   57.8
## 19   18  0.880 -1.370  0.95600   8.42   4.140   52.6
## 20   19  0.897 -1.360  0.96800   7.33   3.400   48.0
## 21   20  0.903 -1.350  0.96700   6.42   2.830   43.9
## 22   21  0.922 -1.350  0.97700   5.64   2.390   40.3
## 23   22  0.936 -1.330  0.98500   4.98   1.980   37.0
## 24   23  0.944 -1.340  0.98900   4.41   1.670   34.0
## 25   24  0.953 -1.320  0.99500   3.92   1.390   31.3
## 26   25  0.956 -1.310  0.99300   3.50   1.140   28.9
## 27   26  0.958 -1.300  0.98900   3.14   0.953   26.7
## 28   27  0.964 -1.280  0.99300   2.82   0.807   24.8
## 29   28  0.970 -1.270  0.99400   2.54   0.690   22.9
## 30   29  0.974 -1.260  0.99400   2.29   0.584   21.3
## 31   30  0.976 -1.250  0.98900   2.08   0.501   19.8
```

We set the gene co-expression network analysis to a power of 18:

```
softPower = 18

adjacency = adjacency(datExpr, power = softPower, type = "signed")

#translate the adjacency into topological overlap matrix and calculate the corresponding

dissimilarity:

TOM = TOMsimilarity(adjacency, TOMType="signed")

# specify network type

## ..connectivity..## ..matrix multiplication (system BLAS)..## ..normalization..## ..done.

dissTOM = 1-TOM

# generate a clustered gene tree

geneTree = flashClust(as.dist(dissTOM), method="average")

#this sets the minimum number of genes to cluster into a module

minModuleSize = 30

dynamicMods = cutreeDynamic(dendro= geneTree, distM= dissTOM, deepSplit=2,

pamRespectsDendro= FALSE, minClusterSize = minModuleSize)

##  ..cutHeight not given, setting it to 0.997  ===>  99% of the (truncated) height range in

dendro.

##  ..done.

dynamicColors= labels2colors(dynamicMods)

#plot dendrogram with module colors below It

plotDendroAndColors(geneTree, cbind(dynamicColors), c("Dynamic Tree Cut"),

dendroLabels= FALSE, hang=0.03, addGuide= TRUE, guideHang=0.05)
```

Now we can map the modules to traits.

```
#define number of genes and samples

nGenes = ncol(datExpr)

nSamples = nrow(datExpr)

#recalculate MEs with color labels

MEs0 = moduleEigengenes(datExpr, dynamicColors)$eigengenes

MEs = orderMEs(MEs0)moduleTraitCor = cor(MEs, datTraits, use= "p")

moduleTraitPvalue = corPvalueStudent(moduleTraitCor, nSamples)

#print correlation heatmap between modules and traits

textMatrix= paste(signif(moduleTraitCor, 2), "\n(",  signif(moduleTraitPvalue, 1), ")", sep= "")

dim(textMatrix)= dim(moduleTraitCor)

par(mar= c(6, 8.5, 3, 3))#display the correlation values with a heatmap plot (Figure 6)

labeledHeatmap(Matrix= moduleTraitCor,

        xLabels= names(datTraits),

        yLabels= names(MEs),

        ySymbols= names(MEs),

        colorLabels= FALSE,

        colors= blueWhiteRed(50),

        textMatrix= textMatrix,

        setStdMargins= FALSE,

        cex.text= 0.5,

        zlim= c(-1,1),

        main= paste("Module-trait relationships"))
```

4.6 Functional/ Knowledge Database-Based Enrichment Analysis

While the differential expression and co-expression network analysis provides a way to screen the targets measured in antibody array studies, it is desirable to extend our sight beyond the targets observed by their connection to those unmeasured. Enrichment analysis is based on biological knowledge, e.g., signaling pathways, gene ontology terms, and other categories/clusters of biomarkers, and provides the power to identify the biological mechanism of which the differentially/co-expressed proteins are involved. There are two methods for knowledge database-based enrichment analysis. The first method is called "overrepresentation," and it counts the number of selected proteins falling into a specific pathway/term and then estimates the probability according to hypergeometric distribution. The second method, gene set enrichment analysis (GSEA) [7], uses the fold changes of all the targets between two groups and calculates an enrichment score for each pathway/term with the fold changes of targets falling into it. An example using the R package *clusterProfiler* [8] implementing both methods for analyzing overrepresentation of significantly differential targets among all the biomarkers regarding KEGG pathway and gene ontology terms is shown below:

```
# load R package

library(clusterProfiler)# load mouse gene database

library(org.Mm.eg.db)

# gene id for significantly differential targets

sig_bioms

## [1] "16009" "12985" "15894" "16193" "16456" "18133"

# gene id for 200 targets measured

length(all_bioms)

## [1] 198

# KEGG pathway enrichment, 0 identified

kk = enrichKEGG(gene=sig_bioms, universe=all_bioms, organism='mmu', pvalueCutoff=1,

keyType = "ncbi-geneid")
```

```
head(kk)

## [1] ID Description GeneRatio BgRatio pvalue p.adjust ## [7] qvalue geneID
Count ## <0 rows> (or 0-length row.names)

# GO biological process enrichment, 0 go term with qvalue<0.10go_res =
enrichGO(gene=sig_bioms, universe=all_bioms, OrgDb=org.Mm.eg.db, ont='BP',
keyType="ENTREZID", pvalueCutoff=1, qvalueCutoff=1, readable=T)

head(go_res)

##                ID                          Description

## GO:0030036 GO:0030036              actin cytoskeleton organization

## GO:0051051 GO:0051051             negative regulation of transport

## GO:0030029 GO:0030029               actin filament-based process

## GO:0051128 GO:0051128 regulation of cellular component organization

## GO:0007010 GO:0007010                 cytoskeleton organization

## GO:0046883 GO:0046883             regulation of hormone secretion

##           GeneRatio BgRatio      pvalue  p.adjust    qvalue

## GO:0030036       3/6  11/196 0.002428528 0.5168014 0.5019756

## GO:0051051       4/6  26/196 0.003103004 0.5168014 0.5019756

## GO:0030029       3/6  12/196 0.003199254 0.5168014 0.5019756

## GO:0051128       6/6  79/196 0.003813596 0.5168014 0.5019756
```

```
## GO:0007010       3/6  14/196 0.005166627 0.5168014 0.5019756
## GO:0046883       3/6  15/196 0.006380135 0.5168014 0.5019756
##                                 geneID Count
## GO:0030036              Csf3/Icam1/F11r     3
## GO:0051051          Igfbp3/Icam1/Il6/Ccn3     4
## GO:0030029              Csf3/Icam1/F11r     3
## GO:0051128 Igfbp3/Csf3/Icam1/Il6/F11r/Ccn3     6
## GO:0007010              Csf3/Icam1/F11r     3
## GO:0046883              Igfbp3/Il6/Ccn3     3
```

Gene set enrichment analysis using the log2 fold-change of all the biomarkers measured between two groups:

```
# log2 fold-change of all the biomarkers

head(fc)

##    21948    22035    70835    17395    22164    14205 ## 12.905478 11.481549  9.930964
2.937867  2.423868  1.531103

# GSEA with KEGG pathway

gsea_kk <- gseKEGG(geneList=fc, organism= 'mmu', nPerm=1000, minGSSize=10,
        pvalueCutoff = 1, keyType = "ncbi-geneid")

## preparing geneSet collections...

## GSEA analysis...

## Warning in fgsea(pathways = geneSets, stats = geneList, nperm = nPerm,

## minSize = minGSSize

## leading edge analysis...

## done...
```

```
head(gsea_kk)

##              ID                    Description setSize enrichmentScore
## mmu04630 mmu04630      JAK-STAT signaling pathway      32      -0.8017727
## mmu05321 mmu05321 Inflammatory bowel disease (IBD)      19      -0.8823569
## mmu05310 mmu05310                         Asthma      10      -0.8891131
## mmu04657 mmu04657         IL-17 signaling pathway      24      -0.8122916
## mmu05152 mmu05152                     Tuberculosis      13      -0.8645117
## mmu04658 mmu04658 Th1 and Th2 cell differentiation      10      -0.8769430
##              NES      pvalue  p.adjust    qvalues rank
## mmu04630 -1.520057 0.004160888 0.1058824 0.08591331   30
## mmu05321 -1.559277 0.004411765 0.1058824 0.08591331   24
## mmu05310 -1.466272 0.018707483 0.1971831 0.15999506   13
## mmu04657 -1.489864 0.019746121 0.1971831 0.15999506   18
## mmu05152 -1.459415 0.026813880 0.1971831 0.15999506   24
## mmu04658 -1.446202 0.028911565 0.1971831 0.15999506   22
##                        leading_edge
## mmu04630 tags=48%, list=15%, signal=49%
## mmu05321 tags=53%, list=12%, signal=51%
## mmu05310  tags=60%, list=7%, signal=59%
```

```
## mmu04657  tags=33%, list=9%, signal=34%

## mmu05152 tags=46%, list=12%, signal=43%

## mmu04658 tags=60%, list=11%, signal=56%

##                                                    core_enrichment

## mmu04630
16168/16196/83430/60505/16159/16160/16184/12983/13645/16163/16187/12985/16193/15978/
16191

## mmu05321
60505/16159/16160/16163/21926/16193/16171/15978/16191

## mmu05310                                          21939/16163/16187/21926/16191##
mmu04657                                    16163/12985/21926/16193/16171/15978/16191

## mmu05152                                          16159/16160/21926/16193/15978

## mmu04658                                          16160/16184/16163/15978/16191
```

```
# GSEA with GO biological processgsea_go <- gseGO(geneList=fc, OrgDb=org.Mm.eg.db,
nPerm=1000, minGSSize=10, ont='BP', pvalueCutoff = 1, keyType="ENTREZID" )

## preparing geneSet collections...## GSEA analysis...

## Warning in fgsea(pathways = geneSets, stats = geneList, nperm = nPerm,

## minSize = minGSSize

## leading edge analysis...

## done...
```

```
head(gsea_go)

##                 ID                                Description
## GO:1903706 GO:1903706                  regulation of hemopoiesis
## GO:0018108 GO:0018108              peptidyl-tyrosine phosphorylation
## GO:0018212 GO:0018212               peptidyl-tyrosine modification
## GO:0008104 GO:0008104                     protein localization
## GO:0018193 GO:0018193              peptidyl-amino acid modification
## GO:0050730 GO:0050730 regulation of peptidyl-tyrosine phosphorylation##            setSize
enrichmentScore       NES       pvalue p.adjust## GO:1903706      46      -0.7581617 -1.498970
0.001335113 0.283741
## GO:0018108      45      -0.7907203 -1.559996 0.001342282 0.283741
## GO:0018212      45      -0.7907203 -1.559996 0.001342282 0.283741
## GO:0008104      49      -0.7633553 -1.535373 0.002604167 0.283741
## GO:0018193      49      -0.7692424 -1.547214 0.002604167 0.283741
## GO:0050730      42      -0.7944174 -1.555642 0.002713704 0.283741
##            qvalues rank                 leading_edge
## GO:1903706 0.2565695   30 tags=37%, list=15%, signal=41%
## GO:0018108 0.2565695   31 tags=40%, list=16%, signal=44%
## GO:0018212 0.2565695   31 tags=40%, list=16%, signal=44%
## GO:0008104 0.2565695   14 tags=16%, list=7%, signal=20%
```

```
## GO:0018193 0.2565695   31 tags=37%, list=16%, signal=41%
## GO:0050730 0.2565695   31 tags=40%, list=16%, signal=43%
##                                                  core_enrichment
## GO:1903706
16168/16196/16323/83430/60505/16159/16160/16184/16542/16187/12985/21926/16193/16171/
15978/16191
## GO:0018108
16183/16168/12491/16196/83430/60505/16159/16160/16542/13645/16163/16187/12985/21926/
16193/15978/16191
## GO:0018212
16183/16168/12491/16196/83430/60505/16159/16160/16542/13645/16163/16187/12985/21926/
16193/15978/16191
## GO:0008104
16163/21926/16193/16171/15978/16191/16456
## GO:0018193
16183/16168/12491/16196/83430/60505/16159/16160/16542/13645/16163/16187/12985/21926/
16193/15978/16191
## GO:0050730
16183/16168/12491/16196/83430/60505/16159/16160/13645/16163/16187/12985/21926/16193/
15978/16191
```

4.7 Statistical Modeling

Statistical modeling/machine learning techniques provide us powerful tools to classify samples and/or identify important underlying biomarkers, when we have sufficient samples with antibody array data. With R package caret [9], data preprocessing, feature selection, dataset splitting, model training, and validation can be conducted. An example of statistical modeling analysis with this

package, for example, data of 170 samples and 28 biomarkers, is shown below:

```
# 170 samples with 38 targets measured

print(paste('# targets:', ncol(data_matrix), ' # samples:', nrow(data_matrix)))

## [1] "# targets: 38  # samples: 170"

# Two groups

table(group)

## group

## Cancer Health

##     90     80
```

The targets with high correlation may compromise the modeling performance. We can identify them with pairwise correlation analysis:

```
correlations <- cor(data_matrix)

highCorr = findCorrelation(correlations, cutoff = .7)

highCorrBioms = colnames(data_matrix)[head(highCorr)]highCorrBioms

## [1] "IL-2 Ra" "IL-1 R6" "MIF"     "IL-6"    "IGFBP-4" "AgRP "
```

We can transform the original data with different algorithm in caret for better normality, which may improve the performance of some modeling techniques:

```
#YeoJohnson transformation

dataTrans = preProcess(data_matrix,method=c("YeoJohnson"))

data_matrix_transYJ = predict(dataTrans,data_matrix)
```

Screening the targets for the combination of better performance using recursive feature elimination technique with a random forest algorithm and a threefold cross-validation. A combination of 19 biomarkers was reported as the best in the selection run:

```
# set randomization seed number for reproducible analysis

set.seed(123)

rfeCtrl = rfeControl(functions=rfFuncs, method="cv",number=3, repeats=10)

rfeRes = rfe(data_matrix_transYJ, factor(group, levels=c("Health", "Cancer")), size=c(1:38),

rfeControl=rfeCtrl)

rfeRes

 ## Recursive feature selection

## Outer resampling method: Cross-Validated (3-fold)

## Resampling performance over subset size:

## Variables Accuracy  Kappa AccuracySD KappaSD Selected

##         1   0.7474 0.4924    0.07168 0.14603

##         2   0.8178 0.6329    0.05583 0.11105

##         3   0.8415 0.6826    0.04535 0.08930

##         4   0.8588 0.7158    0.03512 0.07041

##         5   0.9003 0.8001    0.05319 0.10521

##         6   0.8885 0.7765    0.04357 0.08596

##         7   0.8768 0.7528    0.05201 0.10311

##         8   0.8885 0.7759    0.03582 0.07104

##         9   0.8943 0.7878    0.03446 0.06806
```

```
##      10  0.8943 0.7878  0.03446 0.06806
##      11  0.9003 0.7999  0.04365 0.08684
##      12  0.8944 0.7880  0.05216 0.10406
##      13  0.9062 0.8118  0.05326 0.10615
##      14  0.9003 0.7997  0.04365 0.08654
##      15  0.9062 0.8118  0.05326 0.10615
##      16  0.9003 0.7997  0.04365 0.08654
##      17  0.9120 0.8234  0.03462 0.06820
##      18  0.9060 0.8112  0.02626 0.05109
##      19  0.9179 0.8355  0.04382 0.08699    *
##      20  0.9120 0.8234  0.03462 0.06820
##      21  0.9121 0.8237  0.05232 0.10414
##      22  0.9178 0.8352  0.02629 0.05148
##      23  0.9179 0.8355  0.04382 0.08699
##      24  0.9002 0.7994  0.03602 0.07089
##      25  0.9120 0.8234  0.03462 0.06820
##      26  0.9003 0.7997  0.04365 0.08654
##      27  0.9121 0.8237  0.05232 0.10414
##      28  0.9179 0.8352  0.04382 0.08741
```

```
##         29   0.9121 0.8237    0.04606 0.09171

##         30   0.9002 0.7991    0.03602 0.07147

##         31   0.9178 0.8350    0.02629 0.05182

##         32   0.9003 0.7997    0.05319 0.10584

##         33   0.9060 0.8112    0.02626 0.05109

##         34   0.9120 0.8231    0.03462 0.06866

##         35   0.9062 0.8118    0.05326 0.10615

##         36   0.9120 0.8234    0.03462 0.06820

##         37   0.9061 0.8116    0.04372 0.08660

##         38   0.9061 0.8116    0.04372 0.08660


 ## The top 5 variables (out of 19):

##    MSPa , ApoA1, EGF , PDGF Ra, CA125

# list of biomarkers selected by recursive feature elimination

predictors(rfeRes)

##  [1] "MSPa "      "ApoA1"      "EGF "       "PDGF Ra"    "CA125"

##  [6] "BDNF"       "EGF R"      "PDGF-AA "   "PDGF Rb "   "B2M"

## [11] "OPN"        "TIMP-4"     "IL-6"       "Mesothelin" "IL-6 sR"

## [16] "TIMP-2"     "Leptin "    "CEA"        "VEGF"
```

Splitting the dataset into training/testing for model training and validation, respectively:

```
# set seed of randomization for reproducible analysis

set.seed(1005)

trainIdx = createDataPartition(group,p=.75,list=F)

trainData = data_matrix[trainIdx,]

testData = data_matrix[-trainIdx,]

trainGroup = factor(group[trainIdx], levels=c("Health", "Cancer"))

testGroup = factor(group[-trainIdx], levels=c("Health", "Cancer"))

print(paste("# training:", nrow(trainData), "  # testing:", nrow(testData)))

## [1] "# training: 128   # testing: 42"
```

Both the training and testing datasets were transformed with parameters learned from the training dataset:

```
# retrieve transforming parameters from training data

dataTransByTraining<-preProcess(trainData,method=c("YeoJohnson"))# data transformation of

training/testing data with same parameters from training data

trainData = predict(dataTransByTraining,trainData)

testData = predict(dataTransByTraining,testData)
```

There are hundreds of modeling algorithms available in the caret package. Three of them, logistic regression (LR), linear discriminant analysis, (LDA) and random forest (RF), were applied on the training dataset of targets selected by recursive feature elimination. Please note that results from other feature selection techniques can also serve as inputs.

```
# model training with three algorithms
ctrl = trainControl(method="repeatedCV",repeats=5, number=3,
#summaryFunction=twoClassSummary,       classProbs=T)
## Warning: `repeats` has no meaning for this resampling method.
lrFit = train(trainData[, 1:5], y=trainGroup, method="glm",metric="Accuracy", trControl=ctrl,
preProcess=c("center","scale"))
ldaFit = train(trainData[, 1:5], y=trainGroup, method="lda",metric="Accuracy", trControl=ctrl,
preProcess=c("center","scale"))
rfFit = train(trainData[, 1:5], y=trainGroup, method="rf",metric="Accuracy", trControl=ctrl,
preProcess=c("center","scale"))# summary of modeling perfomance from cross-validation
results = resamples(list(LR=lrFit,LDA=ldaFit,RF=rfFit))summary(results)
## ## Call:
## summary.resamples(object = results)
## ## Models: LR, LDA, RF
## Number of resamples: 15
## Accuracy
##          Min.   1st Qu.    Median      Mean   3rd Qu.      Max. NA's
## LR  0.6904762 0.7411406 0.7674419 0.7608712 0.7906977 0.8139535    0
## LDA 0.6279070 0.6744186 0.6976744 0.7331488 0.7884828 0.9069767    0
## RF  0.6666667 0.7325581 0.7906977 0.7877815 0.8355482 0.9047619    0
 ## Kappa
```

```
##        Min.   1st Qu.    Median      Mean   3rd Qu.      Max. NA's
## LR  0.3809524 0.4755761 0.5295405 0.5190030 0.5806442 0.6285097    0
## LDA 0.2472648 0.3365874 0.3823204 0.4591650 0.5738611 0.8118162    0
## RF  0.3318182 0.4670405 0.5807151 0.5745172 0.6723630 0.8108108    0
```

bwplot(results)

We can validate the model performance with reserved testing data (Fig. 7):

We can plot the classification performance of a model in the test data (Fig. 8):

```
## Setting direction: controls < cases
```

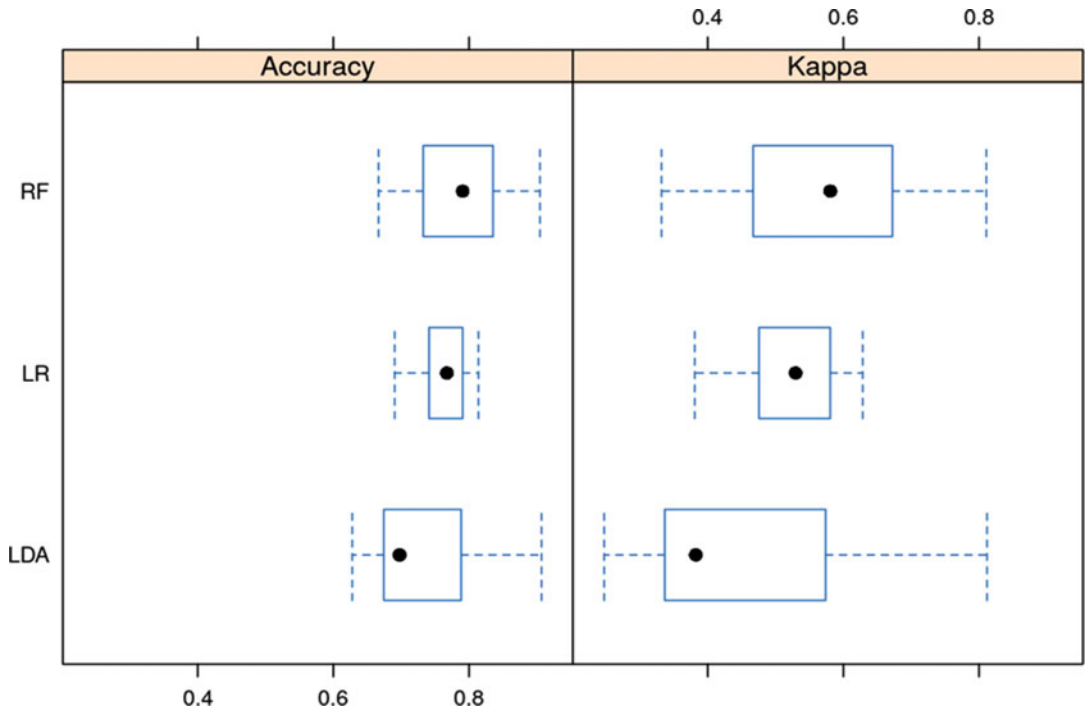

Fig. 7 Model performance in cross-validation in the training dataset

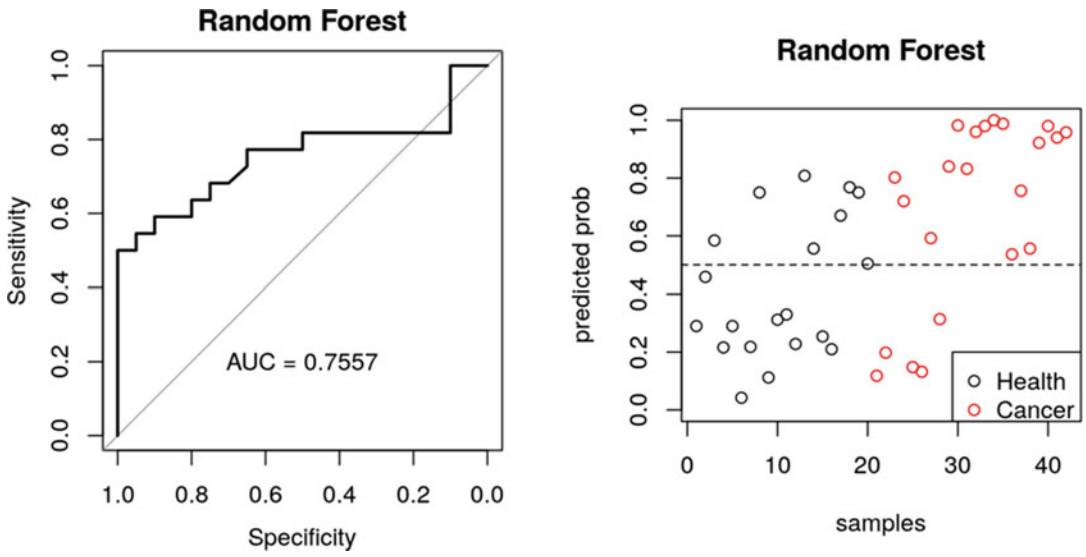

Fig. 8 Model performance in the test dataset

5 Conclusion

The statistical analysis of antibody array data may involve various methods/algorithms/tools. We introduced some basic options with R language and packages in this chapter. There are many other statistical methods that can be applied to antibody array data that are not addressed in this chapter, like different statistical models and other dimension-reduction techniques such as MDS. However, the powerful and flexible R language can be applied to antibody array data with ease.

References

1. Team RC (2013) R: a language and environment for statistical computing. R Foundation for Statistical Computing, Vienna
2. Gu Z, Eils R, Schlesner M (2016) Complex heatmaps reveal patterns and correlations in multidimensional genomic data. Bioinformatics 32:2847–2849. ISSN: 1367-4811 (Electronic)
3. Benjamini Y, Hochberg Y (1995) Controlling the false discovery rate: a practical and powerful approach to multiple testing. J R Stat Soc B (Methodol) 57(1):289–300
4. Tusher VG, Tibshirani R, Chu G (2001) Significance analysis of microarrays applied to the ionizing radiation response. Proc Natl Acad Sci U S A 98:5116–5121. ISSN: 0027-8424 (Print)
5. Smyth GK (2004) Linear models and empirical Bayes methods for assessing differential expression in microarray experiments. Stat Appl Genet Mol Biol 3:3. ISSN: 1544-6115 (Electronic)
6. Langfelder P, Horvath S (2008) WGCNA: an R package for weighted correlation network analysis. BMC Bioinformatics 9(1):559. https://doi.org/10.1186/1471-2105-9-559
7. Subramanian A, Tamayo P, Mootha VK, Mukherjee S, Ebert BL, Gillette MA, Paulovich A, Pomeroy SL, Golub TR, Lander ES, Mesirov JP (2005) Gene set enrichment analysis: a knowledge-based approach for interpreting genome-wide expression profiles. Proc Natl Acad Sci 102(43):15545. https://doi.org/10.1073/pnas.0506580102
8. Yu G, Wang L-G, Han Y, He Q-Y (2012) clusterProfiler: an R package for comparing biological themes among gene clusters. OMICS 16:284–287. ISSN: 1557-8100 (Electronic)
9. Caret: classification and regression training (2019).

INDEX

A

Aminosilanes 191–197
Antibodies 1–9, 11–37, 39–53, 55–66, 72–74, 83–91, 94, 95, 98, 99, 101, 104, 107, 109, 112–114, 116–118, 120, 123–126, 128, 132–135, 137, 138, 142, 143, 148, 151–153, 157, 158, 166–170, 186, 191, 192, 199–205, 207, 208, 211, 214, 217–223, 225–235, 237–244, 247–254, 257–261, 263–273, 277–314
Antibody array
  cytokine antibody arrays 4
  membrane arrays 135
  microarrays 152, 238, 239, 268, 291
  quantibody array 2
  quantitative array 2
  reverse phase protein array (RPPA) 104
Apoptosis 230

B

Biomarkers 45, 69–81, 84, 88, 152, 207, 208, 210, 237–244, 267, 285, 300, 302, 306, 307
Biomolecular interactions 55–66
Biotin labeling 47, 49
Biotinylated Phos-tag 240

C

Chemokines 46, 83, 248, 252
Chips 41, 46, 56, 94–99, 101, 152, 180
Chip-to-chip 141–149
Conjugates 12, 20, 23, 29–31, 35–37, 72, 95, 98, 99, 101, 132, 137, 185
Cross-reactivity 2, 12–17, 45, 79, 142, 152, 204, 239, 242–244
Cytokines 4, 5, 7, 9, 46, 83, 84, 123–128, 132, 201, 202, 204, 248, 252

D

Data analysis 24, 42, 88, 114, 257, 258, 263, 265, 271, 272, 277, 283
Databases 257–259, 272
Data preprocess 264–265, 306
Dendrimers 208, 210–212, 214
Detection
  enhanced chemiluminescence (ECL) 132, 220, 230
  fluorescence detection 7, 50, 128
Diagnostics 13, 69, 169, 199, 207, 238, 267
Differential expression analyses 263, 265, 267, 285
Dried blood sample 199
Drug discovery 170

E

Enhanced protein array 123–128

F

Fluorescence 2, 9, 39, 43, 83, 94, 97, 99, 118, 128, 129, 143, 144, 169, 180, 186, 187, 191, 192
Functional phenotype 103

G

Gene ontology (GO) 271, 272, 286, 300
Glass coatings 193
Glycosylation 129, 208, 210, 215

H

High-throughput 45, 56, 83–85, 88, 123–128, 142, 155, 158, 170, 200, 207, 226, 257, 263, 267, 285, 294

I

Image analysis 7, 24
Immobilization 11, 20–21, 25, 29, 31, 33, 36, 56, 62, 65, 152, 153, 169, 179
Immunoarrays 69–82
Immunoassay
  enzyme-linked immunosorbent assays (ELISA) 22, 200
  sandwich immunoassays 12
Intestines 247–254
Intraepithelial lymphocytes (IEL) 250, 254

Kelly C. Whittaker and Ruo-Pan Huang (eds.), *Antibody Arrays: Methods and Protocols*, Methods in Molecular Biology, vol. 2237, https://doi.org/10.1007/978-1-0716-1064-0,

K

Kyoto Encyclopedia of Genes and Genomes (KEGG) 272, 300

L

β-Lactoglobulin 56, 58, 63
Lamina propria lymphocytes (LPL) 249, 251, 254
Layer-by-layer 70
Ligands 9, 56, 63, 164, 225

M

MAPK 226, 230
Mass spectrometry (MS) 55, 56, 60, 64, 66, 155, 185, 200, 217, 226, 238
Matrix-assisted laser desorption/ionization (MALDI) 56, 58, 60, 63, 64, 66, 238
Microfluidics 69–81, 158, 160, 162, 169, 183
Microplates 14, 34, 35, 86, 88, 110
Molecular bridging 11, 21, 29–31
Multiplexes 11–13, 17, 20, 22, 25, 29, 31–33, 55–66, 83–91, 93–101, 113, 141–149, 151, 200, 218, 248

N

Nitrocellulose 1, 18, 35, 104, 107, 111, 114, 116, 117, 119–121, 123, 129, 208, 211, 214, 222, 226

O

Oligonucleotides 29, 94, 97, 98, 101
One-step 39

P

Peyer's patches (PPs) 250
Poly(ethylene glycol) (PEG) 56, 70–72, 77, 158, 180, 193, 218
Post-translational modification ..... v, 103, 104
Protein
protein detection 1–9, 151, 244
protein immobilization 165
protein phosphorylation 217–223, 226
protein profiling 123–128, 199–204, 238
Proteomics 45, 69, 93, 151, 200, 217, 238, 257, 267

Q

Quantitation 210

R

R 258–261, 269, 272, 277–279, 282–289, 291–294, 300, 306, 314

S

Sandwich assays 80, 142, 143
Screening 13, 45, 151, 153, 199, 307
Self-assembly
self-assembly peptide hydrogels 179–188
Signaling pathways 1, 221, 225–235, 286, 300
Silanes 193, 196
Snap chip 142
Solid pins 14, 104, 109, 113, 130
Sourcing 11
Supervised classification 269, 270
Surface modifications 179
Surface plasmon resonance 55–66

U

Unsupervised classification 269, 270